TERRAIN STUDIES FOR SLOPE INSTABILITY IN PARTS OF TEHRI DISTRICT, GARHWAL HIMALAYA, U.P., INDIA

A THESIS

submitted in fulfilment of the
requirements for the award of the degree
of
DOCTOR OF PHILOSOPHY
in
APPLIED GEOLOGY

246562
27-1-95
ROORKEE

By

SAEID HASHEMI TABATABAEI

28/12/92
Professor and Head
Department of Earth Sciences
University of Roorkee
ROORKEE

DEPARTMENT OF EARTH SCIENCES
UNIVERSITY OF ROORKEE
ROORKEE-247667 (INDIA)

DECEMBER, 1992

Dedicated To The Harmony Of Nature

My Wife & Parents

Who Lifted My Eyes To The Hills

CANDIDATE'S DECLARATION

I hereby certify that the work which is being presented in the thesis entitled **"TERRAIN STUDIES FOR SLOPE INSTABILITY IN PARTS OF TEHRI DISTRICT, GARHWAL HIMALAYA, U.P., INDIA"** in fulfilment of the requirement for the award of the Degree of Doctor of Philosophy, submitted in the Department of Earth Sciences, University of Roorkee, is an authentic record of my own work carried out during the period from January 1987 to December 1992 under the supervision of Dr. A.K. Awasthi, Dr. B. Singh and Dr. G.S. Mehrotra.

The matter embodied in this thesis has not been submitted by me for the award of any other degree.

(SAEID HASHEMI TABATABAEI)

This is to certify that above statement made by the candidate is correct to the best of our knowledge.

(Dr. G.S. MEHROTRA)	(Dr. BHAWANI SINGH)	(Dr. A.K. AWASTHI) 26/12/92
Scientist E-II	Professor	Professor in Geology
Geotechnical Engg.Divn.	Deptt. of Civil Engg.	Deptt. of Earth Sciences
Central Building	University of Roorkee	University of Roorkee
Research Institute	ROORKEE, INDIA	ROORKEE, INDIA
ROORKEE, INDIA		

Date: 26.12.92

The Ph.D. viva-voce examination of Mr. S.H. TABATABAEI, Research Scholar has been held on 27.5.93.

Signature of Guide(s) Signature of External Examiner

ACKNOWLEDGEMENTS

The work embodied in this thesis was carried out under the supervision of Prof. A.K. Awasthi, Prof. Bhawani Singh and Dr. G.S. Mehrotra to whom I am highly indebted for their constant encouragement, inspiration, guidance and discussions. I wish to particularly thank Prof. A.K. Awasthi for proposing this topic and for offering many valuable suggestions and advice, throughout this work.

Facilities for carrying out the investigations were generously provided by Department of Earth Sciences, University of Roorkee, Roorkee for which I am grateful to Professors A.K. Jain and Late R.K. Goel. Words fail to express my deep sense of gratitude to beloved Late Prof. R.K. Goel, who shaped my carrier.

My sincere thanks are also due to Messers C. Magh Raj, R.Kandpal, S.K. Sharad , A. Asokant and R. Dharmaraju for their help at one or the other stages of this work.

I wish to record my heartful appreciation to Drs. R. Anbalagan, A.K. Pachauri, V.N. Singh and R.C. Patel for many valuable technical discussions.

I am thankful to Prof. M.J. Crozier (Wellington, Newzealand) and G. Kumar, Director, Geological Survey of India (N.R.) for providing technical manuscripts and advice.

Assistance rendered by Messers R.C. Punj and R.D. Misra in preparation of rock samples (cubes) is highly appreciated.

The cooperation and moral encouragement received through my friends namely, Doctors Changiz Fooladi, Jamaloddin Noorzai and Messrs H. Afshari, H. Fahimi, C. Chafghazi, M. Ghazi, A. Taheri, L.P. Singh ,Pankaj Gupta and P.V. Gupta are thankfully acknowledged.

Financial assistance received from University Grants Commission is gratefully acknowledged.

Consistent encouragement and deep interest shown by family members, especially my wife Parissa, have provided necessary inspiration. I appreciate their thoughtfulness in bearing with me the inconvenience due to my constant occupation with this work in the final stage.

I have my humble thanks for all those who, in any manner, directly or indirectly put a helping hand in every bit of this investigation.

(SAEID HASHEMI TABATABAEI)

ABSTRACT

Himalaya is the youngest mountain range in the world. They owe their origin to the collision of Indian Plate with the Eurasian plate. With the continual subduction of Indian Plate, the Himalaya is still rising, thus, form a very unstable belt on the northern part of India. On the basis of lithotectonic characters, this mountain range has been classified in to six longitudinal zones - as sub-Himalaya in the south, followed northerly by lesser Himalaya, Higher (or greater or central) Himalaya, Tibetan (or Tethys) Himalaya, Indus-Tsangpo suture zone and Trans-Himalaya (Schawn, 1981). During rainy seasons Himalaya witnesses inumerable landslides which cause major hazards. In general, it has been observed that the Lesser Himalayan region is more affected by landslide activity as compared to sub-Himalayan region (Joshi, 1987). In the Garhwal region of the Lesser Himalaya, a study conducted by Central Building Research Institute, Roorkee indicates annual land degradation of 120 sq.m per kilometer of roads.

Although these areas are highly landslide prone, it appears that land failure phenomena are not observed every where. They are found to occur and recur in the areas characterised mainly by unique combination of topographic, structural, lithologic, hydrologic, climatic and vegetative features. These features to gether with mass wasting play important role in changing the geomorphic regime of an area, both on long and short term basis. Hence, the present study is an endeavour towards identification,

evaluation and forecasting such hazardous zones of instability due to landslide mainly through geomorphological signatures in the Garhwal region of the Lesser Himalaya of a part of Tehri district, U.P., India.

Geologically, the area is made up of two major lithostratigraphic succession - the Bijni Member of the Lansdwone Formation and the Younger succession of Blaini, Krol, Tal and the Subathu Formations, consisting mainly of quartzite, limestone/ dolomite, siltstone, slate and shale. The Bijni quartzite of Lansdowne Formation has angular unconformable contact with the overlying younger stratigraphic units. Also, the contacts between Phulchatti Quartzite and Manikot Shell Limestone of Upper Tal and the Subathu Formation with underlying rocks is marked by an unconformity. In the south-western part of the area, Bijni Member overlies the Subathu (Eocene) Formation and this abnormal position is due to a major fault known as Singtali Fault or Garhwal Thrust, which trends, in general, WNW-ESE with steep southerly dip varying between 70° to 80°. These rocks in general, have four sets of joints dipping NE, SSW, ESE and NW direction.

The terrain under study is characterised by rugged topography and typical ridge and valley features. The slopes are found to be highly variable and in general steep. Approximately 90% of the hillface is occupied by natural vegetation cover. Landslide affected areas in the terrain are found to occur at any elevation which ranges from about 500 m to more than 2200 m. In

general, with increase in elevation, the landslide affected area though tends to increase, yet is not uniformly distributed. Such areas are prominently found to occur mostly at elevations above 1800 m, 1500 - 1600 m and 1100 - 1300 m, close to the upper part of the ridges, and also at elevation of 500 - 600 m which is generally found along the hillslope near the road running almost parallel to the river Ganga. Slopewise also, the percent landslide affected area is not uniformly distributed in different slope facets. It is maximum in facets with slope angle between 30 to 35°. Landslide distribution has also been found to have intimate relation with vegetation cover. It is observed that maximum landslide affected areas fall within barren to sparsely vegetated land, of which barren lands have been affected the most, and found associated with steeper slope areas of upper part of ridges. The effect of lithology on the landslide area distribution is not conspicuous as most of the area (about 80%) is occupied by a single rock type i.e. quartzite. However, a careful observation indicates that the argillites and carbonates of the Lower Krol Formation, the quartzite of the Bijni Member of Lansdowne Formation and Blaini Formation have been affected the most. The steep sided valleys have led to increase in the susceptibility of the rocks to landslide activities. The slope movement is also governed by occurrence, orientation and trend of local structures, such as bedding plane and joints.

Various workers like Horton (1932, 1945), Strahler (1952, 1971) Schuum (1956), Morissawa (1962,1963,1968,1985) have studied

landforms and proposed a number of morphometric parameters which are used for terrain evaluation. Despite their wide use for morphometric studies, little attempt has been made to assess them as instability indicators. The basins of the third order which formed good working units, were the targets of study on morphometry vis-a-vis instability of the area.

The correlation matrix prepared from twenty variables indicates that Fraction landslide area (Ls) in a basin has statistically significant correlation coefficient of about 0.86, 0.84, 0.68 and -0.55 (99% confidence level) with Drainage texture (DT), Stream frequency(SF), Drainage density (DD), and Basin circularity (BC) respectively. Drainage density is sensitive to changes in lithology, vegetation cover, slope, structure, and hydrologic aspect of stream system (Carlston, 1963; Strahler, 1964). Stream frequency is largely dependent on rock type. Therefore drainage texture is one single morphometric parameter in a basin that has in it, the influence of many morphometric parameters which in turn, are reflection of the sum effect of elevation, slope, lithology, structural features, vegetation and hydrological condition. Based on regression analysis the following relationship between Fraction landslide area and Drainage texture (DT) has been worked out.

$$Ls = 0.0279 + 0.0052\ DT$$

This relationship when tested to estimate Fraction landslide area in four randomly selected drainage basins in the area was found

to be useful within the error limit of 25 percent.

Despite the usefulness of Drainage texture as an indicator of instability of a terrain, this parameter cannot be used to study instability condition at local level of a particular hillslope section. Also, it does not indicate the nature of failure and processes of instability involved on the hillslope. Nevertheless, it indicates that morphological features can be very useful in investigation of stability of hillslopes in a watershed. Morphology of slopes can dictate type of movement and extent of instability (Crozier, 1973). He showed that significant morphometric indices can be obtained from a landslip as indicators of slope movement processes. Crozier investigated slope morphology on the basis of sixty six landslips as observed in a terrain made up largely of concavo-convex slopes with very few bedrock outcrops and free faces associated with a thick soil and regolith mantle cover in Newzealand. In the present investigation, a similar approach has been made on the basis of sixty transverse slope profiles in the twelve randomly selected drainage basins. However, critical values of various indices namely classification index, dilation index, flowage index, displacement index and tenuity index given by Crozier (1973) could not be applied as such in this area. Hence, these critical values as predictive limits for likely process of slope movement were modified. The modified mean values of five morphometric indices namely classification, dilations, flowage, displacement and tenuity indices were calculated to be 7.68, 0.35, 75.92,

48.04 and 1.20 respectively for rotational slide (RS). Likewise the mean values for five above mentioned indices for planar slide were calculated to be 7.22, 0.36, 44.0, 73.31 and 0.62 respectively. Similarly, for slide flow (SF) the mean values of classification, dilation, flowage, displacement and tenuity indices were calculated to be 4.39, 0.70, 73.94, 54.25 and 1.62 respectively. The calculated mean values for fluid flow (FF) were found to be 1.88, 1.78, 215.95, 53.22 and 2.37 for classification, dilation, flowage displacement and tenuity indices respectively. The efficacy of the modified parameters as predictive limits for the slope movement processes involved on a hillslope was established when this approach was applied successfully to three different areas of similar topography located at 122 km NNW (Mussoorie ByPass); 80 km NNE (Kaliasaur) and 57 km SSW (Chilla) of the area of study.

Displacement index (DPI) appears to indicate the potential of failure of a section. A section is likely to become unstable and fail by rotational slide, planar slide, slide flow and fluid flow if the displacement index is less than 48.04, 73.31, 54.25 and 53.22 respectively.

With a view to work out a simple quantitative statistically significant criteria to differentiate between the various slope movement processes based on simultaneous use of all the five morphometric indices, multivariate discriminate function analysis was used. The multivariate criteria have been developed and tested successfully to discriminate slide flow from fluid flow,

fluid flow from planar slide, fluid flow from rotational slide, planar slide from slide flow, rotational slide from slide flow and planar slide from rotational slide.

Discriminant analysis when used as search technique, indicated that of all the morphometric indices, classification, dilation and tenuity indices contribute significantly in discriminating various slope movement processes. Based on these indices, bivariate and unvariate plots have been prepared. These plots can also be used as tools to screen and find out the slope movement process at a given site.

The developmental activity has affected the hillslope adjoining the road sections at a number of places by various types of slope movement, particularly planar and wedge failure. In order to evaluate the hillslope failure along the road, twenty one landslides were identified between Byasi to Devaprayag in the study area. Six sites, designated herein as L_1, L_5, L_6, L_7, L_9 and L_{14} were selected for detailed study. Slope orientation, joint orientation, weathering of joint wall, joint continuity, spacing, filling and separation of joints were measured. Stability analyses were performed using Slope Mass Rating (SMR) and limit equilibrium technique (Hoek and Bray, 1981). To use SMR it was necessary to determine joint wall (JCS) and uniaxial compressive strength of rock material. The L-type Schmidt hammer (rebound hammer) is in use by many research workers world over, for determination of JCS. The correlation coefficient between joint wall uniaxial compressive strength (JCS) measured

in the laboratory on rock samples (on cubes of 25 mm length) and the rebuond hammer test data on natural discontinuity surfaces (using Miller equation, 1965) was found to be significantly low i.e. close to zero. A close scrutiny of samples and data revealed that hammer can give acceptable strength (JCS) of joint wall, if the surface is dry and smooth, and not relatively uneven, which occures in most cases in field.

Slope Mass Rating of six selected sites indicates that the rating for sites L_1, L_5 and L_{14} are 22, 28 and 42 respectively. These conclusions proved correct on field observations. However, rating for sites L_6, L_7 and L_9 was calculated to be 18, 24 and 6 respectively and do not represent the stability condition as observed in the field. It therefore, indicates that SMR method of stability analysis is not a foolproof approach of indicating stability condition.

A critical examination of these sites indicates that when the continuity along the dip of a discontinuity surface is less than five percent of the total height of affected slope, it appears that the SMR technique does not depict the true picture of stability condition and extent of failure.

Slope stability analysis based on short solution of Hoek and Bray (1981) suggests that all these slopes are unstable in wet condition and are stable under dry dynamic (earthquake) condition. The conclusion draws its support from the fact, that year after year, these slopes fail only during the monsoon

season, due to dual action of pore water which exerts pressure to destabilise the slope on one hand and decreases the strength of wet rock mass along discontinuity surfaces on the other hand. It is also important to note that these sites remained unaffected by an earthquake of 6.5 on Richter scale which devastated the area in and around Uttarkashi (situated 35 km to the north of study area). Computer slope analysis recommends provision of adequate drainage in form of drill holes with folded geofabrics to stabilise rock slopes.

The study, in short indicates that i) Slope movement in the area is the out-come of the action and interaction of factors like, topographic elevation, slope, structural, lithological, hydrological conditons, vegetation cover. The sum effect of these factors is also reflected in the morphometric signature of a terrain. ii) L-type rebound hammer should be used on smooth natural surfaces only iii) It appears when continuity along dip of a discontinuity surface is less than five percent of total height of affected slope, SMR may not give adequate picture of stability condition. (iv) Slope movement along the road is due to excess pore water pressure build ups and decrease in the strength of rock mass during rainy season. The slopes remain stable under dry dynamic (earthquake) condition.

CONTENTS

		Page
	CERTIFICATE	(i)
	ACKNOWLEDGEMENT	(ii)
	ABSTRACT	(ix)
	LIST OF FIGURES	(xvii)
	LIST OF TABLES	(xxii)
CHAPTER		
1.	**INTRODUCTION**	1
	1.1 General	1
	1.2 Area of Study	2
	1.3 Physiography-A Synoptic view	4
	1.4 Climate and Vegetation	5
	1.5 Seismicity	6
	1.6 Accessibility	7
	1.7 Previous work	8
	1.8 Scope and Objectives of the Study	10
2.	**GEOLOGY OF THE AREA**	12
	2.1 The Himalaya	12
	2.2 Regional Sub-divisions of Himalaya	13
	2.2.1 Lithotectonic Subdivisions	17
	2.3 Geological FrameWork	17
	2.3.1 Stratigraphy of the Area of Study	20
	2.3.2 Structure of the Area of Study	26
	2.4 SUMMARY	28

3. TERRAIN, LANDSLIDES AND MORPHOMETRY 30

3.1 Introduction 30

3.2 Terrain 31

3.2.1 Elevation 32

3.2.2 Slope Classification Map 35

3.2.3 Vegetation Cover 38

3.2.4 Lithological and Structural Character 44

3.3 Identification Techniques of Landslides 46

3.3.1 Remote Sensing Technique 46

3.3.1.1 Diagnostic Features of Landslides on Aerial Photographs 47

3.3.2 Map Technique 48

3.3.2.1 Diagonstic Features of Landslides on Topographic Map 49

3.3.3 Field Investigation 49

3.3.4 Landslide Map of the Area 50

3.4 Distribution of Landslides in the Terrain 50

3.4.1 Landslide Distribution in Relation to Topographic Elevation 52

3.4.2 Landslide Distribution in Relation to Slope 56

3.4.3 Landslide Distribution in Rlation to Landuse (vegetation cover) 59

3.4.4 Landslide Distribution in Relation to Stratigraphic Units 63

3.4.5 Landslide Distribution in Relation to Structure 66

3.5 Morphometric Parameters and Landslides 70

3.5.1 Correlation Between Landslide Area and Geomorphometric Parameters 79

3.5.2 Analysis 80

3.5.3 Relationship Between Landslide Area and Drainage Texture 85

3.5.3.1 Efficacy of the Regression Model Developed 86

3.6 Summary 87

4. TYPE AND PROCESS OF SLOPE MOVEMENT -A MORPHOMETRIC APPROACH 90

4.1 Introduction 90

4.2 Slope Profiles and Genetic Processes 91

4.3 Slope Profile Morphometry and Land Instability of the Terrain 97

4.3.1 The Classification Index 97

4.3.2 The Dilation Index 100

4.3.3 The Flowage Index 101

4.3.4 The Displacement Index 103

4.3.5 The Tenuity Index 105

4.3.6 Statistical Summary of Slope Morphometric Indices 106

4.3.7 Test Cases 108

4.3.8 Inference 115

4.4 Multivariate Discrimination Criteria for Slope Movements 116

4.4.1 Philosophy of Discriminant Function Analysis 116

4.4.2 Application of Discriminant Function Analysis 118

4.4.3 Discriminant Function and Discriminant Criteria 119

4.4.4 Discriminant Function as Search Technique 123

4.4.5 Bivariate and Univariate Plots as Tool for Discrimination 128

4.4.6 Usefulness of Bivariate and Univariate Plots 135

4.5 Summary 135

5. LANDSLIDES IN RELATION TO DEVELOPMENTAL ACTIVITIES IN THE AREA 138

5.1 Introduction 138

5.2 Classification of Roadside Slope Instability in the Area-General 138

5.3 Types of Hillslope Instability along the Road 142

5.4 Determination of Parameters for Stability Analysis 162

5.4.1 Stability Parameters 162

5.5 Stability Analysis 185

5.5.1 Slope Mass Rating of Sites Under Study 186

5.5.2 Efficacy of SMR Approach of Stability Analysis 191

5.6 Three Dimensional Stability Analysis 192

5.7 Result and Discussion 194

5.8 Summary 213

6. SYNTHESIS, SUMMARY AND CONCLUSION 215

6.1 Conclusions 232

REFERENCES 234

APPENDICES

AI. Calculation of Slope Mass Rating (SMR) 252

AII. Short Method of Analysis of Tetrahedral Wedge (Hock and Bray, 1981) 255

AIII. Estimation of `c' and `ϕ' from RMR_{basic} 266

AIV. Slope Morphometric Indices for Sixty Slope Profiles in the area of study 267

LIST OF FIGURES

		Page
1.1	Location Map of the Area	3
2.1	Geographic Subdivisions of Himalaya (after Gansser, 1964)	14
2.2	Litho-Tectonic Zones of the Himalaya (After Schwan, 1981)	15
2.3	Litho-Tectonic Divisions of Garhwal-Kumaun Himalaya, Uttar Pradesh showing Major Tectonic Features (after Kumar, 1981)	18
2.4	Geological Map of a Part of "Garhwal Synform" (After Kumar and Dhaundiyal, 1979)	22
2.5	Geological Map of the Area (Modified After Kumar and Dhaundiyal, 1979)	23
2.6	Geological Cross Section along the line x,y on Geological Map (Fig. 2.5)	27
3.1	Contour Map of the Area Based on Toposheet No. 53J/8, 53J/12	33
3.2	Slope Classification Map of the area	36
3.3	Landuse Map (Vegetation Cover) of the Area	42
3.4	Map Showing Landslide Areas in the Terrain (Based on Aerial Photographs and Field Survey)	51
3.5	Distribution of Landslide Area with Elevation	54
3.6	Distribution of Landslide Area with Slope	57
3.7	Rock and Debris Slide in Well Jointed and Weathered Slate (38 km from Rishikesh)	60
3.8	Rock cum Debris Avalanches in Highly Weathered Phyllite (65 km from Rishikesh)	60
3.9	Distribution of Landslide Area with Landuse (Vegetation Cover)	62
3.10	Distribution of Landslide Area with Respect to Stratigraphic Units	65
3.11	Rock Slide on Dip-Slopes of Quartzite Caused by Toe Excavation (32 km from Rishikesh)	68

3.12	Rock fall from Over Hanging Scar Face of the Quartzite (52 km from Rishikesh)	68
3.13	Rock Slide in Highly Jointed Quartzite (46 km from Rishikesh)	69
3.14	Axial Zone of a Minor Fold, Forms Landslide Susceptible Area While Disturbed Exogenically (58 km from Rishikesh)	69
3.15	Drainage Map of the Area	71
3.16	Rose Diagram of Drainage Azimuth of First order Stream in the Area	76
3.17	Rose Diagram of Drainage Azimuth of second order Stream in the Area	76
3.18	Rose Diagram of Drainage Azimuth of Third order	76
3.19	Showing Correlation Coefficients Between Fractional Landslide Area (LS) and Geomorphometric Parameters (Figures Along the Lines Indicate Correlation Coefficients)	82
3.20	Showing Comparison of Computed and Observed Fraction Landslide Area with Location of Test Samples.	88
4.1	Diagrammatic Respresentation of a Hypothetical Nine Unit Landsurface Model (Dalrymple et al., 1968)	92
4.2	Terminology Use in the Morphometric Classification (Crozier, 1973)	95
4.3	Landslip Terminology and Measurements Used in the Morphometric Indices	98
4.4	Panoramic View of Mussoorie Bypass	112
4.5	Panoramic View of Kaliasaur	
4.6	Panoramic View of Chilla	114
4.7	Location of Samples on Discriminant Function Line for Differentiation Between Slide Flow (SF) and Fluid Flow (FF)	124
4.8	Location of Samples on Discriminant Function Line for Differentiation Between Planar Slide (PS) and Fluid Flow (FF)	124

4.9	Location of Samples on Discriminant Function Line for Differentiation Between Rotational Slide (RS) and Fluid Flow (FF)	125
4.10	Location of Samples on Discriminant Function Line for Differentiation Between Planar Slide (PS) and Slide Flow (SF)	125
4.11	Location of Samples on Discriminant Function Line for Differentiation Between Rotational Slide (RS) and Slide Flow (SF)	126
4.12	Location of Samples on Discriminant Function Line for Differentiation Between Rotational Slide (RS) and Planar Slide (PS)	126
4.13	Location of Test Samples on the Bivariate Plot Between Classification (D/L) and Dilation (Dx/Dc) Indices Showing Distinct Fields for Slide Flow (SF) and Fluid Flow (FF)	131
4.14	Location of Test Samples on the Bivariate Plot Between Classification (D/L) and Tenuity (Lm/Lc) Showing Distinct Fields for Planar Slide (PS) and Fluid Flow (FF)	131
4.15	Location of Test Samples on the Bivariate Plot Between Classification (D/L) and Dilation (Dx/Dc) Indices Showing Distinct Fields for Planar Slide (PS) and Fluid Flow (FF)	132
4.16	Location of Test Samples on the Bivariate Plot Between Tenuity (Lm/Lc) and Dilation (Dx/Dc) Indices Showing Distinct Fields for Planar Slide (PS) and Fluid Flow (FF)	132
4.17	Location of Test Samples on the Bivariate Plot Between Classification (D/L) and Dilation (Dx/Dc) Indices Showing Distinct Fields for Rotational slide (RS) and Fluid Flow (FF)	133
4.18	Location of Test Samples on the Bivariate Plot Between Classification (D/L) and Tenuity Indices Showing Distinct Fields for Planar Slide (PS) and Slide Flow (SF)	133
4.19	Location of Test Samples on the Bivariate Plot Between Classification (D/L) and Dilation Indices Showing Distinct Fields for Rotational Slide (RS) and Slide Flow (SF)	134

4.20	Location of Test Samples on the Univariate Plot of Tenuity (Lm/Lc) Showing Distinct Fields for Rotational Slide (RS) and Planar Slide (PS)	134
5.1	Inventory of Landslide Areas Investigated Along the Road	144
5.2	Planar Slide in Well Jointed and Fractured Quartzite (32 km from Rishikesh)	151
5.3	Rock Avalanches in Jointed Quartzite (35 km from Rishikesh)	152
5.4	Occasional Wedge Failure and Rock Fall in Jointed Quartzite (35.3 km from Rishikesh)	152
5.5	Large Planar Failure in Well Jointed Quartizte (38.5 km from Rishikesh)	153
5.6	Wedge Failure in Highly Jointed and Fractured Quartzite (42 km from Rishikesh)	154
5.7	Occassional Planar Failure in Well Jointed Silt -stone (42 km from Rishikesh)	154
5.8	Planar Slide in Highly Jointed and Fractured Quartzite (46 km from Rishikesh)	155
5.9	Rock Avalanches in Jointed and Weathered Limestone (43 km from Rishikesh)	156
5.10	Wedge Failure in Well Jointed Quartzite (52.8 km from Rishikesh)	156
5.11	Wedge Cum Planar Failure in Well Jointed Quartzite (52.5 km from Rishikesh)	157
5.12	Planar Slide Cum Debris Avalanches in Well Jointed Quartzite (61 km from Rishikesh)	158
5.13	Debris slide in Weathered Phyllite (65 km from Rishikesh)	159
5.14	Debris Slide in Weathered Phyllite and Quartzite (65 km from Rishikesh)	159
5.15	Rotational Slide in Highly Weathered Phyllite (70 km from Rishikesh)	160
5.16	Measurement of Uniaxial Compression Strength (JCS) by L-type Rebound Hammer	167

5.17	Rock Cubes Preparation for Measurement of Uniaxial Compressive Strength (JCS)	167
5.18	Determination of JCS by 10 Tons Universal Testing Machine	168
5.19	Observed vs. Computed Joint Wall Compressive Strength (Miller, 1963) in Dry Condition	172
5.20	Observed vs. Computed Joint Wall Compressive Strength (Miller, 1963) in Wet Condition	173
5.21	Observed vs. Computed Joint Wall Compressive Strength in Wet Condition	174
5.22	Stereographic Plots of Joints and Slope at Sites L_1(A), L_6(B) and L_9(C)	181
5.23	Stereographic Plots of Joints and Slope at Site L_5	182
5.24	Stereographic Plots of Joints and Slope at Site L_7	183
5.25	Stereographic Plots of Joints and Slope at Site L_{14}	184

LIST OF TABLES

		Page
2.1	Stratigraphy of `Garhwal Synform', Tehri District, Uttar Pradesh	21
3.1	Elevation Distribution in the Area	34
3.2	The Facets of the Area	37
3.3	Slope Facet Distribution in the Area	38
3.4	Interpretation key for Landuse Types on Aerial Photographs	40
3.5	Landuse Class Distribution in the Area	43
3.6	Areas Occupied by Various Stratigraphic Units	45
3.7	Landslide Area Distribution at Different Elevation	53
3.8	Landslide Area Distribution at Different Slope Facets	56
3.9	Landslide Area Distribution at Different Landuse class	61
3.10	Landslide Area Distribution at Different Stratigraphic Units.	64
3.11	Geomorphometric Parameters Used	73
3.12	Measures of Drainage Basin Shape (compiled from Gregory et al. 1973)	78
3.13	Pearson's Correlation Matrix Showing all Possible Correlation Coefficients among Geomorphometric Parameters.	81
3.14	Showing Theoretically Computed and Observed Values of Fraction Landslide Area for Four Test Basins.	81
4.1	Morphometric Indices (Crozier, 1973)	94
4.2	Process Groups used in Morphometric Analysis (Crozier, 1973)	94
4.3	Statistical Summary of the Values Calculated for the Morphometric Indices of the Landslip found in Eastern Otago (After Crozier, 1973)	96
4.4	Comparison of the Mean Values for Classification Index	99

4.5	Comparison of the Mean Values for Dilation Index	101
4.6	Comparison of the Mean Values for Flowage Index	103
4.7	Comparison of the Mean Values for Displacement Index	105
4.8	Comparison of the Mean Values for Tenuity Index	106
4.9	Statistical Summary of Morphometric Indices of Each Process in the Area of Study (Modified after Crozier, 1973)	107
4.10	Landslip Morphometric Indices at Mussoorie Bypass	110
4.11	Landslip Morphometric Indices at Kaliasaur	111
4.12	Landslip Morphometric Indices at Chilla	115
4.13	Discriminant Constants for Discrimination Betwee Various Slope Movement Process Group	118
4.14	Discriminant Score Means and Distance Measure D^2	119
4.15	Relative Contribution of Each Indices to Discriminate Between Various Slope Movement Process	128
5.1	Classification of Slope Movements	140
5.2	Details of Reconnaissance Survey of the Area along the Road Between Byasi to Devaprayag	145
5.3	Showing the Density of Rock Mass and Rebound Number (L-type hammer) under Dry and Wet Conditions	170
5.4	Calculated Jv and RQD values for six selected sites	175
5.5	Basic Geological Parameter and Measurement of Site-I (L_1)	199
5.6	Basic Geological Parameter and Measurement of Site-II (L_5)	200
5.7	Basic Geological Parameter and Measurement of Site-III (L_6)	201
5.8	Basic Geological Parameter and Measurement of Site-IV (L_7)	202

5.9	Basic Geological Parameter and Measurement of Site-V (L_9)	203
5.10	Basic Geological Parameter and Measurement of Site-VI (L_{14})	204
5.11	Basic Rock Mass Rating for Selected Sites	205
5.12	SMR Value and Factor of Safety of Site-I (L_1)	206
5.13	SMR Value and Factor of Safety of Site-II (L_5)	207
5.14	SMR Value and Factor of Safety of Site-III (L_6)	208
5.15	SMR Value and Factor of Safety of Site-IV (L_7)	209
5.16	SMR Value and Factor of Safety of Site-V (L_9)	210
5.17	SMR Value and Factor of Safety of Site-VI (L_{14})	211

CHAPTER - 1

INTRODUCTION

1.1 GENERAL

On the northern fringe of the Indian subcontinent, the Himalaya forms a very conspicuous physiographic terrain. This high mountain range is the youngest of other such ranges in the world. It owes its origin to the collision of Indian plate with the Eurasian plate. As the Indian plate is continually subducting, the Himalaya is rising up. The range is, thus, undergoing geodynamic activities, leading to high seismicity, intense tectonism and higher topographic relief observed in this belt. Besides high seismicity, this region is witnessing high amount of mass-wasting mainly through fluvial, glacial and gravity controlled processes (rock and debris slide, avalanches, creep, etc.). During rainy season, many hillslopes undergo innumerable changes and cause landslides and related phenomena. The severity of the landslide can be judged from the fact that as many as 20,000 landslide events are estimated to have occurred in one monsoon season in Nepal region only (Ives and Messereli, 1981).

In general, it has been observed that the Lesser Himalaya, a lithotectonic unit, is more affected by landslide activities as compared to southerly located belt of sub-Himalayan region (Joshi, 1987). In Garhwal region of the Lesser Himalaya, a study conducted by Central Building Research Institute, Roorkee,

indicates annual land degradation of the order of 120 sq.m per kilometer of roads.

Although these areas are highly landslide prone, it appears that landslide phenomena are not observed every where. The slides are found to occur and recur in the areas characterised mainly by unique combination of topographic, structural, lithologic, hydrologic, climatic and vegetative features. These features together with the mass wasting phenomena play important role in changing the geomorphic regime of an area, both on long term and short term basis. If this is so, then the geomorphic parameters, singly or in combination may indicate areas of instability which in this terrain, is found to be mainly related to landslides. Hence, the present study is an endeavour towards identification, evaluation and forecasting such hazardous zones of instability due to landslide mainly through the geomorphic signatures in the Lesser Himalaya in a part of Tehri district ,U.P., India.

1.2 AREA OF STUDY

The area of study lies in Garhwal region of the Lesser Himalaya, in the district Tehri Garhwal (Fig. 1.1). It falls within the longitudes $78^{o}25'E$ to $78^{o}37'E$ and latitudes $30^{o}3'N$ to $30^{o}10'N$ and forms parts of toposheet No. 53J/8 and 53J/12 of Survey of India. The river Ganga girdles the area of study in the east between Devaprayag to Debri village, in the south between Debri to Monjigaon village and in the west between village Monjigaon to Gal. The northern boundary of the area is

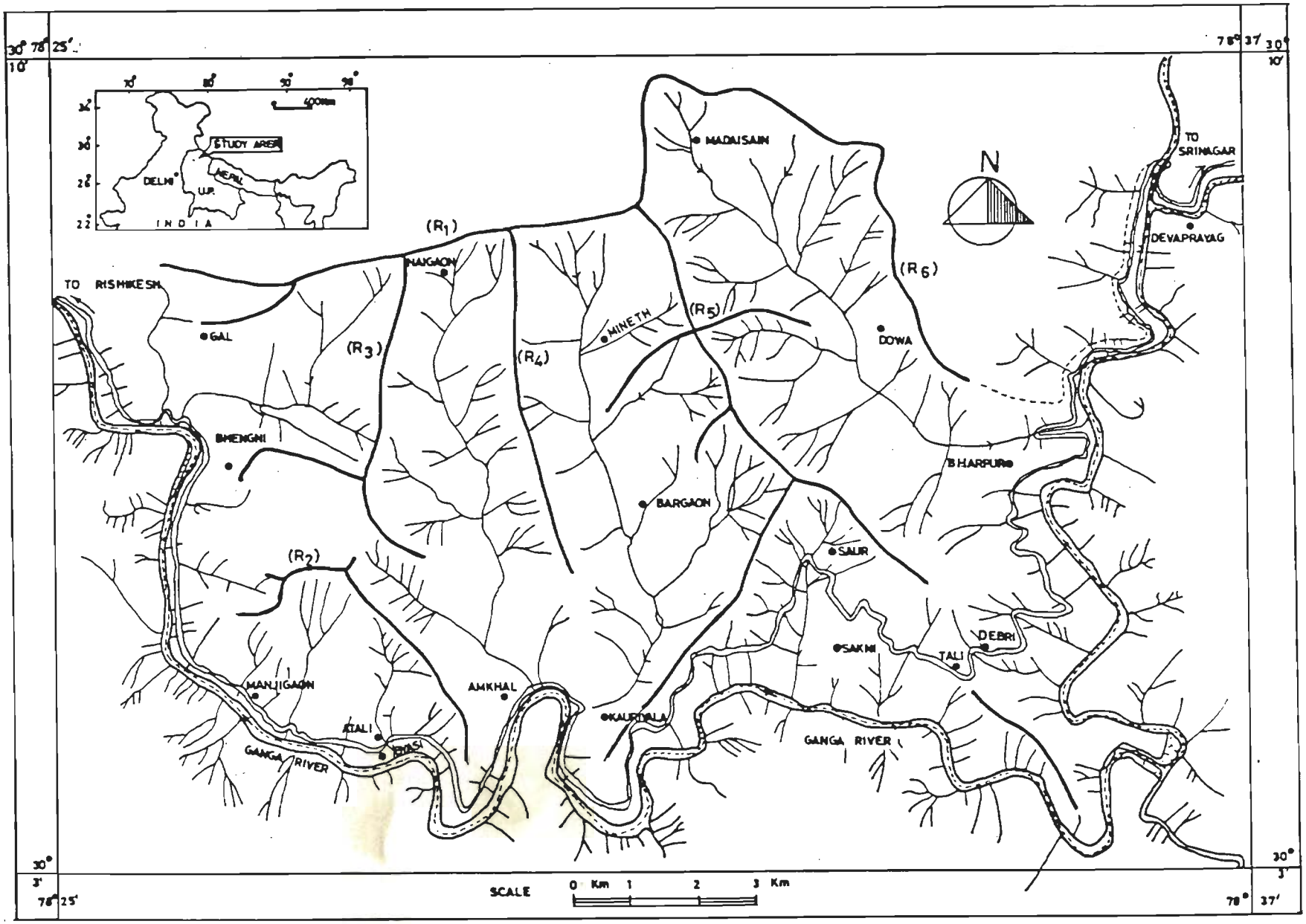

Fig.1.1: LOCATION MAP OF THE AREA

demarcated by a prominent topographic ridge between Gal and Madaisain village as shown in Figure 1.1. The area of study is about 102 sq.km with strategically important road connecting Rishikesh to Badrinath.

Landslide susceptible Lesser Himalaya, with its ridge and valley topography, travesed by an all weather motorable road of stratagic importance, offered excellent opportunity for carrying out the present investigation in this part of closely located Garhwal Himalaya.

1.3 PHYSIOGRAPHY - A SYNOPTIC VIEW

The area belongs to a hilly terrain which have been formed by orogenic activities and modified by external agencies to the present form. It exhibits the following physiographic features conspicuously.

Ridges - The area displays rugged topography with sharp and steep ridges linearly extending hill crests. They form water divide and are the result of head water erosion in the drainage basins which have been dealt with in detail in Chapter 3. The prominent ridges in the area are shown on the map (Figures 1.1 and 3.3). The R_1 ridge trends in general in E-W direction with elevation difference ranging from 500 m in the east to 2200 m in the west.The north-south running ridges (R_3 ,R_4,R_5,Fig. 1.1) take turn south westerly, when one approaches center of the area, and these ridges run against the general strike of the rocks, with maximum elevation of 1500 m. The R_5 ridge constitutes the longest

ridge in the area trending NW-SE with substantial elevation difference ranging from 500 m to 2100 m.

Valleys- These are the prominent negative landforms in the area, formed dominantly by fluvial erosion, in between the ridges filled up by alluvial and colluvial materials. The valleys are deep and narrow (narrow flood plain and steep sides slopes). Their axes are occupied by perennial or intermittant streams which display appreciable sinuousity along their path of flow. They vary in dimension and shape and may be distinguished into features like `rill (small channels formed on the surface of soil), `gully' (advance stage of rill formed due to large erosion of surface soil-much deeper than the rill) and `gorge' (deep, steep sided, rocky river valley). The size of the valley could be inferred from the width of separation of water divides (or ridges). The area displays in general trellis drainage pattern (Figures 1.1 and 3.1).

1.4 CLIMATE AND VEGETATION

In general the altitude of the area governs the climatic conditions. The meterological data collected from Devaprayag weather station indicates that annual rainfall varies from 411 mm in 1982 to 965 mm in 1985. On average it is of the order of 765 mm. The maximum precipitation is during the months of June, July and August and is of the order of 163 mm to 632 mm . Average rainfall is 432 mm at elevation of 1600 m and above this level it begins to decline. Thus, while it is highest at middle slope

(at elevation of 1000 m to 1500 m), it is low over hill tops.

The maximum temperature is during months of May and June which ranges on an average between 16^{o}C to 38^{o}C during day and night respectively. It is minimum during the months of December and January, having a range of 3^{o}C to 18^{o}C during day and night respectively.

The wind velocity, in general is moderate (approximately 4-10 km ph).It is highest during the months of May to August (average highest 42 km ph). The wind direction is variable and it may blow from NE, SW, NW, SE directions.

The relative humidity is high during the monsoon season, generally it exceeds 65% on the average. The driest part of the year is the pre-monsoon period when the humidity may drop to 35%. The highest and lowest percentage of humidity in the area is 94 and 34 respectively.

The type of vegetation is governed by altitude of the area and is in the form of deciduous plant e.g. shorea robutsta., Tectona grandis etc. at lower elevation. The pine forests e.g. Pinus roxburghii are found at higher elevation. In general, it has been observed that the valleys are densely vegetated, the hill tops on the other hand have scanty vegetation. A detail account of vegetation distribution is dealt in Chapter 3.

1.5 SEISMICITY

The convergence of Indian plate with Eurasian plate leads to occurrences of earthquakes along the Himalaya mountain. In

western sector of this chain the greatest earthquake event so far recorded was in the Kangra valley in the year 1905. It was of the magnitude 8.6 on Richer scale. The latest strong earthquake of 6.6 M occurred in Garhwal region (Uttarkashi) on 20th Oct. 1991. Besides these strong events many small magnitude earthquakes have been recorded in Garhwal Himalaya by Khattri et al. (1987). During the studies no microearthquakes were recorded along Main Boundary Thrust (MBT). But 70 km north of this region, a good cluster of microearthquakes was observed along the Main Central Thrust (MCT).

The area of study in the present work is bounded in the south by the Main Boundary Thrust (MBT) and in the north by Main Central Thrust (MCT). It is close to the former where little seismicity has been recorded.

1.6 ACCESSIBILITY

The area has poor accessibility due to rugged topography and thick natural vegetation. Rishikesh - Devaprayag road running almost parallel to the right bank of the river Ganga which forms roughly the southern, western and eastern limit of the study area, is the only approach road in this terrain. Villages located sparsely, can be visited in general, either by mule tracks or by walk on foot. The field investigation in the interior parts of the area could be done in the valleys between the ridges and the ridge slope through rock climbing.

1.7 PREVIOUS WORK

Since the middle of nineteenth century, the studies on the geology of Kumaun HImalaya has been carried out by many workers.

Herbert (1848) gave the first geological map of mountain provinces between Satluj and Kali river. Auden (1937) described the lithological sequence of Garhwal Himalaya. In 1949, he renamed `Barahat series' as `Garhwal series'. Later on, several workers carried out investigations on several aspects like geology, tectonics, stratigraphy etc. of various parts of Garhwal - Kumaun Himalaya (Jain, 1971; Saklani, 1971, 1972a, 1972b; Kumar et al., 1974, 1975, 1979; Rupke, 1974; Sharma and Virdi, 1976; Ganeshan and Thussu, 1978; Valdiya, 1978, 1980a, 1980b; Fuches and Sinha, 1978; Srivastava and Ahmad 1979; Prasad and Rawat, 1985; Virdi, 1986; Roy and Valdiya, 1988).

Raina (1972), Sharma (1977), Bharktia and Gupta (1982), Shandilya and Prasad (1982), Goel et al. (1987) and Jain (1987) used remote sensing techniques for different geological studies in the Garhwal - Kumaun Himalaya.

The geomorphological studies in Garhwal-Kumaun Himalaya were first carried out by Strachey (1851), Langstaff (1928) and Gillbert and Auden (1932) studied the Nanda and Gangotri-Badrinath group of glacier respectively. Bose (1966) worked on the fluvio-glacial geomorphology in the Alaknanda river. Chansarkar (1970) proposed tentative terrain types in Kumaun hills. Kumar (1970) and Nityanand and Prasad (1972) gave

the geotechnical evaluation and geomorphological appraisal respectively of floods of Alaknanda river in the year 1970. Hazara and Raina (1972) focussed on the occurrence of raised terraces and on the dissection of Himalayan mountain chain by rivers. Kaushik (1972) described the salient features of rejuvenation in the Garhwal region. Kaushik and Sharma (1972a, 1972b) studied the Bugyal ridges in Garhwal and transverse gorge of the Alaknanda river. Mithal et al. (1972) gave various morphometric parameters to evaluate geomorphic processes operating in the river regime of Birahiganga.

Pant (1975) studied the development of epigenetic gorges in the Bhagirathi and Alaknanda rivers. Khan et al. (1982) gave an account of the geomorphic evaluation of fluviatile landforms of Ganga valley river complex during Holocene. Pandey (1986) gave an account of lithological control on morphometric parameters in the Lesser Himalaya.

Kalvoda (1972), Saxena (1980), Prasad and Verma (1980), Negi et al. (1982), Mehrotra and Bhandari (1988), Anbalagan et al. (1990), Anbalagan (1992a,1992b), Pachauri et al. (1992) studied the phenomena of landslides and slope stability in the Alaknanda river valley and other parts of Garhwal Kumaun Himalaya. Although so many studies have been carried out, not much efforts have been made to investigate in details the correlationship between geomorphic parameters and landslide.

1.8 SCOPE AND OBJECTIVES OF THE STUDY

A review of the previous work done by many workers clearly indicates that although many geological, structural, seismic, geomorphic and slope stability studies have been carried out by geoscientists since middle of nineteenth century, very little attention have been made to study geomorphometric parameters in a terrain in relation to slope instability. This therefore, left enough scope to take up such an investigation in the present study.

The basic objectives of the present investigations are to study and develop, if possible, geomorphological approach towards identification of probable zones of instability in relation to landslides of hill-slopes, of the area of study. Thus, the main thrust of this terrain study is on the following aspects.

i) Studies of geomorphic parameters in relation to instability of hillslopes and to establish their relative importance as instability indicator;

ii) To evaluate slope developments and their effect on type of movement and stability of slope;

iii) To identify and evaluate cause and type of landslide movements, along the road in the area of study and evaluate applicability of Slope Mass Rating (Romana,1985).

The result of these studies are given in the form of six chapters. Chapter 1 deals with the rationale and objectives of

study.

A brief description of the geology of the area is given in Chapter 2.

Chapter 3 deals with the terrain characteristics and spatial location of landslide areas in relation to slope, lithology, structure, elevation, vegetation etc. and multivariate aprroach to develop a geomorphic model for forecasting and assessing instability.

Chapter 4 deals with slope development and morphology in relation to slope instability and type of movement.

Chapter 5 deals with evaluation of slope movement along the road and stability analysis of selected sites by SMR technique and three dimensional slope analysis by computer program.

In chapter 6 all the results of this study are summarised along with concluding remarks.

CHAPTER - 2

GEOLOGY OF THE AREA

2.1 THE HIMALAYA

The Himalaya constitutes a prominent physiographic feature in south central part of Asia. They trend strike wise from Arunachal Pradesh in east to Kashmir in the west for about 2400 km with width ranging from 230 to 320 km. It represent the youngest mountain range in this region.

For over a century many workers have made geological investigations on Himalaya. Among the earliest workers the work done by Strachey (1851); Medlicott (1864); Oldham (1883) and Middlemiss (1885, 1887a and b, 1890) is noteworthy. During the first half of the twentieth century, the studies of Pilgrim and West (1928), Auden (1934, 1937), and Heim and Gansser (1939) have been of particular importance. An excellent account of the regional geology of the Himalaya is given by Gansser (1964), which still forms the base for any studies to be carried out. In the recent years the work done by Valdiya (1964, 1975, 1978, 1980a, 1980b); Saklani (1970, 1971); Pande (1974); Raina (1978); Kumar et al. (1979); Power (1980); Kumar (1981) and Jain (1987) are of immense value.

2.2 REGIONAL SUB-DIVISIONS OF HIMALAYA

The Himalaya has been cut transversely by a number of major rivers, like the Indus, Jhelam, Satluj, Alaknanda-Ganga, Kali, Tista and Brahmputra (Fig.2.1). The mountain ranges between Indus up to Jhelam river, Jhelam and Satluj river, Satluj and Alaknanda-Ganga and Alaknanda-Ganga to Kali river, Kali and Tista river, Tista and Brahmputra river are known as as Kashmir Himalaya, Himachal Himalaya, Garhwal HImalaya, Kumaun Himalaya, Nepal Himalaya and the Assam Himalaya respectively.

2.2.1 Lithotectonic Subdivisions

Longitudinally the Himalaya has been divided in to six zones on the basis of litho-tectonic characters as shown in Figure 2.2 (Schwan, 1981). These zones are briefly discussed below.

i) Sub-Himalaya

The late Tertiary Siwalik ranges form the southern hilly terrain of the Himalayas and are called as sub-Himalaya. These ranges are made up of molasse deposits. The deposits are folded and thrusted. The northern limit of sub-Himalaya is marked by Main Boundary Fault (Fig. 2.2), a set of multiple thrusts (Talukdar and Sudhakar, 1963; Acharya and Rao, 1981).

ii) Lesser Himalaya

This division is bounded in the south by the sub-HImalayas (with Main Boundary Fault in between), and in the north by Main Central Thrust. It comprises of dominantly the unfossiliferous sedimentary sequences and the low to high grade metamorphics

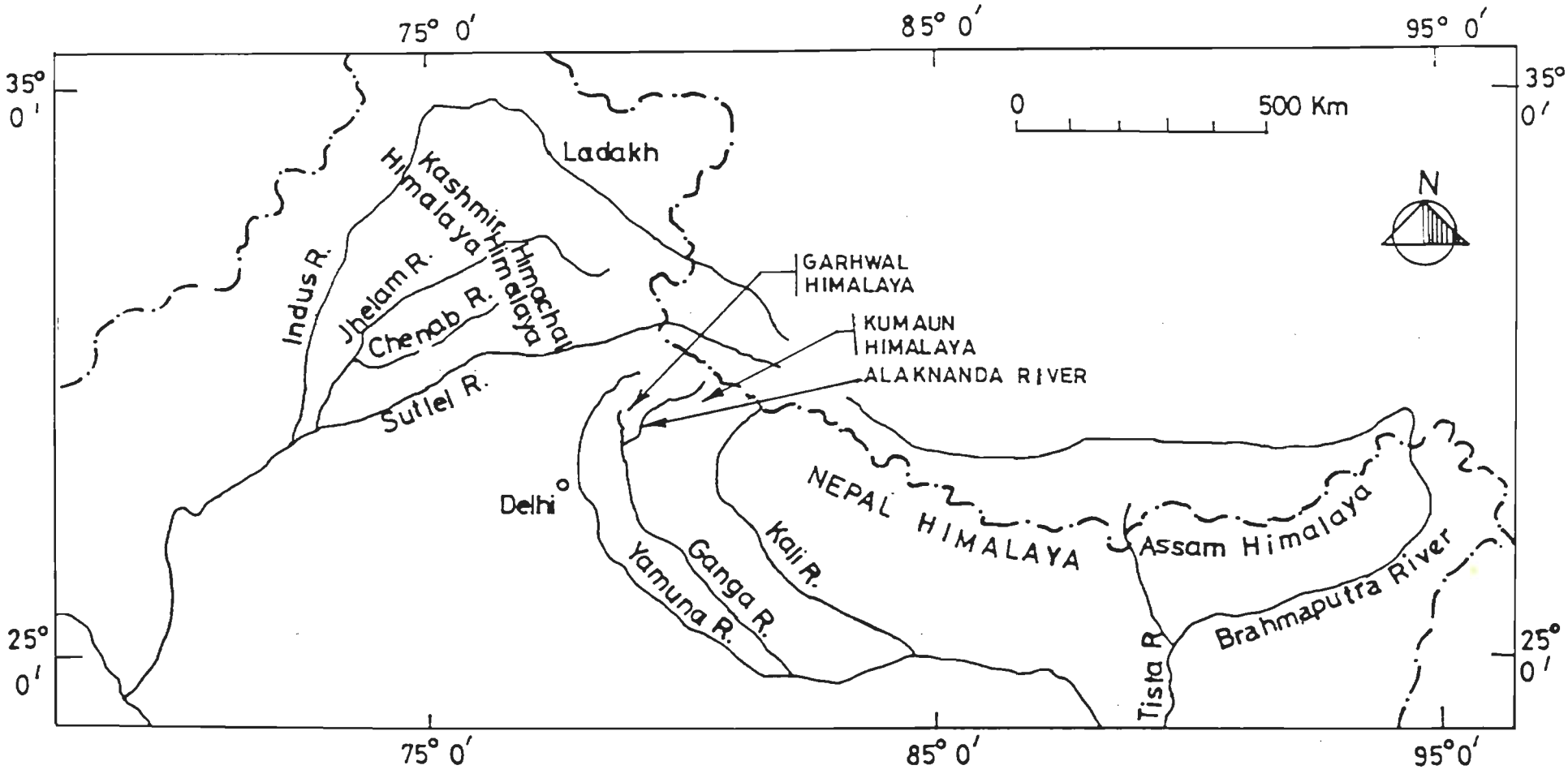

Fig. 2.1 : GEOGRAPHIC SUBDIVISIONS OF HIMALAYA (GANSSER, 1964)

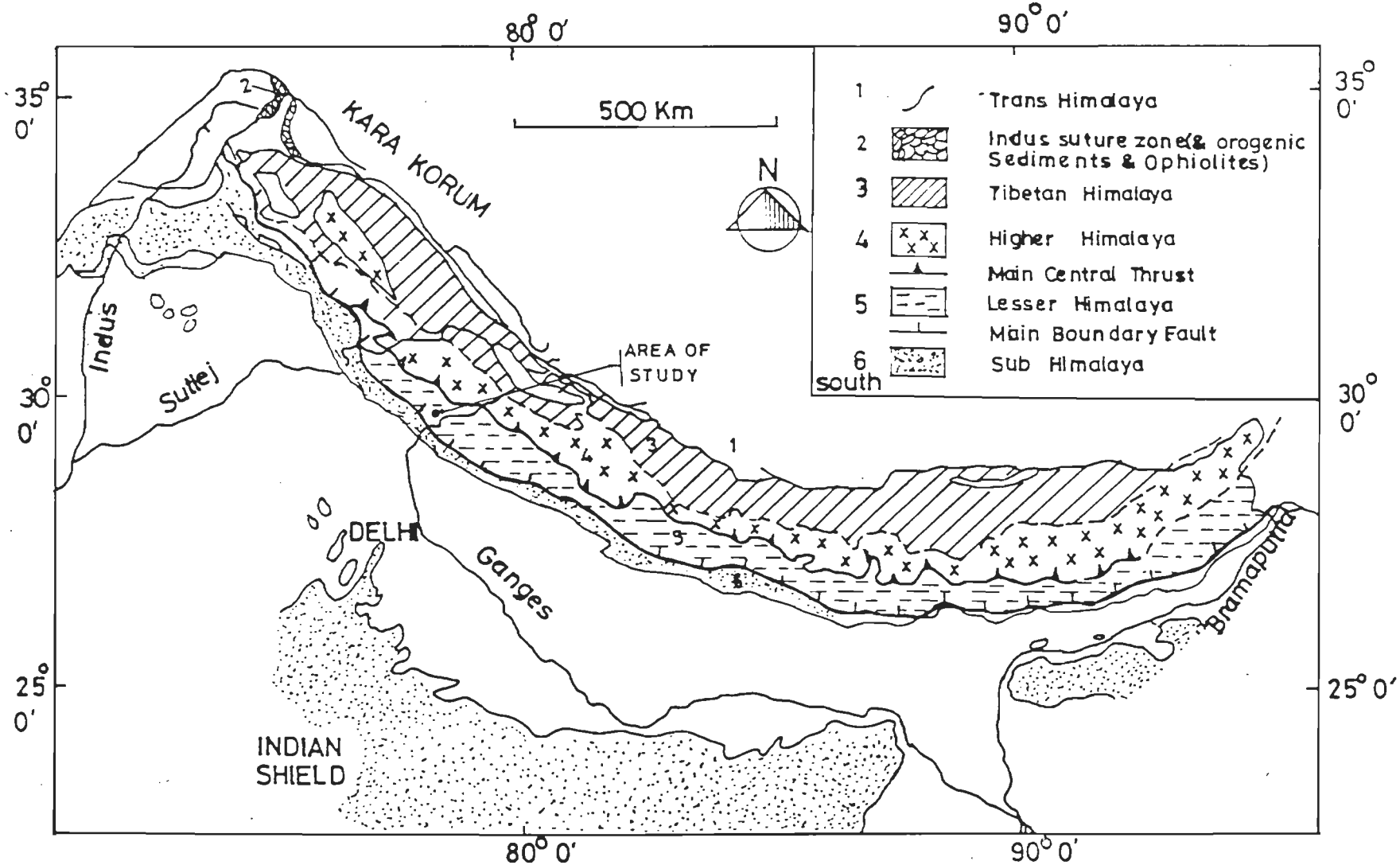

Fig.2.2: LITHO-TECTONIC ZONES OF THE HIMALAYA (AFTER SCHWAN, 1981)

ranging in age from Pre-cambrian to Eocene.

iii) Higher Himalaya

This forms the zone of greatest vertical uplift. Main Central Thrust marks the boundary between Lesser and Higher Himalaya. This part is characterised by low to high grade metamorphic rocks like schists, gneisses, granite and complex sequences of para-ortho-metamorphites with igneous intrusions of Precambrian to Tertiary age.

iv) Tibetan or Tethys Himalaya

Forming a broad thick belt of normal sequence of fossiliferous sediments, the Tibetan Himalaya lies north of the Higher Himalaya. The rocks of this part range in age from Palaeozoic to Mesozoic.

v) Indus-Tsangpo suture zone

North of the Tibetan Himalaya, lies a succession of geosynclinal deposits of Cretaceous to Paleogene time. The presence of Ophiolites in it suggest a subduction zone and collision of Indian plate from south to the Eurasian plate in the north, at the Indus Tsangpo suture zone.

vi) Trans - Himalaya

It forms the northernmost part of Himalaya and consists of a north ward thrust mass of Cretaceous flysch with basic and ultra basic exotics which rest on Paleogene molasses.

2.3 GEOLOGICAL FRAME WORK

For better appreciation of geology and tectonic set up of the area of study, it is useful to analyse synoptically the regional frame work of the area.

The area of present study lies entirely in the Lesser Himalaya lithotectonic zone of the so called Kumaun tectonic zone of Garhwal Himalaya. Tectonically the Garhwal Himalaya has been classified into two units by what is called as North Almora Thrust. (Kumar, 1981). The southern unit is known as Kumaun tectonic unit - and the northern as the Garhwal tectonic unit (Fig.2.3).

The Lesser Himalayan terrain of the Garhwal Himalaya have been broadly classified into three distinct sub-tectonic belts by Kumar et al.(1974) and Jain (1981). Jain (1987) describes them as follows.

i) Inner Lesser Himalaya

The region is made up of two tectonic units of the para-authochthonous, antiformally-folded quartzite, slate and limestone in the Dunda and Uttarkashi windows and the over thrust quartzite of the Uttarkashi Thrust sheet. The former is comprised of three Lithofacies: (i) a lower orthoquartzite slate sequence exposed only at places where carbonate sequence intervene, (ii) widespread argillo-calcareous intertonging sequence and (iii) and upper orthoquartzite - carbonate stable shelf sequence (Jain et al., 1971).

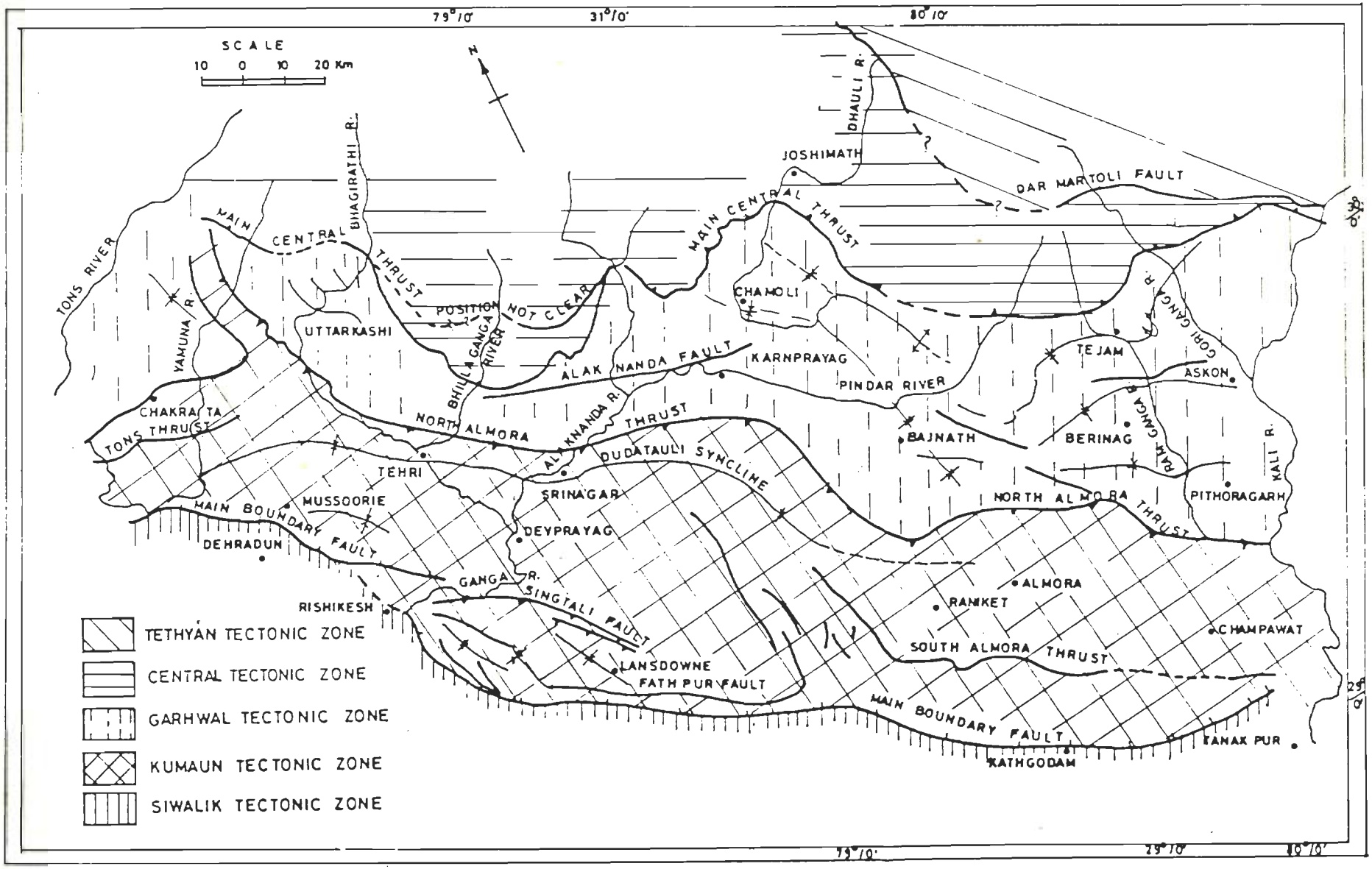

Fig.2.3:LITHO-TECTONIC DIVISIONS OF GARHWAL-KUMAUN HIMALAYA, UTTAR PRADESH SHOWING MAJOR TECTONIC FEATURES (AFTER KUMAR, 1981)

ii) Middle Lesser Himalaya

Predominantly argillo-calcareous meta-sediments in central parts of the Lesser Garhwal Himalaya belong to synformally-folded Simla-Dundatoli-Almora Thrust sheet. These are bound by southerly hading North Almora Thrust and the Tons Thrust. The former thrust has been named differently as the Srinagar Thrust between Rudraprayag and Srinagar, the Dharkot Thrust in the Jalkur valley, Tehri tear fault and the Dharasu Thrust along left bank of the Bhagirathi valley. The Simla-Dudatoli-Almora Thrust sheet is comprised of the following three main units with facies variation. The Mandhali-Deoban group carbonate in the north western part in the region of the Yamuna, Tons valleys, (ii) The Dharasu Group of meta-arenites, meta-pelites, schists and gnesises extending southeastward in the Kumaun Himalaya as the Almora Nappe.

iii) Outer Lesser Himalaya

The outer Lesser Himalaya comprising of two main thrust sheets is a para-autochthon of Late Precambrian Jaunsar Group sediments with unconformably overlying and synclinally folded Krol and Tal Groups in the lower Krol Thrust sheets. The upper Garhwal thrust sheet is comprised of the fossiliferous Permain Raitpur Formation, the metamorphics and Lansdowne Granite (Jain, 1981). The lower thrust sheet is bound by northeasterly-hading krol Thrust, while the upper sheet is delineated by Garhwal Thrust (Valdiya, 1976).

2.3.1 Stratigraphy of the Area of Study

Although a number of studies have been made by various workers such as Prakash et al. (1961); Rupke (1968); Saklani (1970, 1971, 1972a, 1972b); Kumar et al. (1974,1979); Gairola (1975); Thakur (1980); Kumar (1981); and Jain (1981, 1987) the stratigraphic correlation among various units and their structural relationships have been a subject of debate. However for present study the lithologic characteristics and local structural features of various rocks are more important than their stratigraphic position, as these characters would bear intrinsic relationship with various geomorphological features and surface process such as erosion, deposition and landslide etc. As such only descriptive aspects related to lithology and local structures are considered without going in to details of structural and stratigraphic correlation.

The study area is situated in northern part of Garhwal synform (Kumaun tectonic zone) in Outer Lesser HImalaya (Fig. 2.4) which had been studied by a number of workers like Medlicott (1864); Middlemiss (1885, 1887a,1887b); Auden (1937); Bassi (1968); Goswami (1977); Gaur (1978); Kumar et al. (1979); Kumar (1981) and Jain (1987). The stratigraphy of `Garhwal Synform' as worked out by Kumar and Dhaundiyal (1979) is given in Table 2.1, and forms the basis of the present studies.

Field investigations in the area almost fully corroborate the stratigraphic and geologic observations of Kumar and Dhaundiyal (1979) with little modification necessiated by two

thin outcrops of Manikot Shell Limestone of Upper Tal and Subathu formations (Figures 2.4, 2.5).

Table 2.1: Stratigraphy of `Garhwal Synform' Tehri District, **Uttar Pradesh (Modified after Kumar et al.,1979)**

Stratigraphic unit	**age**
River terraces and Dun Gravel	Pliestocene
Siwalik Group	Middle Miocene to Lr. Pleistocene
Subathu Formation	Eocene
-Unconformity-	
Manikot Shell Limestone -Up Cret. to Lr. Paleocene -Locally unconformable- Phulchatti Quartzite	Jurassic to Cretaceous
Tal* (Upper Tal Member)	
Lower Tal Member Upper Krol (C+D) Member Krol* Middle Krol (B) Member Lower Krol (A) Member	Permian to Triassic ?
Blaini*	Permocarboniferous ?
Binj	Middle to Upper Palaeozoic? (Lower Carboniferous?)
-Angular unconformity-	
Amri-Pauri Phyllite Member	
Lansdowne-Saknidhar Formations	Precambrian ?
Bijni Member	

* Age controversy

Blaini and Krol Formations - Cambrian to Late Precambrian (Azmi et al. 1981,1983). Precambrian (Prasad et al.1990)

Tal Formation - Lower Tal (Cambro-Ordovician, Azmi et al. 1981,1983). Tal (Cambrian, Prasad et al. 1990)

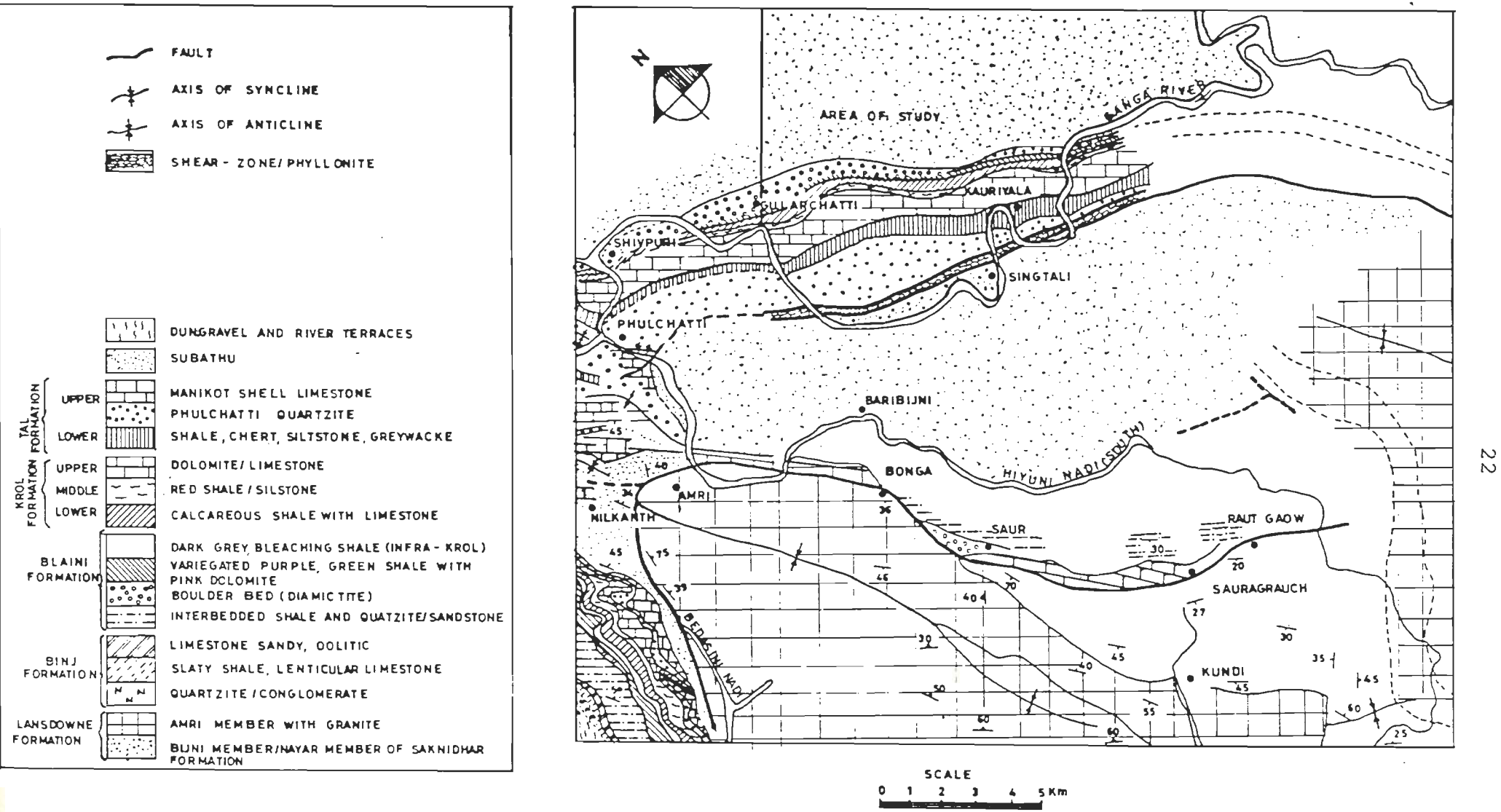

Fig.2.4: GEOLOGICAL MAP OF PART OF "GARHWAL SYNFROM" (AFTER KUMAR AND DHAUNDIYAL, 1979)

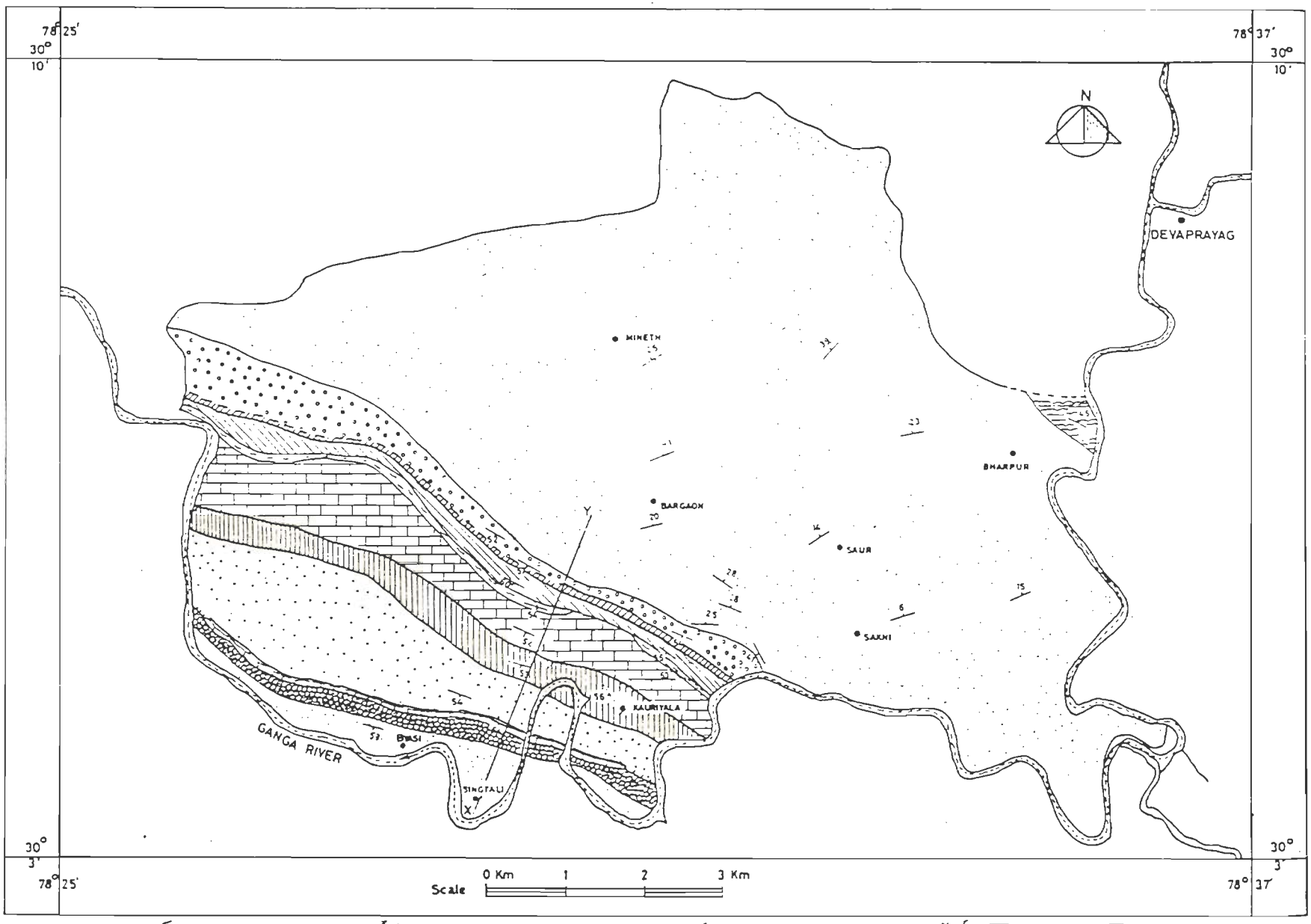

Fig. 2.5 GEOLOGICAL MAP OF THE AREA (MODIFIED AFTER KUMAR & DHAUNDIYAL, 1979)

In the following pages the various stratigraphic units are briefly described in terms of their lithology and structure.

i) Lansdowne Formation - It is divisible into two members, the Bijni and Amri (Dhaundiyal and Kumar, 1976). The Bijni member comprises purple, greenish grey, bluish grey, variegated purple white, white quartz granite with bands of shale and phyllite in upper part. The upper member Amri comprises phyllite and interbedded white to buff coloured flaggy quartzite and sericite-quartz schist. The rocks of Bijni member are characterised by four sets of joints, associated with many irregular fractures specially in south western part of the area, due to faulting which brings Subathu in Juxta-position with Bijni. In central part of the area the Bijni formation is also highly fractured and thinly bedded. In eastern side of the area they are of tabular form. Ripple marks, cross bedding and fan folding are observed in these rocks. The quartzite being hard and resistant rocks form steep topographic hills and peaks. The Amri Formation is exposed in extreme north-eastern side of the area.

ii) Blaini Formation - It consists mainly of greenish grey boulder bed with lenticular purple shale and Sandy greyish dolomite, variegated purple green shale and siltstone, greenish white quartzite and dark grey laminated shale. This formation is exposed along th road section near Saur village. The boulder bed is competent and well jointed. The upper units are incompetent and amenable to weathering. The upper most unit of this formation form a thin out-crop varying in width from 5 m to 20 m.

iii) Krol Formation - A thick sequence of dominantly limestone and dolomite overly conformably over the Blaini rocks, was named by Medlicott (1864) as the Krol series in Himachal Pradesh (Punjab Himalaya). The Krol is well developed in the area and comprises massive limestone and dolomite, red shale and siltstone, calcareous shale with limestone, which are sometimes poorly jointed. The Krol limestones and dolomites are generally competent and comparatively resistant rock types. However, at few places the limestone is weathered and displays elephant skin weathering.

iv) Tal Formation - It is well developed in the area and has been divided in to lower and upper member. The lower member comprises of dark green to black chert with intercalation of black shale with calcareous nodules, siltstone and greywacke.

The upper Tal consists of gritty to fine grained felspathic, white to purple and bluish grey quartzite and oolitic, sandy, current bedded grey Manikot Shell Limestone. Phulchatti Quartzite is exposed in south-western part of the area and due to its proximity to shear zone, like Bijni Quartzite, shows variable joint orientation and many irregular fractures. The rocks are, in general, competent. The siltstone of Lower Tal are highly competent rock and exhibit four well developed sets of Joints.

v) Subathu Formation - The name Subathu was first given to these rocks by Medlicott (1864) after township of Subathu, in Himachal

Pradesh (Punjab HImalaya). Subathu is the youngest lithostratigraphic unit (Eocene) of the Lesser Himalaya and lies unconformaly over Tal Formation. It consists of greenish grey splintery shale and greenish grey and red shales and ferruginous quartzite. It occurs as a narrow belt in the area. The rocks are highly incompetent and amenable to weathering.

2.3.2 Structure of the Area of Study

As mentioned earlier, the Lesser Himalaya is bounded by two tectonic boundary thrusts. The southern one is known as the Main Boundary Fault (MBF) and northern delimiting boundary is the Main Central Thrust (MCT) which separates it from Higher Himalaya. However, the Lesser Himalaya, on the basis of lithotectonic characters, is further divided into two zones, namely Kumaum and Garhwal tectonic zone (Kumar, 1981). The area of study lies in Kumaun tectonic zone which is seperated in the north from Garhwal tectonic zone by North Almora Thrust and from the Siwaliks (Middle Miocene) in the south by Main Boundary Fault.

The Bijni member of Lansdowne Formation (Precambrian) has angular unconformable contact with the overlying younger stratigraphy units. This member appears to have acted as antiformal base for deposition of Blaini, Krol, Tal and Subathu Formations (Fig. 2.6). The Blaini, Krol and Lower Tal Formations dip at angles varying from 42^{o} to 65^{o} toward SSW.

Between Phulchatti Quartzite and Manikot shell Limestone a unconformity exist. The contact of the Subathu Formation with

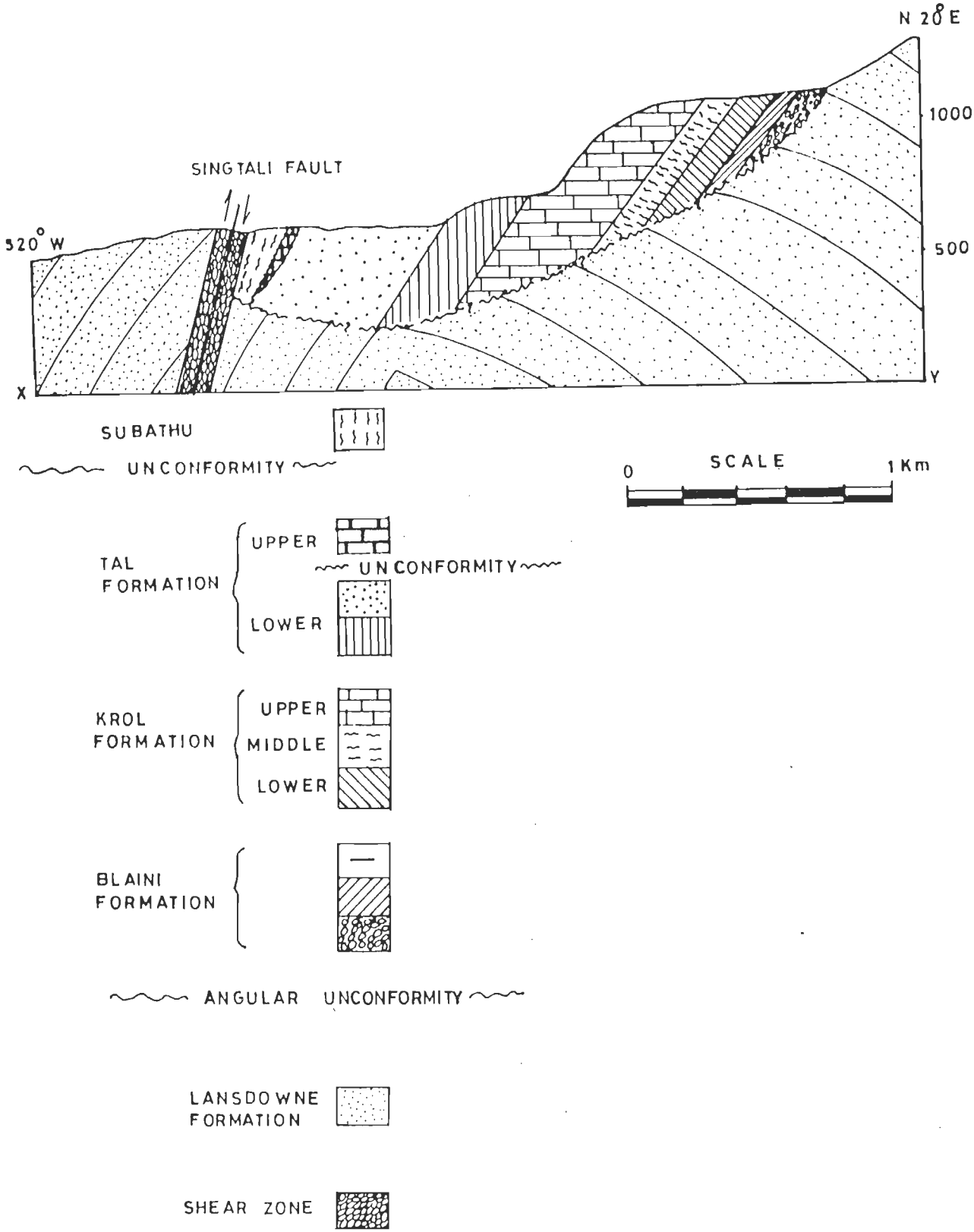

Fig. 2.6 : GEOLOGICAL CROSS SECTION ALONG THE LINE X Y ON GEOLOGICAL MAP (Fig. 2.5)

the underlying stratigraphic unit is a disconformity (Kumar, et al. 1979).

These sequence in the south are highly sheared and faulted. The fault is termed as Singtali Fault (Kumar et al. 1979) and the Garhwal Thrust by Auden (1937). It trends, in general WNW-ESE with steep southerly dip varying from 70 to 80^{o}. This reverse fault has brought the Bijni Quartzite of Lansdowne Formation (Precambrian) in juxtaposition with the younger Subathu Formation (Eocene).

Besides these major structures, the rocks have also been affected by a number of joints forming four major sets, the detailed study of which has been done seperately along with the slope stability analysis in Chapter 5.

2.4 SUMMARY

The Lesser Himalaya is bounded by two major tectonic boundaries. The southern limit of the Lesser Himalaya is formed by Main Boundary Fault (MBF) and northern delimiting boundary is Main Central Thrust(MCT) which separates it from Higher Himalaya. However, the Lesser Himalaya on the basis of lithotectonic characters is further divided in to two zones, namely Kumaun and Garhwal tectonic zone. The area of study lies in Kumaun tectonic zone of Garhwal Himalaya which is separated in the north from Garhwal tectonic zone by North Almora Thrust and from Siwalik in the south by Main boundary Fault.

The rocks exposed in the area form part of two major lithostratigraphic successions- The Bijni Quartzite(Lansdowne Formation) of the Precambrian Kumaun Super Group, and the younger succession of Blaini, Krol,Tal and Subathu Formations, consisting mainly of quartzite, limestone/dolomite, siltstone, slate and shale. The Bijni member of Lansdowne Formation has angular unconformable contact with the overlying younger stratigraphic units. This member appears to have acted as antiformal base for deposition of younger rocks. Between Phulchatti Quartzite and Manikot Shell Limestone of Upper Tal a uncoformity exists, and the contact of Subathu Formation with underlying rocks is marked by a disconformity. In the southwestern part of the area, Bijni Quartzite overlies the Subathu(Eocene) and this abnormal position is due to a major reverse fault known as Singtali Fault (Kumar et al., 1979) or Garhwal Thrust (Auden, 1937), which trends in general, W.N.W. -E.S.E. with steep southerly dip varying between 70^{o} to 80^{o}. These rocks in general have four sets of joints.

CHAPTER - 3

TERRAIN, LANDSLIDES AND MORPHOMETRY

3.1 INTRODUCTION

A terrain of an area is a part of earth which is characterised by a set of factors like topography, lithology (rock type and soil), structure of rocks, vegetation, climate and hydrological features. These factors, besides seismicity, control the stability of the terrain and its morphology. Their actions and interactions change continually the sculpture of the terrain. Constructive combination and interaction of these factors result in relatively stable lands which undergo very slow sculptural change. However, adverse interactions of these factors, in contrast, may cause relatively fast and sudden instabilities on the face of a land. If this is so, then, there may exist a pattern in the distribution of instability of land vis-a-vis these factors or the terrain attributes. Hence, with the changing face of the land, the morphology of the terrain can give clues to the possible areas of instability. With this premise, an attempt has been made in this chapter to investigate and decipher possible patterns of occurrence of areas of instability with respect to various terrain attributes. Besides this, an attempt has also been made to evaluate correlationships between

morphometric parameters and the area of instability found in this terrain.

3.2 TERRAIN

The terrain in the area is characterised by a typical rugged ridge and valley topography (Figs. 1.1, 3.1, 3.4). The area is bounded in the east, south and west by the river Ganga and in the north by a ridge (R_1). This ridge (R_1) trends roughly east-west with swings towards N-S and NW-SE directions. The minimum and maximum altitude of this ridge is 500 to 2276 m. Besides this northern ridge, there are five more ridges designated as R_2, R_3, R_4, R_5 and R_6. The ridges R_3, R_4, R_5 and R_6 run sub parallel to each other with substantial variation in attitude. The ridge R_2 stretches for about 1 km from north to south and then turns towards NW-SE and swings in E-W, NE-SW and again E-W directions for about 3.15, 1.17, 0.65 and 0.54 km respectively. The R_3 (ridge) trends in NE-SW direction for about 4 km and then bifurcates towards SE (2 km) and NW (1.62 km) directions. The R_4 ridge which is situated in the central part of the area has a N-S direction for about 3 km and changes its trend approximately 3.4 km in SE direction. The R_5 ridge on the eastern part of the area is the longest among ridges (R_2, R_3, R_4 and R_6). It stretches in NW-SE direction for about 6 km and then bifurcates at altitude of 1700 m and 1600 m. The major bifurcation (length-wise) is at 1600 m altitude and bifurcated ridges stretch in NE-SW and NW-SE directions for about 6 km respectively. There is a substantial

difference of altitude along this ridge which ranges from 400 to 2078 m. The R_6 ridge trends in general in NW-SE direction for about 3.78 km. The maximum elevation of this ridge is 2064 m. Field observations indicated that valleys have small flood plains and relatively steep walls.

3.2.1 Elevation

The terrains shows high topographic relief. The elevation in this terrain varies from more than 2200 m to less than 400 m.

Since there is a substantial difference in the altitude in this terrain, it is interesting to study the elevation distribution in the area. A topographic contour map with 100 m interval was prepared and the area falling between elevation contours of 100 m interval was measured using planimeter. The elevationwise areas thus determined are presented in the Table 3.1.

A scrutiny of Fig. 3.1 reveals that the maximum elevation to the western part of the R_5 ridge, which constitutes more than 2/3 of the area is 1500 m and in general 1300 m. A perusal of Table 3.1 indicates that 88% of the terrain has elevation between 400 to 1500 m. Nearly 38% of the area has elevation less than 900 m and approximately 50% of the area has elevation between 900 to 1500 m of which about 30% falls within 1000 to 1300 m. Approximately about 1% of the terrain has elevation above 1900 m.

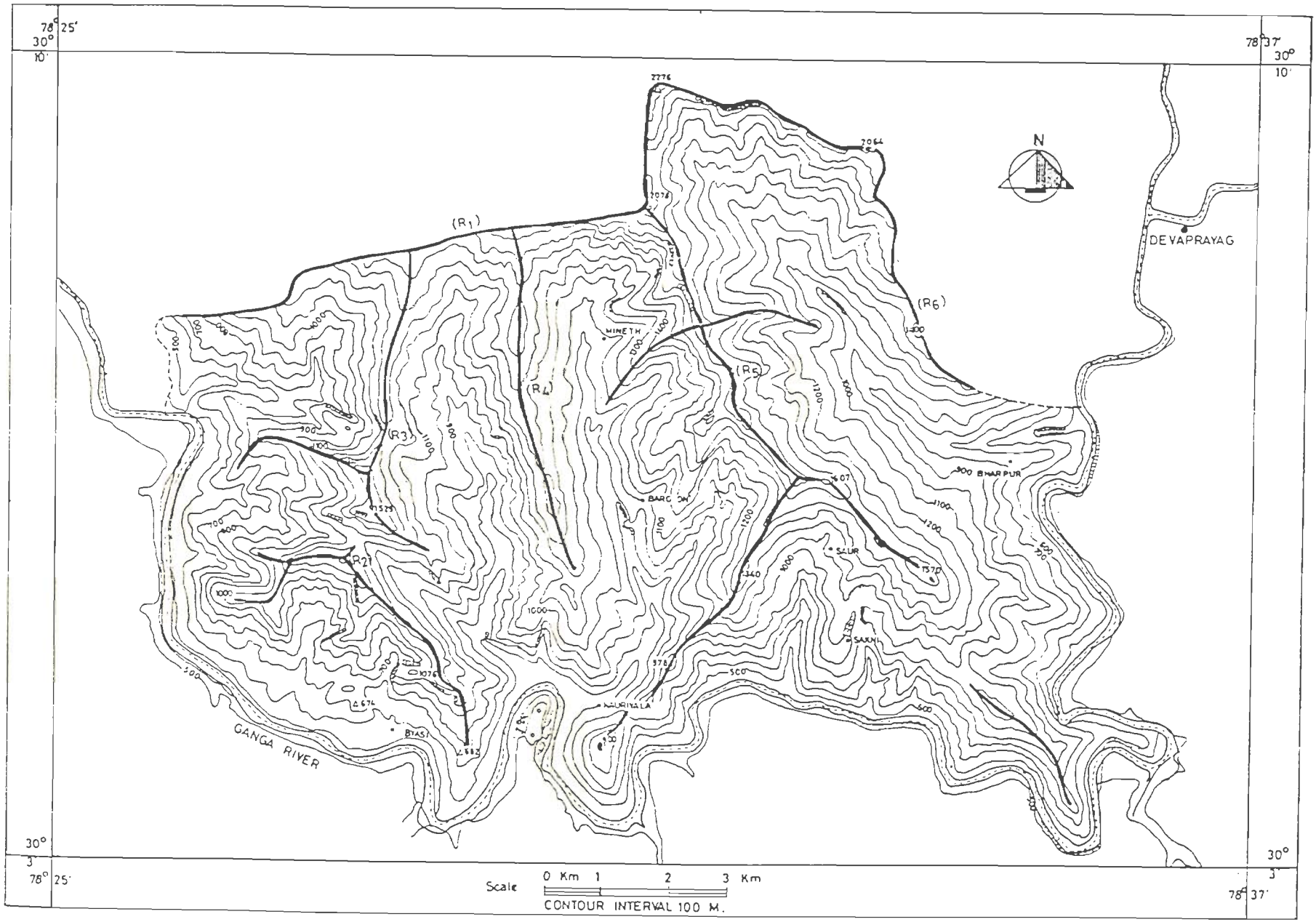

Fig. 3.1: CONTOUR MAP OF THE AREA BASED ON TOPOSHEET NO. 53 J/8 53 J/12

Table 3.1 : Elevation Distribution in the Area

Total area = 102.42 sq.km

Elevation interval (above M.S.L.) (m)	Area of each contour interval	Percentage (out of total area)	Cumulative percentage
400-500	6.02	5.88	5.88
500-600	7.15	6.98	12.86
600-700	6.27	6.12	18.98
700-800	9.60	9.37	28.35
800-900	9.65	9.42	37.77
900-1000	10.36	10.11	47.88
1000-1100	10.40	10.15	58.03
1100-1200	9.48	9.26	67.29
1200-1300	8.24	8.04	75.33
1300-1400	7.18	7.01	82.34
1400-1500	6.09	5.95	88.29
1500-1600	4.08	3.98	92.27
1600-1700	3.02	2.95	95.22
1700-1800	2.05	2.00	97.22
1800-1900	1.24	1.21	98.43
1900-2000	0.99	0.97	99.40
2000-2100	0.37	0.37	99.77
2100-2200	0.23	0.23	100.00

3.2.2 Slope Classification Map

A Terrain can be classified on the basis of several factors such as relief, slope, height, vegetation index, landform etc. In this section, an attempt has been made to classify this terrain on the basis of slope variation. Slope is a major and important factor which forms the foundation of landform generating processes. Since the Himalayas are young and are still active, the rate of erosion is highest in these mountains. Therefore, it is interesting to study the differences in slope distribution in a terrain and their relation with landslide. Similar investigations have been done by Young (1961), Selby (1982), Crozier (1984, 1986) in other parts of world. Terrain classification map (slope distribution) of the area was prepared following the technique described by Pachauri (1970), Pachauri and Krishna (1984). The technique draws its support from experiences in classification by CSIRO Australia and Oxford Mexe groups (Olier, 1977).

The basic smallest unit mapped is the facet which is considered to be consisting of one or more elements and is still reasonably homogeneous. In the present study the facets are the various slope categories. Thus the proposed classification system needs the determination of various slope categories facets which was done with the help of topographic maps of the area (Fig. 3.2). The various facet categories recognized in this way are shown in Table 3.2.

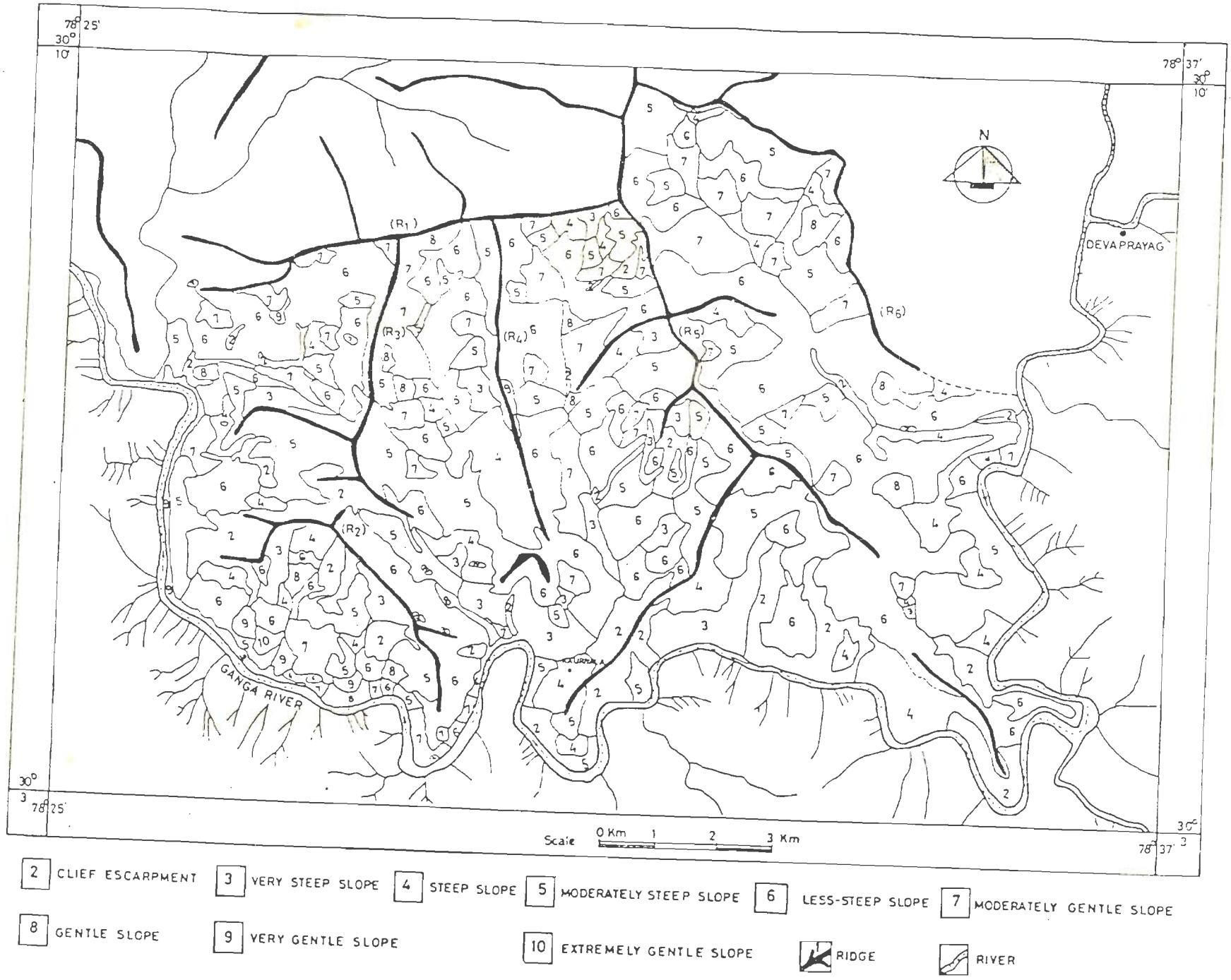

Fig. 3.2: SLOPE CLASSIFICATION MAP OF THE AREA

Table 3.2 : The Facets of the Area

Facet No.	Name of the facet	Slope	Number of contours in one centimeter (contour interval 20 m)
I	Ridge top	-	-
II	Cliff/Escarpment	>45°	>25
III	Very steep slope	40-45°	21-25
IV	Steep slope	35-40°	17.6-21
V	Moderately steep slope	30-35°	14.5-17.6
VI	Less steep slope	25-30°	11.5-14.5
VII	Moderately gentle slope	20-25°	9-11.5
VIII	Gentle slope	15-20°	6.6-9
IX	Very gentle slope	10-15°	4.4-6.6
X	Extremely gentle slope	5-10°	2.18-4.4

The area of each facet was calculated using planimeter and tracing graph paper. The areas of various facets calculated are presented in Table 3.3.

A careful observation of Table 3.3 and Figure 3.2 clearly indicates that the slopes are steep near the ridges and in general highly variable. The hill face having slope angle more than 25° constitutes 86% of the area. Approximately 76% of the hill face is occupied with slope angle varying between 25 to 40°. Slope angle less than 25° constitute 14% of the total area of

which 1% has slope angle between 5 to 15°. The area covered by ridge top is about 3% of the total area. This suggests that the area has high gradient and appears to be in young stage, in other words natural processes like weathering and erosion are active, and th area is undergoing changes depending on prevailing conditions.

Table 3.3 : Slope Facet Distribution in the Area

Total area = 102.42 sq.km

Slope facet	Area (km^2)	Area percentage	Cumulative percentage area
I	2.20	2.15	2.15
II	10.83	10.57	12.72
III	5.60	5.47	18.19
IV	18.07	17.64	35.83
V	22.72	22.18	58.01
VI	28.53	27.86	85.87
VII	9.95	9.72	95.59
VIII	3.31	3.23	98.82
IX	0.84	0.82	99.64
X	0.37	0.36	100.00

3.2.3 Vegetation Cover

With expanding industrialization and civilization, landuse pattern has been changing fast. These activities when carried out in unscientific manner have a great impact on the mountain

ecosystem (Nunnally and Witmer, 1970; Ryabchikov, 1975). In this context hill areas are highly vulnerable because of their topography and sensivity to the natural environment. The foremost after effects are instability of slopes and soil erosion. Thus, there is a great need to study landuse pattern (Selby, 1976).

Rau (1974) has reported that in the western Himalayan ranges, the Lesser HImalayan slopes and in the area of study, slopes up to 1200 m are predominantly forested with Shorea robusta associated with Tectona grandis, Dilbergia sisson etc. The Pinus roxburghii form excellent forests at altitutude above 1200 m upto 1800 m. These pine forests occur in association with Quercus incana and Rhododendron aboreum. The Oak-rododendron forest are developed at altitudes above 1800 m, associated with Lyonia ovalitolia. These forests are densely populated and rich in epiphytes, especially a large variety of orchids, ferns and aroids.

The landuse mapping of the area was carried out using black and white aerial photographs (scale ≈ 1:55,000). The identification of different landuse categories is based upon photo-recognition elements (Table 3.4), supported by selected ground checks (Fig. 3.3). Broadly four landuse categories were identified viz., i) forest land ii) sparsely vegetative land iii) Agricultural land, and iv) Barren land. The forest category was further divided into sub-categories as very dense, dense and modrately dense vegetated lands for better appreciation of the

Table 3.4 : Interpretation Key for Land use types on aerial Photographs

PHOTOGRAPHS (Scale =1:55,000 Approx.)

SL. NO. (1)	LAND USE CATEGORY (2)	SUB-CATEGORY (3)	TONE (4)	TEXTURE (5)	PATTERN (6)	REMARKS (7)
1.	Forest	Very dense	Dark grey	Fine	No definite Pattern irregular and often with sharp bounderies	Dark tone due to thick canopy cover of trees.
		Dense	Medium grey	Medium	No definite pattern irregular and often with sharp boundaries	Medium tone due to comparatively land canopy cover.
		Moderately dense	Grey to light grey mix	Coarse	No definite pattern, irregular boundaries sometimes sharp.	Light tone is due to the exposed land surface because of less canopy cover.
2.	Sparse Vegetation	Grazing field Shrubs and Grass land	Light grey to very light	Coarse	Scattered,no definite pattern	Coarse texture is due to the scattered trees and shrubs.
			Light grey/ grey	Very fine	Scattered, no definite pattern sometimes pattern boundary.	Fine texture and grey tone is due to uniform distribution of thick grasses.
3.	Agricultural land	Agricultural land	Light grey/ white	Fine	Terraced fields with sharp boundaries	Hill slopes and terraces are modified into thin linear steps. Grey tone when crop is there,while white tone when they lack crops.

Contd.. Table 3.4

SL. NO. (1)	LAND USE CATEGORY (2)	SUB-CATEGORY (3)	TONE (4)	TEXTURE (5)	PATTERN (6)	REMARKS (7)
4.	Barren land	Expooed rock surfaces	White (bright)	Fine	Scattered no definite pattern	White tone is due to exposed rock surfaces or dry soil cover on surfaces.
		Sands	Light grey/ white	Fine	Generally found linearly along the river.	Grey tone when it is saturated with water and white when sand is dry or without moisture.
5.	Water body	Drainage	Grey/Dark grey	Fine	Linear water body straight and sinuous pattern	Grey when drainage is laden with silted dark grey when the water is deep and clean

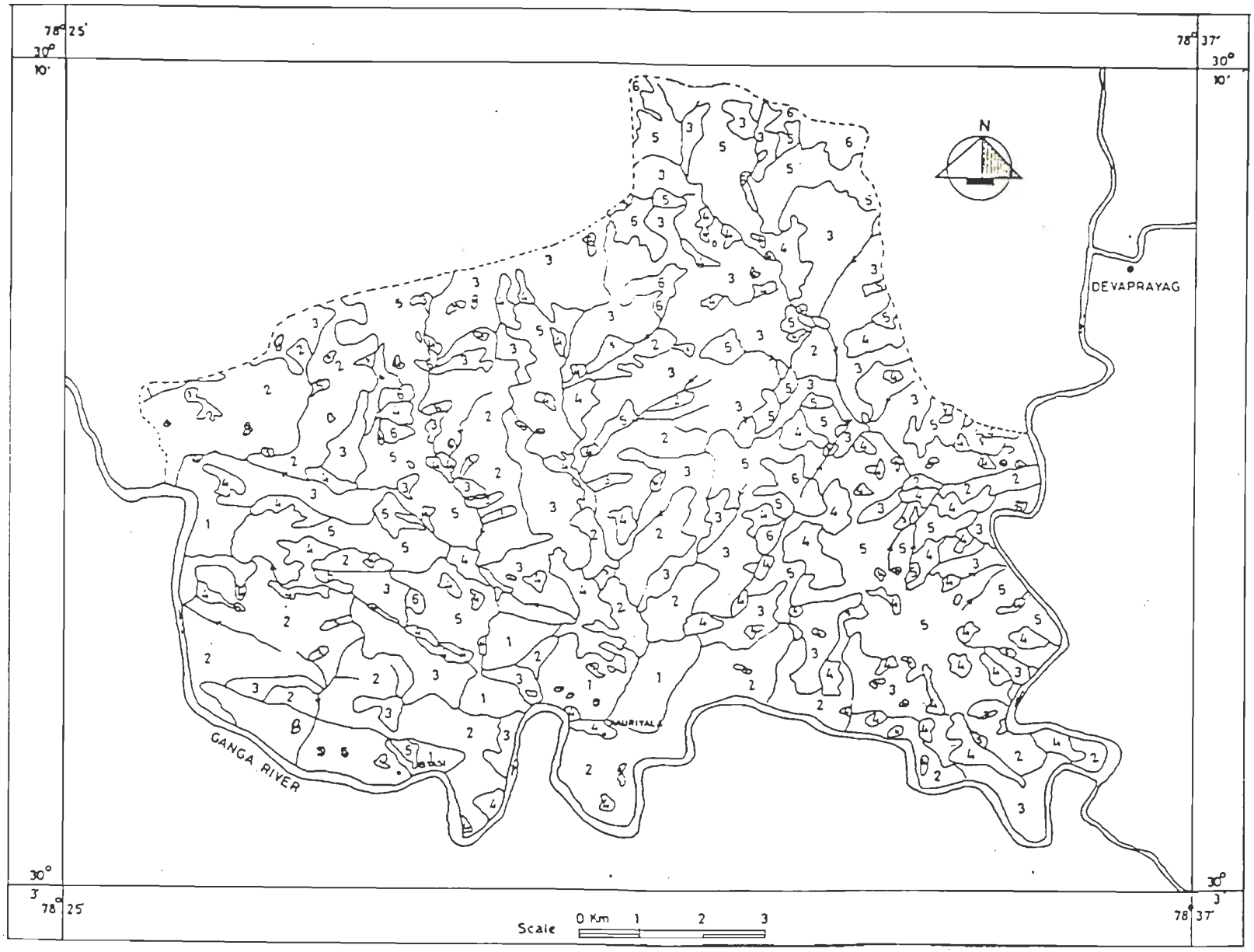

Fig. 3·3: LANDUSE MAP (VEGETATION COVER) OF THE AREA

influence of vegetation cover on the hillslope instability in the area. The area of each category was measured using planimeter and tracing graph paper. The area of various categories are presented in Table 3.5.

Table 3.5 : Landuse Class Distribution in the Area

Total area - 102.42 sq.km

Landuse class	Vegetation cover	Area (sq.km)	Area percentage	Cumulative percentage area
I	Very Dense	7.07	6.90	6.90
II	Dense	27.21	26.57	33.47
III	Mod. Dense	30.62	29.91	63.37
IV	Agriculture	11.24	10.97	74.34
V	Sparse	22.53	22.00	96.34
VI	Barren	3.75	3.66	100.00

Observations from Table 3.5 indicate that nearly 7% of the area is characterised by very dense forest. The vegetation cover for categories of dense and moderately dense is 26% and 30% respectively, implying thereby, that the total forest cover in the area is nearly 63%. Approximately 37% of the area is characterised by sparse agricultural and barren land, of which 22% of hill face is occupied by sparse vegetation. The agricultural land constitutes about 11% of the area and only about 3% of the area is barren. It may be note-worthy to mention that the vegetation cover at higher altitude relatively decreases

(Figures 3.1 and 3.3), specially along the ridges where it ranges from moderately dense and in general sparse. On the other hand, low altitude areas are characterised in general with very dense to dense vegetation cover. Field observations also revealed that with increase of elevation the growth of secondary vegetation decreases.

3.2.4 Lithological and Structural Character

It has long been observed that the lithological character has intrinsic influence on extent of slope stability in an area (Stimpson, 1976). Due to peculiar topography and high variation of slope angle in the area of study, the impact of lithological characters on slope movements are more pronounced. Therefore, a study of rock distribution in terms of their lithological characters was attemped in this area.

The geological map of the area was prepared, using the geological map of Kumar and Dhaundiyal (1979) as base map, coupled with field observations. As mentioned earlier on the basis of these field investigations, the base map was modified (Fig. 2.5). The areas of various outcrops measured using planimeter are presented in the Table 3.6.

A general overview and synoptic evaluation can also bring out the lithological distribution in the area. Table 3.6 suggests that the oldest stratigraphic unit i.e. the Lansdowne Formation consisting mainly of quartzite with some phyllite, constitutes 71% of the area, of which less than 0.5% and about 70% belong to its Amri Member (Phyllitic) and Bijni Member

(dominantly quartzitic) respectively. The Blaini Formation which consists of dark grey laminated shale, variegated purple green shale and boulder bed occupy about 5% of the region. The Krol Formation forms about 10% of the total area of study. It mainly consists of limestone/dolomite, calcareous shale with limestone, red shale and siltstone. The Tal Formation composed of slate, shale, chert, siltstone, quartzite, shell limestone in its Upper and Lower Members constitutes about 12% of the rock type in the area, of which the Upper Member mainly quartzite covers about 9% of the terrain. The Subathu Formation consisting dominantly of splintery green shale, forms less than 1% of the total area. Table 3.6 indicates that quartzite forms approximately 80% of the total area of study.

Table 3.6: Areas Occupied by Various Stratigraphic Units
Total area - 102.42 sq.km

Stratigraphic Units		Area (km^2)	Area percentage	Cumulative percentage area
Formation	Member			
Subathu		0.71	0.69	0.69
Tal	Upper	9.12	8.90	9.59
	Lower	4.01	3.92	13.51
Krol	Upper	7.47	7.29	20.80
	Middle	0.98	0.96	21.76
	Lower	2.22	2.17	23.93
Blaini		5.26	5.14	29.07
Lansdowne	Amri	0.49	0.48	29.55
	Bijni	72.16	70.45	100.00

The Bijni Member of Landsdowne Formation acts as antiformal base for deposition of younger strata. These rocks in general have four sets of joints dipping in NE, SSW, ESE and NW directions. The area is also characterised by a major reverse fault which trends in general WNW-ESE with steep southerly dips varying between 70 to 80° (Kumar and Dhaundiyal, 1979). A detailed account of lithology and structure has already been discussed in Chapter 2.

3.3 IDENTIFICATION TECHNIQUES OF LANDSLIDES

The instability of slopes in mountain range is one of hte major hazards witnessed specially during the rainy season. Landslides are the major causes of instability in the area of study. The implications of landslides are manifold. Among the direct and foremost effects to man kind are loss of life, damage to developmental projects like road, dams, communication lines bridges etc. Therefore, it is important to know the severity of landslide in an area.

The techniques used for identification and damarcation of landslides are:

i) Remote sensing Technique

ii) Map Technique

iii) Field Investigation

3.3.1 Remote Sensing Technique

The aerial photographic studies have proved to be very effective in recognizing and determining the areas of landslide.

No other technique can provide a three-dimensional overview of the terrain from which land instability can be easily identified. Therefore, in the present investigations the available black and white aerial photographs, taken in Oct. 1973 of the scale of 1 ≈ 55,000 have been used for preparation of landslide map. The features by which landslides can be identified are mentioned below.

3.3.1.1 Diagnostic Features of Landslides on Aerial Photographs

On the basis of distinct tonal, textural contrast on the aerial photographs, the following discernible features on aerial photographs are found to be typical of landslides or landslide susceptible terrains (Belchers, 1960; Rib and Liang, 1978). These features which may not be very evident for each slides are listed below

i) Land masses under cut by streams;

ii) Steep slopes having large masses of loose soil and rock;

iii) Sharp line of break at the scarp (head end) or presence of tension crack or both;

iv) Hummocky surface of sliding mass below the scarp;

v) Unnatural topography such as spoon shaped trough in the terrain;

vi) Seepage zone;

vii) Elongated undrained depressions in the area;

viii) Closely spaced drainage channels;

ix) Accumulation of debris in drainage channels or valleys;

x) Appearance of light tones where vegetation and drainage have

not been restablished;

xi) Distinctive change in photograph tones from lighter to darker, the darker tones indicating higher moisture content;

xii) Distinctive change in vegetation indicative of changes in moisture;

xiii) Relatively lighter tone on the slided area than the adjoining stable area; and

xiv) Relatively uneven top surface of the agricultural fields (if the fields are developed over the slide mass).

3.3.2 Map Technique

The acquisition and analysis of the various types of maps constitute one of the first steps in landslide investigation. The nature and quality of the informations related to the presence of landslides or potential areas for landslides that can be derived from the existing maps, depend on the purpose, type, scale and details used in preparing the map. From most of the maps only a general indication of landslide susceptibility can be derived. Maps have certain inherent advantage for landslide studies. They are prepared at a uniform scale and, therefore, are subject to direct measurement. Further planimetric information is often included, thereby minimizing uncertainities in superimposing other informations. The disadvantage is that they are outdated as soon as they are published. Unless the maps are updated periodically or no changes occur, the maps will not show the most recent terrain features.

Major landslide areas that are closely evident are sometimes labelled on topographic maps. On some maps the boundaries of landslide and arrows pointing towards the direction of movement are also shown.

3.3.2.1 Diagnostic Features of Landslide on Topographic Map

Small slides, the type most commonly encountered along the road and other engineering works are not usually labelled on such maps. Indication of these smaller slide or unlabelled larger slides can be accomplished by noting certain features on the topographic maps. In the present investigations the following features on topographic maps of the area in the scale 1:50,000, helped in identifying landslide areas

i) Topographic expression observed, for example, steep slope (closely spaced contour) at the head of slide;

ii) Hummocky topography in slide mass (irregular unsymmetrical contour pattern with shallow depression;

iii) Wavy contour lines; and

iv) Minor movements or irregularities at "vulnerable location" i.e. steep slopes, cliffs, banks under cut by streams and areas of drainage concentration.

3.3.3 Field Investigation

Field investigations were carried- out in some selected sections with two objectives i) to check and confirm the interpretations made on the basis of aerial photographs and the

topographic maps, and ii) to obtain the information of questionable areas and to demarcate small landslide areas. The observations made in the field helped in the preparation of landslide map of the area.

3.3.4 Landslide Map of the Area

To carryout the landslide mapping from aerial photographs, first the uncontrolled mosaics of the aerial photographs in a strip were prepared for an overall view of the area. Likewise indications of possible landslides on topographic maps were also noted. This was followed by a detailed stereoscopic study or aerial photographs. The informations from aerial photo-study and field investigations were transferred on to the survey of India toposheet maps using ground points.

Based on the above techniques for landslide detection and field observation, a landslide distribution map of the area has been prepared (Fig. 3.4). Measurement of landslide areas indicated that sum total of 13.42 sq.km of the area has been affected by it.

3.4 DISTRIBUTION OF LANDSLIDES IN THE TERRAIN

Landslides are intimately linked with terrain attributes such as topographic elevation, slope, vegetation cover, lithology and structure etc. (Joshi, 1987; Zimmerman et al, 1986; Choubey and Litoria, 1990; Anabalagan, 1992a, 1992b). Therefore, an attempt has been made to know the distribution of landslides and their possible link with the above mentioned parameters in the

246562

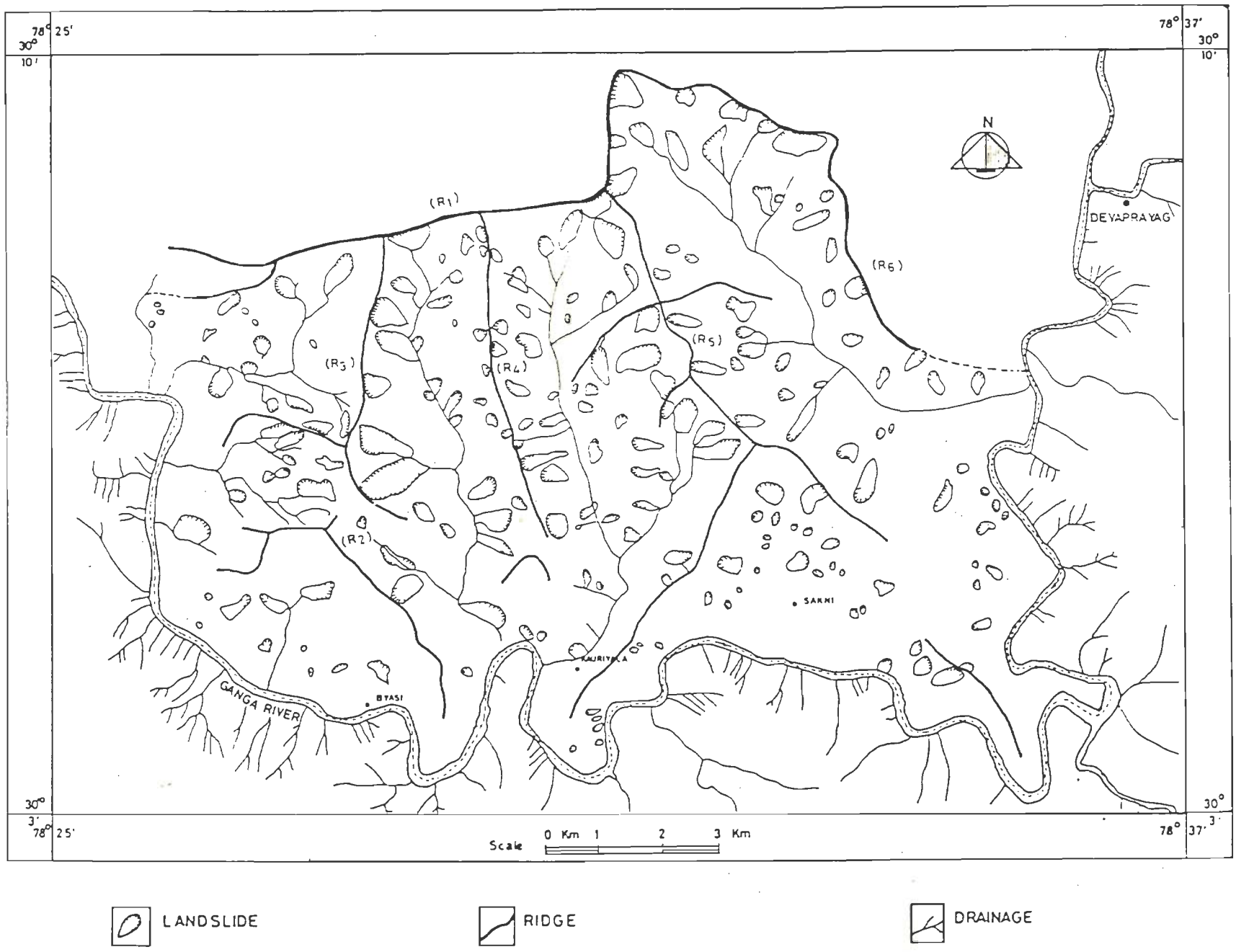

Fig. 3.4: MAP SHOWING LANDSLIDE AREAS IN THE TERRAIN
(based on aerial photographs & field survey)

area.

3.4.1 Landslide Distribution in Relation to Topographic Elevation

A general view and synoptic elevation of landslide map (Fig. 3.4) of the area brings out the relationship of landslide activity with the topographic elevation. It is seen that, in general, landslide density is high close to the ridges. For better appreciation of mutual relation of topographic elevation with landslide activity, contour map of the area prepared from toposheets (Fig. 3.1) was superimposed on landslide map. The percent landslide affected area (out of total landslide affected area) at each contour interval was measured. The data thus worked out are summerised in Table 3.7 and presented in Figure 3.5.

A perusal of Table 3.7 and Figure 3.5 indicates that landslide activity is found to occur at any elevation but it is not uniformly distributed. It indicates that, in general, with increase in elevation, the landslide affected area tends to increase. Nevertheless the landslide area distribution in Figure 3.5 shows four modes (peaks). As evident the primary mode indicates that the maximum percent landslide area is found at elevations above 1800 m. Such regions are of very small aerial extent (only about 1.5% of the total area of the terrain). They are found on hillslopes close to the ridges (Figs. 3.1, 3.4 and Table 3.1). These landslide prone areas are poor or devoid of vegetation.

Table 3.7: Landslide Area Distribution at Different Elevation

Total area - 102.42 sq.km

Total landslide area - 13.42 sq.km

Elevation Interval (above MSL) (m)	Landslide area at each elevation (km^2)	Area of each elevation	Landslide area per unit area in percent
400 - 500	0.03	6.02	0.50
500 - 600	0.79	7.15	11.05
600 - 700	0.40	6.27	6.38
700 - 800	0.77	9.60	8.02
800 - 900	0.93	9.65	9.64
900 - 1000	1.23	10.36	11.87
1000 - 1100	1.14	10.40	10.96
1100 - 1200	1.85	9.48	19.51
1200 - 1300	1.79	8.24	21.72
1300 - 1400	1.12	7.18	15.54
1400 - 1500	0.95	6.09	15.60
1500 - 1600	0.81	4.08	19.85
1600 - 1700	0.41	3.02	13.58
1700 - 1800	0.19	2.05	9.27
1800 - 1900	0.34	1.24	27.74
1900 - 2000	0.38	0.99	38.38
2000 - 2100	0.18	0.37	48.65
2100 - 2200	0.11	0.23	47.83

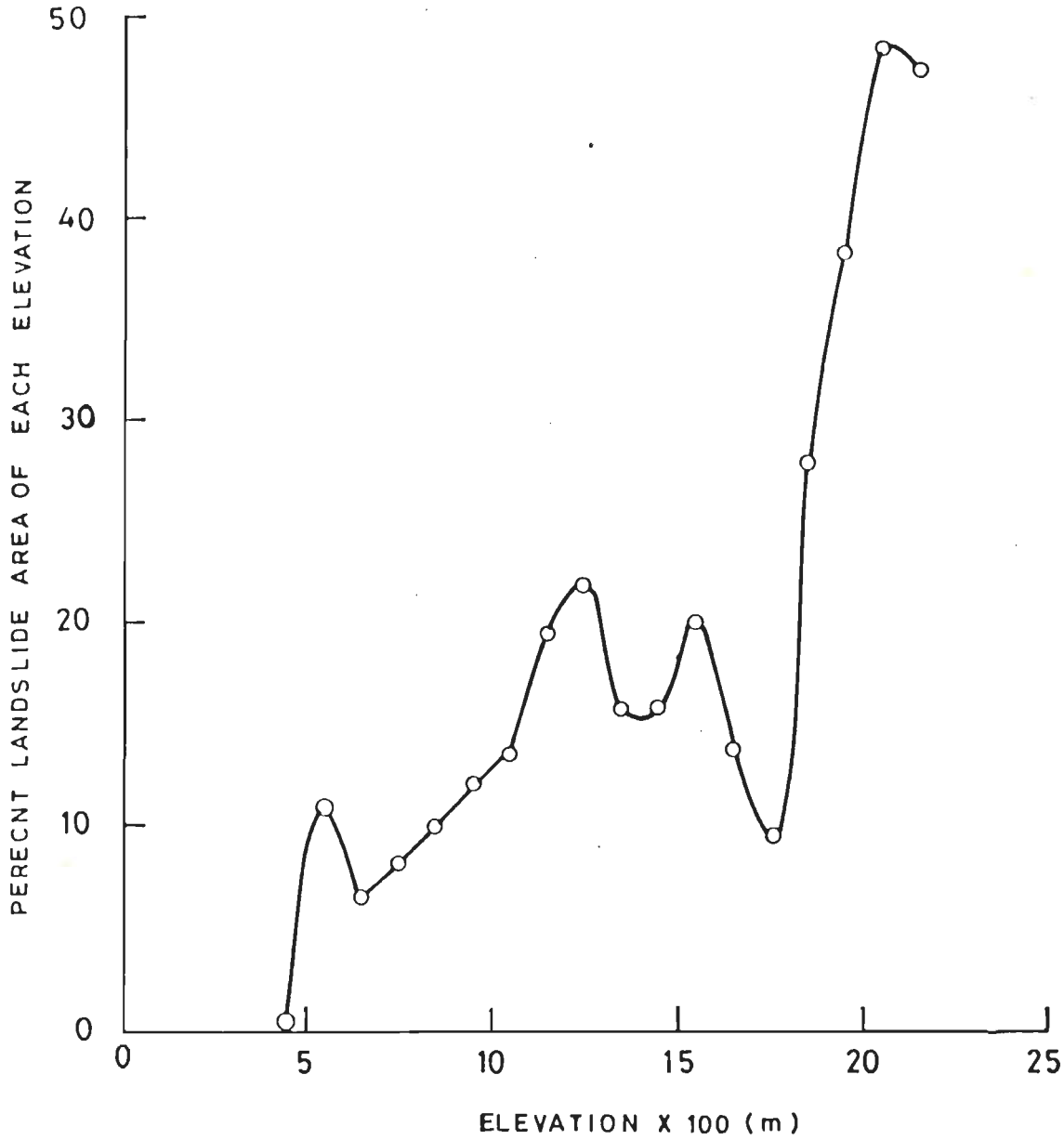

Fig. 3.5: DISTRIBUTION OF LANDSLIDE AREA WITH ELEVATION

It is also observed that the second, third and fourth modes related to landslide areas are found at elevation ranges of 1100 - 1300 m, 1500 - 1600 m and 500 - 600 m with aerial extents of about 17, 4 and 7 percent of the total terrain. It is seen from Figure 3.1 that areas to the west of ridge R_5 have maximum elevation of 1500 m in form of hill peaks. The rainfall pattern during monsoon in this area indicates that the amount of precipitation is more in the western part as compared to the eastern side of this ridge which acts as a physiographic barrier to the easterly moving monsoon laden clouds. The landuse map (Fig. 3.3) reveals that vegetation cover near the ridges with hillslope at elevations 1100-1300 m and 1500 - 1600 m are moderately dense and, in general sparse. It is appropriate to mention that at elevations of 1200 to 1800 m, nature of vegetation changes and canopy cover decreases. Field observations indicated that with increase of elevation, scanty growth of secondary vegetation decreases. Further slopes, in general, are steeper near the ridges as compared to low level areas. Moreover, it is important to mention that slopes, in general, are retreating towards ridges. Thus erosion near ridges is intensified. This fact is supported by sharp edge of ridges. The fourth mode of slope failure is at elevation 500-600 m which is generally found along hill slopes near the road running parallel to the river Ganga. Hence, these factors singly as well as their mutual interaction, whenever acted adversely, might have caused slopes to fail.

3.4.2 Landslide Distribution in Relation to Slope

With a view to investigate the relationship of landslide distribution with slope, landslide map was superimposed on slope classification map. The percent landslide affected area at different slope facet was determined (Table 3.8).

Table 3.8: Landslide Area Distribution at Different Slope Facets

Total area : 102.42 sq.km

Total landslide area : 13.42 sq.km

Slope Category	Facet Angle	Landslide area at each facet (km^2)	Area of each facet (km^2)	Percentage of landslide area in each facet
II	>45°	0.93	10.83	8.58
III	40-45°	0.89	5.60	15.89
IV	35-40°	1.68	18.07	9.30
V	30-35°	4.41	22.72	19.41
VI	25-30°	3.82	28.53	13.39
VII	20-25°	1.32	9.95	13.27
VIII	15-20°	0.32	3.31	9.67
IX	10-15°	0.04	0.84	4.76
X	5-10°	0.01	0.37	2.70

Experience of various workers like Young (1961) and Selby (1982) indicates that the landslides and slopes are intimately related (Table 3.8, Fig. 3.6).

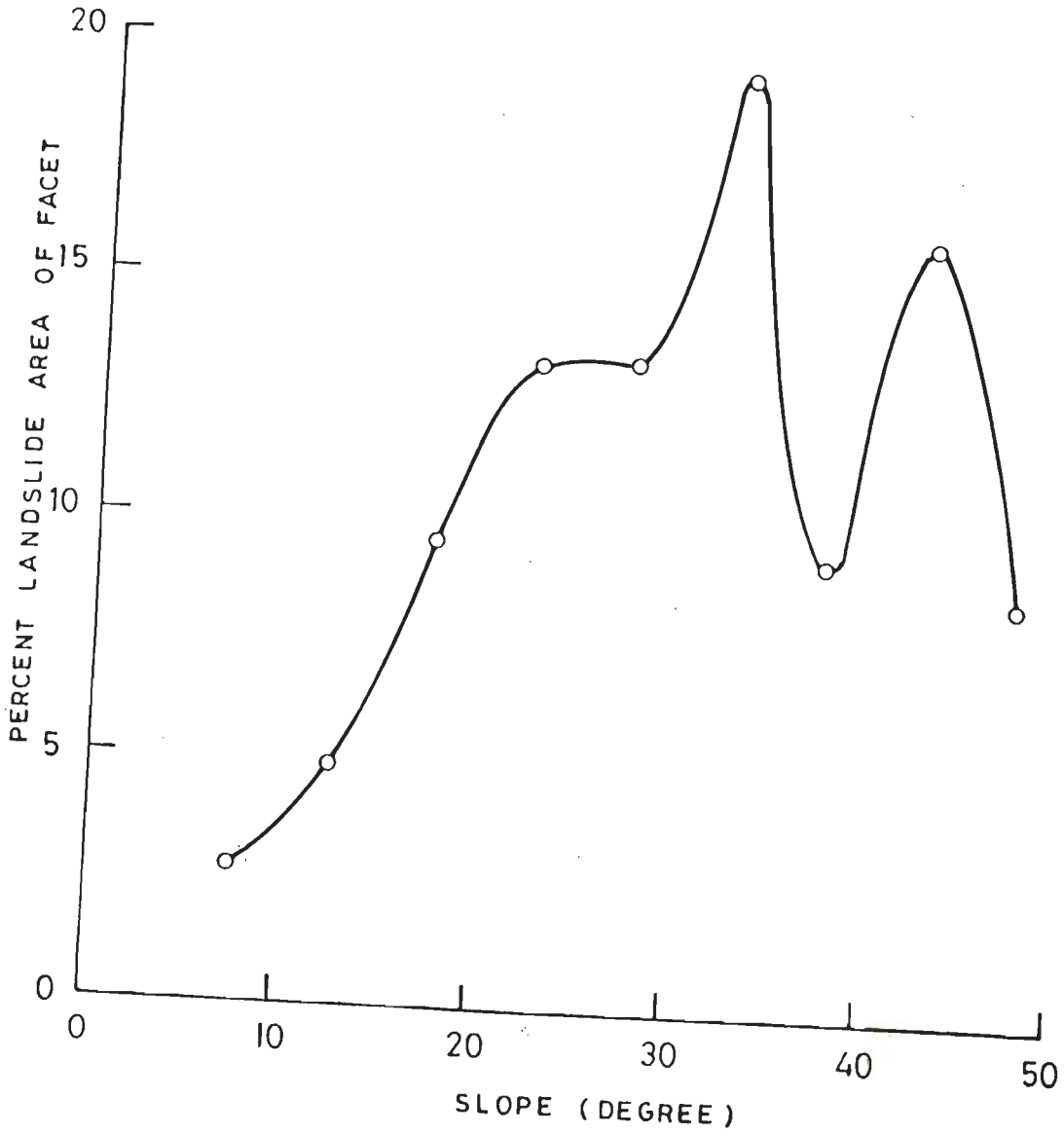

Fig. 3.6: DISTRIBUTION OF LANDSLIDE AREA WITH SLOPE

It is observed from Table 3.8 and Figure 3.6 that landslide activity is not uniformly distributed in different facets. It shows a bimodal pattern of slide area distribution with respect to slope. The primary mode indicates that the maximum slope area failure is found in the facet V with slope angle 30 to 35°. This appears to be due to proximity of this facet in general to ridges (Fig. 3.2) which are characterised by moderate to sparse vegetation cover (Fig. 3.3). Besides this, about 81% of the area consists of quartzite and 30 to 35° facet angle is close to angle of internal friction of these rocks (Hoek and Bray,1981). The landslide activities are also intensified in facets with slope angle between 40-45°. Figure 3.2 indicates that these facets in general are close to the ridges, and vegetation cover in facets with slope angle 40 to 45° ranges between dense to moderately dense (Fig. 3.3). Further observation of Figure 3.2 indicates that the entire facet lies to the west of ridge R_5 where amount of precipitation is relatively more. The facet with slope angle between 20 - 25° has a large aerial extent (Table 3.8) and characterised by moderately dense to barren and dominantly sparse vegetation cover (Fig. 3.3). The aerial extent of facet with slope angle between 25 to 30° is largest in the area (Table 3.8) with dominantly moderately dense to sparse vegetation cover. A synoptic view of Figure 3.4 reveals that landslide areas in general, are elongated. This may be due to the fact that area has high gradient (Table 3.3). Thus, they are directional in their movement.

Field observations indicated that slope provides a natural surface for landslides. The slope on the steep rock face, called free face, is influenced by frequent action of weathering process. The weathering of free face causes debris avalanches and slide (Figs 3.7 and 3.8). These type of failures are common around Bargaon village and frequently observed along the road.

3.4.3 Landslide Distribution in Relation to Landuse (Vegetation Cover)

It is important to understand the relationship of landslide distribution with vegetation cover. The various landuse types considered here include: i) very dense vegetated land, ii) Dense vegetated land, iii) Moderately vegetated land, iv) agricultural land, v) Sparse vegetated land, and vi) Barren land. The relationship of landslide distribution with vegetation cover is worked out by superimposing landslide map on landuse map. The landslide affected area at each landuse category was measured and the following observations and broad conclusions were drawn (Table 3.9).

Table 3.9 and Figure 3.9 indicate that landslide area distribution has intimate relation with vegetation covered. As the density of the natural vegetation cover decreases, landslide area percentage increases. It is observed that maximum landslide area occurs in natural lands. Although the barren lands have relatively low aerial extent of about 3.66 sq.km (Table 3.9), they are affected maximum by landslide activity. Observations from Figures 3.1, 3.2, 3.3 and 3.4 indicate that these areas are

Fig. 3.7 : Rock and Debris Slide in Well Jointed and Weathered Slate (38 km from Rishikesh)

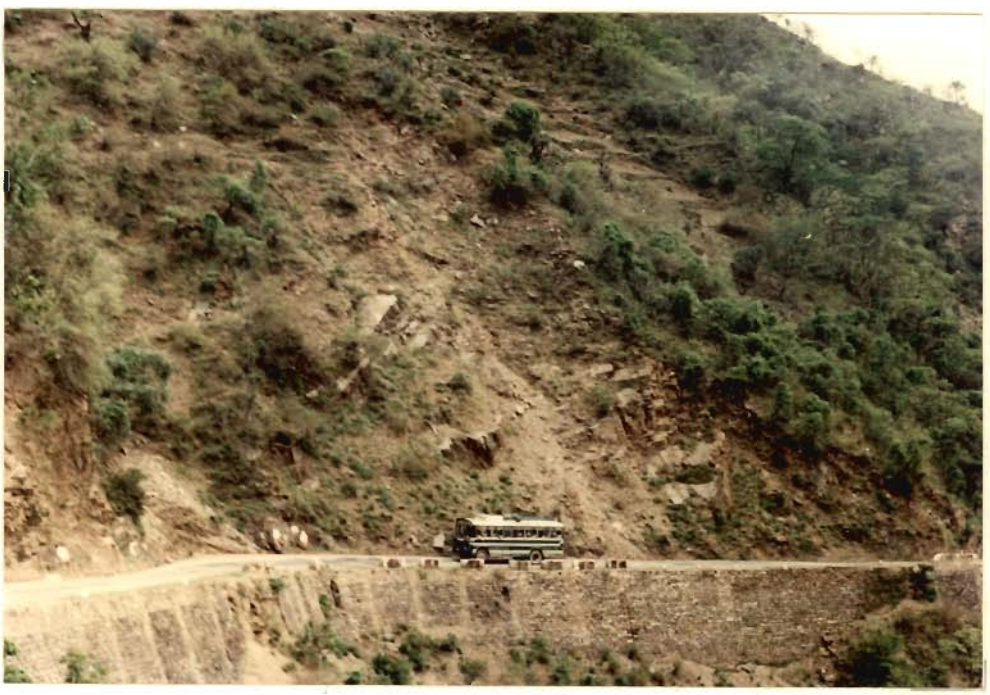

Fig. 3.8 : Rock cum Debris Avalanches in Highly Weathered Phyllite (65 km from Rishikesh)

usually associated with steep slopes near the ridges. It is very clear that vegation plays an important role in the stability of hillslopes in the area. It is observed that sparse, moderately dense and dense vegetation cover have maximum aerial extent. A synoptic view of Figures 3.1 and 3.3 indicates that in general moderately dense to sparsely vegetated lands are associated with ridges, whereas the areas with dense to very dense vegetation cover are at lower elevation.

Table 3.9: **Landslide Area Distribution at Different Landuse Class**

Total area : 102.42 sq.km

Total landslide area : 13.42 sq.km

Landuse class	vegetation cover	Landslide area at each facet (km^2)	Area of each facet (km^2)	Percentage of landslide area at each facet
I	Very dense	0.24	7.07	3.39
II	Dense	2.10	27.21	7.72
III	Moderately dense	4.27	30.62	13.94
VI	Sparse	4.11	22.00	18.68
V	Barren	1.35	3.66	36.88
IV	Agriculture land	1.35	11.24	12.01

From such studies as inferred from Figure 3.9, it is noted that vegetation has a high influence on landslide distribution in the terrain and its effect is more pronounced in combination with other factors, like slope, topographic elevation, structure, etc.

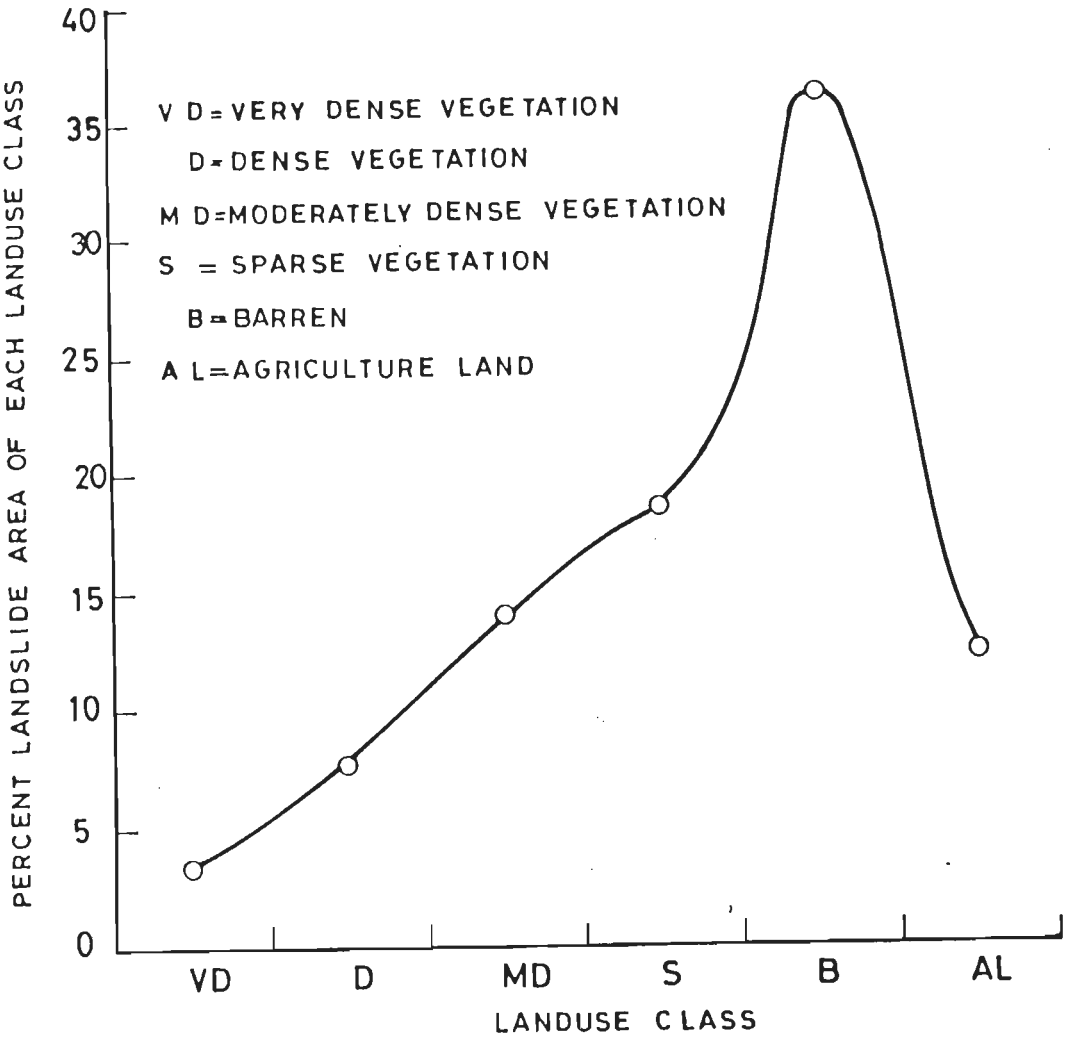

Fig. 3.9: DISTRIBUTION OF LANDSLIDE AREA WITH LANDUSE (Vegetation Cover)

3.4.4 Landslide Distribution in Relation to Stratigraphic Units

It is important to understand the relationship of landslide distrubution with various rock formations. The rocks in the area belong to five stratigraphic units: (i) Lansdowne Formation dominantly consisting of quartzite associated with phyllite of Amri Member, ii) Blaini Formation - chiefly comprised of boulder bed, variegated purple green shale and siltstone, sandy greyish dolomite and associated with dark grey laminated shale, iii) Krol Formation - largely limestone and dolomite associated with calcareous shale with limestone, red shale and siltstone, iv) Tal Formation - made up of quartzite, slate, shale, chert, siltstone and shell limestone, v) Subathu Formation - consisting mainly of greenish grey splintery shale.

Landslide affected areas in each of the rock formations were measured after superimposing the landslide map on geological map. The percent landslide affected area in each of the rock formations are listed in Table 3.10 and pictorially presented in Fig. 3.10.

A perusal of Table 3.10 and Figure 3.10 indicates that the areas underlain by Bijni and Amri Members of the Lansdowne Formation, the Blaini Formation and the Lower Krol Formation are most affected by landslide activity. It may be mentioned here that Bijni quartzite constitutes about 72% of the area of study and therefore shows high percentage of landslide activity. Observation from Figures 2.5, 3.2 and 3.3 indicates that the area

Table 3.10: Landslide Area Distribution at Different Statigraphic Units.

Total area : 102.42 sq.km

Total landslide area : 13.42 sq.km

Stratigraphic unit		Landslide area at each members (km^2)	Area of each member (km^2)	Percentage of landslide area of each member
Formation	Member			
Subathu		0.02	0.71	2.82
TAL	Upper	0.65	9.12	7.13
	Lower	0.44	4.01	10.97
Krol	Upper	0.82	7.47	10.98
	Middle	0.14	0.98	13.28
	Lower	0.40	2.22	18.02
Blaini		0.65	5.26	12.36
Lansdowne	Amri	0.06	0.49	12.19
	Bijni	10.24	72.16	14.19

underlain by phyllite (Amri Member) are characterised by steep slopes and agricultural land and dominantly sparse vegetation cover. Field observation also revealed that weathering processes are intensified in areas underlain by phyllite. Blaini Formation consists of boulder bed, sandy dolomite, variegated purple green shale with dolomite. Lower Krol Formation chiefly is made up of calcareous shale with limestone, hence they are more amenable to weathering processes as compared to quartzites. Observations from Figures 3.2 and 3.3 indicates that hillface occupied by

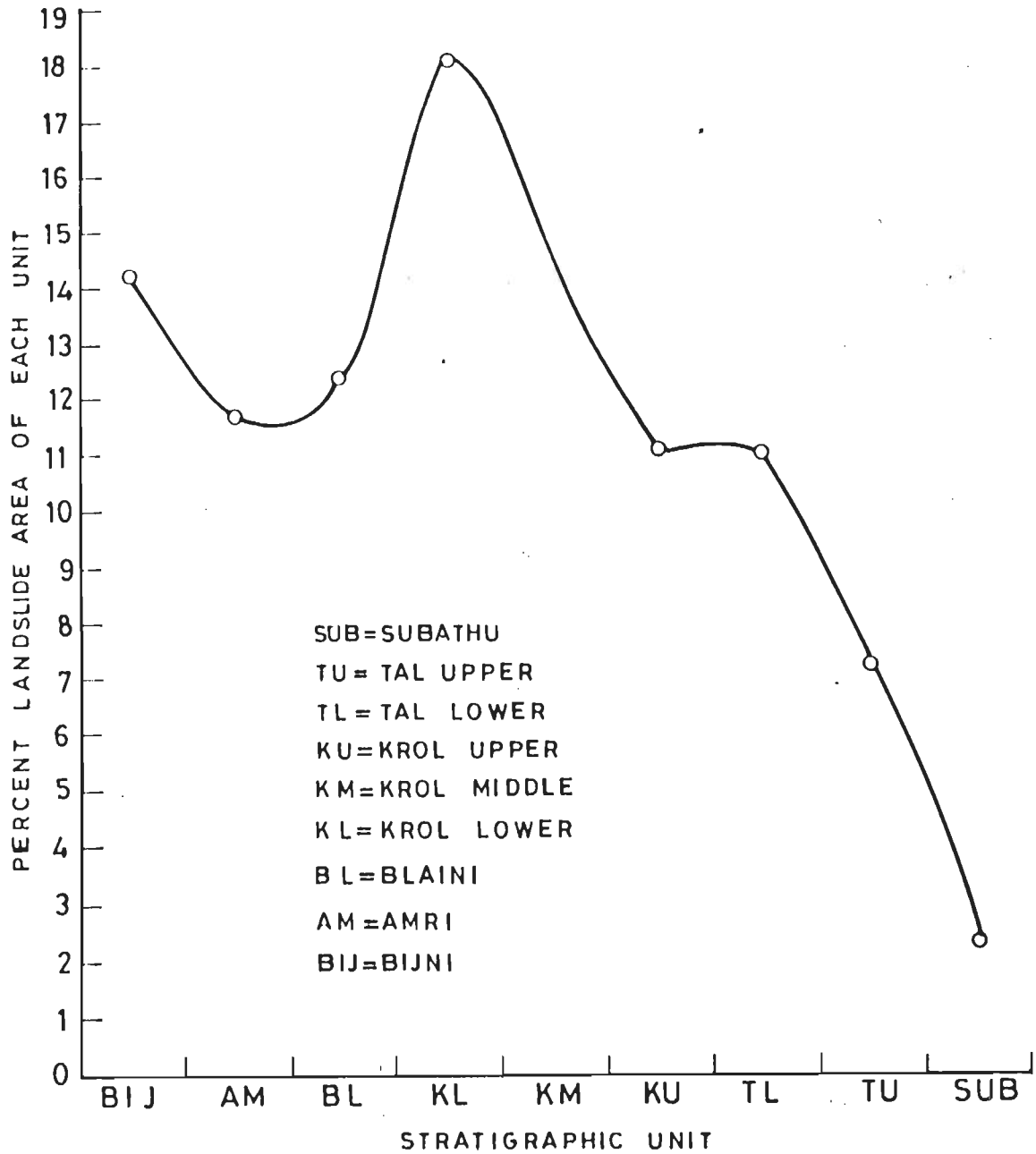

Fig. 3.10: DISTRIBUTION OF LANDSLIDE AREA WITH RESPECT TO STRATIGRAPHIC UNITS

Blaini and Lower Krol Formations are generally characterised with steep slope, dense to sparse vegetation and agricultural land. It is appropriate to mention at this point that the aerial extent of other rock types compared to quartzite is so low, that combination of factors causing landslide get less chance to occur and cause landslide.

3.4.5 Landslide Distribution in Relation to Structure

Landslides are usually intimately linked with the occurrence, trend and orientation of regional and local structural features.

i) Regional structure and landslides - The major structural tectonic feature present in the area is a major fault known as Singtali Fault. In general, areas affected by major fault or thrust are considered highly suceptible to landslide activity. The major fault in the south western part of the area (Singtali Fault) although has caused tremendous fracturing of the Bijni and Phulchatti Quartzites in its proximity, but landslide activity is not a common phenomenon except along the road where in most places it runs parallel to the strike of rocks. This is possibly due to fracturing of the rocks which has affected their weathering characteristics and thus produced relatively low slope angle, good soil and luxuriant vegetation cover in the vicinity of shear zone which in turn has helped in stabilization of slopes.

ii) Local Structures and landslide - The landslide activity has often been found to be governed by occurrence, trend and orientation of local structures in terms of discontinuity planes viz. bedding planes, joints, fractures as suggested by many workers (Hoek and Bray 1981; Johnson et al. 1988). The effect of these local structures is discussed below.

Bedding planes- The bedding planes in the area show variation in their strike within a short distance. Whenever the bedding plane is cutting the topographic slope, the slope becomes vulnerable to landslides. Such slopes when disturbed exogenically may cause frequent slope failure (Fig. 3.11).

Joint Planes - Orientation, frequency and extent of joint planes are very important in controlling the stability of slopes. Rock falls and rock slides are the joint controlled slope failures. Rockfalls often result from steeply dipping joint planes cut across by other sub-horizontal joint planes (Fig. 3.12). Similarly, if the joint planes are steeply inclined and cut across the topographic slopes, the rock slide may occur (Fig. 3.13). The rugged nature of the area characterised by steep sided valleys has led to increase susceptibility of the rocks to landslide activity.

Fold axis - The axial zones of local folds often exhibit intense cracks and fractures (Fig. 3.14), which are vulnerable to landslides, especially if the zone is disturbed exogenetically e.g. road cutting etc. Few examples of such type are seen along the road. A detailed study covering these aspects have been

Fig. 3.11 : Rock Slide on Dip-Slopes of Quartzite Caused by Toe Excavation (32 km from Rishikesh)

Fig. 3.12 : Rock fall from Over Hanging Scar Face of the Quartzite (52 km from Rishikesh)

Fig. 3.13 : Rock Slide in Highly Jointed Quartzite (46 km from Rishikesh)

Fig. 3.14 : Axial Zone of a Minor Fold, Forms Landslide Susceptible Area While Disturbed Exogenically (58 km from Rishikesh)

carried out and presented in Chapter 5.

3.5 MORPHOMETRIC PARAMETERS AND LANDSLIDES

Distribution of landslide area in relation to various attributes as investigated in section 3.5, indicates certain pattern of its occurrence when these factors are considered on univariate basis. The morphometric parameters which result as the sum effect of these factors, may have correlation with landslide areas. In this section, the studies have been carried out in this direction.

The morphology of the area clearly indicates that there are six major drainage basins seperated by major ridges (Fig. 3.15). These basins are physiographic units which collect precipitation and serve as reservoir, or storage basins for water and sediments. These may be considered as systems consisting of hillslopes and stream subsystem. However, these broad basins have a number of sub-basins, the ordering of which has been done following the approach of Strahler (1952). In this method the smallest fingertip tributaries are designated first order. When two first order channels join, a channel segment of second order is formed, and so forth. If a lower order channel meets a higher order channel, there is no change in the order of the higher order channel. The trunk stream through which all discharge of water and sediments passes is, therefore, the stream segment of highest order. The main advantage of this method is that it can be used for mathematical derivations and the results obtained

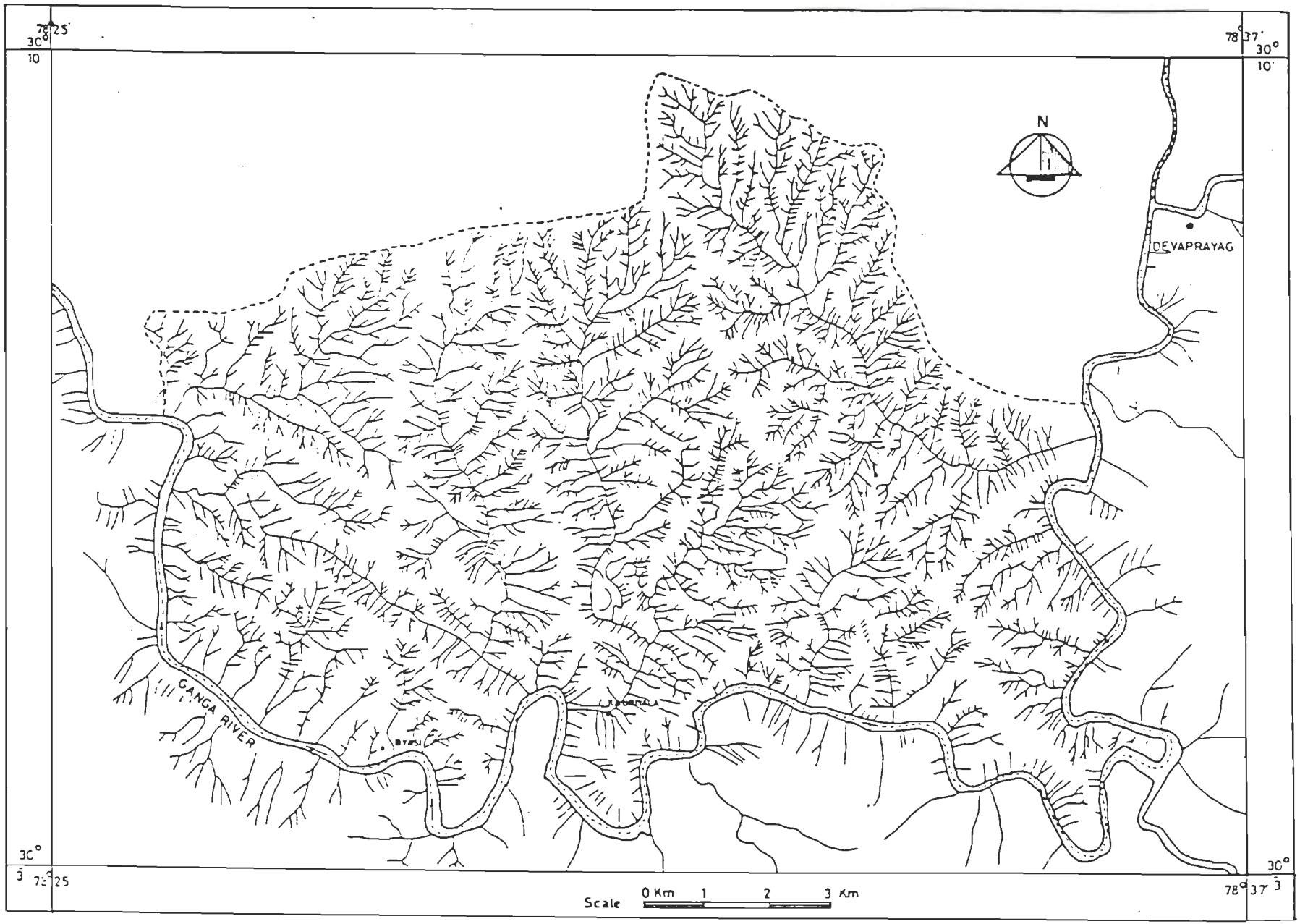

Fig.3.15: DRAINAGE MAP OF THE AREA

through this method can be correlated with that of other basins.

During a rare flood event some first order drainage may form by chance. At the same time two first order drainage can meet to form a second order drainage basin. The possiblilty of third order drainage basin formation during a rare event is very less. Moreover, third order drainage basins are more matured as compared to first and second order basins and provide enough time to components and process to adjust themselves and restore a balance. Therefore third order drainage basins may represent the smallest complete open system. These have been considered as the basic geomorphic units for this study.

The rock type as noted by Yastu (1966) and Burdon (1966) has significant effect on drainage basin. It not only determines the character of weathering and therefore the overlying weathered material but also the basin character particularly relief, drainage density and texture. Therefore, in the present study, the lithology is kept uniform and required parameters were measured from third order drainage basins in quartzite bearing terrain which constitute about 79% of the total area of investigation.

The morphometric parameters presented in Table 3.11 have been worked out from 26 third order drainage basins for further analysis using 1:50,000 toposheets and aerial photographs of scale of 1 $\approx$ 55,000 as basic source data measured by rotometer and planimeter. A brief description of these parameters are

Table 3.11 : Geomrphometric Parameter Used

Sl. No.	Parameters	Symbols	Formula
1.	Fraction Landslide area	Ls	$\frac{\text{Landslide area}}{\text{area of basin}}$
2.	Basin slope	B.SL	BR/BL
3.	Bifurcation ratio	BF_1	F_1/F_2
4.	Bifurcation ratio	BF_2	F_2/F_3
5.	Length ratio	LR_1	L_1/L_2
6.	Length ratio	LR_2	L_2/L_3
7.	Stream frequency	SF	$F_1+F_2+F_3/BA$
8.	Drainage density	DD	$L_1+L_2+L_3/BA$
9.	Drainage Texture	DT	SF x DD
10.	Ruggedness number	RN	DD x BR
11.	Basin Elongation	BE	$BE = \frac{\text{Diameter of circle with same area as basin}}{BL}$
12.	Frequency of First order stream.	F_1	
13.	Frequency of Second & third order stream.	F_2 , F_3	
14.	Length of First order stream.	L_1	
15.	Length of Second order stream.	L_2	
16.	Length of third order stream.	L_3	
17.	Basin relief	BR	
18.	Basin area	BA	
19.	Basin Length	BL	
20.	Basin circulaity	BC	$BC = \frac{BA}{p^2} \times 4\pi$ where 'p' is the basin perimeter

given below.

i) Basin Slope (B.SL) - It is the ratio of maximum basin relief (elevation difference between highest and lowest points in the basin) to the basin length (horizontal distance along the longest dimension of the basin). It is a measure of overall steepness of drainage basin and is an indicator of the intensity of erosion process operating on the slope of a basin (Strahler, 1964).

ii) Bifurcation ratio (BF_1, BF_2) - It is a measure of branching in the network (Horton, 1932) and indicative of topological behaviour of the basin. It is computed as the ratio of the number of streams of order `n' to the number of streams of next higher order `n+1'. Strahler (1964) studied a number of stream networks and observed that in a region of uniform climate and rock type and stage of development values of bifurcation ratio between 3 and 5 are characteristic of natural streams. In the area of study, the value of BF_1 varies from 2 to 6 and that of BF_2 varies between 2 to 10, suggesting that probably the climate or stage of development is not same throughout the area.

iii) Length ratio (LR_1, LR_2) - The ratio of total length `n' order of streams in a drainage basin to the total length of next higher order `n+1' is defined as length ratio. A number of workers including Judson and Andrews (1955) and Beaty (1962) have found a close relation between joints in bedrock and stream length and flow direction. In the present study streams of the area were traced on 1:50,000 toposheets. The azimuth length

analysis of first, second and third order streams was carried out. The azimuths of various order streams were divided into 18 classes with class interval of 10°. Rose diagrams were prepared for azimuth length of streams for the drainage basins (Figs. 3.16, 3.17 and 3.18). These diagrams when compared with mean joint orientation in the area showed that about 32% of first order, 43% of second order and 24% of third order streams are controlled by joints, implying that relation between network and structure is strongest generally in second order segments. The results seem to indicate that first and especially third order streams are not sensitive to joint orientations, perhaps they are more controlled by surface slope.

iv) Stream frequency (SF) - It was proposed by Horton (1945) as the number of stream segments per unit area, which expresses the texture of drainage network and largely depends on lithology.

v) Drainage density (DD) - It is expressed as the total length of stream network per unit area. This is an important parameter which is very sensitive to other basin characteristics. Low drainage density occurs in regions of highly resistant and highly permeable sub-soil materials with dense vegetation cover and low relief, whereas high drainage density is prevalent in regions of weak impermeable sub-surface material which are sparsely vegetated and show high relief (Strahler, 1964). Carlston (1963) determined that drainage density was related to hydrologic aspect of stream systems. It has been proposed that drainage density increases as mean annual precipitation (Williams and Fowler,

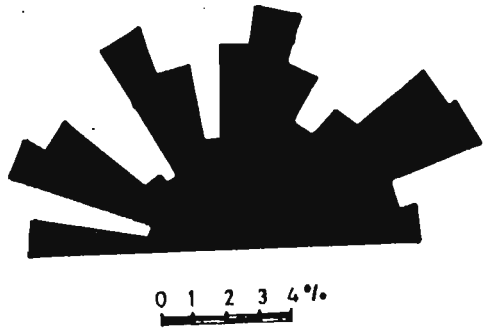

Fig. 3.16: ROSE DIAGRAM OF DRAINAGE AZIMUTH OF FIRST ORDER STREAM IN THE AREA

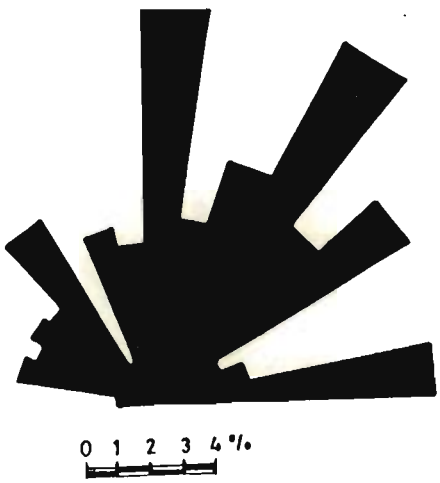

Fig. 3.17: ROSE DIAGRAM OF DRAINAGE AZIMUTH OF SECOND ORDER STREAMS IN THE AREA

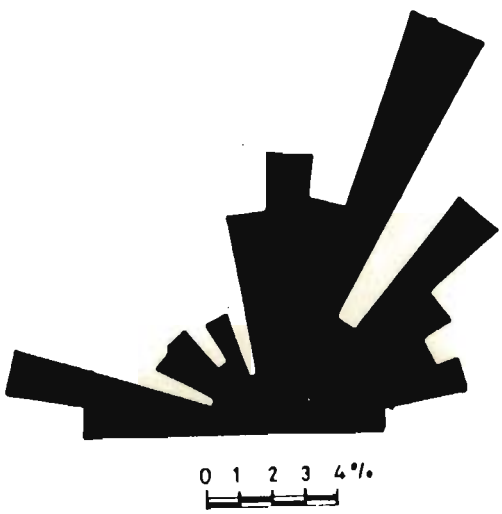

Fig. 3.18: ROSE DIAGRAM OF DRAINAGE AZIMUTH OF THIRD ORDER STREAMS IN THE AREA

1969), rainfall intensity (Chorley 1957; Chorely and Morgan, 1962) and runoff intensity increases.

vi) Drainage texture (DT) - The drainage texture in the present study is calculated on the basis of Horton,s (1945) suggestion, that it is product of drainage density and stream frequency. Strahler (1964) explained that the regions of low drainage density, medium drainage density, high drainage density and very high drainage density have coarse, medium, fine and ultrafine textures respectively. Morgan (1970) in Sungi Klang drainage basin in west Malaysia showed that magnitude of 10 years daily rainfall and seasonality of rainfall regime were the most significant climate controls of drainage texture.

vii) Basin shape - There are a number of methods by which basin shape can be quantitatively measured. Table 3.12 shows some of the important methods.

Basin shape can be significantly influenced by other drainage basin characteristics such as rock type and structure. It is interesting to know unless pronounced structural control is present, drainage basin tends to become more elongated with strong relief and steep slopes (Chorley, 1969). Basin shape has a great influence on the movement of water on hill-surface (Woldenberg, 1969). In elongated basin the overflow is minimised and therefore flow takes place through channels. In the present study, the method derived by Schumm and Miller is used for measuring basin shape.

Table 3.12 : Measures of Drainage Basin Shape (compiled from Gregory et al., 1973)

1-	Form factor (F)	$F = A/L$
2-	Basin elongation (BE)	$BE = \frac{\text{Diameter of circle with same area as basin}}{\text{Basin length}}$
	(Schumm, 1956)	i.e. $BE = \frac{2\sqrt{A/\pi}}{L}$
3-	Basin circularity (BC) (Miller, 1953)	$BC = \frac{\text{Area of basin}}{\text{Area of circle with same perimeter as that of basin}}$
		i.e. $BC = \frac{A}{p^2} \times 4\pi$
4-	Leminscate (K)	Based upon comparison of basin with leminscate curve
	(Chorley, Malm and Progerzeiski, 1957)	$K = \frac{L_2}{4A}$

viii) Ruggedness number (RN) - Strahler (1958) introduced the term ruggedness number which is a product of drainage density and relief. The extremely high values of ruggedness number occur when both variables (relief and drainage density) are high. i.e. when slopes are not only steep but long as well.

ix) Basin relief (BR) is the elevation difference between the highest and lowest point in the basin.

Besides these parameters, there are some other parameters which have been used in this study. F_1 and F_2 are frequency or number of first and second order streams in a basin. L_1, L_2 and L_3 are length of first order, second and third order streams in a basin measured by rotometer. BA is area of the basin measured by planimeter.

3.5.1 Correlation Between Landslide Area and Geomorphometric Parameters

With a view to investigate relationship, if it exists, between the fraction landslide area and 19 morphometric parameters, and also among all possible 171 pairs of 19 morphometric parameter, Pearson's correlation coefficients were computed, using the following simple formula.

$$\Gamma = \frac{\sum_{i=1}^{n} (X_i-\bar{X})(y_i-\bar{y})}{\left[\sum_{i=1}^{n} (X_i-\bar{X})^2 \sum_{i=1}^{n} (y_i-\bar{y})^2\right]^{1/2}} \qquad (3.1)$$

where

Γ = correlation coefficient between the two parameters x and y

X_i = is the ith observation of parameter X

Y_i is the ith observation of parameter Y.

$\bar{X}$ is mean of parameter X.

$\bar{Y}$ is mean of parameter Y.

n is the number of observations.

The correlation coefficient were calculated for all possible 190 pairs of variables from 26 drainage basins and are presented in form of correlation matrix (Table 3.13). These coefficients were tested for their statistical significance at 1% level using methodology given by Dixon and Massey (1969). Since the number of observations in the present study is 26, the correlation coefficient equal or above 0.453 is significant at 1% level.

3.5.2 Analysis

Fraction landslide (Ls) defined as the ratio of landslide area to the total area of basin, is a measure of aerial extent of slope movement in a given basin area. Its relationship with other morphometric parameters, assessed as correlation coefficients is presented in Table 3.13. A perusal of Table 3.13 indicates that Fractional Landslide area (Ls) shows significant correlation of 0.86, 0.82, 0.63 and -0.55 with Drainage Texture (DT), Stream Frequency (SF), Drainage Density (DD) and Basin circularity (BC) respectively. These are represented diagrammatically in Figure 3.19.

Drainage Texture (DT) shows very high positive correlation coefficients of 0.95 and 0.95 with Drainage Density (DD) and Stream Frequency (SF) respectively. Such a correlation is natural to obtain as the drainage texture is defined as the product of drainage density and stream frequency. It also shows negative correlation with BR and BC, suggesting that elongated basins with low relief has maximum drainage texture. But it is not uniform

TABLE 3.13 : Pearson's Correlation Matrix Showing all Possible Correlation Coefficient among Geomorphometric Parameters

	Ls	B.SL	BF_1	BF_2	LR_1	LR_2	SF	DD	DT	B.E	RN	F_1	F_2	L_1	L_2	L_3	BR	BA	BL	BC
Ls	1.00	0.3376	-0.3875	-0.0559	0.3423	-0.0840	0.8382	0.6847	0.8570	-0.3963	0.3567	-0.2440	-0.1456	-0.2064	-0.2990	-0.2603	-0.3855	-0.2662	-0.3312	-0.5547
B.SL		1.0000	-0.5461	-0.7268	-0.0334	0.2219	0.3795	0.1566	0.2896	0.1820	-0.1064	-0.8301	-0.7500	-0.8197	-0.6742	-0.8292	-0.3219	-0.7947	-0.8391	-0.0744
BF_1			1.0000	0.2509	0.2049	0.3632	-0.2949	-0.0390	-0.2309	-0.0013	0.3791	0.5541	0.2706	0.5085	0.4515	0.3652	0.4481	0.4388	0.5230	0.3628
BF_2				1.0000	-0.0193	-0.1715	-0.2404	-0.0935	-0.1690	-0.0246	0.1919	0.8585	0.9184	0.8941	0.7628	0.8855	0.3462	0.8833	0.8269	-0.0715
LR_1					1.0000	-0.3831	0.5432	0.3153	0.3749	-0.1925	0.0825	0.0039	-0.0439	-0.0091	-0.3875	-0.0304	-0.3521	-0.1519	-0.0154	-0.0760
LR_2						1.0000	-0.1621	0.0466	-0.0875	0.1410	0.3011	-0.0846	-0.2288	-0.0696	0.1769	-0.2978	0.2367	-0.0809	-0.0527	0.2990
SF							1.0000	0.8472	0.9484	-0.3600	0.3822	-0.3160	-0.2577	-0.3213	-0.4674	-0.3559	-0.5728	-0.4403	-0.4949	-0.4424
DD								1.0000	0.9516	-0.2885	0.6624	-0.1124	-0.1067	-0.1119	-0.2191	-0.1985	-0.4224	-0.2575	-0.2948	-0.4018
DT									1.0000	-0.3921	0.5508	-0.2410	-0.1959	-0.2394	-0.3405	-0.2764	-0.4758	-0.3502	-0.3934	-0.4952
B.E										1.0000	-0.4051	0.0205	0.0629	0.0486	0.0135	-0.0491	-0.1857	0.0293	-0.1630	0.5550
RN											1.0000	0.3100	0.2173	0.2860	0.3310	0.1880	0.3801	0.2057	0.2796	-0.3311
F_1												1.0000	0.9457	0.9894	0.8581	0.9338	0.4851	0.9529	0.9185	0.0763
F_2													1.0000	0.9570	0.8090	0.9362	0.3767	0.9288	0.8565	-0.0475
L_1														1.0000	0.8435	0.9299	0.4599	0.9626	0.9139	0.0458
L_2															1.0000	0.8315	0.6717	0.9110	0.8962	0.1054
L_3																1.0000	0.4893	0.9587	0.9281	-0.0071
BR																	1.0000	0.5760	0.7119	0.0159
BA																		1.0000	0.9570	0.0459
BL																			1.0000	0.0001
BC																				1.0000

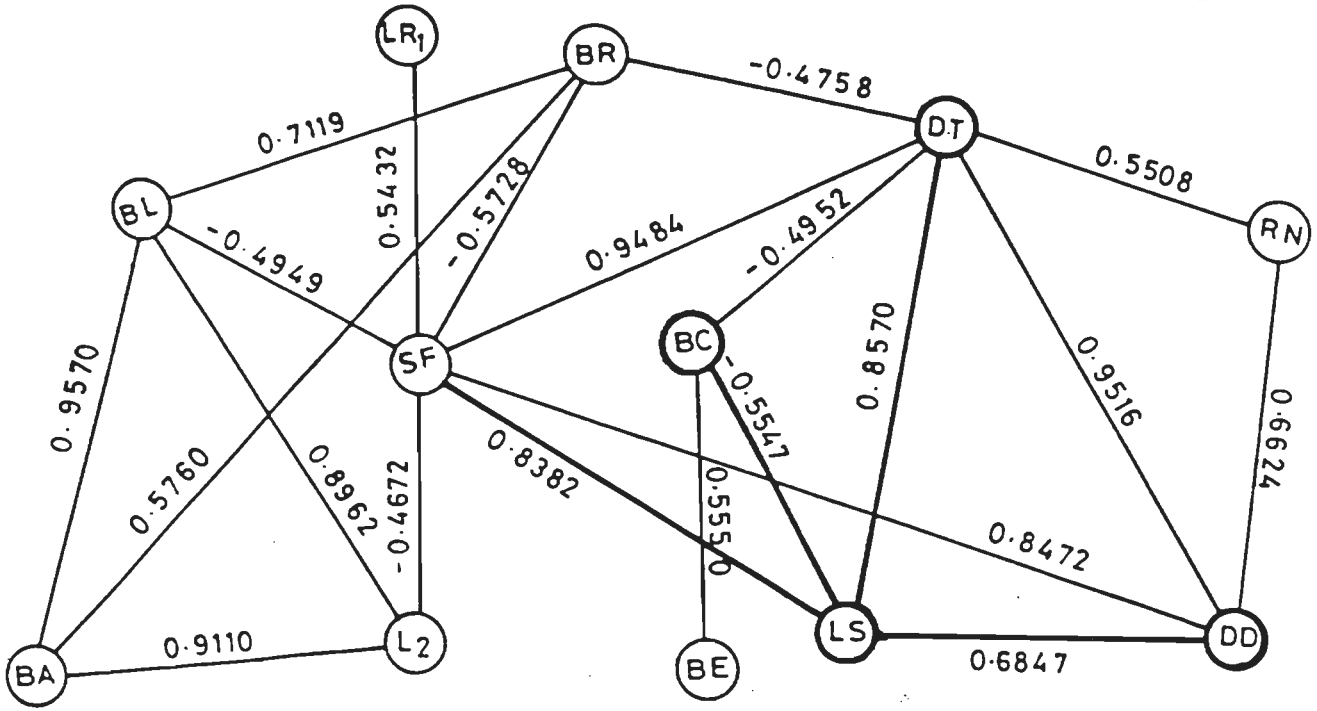

LS = FRACTION LANDSLIDE AREA
FS = STREAM FREQUENCY
DD = DRAINAGE DENSITY
DT = DRAINAGE TEXTURE
RN = RUGGEDNESS NUMBER

BC = BASIN CIRCULARITY
BE = BASIN ELONGATION
BR = BASIN RELIEF
BA = BASIN AREA
BL = BASIN LENGTH

LR_1 = LENGTH RATIO OF FIRST AND SECOND ORDER STREAMS
L_2 = LENGTH OF SECOND ORDER STREAMS

Fig.3.19: SHOWING CORRELATION COEFFICIENTS BETWEEN FRACTIONAL LANDSLIDE AREA (L_S) AND GEOMORPHOMETRIC PARAMETERS (FIGURES ALONG THE LINES INDICATE CORRELATION COEFFICIENTS)

in the area as indicated by low rate of change in correlation coefficient.

Drainage Density (DD) is also correlated positively with Stream Frequency (SF) and Ruggedness Number (RN), besides Drainage Texture (DT). This indicates that, as overall number of drainages in the area increases their overall length also increases and energy entered into system in form of precipitation is dissipiated both through lengthening and expansion of drainage net work. Its correlation with RN indicates that with increase in elevation the energy (rainfall) is dissipiated more through overall lengthening drainage network than its branching. However, it is not uniform throughout the area as indicated by low rate of change in correlation coefficient.

Stream frequency (SF) shows significant positive correlation of 0.54 with LR_1 besides drainage density (DD) and drainage texture (DT), and negative correlation of -0.49, -0.57 and -0.47 with BL, BR and L_2 respectively, This probably indicate that as dissection of the area increases length of first order stream increases. The negative correlation with BL and BR suggest that as dissection increases the length and relief of basin decreases. But these are not confirmed in the area as indicated by low rate of change in correlation coefficient.

Basin circularity (BC) shows positive significant correlation of 0.56 with basin elongation (BE), besides drainage texture (DT). The correlation between BC and BE at the low rate

of change, probably indicates that, there are some structural control which help in development of basin circularity in the area (Chorley, 1969). Basin shape does not show correlation with F_1, F_2, L_1, $L_2$1, L_3, BA and BL and it may prove that basin shape does not have direct pronounced control over drainage network development. Basin area shows high positive correlation of 0.88, 0.95, 0.93, 0.96,. 0.91, 0.967, 0.58 and 0.96 with BF_2, F_1, F_2, L_1, L_2, L_3, BR and BL respectively (Table 3.13). Thus, the ratio of hill slope area occupied by basin to basin length does not increase as drainage network expands in size. Basin relief has significant positive correlation of 0.48, 0.46, 0.67, 0.49, 0.58 and 0.72 with F_1, L_1, L_2, L_3, BA and BL respectively, implying thereby as relief increases the frequency of first order streams, length of first, second and third order streams with different rate of change increases. The rate of change indicates that relief has maximum effect on length of second order streams and minimises on other parameters. Its correlation with BL suggests that tendency is to erode and the area is characterised by retreating slopes which are usually dominated by rill and channel erosion. Hence, it appears that the present topography is the result of accelerated erosion of slopes towards ridges.

From above discussion and Figure 3.19 it becomes apparent that the Drainage Texture is directly related to Drainage Density (DD), Stream Frequency (SF), Ruggedness number (RN) Basin circularity (BC) and Basin Relief (BR). Stream Frequency (SF) is directly related to Basin Length (BL), length of second order

streams (L_2) Basin relief (BR) and LR_1. Morevoer, SF is largely dependent on rock type (Horton, 1945). Drainage Density is a sensitive parameter to other basin character like vegetation cover, slope, structure, mean annual rainfall (Carlston, 1963; Strahler, 1964). Drainage texture is a product of Drainage Density (DD) and Stream Frequency (SF). Therefore, it is amongst all of the morphometric parameters, one single parameter which has in it the influence of so many parameters. Also it is the parameter which shows highest significant correlation coefficient with (0.86) the Fraction landslide Area (Ls) and hence this parameter appears to be of great importance in investigating slope instability in such terrain.

3.5.3 Relationship Between Landslide Area and Drainage Texture

As discussed in the section above the Fraction landslide area has statistically significant, high positive linear correlation coefficient of about 0.86 with Drainage Texture (DT). Therefore, the development of a quantitative relationship between these two parameters may provide a predictive model for estimation of fraction landslide area from drainage texture. For this the regression analysis was applied on 26 observations of Fraction landslide area (Ls) and Drainage Texture (DT) using the regression equation approach (Davis, 1973). The regression of variable y on the variable x is given as:

$$(y-\bar{y}) = \rho \frac{S_y}{S_x} (x-\bar{x}) \qquad (3.2)$$

where

$\bar{y}$ = mean of variable y

$\bar{x}$ = mean of variable x

ρ = correlation coefficient between x and y

S_y= standard deviation of the variable y

S_x= standard deviation of the variable x

If y = LS and x = DT as in the present case

$\bar{y} = \bar{L}_s = 0.3346$, $\bar{X} = \bar{DT} = 59.28$

$S_y = S_{LS} = 0.2346$, $S_x = S_{DT} = 42.35$

Based on these, the regression model is worked out as hereunder:

$$LS = 0.0279 + 0.0052\ DT \qquad (3.3)$$

3.5.3.1 Efficacy of the Regression Model Developed

With a view to test the efficacy of the regression model(eq. 1) as a predictive model for estimation of fractional landslide area knowing the drainage texture (DT), four test basins randomly selected were subjected to this analysis. On the basis of drainage texture (DT), the fracture landslide area were computed using Eq. 3.3 The result of these data are given in Table 3.14.

Table 3.14 : **Showing Theoretically computed and Observed Values of Fraction Landslide Area for Four Test Basins**

Basin	Computed	Observed
1	0.16	0.18
2	0.27	0.28
3	0.69	0.61
4	0.29	0.38

Plot of the computed and observed value of fraction landslide area as shown in Figure 3.20, indicates that all the test samples and most of the observed samples fall close to 45° line, implying usefulness of the model with a possible error of 25 percent.

3.6 SUMMARY

The terrain under study has a rugged topography with ridge and valley feature and thirty subdrainage basins. Landslide affected areas in the terrain are found to occur at any elevation which ranges from about 500 m to more than 2200 m. In general, with increase in elevation, the landslide affected area though tends to increase, but is not uniformly distributed. Such areas with increase in elevations above 1800 m, 1500 - 1600 m and 1100 - 1300 m are close to the ridges, and elevation of 500 - 600 m is generally found along the hillslope near the road running parallel to the river Ganga. When considered slopewise, the percent landslide affected area is not uniformly distributed in different slope facets. It is maximum in facets with slope angle between 30 to 35°. Landslide distribution has also been found to have some relation with vegetation cover. It is observed that maximum landslide affected areas fall within barren to sparsely vegetated land, of which barren lands have been affected the most, and found to be associated with higher slope areas of ridges. The effect of lithology on landslide area distribution is not conspicuous since, quartzite constitute about 80% of the total area and aerial extent of other rock types are low.

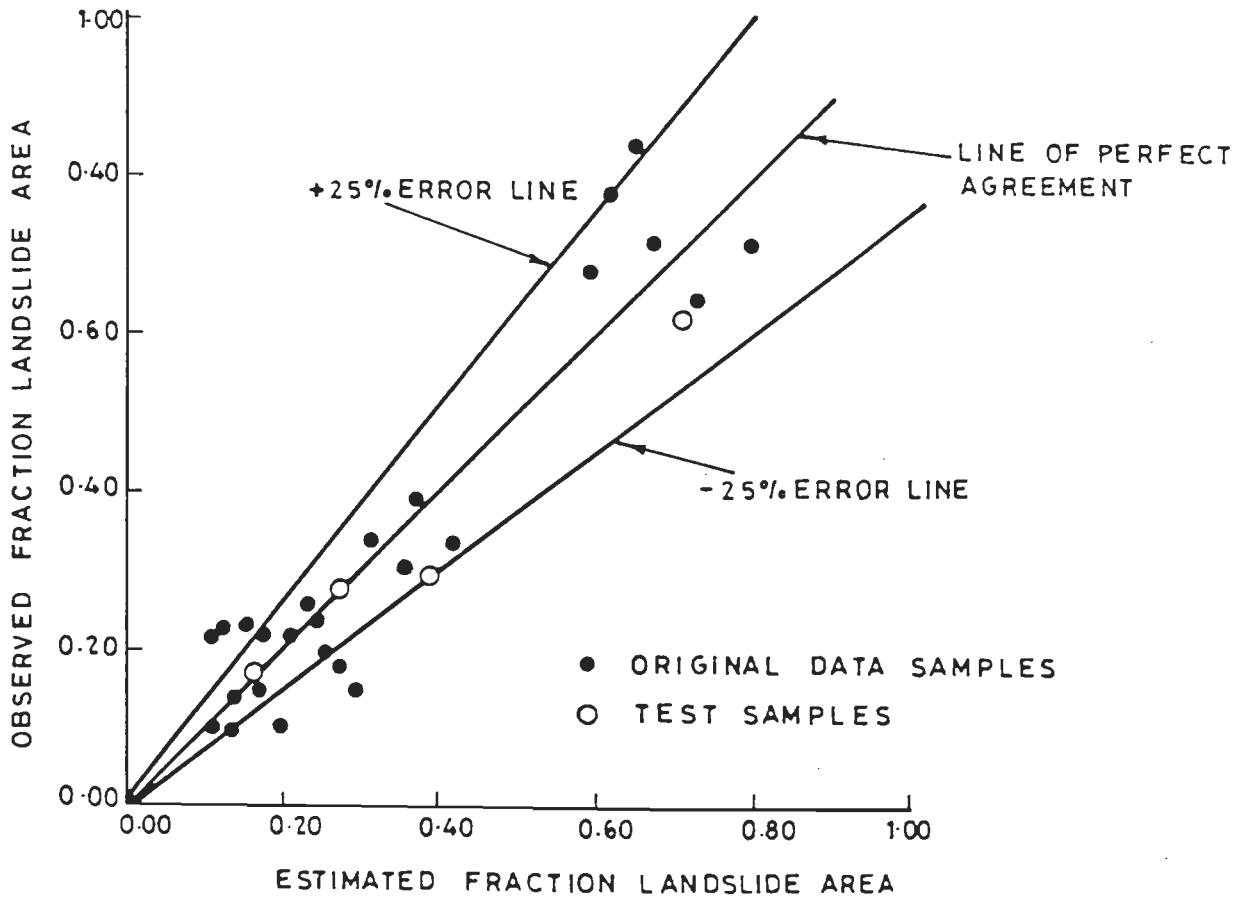

Fig.3.20: SHOWING COMPARISON OF COMPUTED AND OBSERVED FRACTION LANDSLIDE AREA WITH LOCATION OF TEST SAMPLES

However, it has been found Bijni quartzite of Lansdowne Formation, Blaini and Lower Krol formations have been affected the most. The steep sided valleys have led to increase in the susceptibility of the rocks to landslide activity. It has been observed that slope movement is also governed by occurrence, orientation and trend of local structures, such as bedding plane and joints. Data analysis and field observations indicate that the above mentioned parameters and their interaction play an important role in the stability of the area.

The analysis based on 'Pearson's Correlation Matrix' indicated that fraction landslide area (LS) in a basin has highest statistically significant correlation coefficient of about 0.86 with drainage texture (DT). It is one single morphomaetric parameter in a basin that has in it the influence of many morphometric parameters which in turn, are reflections of sum effect of elevation, slope, lithology, structural features, vegetation, climate and hydrological conditions. Based on regression analysis the following relationship between fraction landslide area (LS) and drainage texture (DT) has been worked out.

$$LS = 0.0279 + 0.0052\ DT \qquad (3.3)$$

This relationship when tested to estimate fraction landslide area in four randomly selected drainage basins in the area was found to be useful within the error limit of 25 percent.

CHAPTER - 4

TYPE AND PROCESS OF SLOPE MOVEMENT - A MORPHOMETRIC APPROACH

4.1 INTRODUCTION

The importance of geomorphic parameters has already been described in chapter-3. In the study of stability of hillslopes of a watershed among all the morphometric parameters, the drainage texture, which directly depends upon drainage density and stream frequency, is the most significant parameter of a terrain, as an indicator of instability. It is affected by factors like slope, nature of rocks, structural features, climatic condition, vegetation and hydrological characteristics of the terrain. This single parameter can be used to estimate fractional landslide area in a drainage basin. Higher the drainage texture, higher is the probability of landslide in a basin. Despite its usefulness as an indicator of instability of a terrain on regional three dimensional basis, this parameter can not be used to study instability condition at local level of a particular hillslope section. Also, it does not indicate the nature or type of failure and the processes of instability of a hillslope. Nevertheless, it indicates that morphological features can be very useful in the investigation of stability of hillslopes.

Crozier (1973) investigated the slope morphology of sixty six landslips in a terrain made up largely of concavo-convex slopes with very few bed rock outcrops and free faces, in New-

zealand. His detailed study indicated the usefulness of slope morphology in identifying slope movement processes. In the present investigation, a similar approach has been made on sixty slope sections of the area characterised by rugged topography, steep sided valleys, sharp ridges and free faces, madeup largely of bedrock outcrops with a thin soil and regolith cover. With the hypothesis that slope processes continually sculpture the face of the slope, the facial expression of slope may give the clues regarding the nature or type of movement acting on it.

4.2 SLOPE PROFILES AND GENETIC PROCESSES

It has been observed that the slope profiles generally have two segments. The upper segment is convex and the lower concave, as viewed from above. However, some slopes show a straight segment between its upper and lower segments. Darlymple et al. (1968) identified a total of nine slope segments (Fig. 4.1). In this generalised classification each slope segment or component is associated with a particular assemblage of processes. The upper slope profile segments 1 and 2 are gently sloping (upto 4°) summit part of the slope, characterised mainly by pedogenetic and water seepage processes. Segment 3 with slopes at high angles (but less than 45°) is associated with creep phenomenon. Segment 4 is steeply sloping part (normally with slopes over 65°) and is dominated with fall processes. Segment 5 with slopes frequently at angles between 25-35° is associated with mass wasting or movements (flow slide, slump creep). Fan formation by redeposition of material by mass movement is found in segment 6.

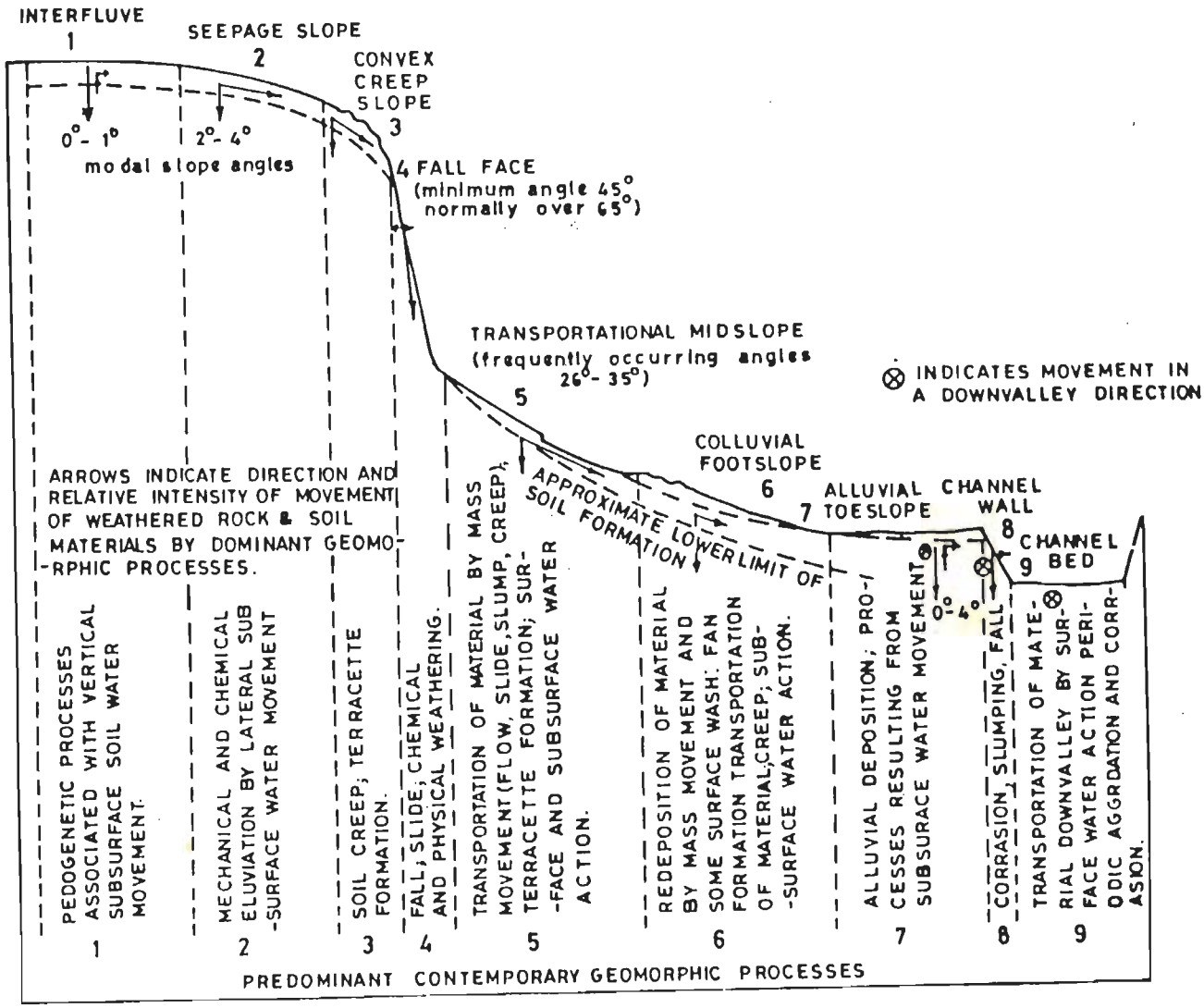

Fig. 4.1: DIAGRAMMATIC REPRESENTATION OF A HYPOTHETICAL NINE UNIT LAND-SURFACE MODEL (DALRYMPLE, ET AL., 1968)

Segment 7 is characterised by alluvial deposition. Corrasion slumping and fall are observed in the channel wall segment number 8 and channel bed processes of transporation and deposition are associated with the segment 9.

Under different climatic and morphogenetic conditions, different combinations of these segments may be found in a slope section. A semi-arid slope may consist of segments 1,4,5,6 and 7, in which slope wash and rock fall are dominant. In humid-temperate climatic conditions, the phenomenon of creep assumes significance with the slope segments 1,2,3,5,7,8 and 9 forming slope profile.

As mentioned earlier, Crozier (1973) carried out a study of various form characteristics of shallow slope movements in the south Island of Newzealand. Most of these landslides exhibited translational flow movement. He observed that the morphology of landslip is closely related to its dominant genetic processes. With this as an aim to characterise the degree and type of movement, using morphometric parameters, he carried out intensive studies and developed six indices (Table 4.1) and five process groups (Table 4.2) namely fluid flow, viscous flow, slide flow, planar slide and rotational slide for 66 failed slopes using the descriptive criteria of Varnes (1958).

The morphometric indices used by Crozier can be calculated using measurements defined and indicated in Figure 4.2. Based on these studies, Crozier (1973) proposed limiting values of various

indices (Table 4.3) to identify different types of slope movement.

Table 4.1: Morphometric Indices (Crozier, 1973)

Morphometeric Parameter	**Measured as**
Classification Index	$D/L \times 100\%$
Dilation Index	W_x/W_c
Tenuity Index	L_m/L_c
Flowage Index	$\left\lvert \frac{W_x}{W_c} - 1 \right\rvert \frac{L_m}{L_c} \times 100\%$
Viscous flow Index	L_f/L_c
Displacement Index	L_r/L_c

for symbols, please refer to Figure 4.2.

Table 4.2: Process Groups used in Morphometric Analysis **(Crozier, 1973)**

Process Group	**Class of Movement**
Fluid-Flow (FF)	Mud flows, debris flow, debris avalanches
Viscous-Flow (VF)	Earth flows, bouldery earth flows
Slide-Flow (SF)	Slump/flow
Planar Slide (PS)	Turf glide, debris slide, rock slide
Rotational Slide (RS)	Earth and rock slumps

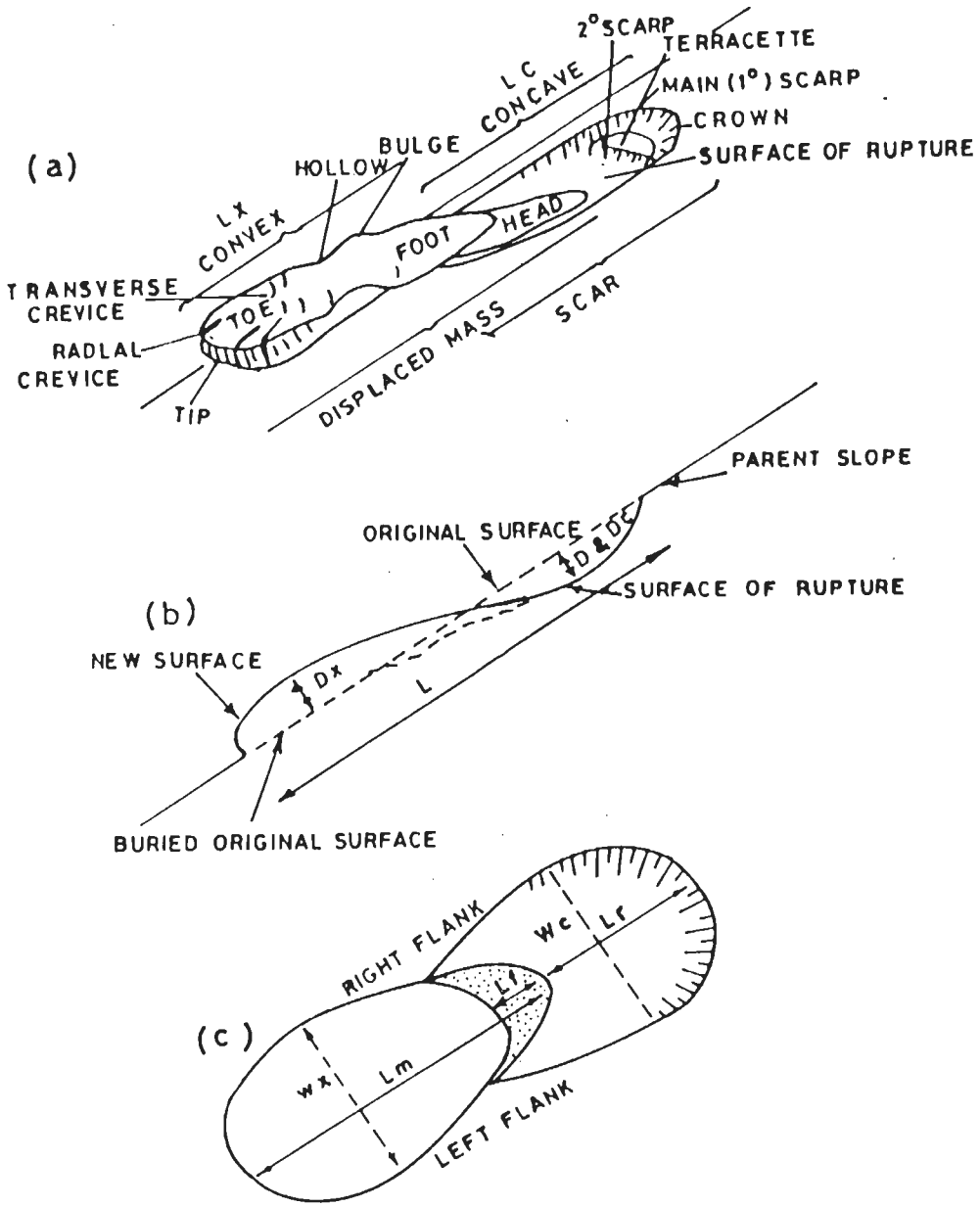

Fig. 4.2: TERMINOLOGY USED IN THE MORPHOMETRIC CLASSIFICATION (CROZIER, 1973)

Table 4.3: Statistical Summary of the Values Calculated for the **Morphometric Indices of the Landslips found in Eastern Otago (After Crozier, 1973)**

Morphometric Index		Process Group				
		RS	PS	SF	VF	FF
Classification Index	m	24.23	7.66	4.98	3.34	1.47
	s	19.28	5.92	1.95	1.39	1.00
	m+s	43.51	13.58	6.93	4.73	2.47
	m-s	4.95	1.74	3.03	1.95	0.47
Dilation Index	m	0.99	0.95	0.94	1.09	0.89
	s	0.10	0.09	0.19	0.37	0.41
	m+s	1.09	1.04	1.13	1.46	1.30
	m-s	0.89	0.86	0.75	0.72	0.48
Flowage Index	m			16.01	5.39	12.14
	s			5.88	4.57	10.59
	m+s			21.89	9.96	22.73
	m-s			10.13	0.82	1.55
Displacement Index	m	68.10	79.87	56.89	29.28	59.06
	s	12.03	6.00	20.47	30.30	30.87
	m+s	80.13	85.87	77.36	59.58	89.93
	m-s	56.07	73.87	36.42	0	28.19
Viscous Flow Index	m				3.66	
	s				2.41	
	m+s				6.07	
	m-s				1.25	
Tenuity Index	m	13.19	1.17	3.07	1.71	3.33
	s	24.15	0.04	0.20	0.71	1.94
	m+s	37.34	1.21	3.27	2.42	5.27
	m-s	0	1.13	2.87	1.00	1.39

m = mean
s = one standard deviation
RS = Rotational Slide
PS = Planar Slide
SF = Slide-Flow
VF = Viscous-Flow
FF = Fluid-Flow

4.3 SLOPE PROFILE MORPHOMETRY AND LAND INSTABILITY OF THE TERRAIN

As discussed above, Crozier (1973) established relationship between the landslip form and landslip processes and developed morphometric indices on the basis of his studies in a terrain of low relief with thick mantle cover in New Zealand. In the present terrain of high relief, rugged topography, poor soil and regolith cover, a similar approach has been made on the basis of sixty transverse slope profiles in the twelve randomly selected drainage basins with known slope instability conditions (Appendix -IV). Toposheets number 53J/8 and 53J/12 of Survey of India were enlarged to the scale of 1:3250 and slope profiles prepared along the zones of weaknesses occupied by drainage for this investigation. The five morphometric indices defined and measured on the profiles are depicted in Figure 4.3. A brief description of these indices is given herewith.

4.3.1 The Classification Index

The classification index is defined as the ratio of maximum depth (D) of the displaced mass, prior to its displacement (true depth), to the overall length or maximum length (L) measured up the slope, expressed as percentage (Fig. 4.3).

This is the most readily derived morphometric parameter which was used for the first time by Skewpton (1953) for the investigation of landslips in the boulder clay of west Durham, England. According to him "The geometry of landslopes may be characterised by the ratio of the maximum thickness of moving mass to the length as measured up slope." Later on the importance of classification index D/L ratio has been

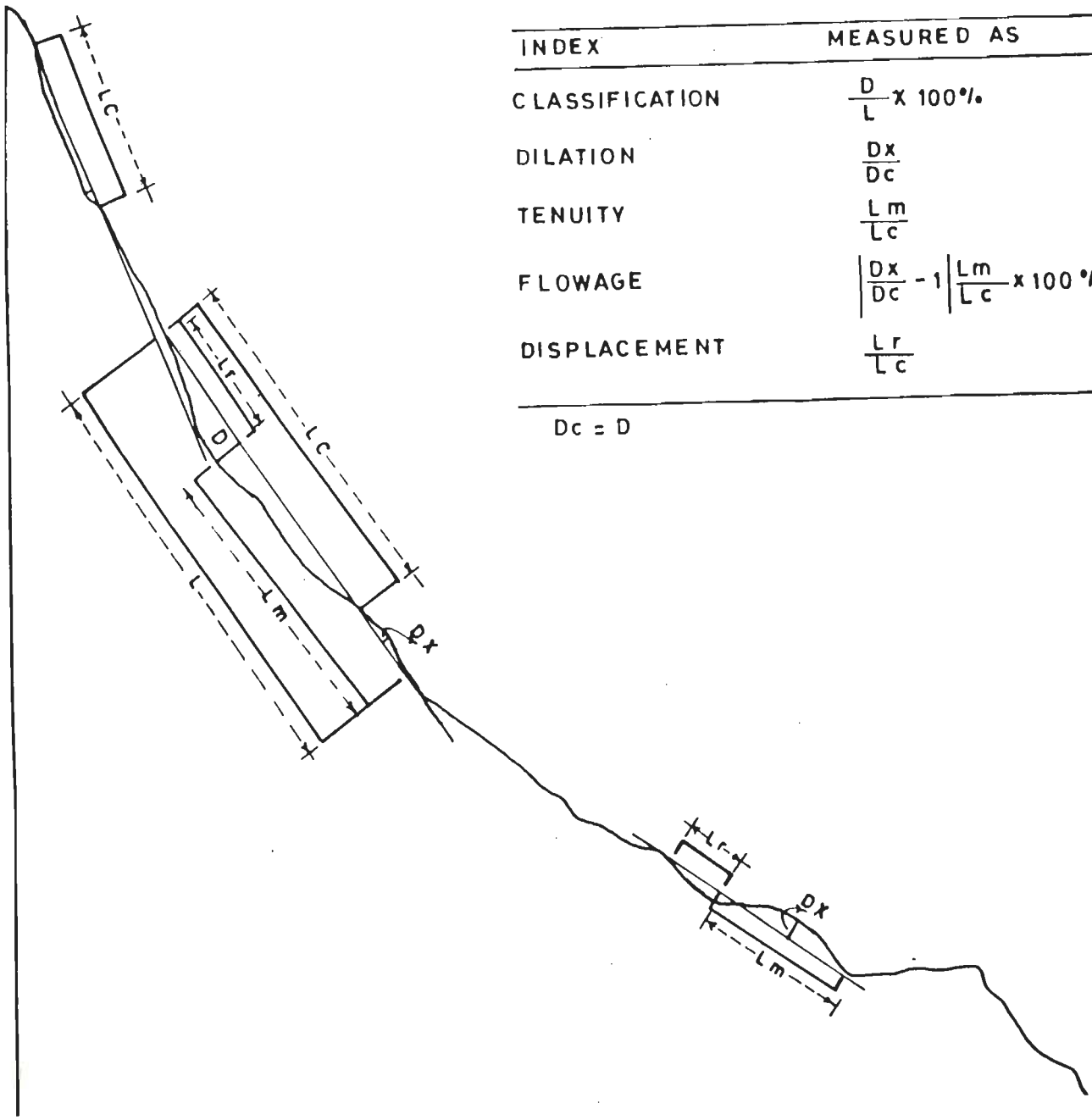

INDEX	MEASURED AS
CLASSIFICATION	$\frac{D}{L} \times 100\%$
DILATION	$\frac{Dx}{Dc}$
TENUITY	$\frac{Lm}{Lc}$
FLOWAGE	$\left\lvert\frac{Dx}{Dc} - 1\right\rvert \frac{Lm}{Lc} \times 100\%$
DISPLACEMENT	$\frac{Lr}{Lc}$

$Dc = D$

Fig.4.3: LANDSLIP TERMINOLOGY AND MEASUREMENTS USED IN THE MORPHOMETRIC INDICES

investigated by Seleby (1967), Mclean and Davidson (1968), Crozier (1968, 1969a, 1969b, 1973), Cooke and Doornkamp (1974) and East (1978).

Skempton (1953) found D/L ratios a suitable means of distinguishing between the "surface slip", and `slumps'. The D/L ratios in classification of processes was also emphasized by Seleby (1967) for the Waikato hill country of Newzealand.

In the present study the D/L ratio was worked out for 60 individual slips derived from profiles drawn from topographic contour map prepared in the scale of 1:3250. The dominant process were confirmed through field checks at various locations in the area of study. Mean value of classification Index (D/L) was found for each group (Table 4.9). It is observed that D/L ratio averaging 7.68, 7.22, 4.39 and 1.88 are characteristic values of Rotational slide, Planar slide, Slide flow and Fluid flow respectively. A comparison of the average values for depth/length ratio with those given by Crozier (1973) is shown in Table 4.4.

Table 4.4 :Comparison of the Mean Values for Classification Index

Process Group	**Present study (D/L)**	**Crozier (1973) (D/L)**
Rational Slide (RS)	7.68	24.23
Planar Slide (PS)	7.22	7.66
Slide Flow (SF)	4.39	4.98
Viscous flow (VF)	D.N.	3.34
Fluid flow (FF)	1.88	1.47

D.N. = Data not available

A perusal of Table 4.4 indicates that barring the Rotational slide, D/L ratio in the present study is comparable with those given by Crozier (1973) for other process group. The difference in D/L values for Rotational slide may possibly be due to the marked difference in the geological field conditions. The terrain in the present area of study is characterised by immature, rugged topography with thin mantle of weathering products of the underlying rocks or slope deposits and therefore shallow slope movements, as compared to the area studied by Crozier (1973) which is characterised by a thick mantle of loess or loess derived regolith in which deep, viscous earth flows were more common than shallower movements. It may also be due to difference in climatic conditions.

4.3.2 The Dilation Index

Crozier defined and calculated the dilation index as the ratio of W_x/W_c, where W_x represent the width of convex part and W_c the width of concave part in longitudinal slope section. However, in the present study dealing with the two dimensitional transverse slope section, it is proposed and defined as the ratio of maximum height of convex part (D_x) and the maximum depth of concave part (Dc) with respect to parent slope (Fig. 4.3).

The D_x/D_c ratio is designated primarily to help in flow studies. It is precisely a measure for landslip shape, and hence a useful parameter to identify the movement processes. It is observed that D_x/D_c ratio averaging 0.35, 0.36, 0.70 and 1.78 are characteristic values of rotational slide, planar slide, slide

flow and fluid flow respectively.

Table 4.5: Comparison of Mean Values of Dilation Index

Process Group	Present study (D_x/D_c)	Crozier (1973) (W_x/W_c)
Rotation slide (RS)	0.35	0.99
Planar slide (PS)	0.36	0.95
Slide flow (SF)	0.70	0.94
Viscous flow (VF)	D.N.	1.09
Fluid flow (FF)	1.78	0.89

D.N. = Data not available

The spreading of the flowing mass in the form of channel-like body or fan-like body on the slope face depends on the slope angle, the degree of saturation and the thickness of soil cover. If potential moving mass of small thickness becomes highly saturated during rainy season on the relatively steeper slopes, the flow characteristically becomes channel-like. This is indicated by high value of dilation index for fluid flow. The area has such a feature and therefore has relatively higher value of dilation index for fluid flow as compared to the area of low relief, low gradient and thick mantle cover described by Crozier.

4.3.3 The Flowage Index

The flowage index is defined here as product of $|D_x/D_c-1|$ x L_m/L_c x 100%, where L_m is the length of displaced material or convex part and L_c the length of concave part (Fig. 4.3). In

case $D_x/D_c = 1.0$, the increase over 1.0 of L_m/L_c alone may be taken and treated as flowage index as has been opined by Crozier (1973).

On the basis of the known behaviour of viscous fluids, and on what has been observed at some locations in the field, it is expected that the value derived from this formula will reflect the fluidity (controlled by the water content) and the effect of slope angle and thus speed of action at the time of landslip occurrence. For a particular slope angle, the more fluid like the material is at the time of displacement, the more deformation is likely to occur. Deformation is measured by D_x and L_m, compared to their original values as indicated by D_c and L_c respectively. It is considered that a deviation from a value of 1.0 in case of D_x/D_c and increase over a value of 1.0 with L_m/L_c, is proportional to the amount of deformation that has occurred in the displaced material. By way of explanation, if the displaced mass is very fluid and lateral spreading consequently occurs the value of D_x/D_c will be less than 1.0. Thus, any value derived from the formula will measure the flowage of a landslip as indicated by lateral deformation in reference to its tenuity (measured by L_m/L_c) or in other words, it is a measure of biaxial spread. This value will increase with the slope angle and therefore does not offer a measure of fluidity, but rather the amount of flowage which in turn indicates relative velocity. The flowage index when applied to rotational slide and planar slide may indicate mutual displacement of individual components within

the displaced material.

Mean values of twenty seven landslips involving flows were computed (Table 4.9). It is observed that flowage index averaging 73.94 and 215.95 are characteristic values of slide flow and fluid flow respectively. A comparison of the average values for flowage index of twenty seven landslips with those given by Crozier (1973) is presented in Table 4.6.

The large difference in flowage index value may be due to difference of geological field conditions. As mentioned earlier, the present area is characterised by high gradient and thin mantle cover as against the area studied by Crozier (1973), which is characterised by thick mantle cover, low relief and low gradient.

Table 4.6: Comparison of the Mean Values for Flowage Index

Process Group	Present study Flowage Index Value	Crozier Flowage Index Value
Slide flow (SF)	73.94	16.01
Viscous flow (VF)	D.N.	5.39
Fluid flow (FF)	215.95	12.14

D.N. = Data not available

4.3.4 The Displacement Index

The displacement index is defined as ratio between length of surface of rupture (L_r), exposed in the concave part, and L_c,

length of the concave part (Fig. 4.3).

This ratio can give a measure of the amount of displacement of the material from its original position on slopes. Any material retained within concave part of slope is highly unstable and likely to be reactivated. This may be due to collection of water in the concave part, which saturate pores and increases pore water pressure and decreases the strength of the mass. The steepness of the slope near crown at the contact with the surface of rupture further adds to the instability. Thus, this parameter can also assess the equilibrium state of landslip and gauge the likelihood of renewed movement, and thereby it helps in indicating the probable stage of development of landslip. A value of 100% for this ratio, therefore, indicates, the most stable situation, where material has been entirely removed from the concave part. While the lower values of slip displacement with respect to the each group mean indicate unstable condition, where the material has partly been removed from concave part. In the present investigation, the mean values of 48.04, 73.31, 54.25 and 53.22 for rotational slide, planar slide, slide flow and fluid flow respectively were taken as a level below which any displacement value will indicate an unstable landslip. A comparison of average values for diplacement index for sixty landslips with those given by Crozier (1973) is presented in Table 4.7.

Table 4.7: Comparison of the Mean Values for Displacement Index

Process Group	Present study (L_r/L_c)	Crozier (L_r/L_c)
Rotational slide (RS)	48.04	68.10
Planar slide (PS)	73.31	79.87
Slide flow (SF)	54.25	56.89
Viscous flow (VF)	D.N.	29.28
Fluid flow (FF)	53.22	59.06

D.N. = Data not available.

4.3.5 The Tenuity Index

The tenuity index is the ratio of L_m/L_c, where L_m represents the length of displaced material or convex part and L_c the length of concave part (Fig. 4.3).

This index will reflect tenuity of the displaced mass in relation to its original size (determined by L_c). Although tenuity is affected by fluidity of the displaced material at the time of landslip occurrence, the index could not be considered as true measure of fluidity because it does not take into account lateral spreading or the effect of slope inclination. Nevertheless, it has the potential of indicating the effect of slope inclination and the micro-relief features conducive to channeling flow downslope.

Mean of tenuity index of each group was computed (Table 4.9). It is observed that L_m/L_c ratio averaging 1.20, 0.62, 1.62

and 2.37 are found associated with rotational slide, planar slide, slide flow and fluid flow respectively. A comparison of the average values for L_r/L_c for sixty landslips as against those given by Crozier (1973) is presented in Table 4.8.

Table 4.8: Comparison of the Mean Values for Tenuity Index

Process Group	Present study (L_m/L_c)	Crozier (L_m/L_c)
Roational slide (RS)	1.20	13.19
Planar slide (PS)	0.62	1.17
Slide flow (SF)	1.62	3.07
Viscous flow (VS)	D.N.	1.71
Fluid Flow (FF)	2.37	3.33

4.3.6 Statistical Summary of Slope Morphometric Indices

The slope profile morphometric indices based on sixty landslips, thus worked out for each of the slope movement process group, have been statistically tested for their significance and presented as mean and standard deviation in Table 4.9. These modified indices may be terrain specific and may be used in similar hilly terrains with rugged topography, high relief and poor soil cover of the Lesser Himalaya and foothills.

A perusal of Table 4.9 indicates that no single morphometric index can be used to predict slope movement process. A combination of these can help in identification of the slope movement and processes involved in it. However, field observation

Table 4.9 : Statistical Summary of Morphometric Indices of Each **Process in the Area of Study (Modified after Crozier, 1973)**

Morphometric Index		Process Group			
		RS	PS	SF	FF
Classification Index	m	7.68	7.22	4.39	1.88
	s	2.61	3.76	0.91	0.46
	m+s	10.29	10.98	5.30	2.34
	m-s	5.07	3.46	3.84	1.42
Dilation Index	m	0.35	0.36	0.70	1.78
	s	0.13	0.23	0.23	0.85
	m+s	0.48	0.59	0.93	2.63
	m-s	0.22	0.13	0.47	0.93
Flowage Index	m	75.92	44.00	73.94	215.95
	s	15.82	17.32	39.82	195.11
	m+s	91.47	61.32	113.76	411.06
	m-s	60.1	26.68	34.12	20.84
Displacement Index	m	48.04	73.31	54.25	53.22
	s	14.12	16.80	16.43	14.70
	m+s	62.16	90.11	70.68	67.92
	m-s	33.92	56.51	37.82	38.52
Tenuity Index	m	1.20	0.62	1.62	2.37
	s	0.11	0.24	0.44	1.20
	m+s	1.31	0.86	2.06	3.57
	m-s	1.09	0.38	1.18	1.17

m = mean
s = one standard deviation
RS = Rotational Slide
PS = Planar Slide
SF = Slide-Flow
FF = Fluid-Flow
FF = Fluid-Flow

suggests that the displacement index can give indication about stability of hill slopes. Slopes are likely to fail by rotational slide if displacement index (DPI) is less than 48.04, by planar slide, if DPI is less than 73.31, by Slide flow, if DPI is less than 54.25 and by fluid flow, if DPI is less than 53.22 .

4.3.7 Test Cases

With a view to evaluate the usefulness of the proposed critical limits of various slope morphometric indices, three test areas namely the Mussoorie by pass, the Kaliasaur and the Chilla hillslope were subjected to this investigation. In order to remove subjectivity or human bias, the geologists of Central Building Research Institute, Roorkee were approached to test the usefulness of the proposed indices. The efficacy of these modified values of various slope morphometric indices (Table 4.9) as critical limits for prediction of slope movement processes involved in landslide was established in all the three landslide areas of similar topography. A brief description of these sites are given below:

Test Site I- Mussoorie By pass: This slide area (Fig. 4.4) is located 122 km NNW of the area of study. Geologically, rocks exposed in and around the slide area, belong to Late Precambrian age of dolomite and dolomite limestone. The eastern and western sides of the slide zone consist of hard and compact dolomite, whereas the central region contains moderate to highly weathered dolomites covered with colluvium and debris. The beds dip

northwesterly ranging from 20° to 45°. The rocks in this zone show numerous types of folds in a stretch of 150 m along the road. The structural features in this area show the presence of plunged overturned and recumbent folds. As a result the rocks get fractured and pulverised. There appears to be two fault zones in NNW and SSE directions which hade towards each other. The bulging in the central zones of the slide area may be due to effect of these two high angles faults. Both the faults meet at toe. In addition, two sets of joint pattern are commonly present in the rocks of the slide area.

Elevation contour map of the area was prepared on the scale of 1:1200 with 5 m contour interval. The study has shown the presence of some newly formed stream of first and second order passing through the landslide area. These two second order streams ultimately meet at toe to form a third order stream.

Slopes were analysed with the help of morphometric indices as shown in Table 4.10. On interpretation, using Table 4.9, the dominant type of movement works out to be rotational slide as indicated by classification and tenuity indices. The slope movement reactivate due to its low value of displacement index of 35.9. This prediction was found out to be correct on field checks.

Table 4.10: Landslip Morphometric Indices at Mussorrie By pass

Morphometric Index	Process Group			
	RS	PS	SF	
			S_1	S_2
Classification Index	5.9	6.5	6.5	3.4
Dilation Index	0.35	0.44	1.2	1.01
Flowage Index	40	13	140	173
Displacement Index	35.9	84.4	72	70.7
Tenuity Index	1.14	0.32	1.16	1.7

RS - Rotational Slide PS - Planar slide SF-Slide Flow
S - Slope section 1,2 - Slope section number

Test Site II- Kaliasaur Slide: The slide area (Fig. 4.5) is located about 80 km NNE of the area of study (at km 147 on Hardwar-Badrinath road). Geologically, this landslide is located in Garhwal group of rocks. The main rocks in this area are purple white and light green quartzite, interbedded with maroon shales. Quartzites in western side of the slide zone have a general southward dip with amount ranging from 25° to 60°. These quartzite end up abruptly along a scree zone, beyond which massive well jointed purple quartzites dipping southeast ranging from 30° to 40° are exposed and continue up to western flank of slide zone where they end up against the slide debris. On the eastern side of the slide zone, the quartzite exposed have maroon shales with southeasterly dip ranging from 30° to 60° and end up

abruptly against a small scree zone and reappear in massive form with a southeasterly dip of 30° to 40°. Structural features in the area show presence of a fault with a roughly E-W trend which passes through the crest of slide zone.

Elevation contour map of the slide area was prepared on the scale of 1:1200 with 5 m contour interval. The study has shown the presence of some old and newly formed streamlets over the escarpment which meet the river at high angle. Indices obtained on the basis of slope profile (Table 4.11) suggested that dominant mode of movement is planar slide as inferred by classification and Tenuity indices. The movement can reactivate as indicated by low value of displacement of 38. The conclusion drawn was confirmed through field check at this location.

Table 4.11 : Landslip Morphometric Indices at Kaliasaur

Morphometric Index	Process Group		
	FF	PS	
		S_1	S_2
Classification Index	2.53	10.7	8.04
Dilation Index	2	1.3	0.85
Flowage Index	501	14.9	28.4
Displacement Index	63	69	38
Tenuity Index	3.1	0.62	0.71

FF - Fluid Flow
S - Slope section
PS - Planar Slide
1,2 - Slope section number

Fig. 4.4 : Panoramic View of Mussoorie Bypass

Fig. 4.5 : Panoramic View of Kaliasaur

Test Site III- Chilla Slide: The slide area (Fig. 4.6) is located about 57 km SSW of the study area. The rocks exposed in the slide area consist predominantly of sandstone and shale, belonging to Subathu Formation of Eocene age. The outcrops are found exposed near the slip surface and in the lower horizons.

The shales are generally moderate to highly weathered and fractured associated with hard sandstone. The inclination of the beds is towards the hill with E-W strike and 20° - 30° dip towards south. At many places, the presence of sheared and pulverised material indicated possibility of presence of shear zone, but the extent and nature could not be traced out precisely due to lack of continuous rock exposure on slip region and also due to thick vegetation cover at some locations in form of trees and bushes. However, based on the variations in the attitude of the beds, the presence of fold as well as shear zone in the slip region can not be ruled out.

Elevation contour map of the area was prepared on the scale of 1:2000 with 5 m contour interval. The slide zone is characterised by presence of small as well as large streamlets which usually meet the river at high angle. Morphometric analysis based on slope profiles indicated that this location is characterised by complex mode of failure involving fluid flows, slide flow. Rotational slide is associated with planar slide. These modes of failures are inferred using classification, Dilation and Tenuity indices. The possibility of its reactivation is inferred by low valus of Displacement index for

Fig. 4.6 : Panoramic View of Chilla

each process group which is estimated to be 24.19, 45.5, 28.30, and 35 for rotational slide, planar slide, slide-flow and fluid flow respectively (Table 4.12). The prediction proved to be correct on field checks.

Table 4.12 : Landslip Morphometric Indices at Chilla

Morphometric Index	Process Group							
	RS		PS			SF	FF	
	S_1	S_2	S_1	S_2	S_3		S_1	S_2
Classification Index	6.44	6.68	5.3	4.3	6.34	4.12	2.2	2.4
Dilation Index	0.49	0.42	0.35	0.47	0.54	0.48	2	1.7
Flowage Index	96.65	65.03	69.03	49.47	65.03	64.32	401	469
Displacement Index	24.19	63.60	66.80	45.50	66.90	28.30	49.3	35
Tenuity Index	1.67	1.5	0.86	0.88	0.81	1.27	1.88	3.3

SF - Slide flow
S - Slope section
FF - Fluid Flow
1,2,3 - Slope section number

4.3.8 Inference

The interpretations regarding slope movement processes made on the basis of modified slope morphometric indices (Table 4.9), particularly classification, Dilation, Displacement and Tenuity indices have proved their efficacy on field checks for all the three test sites mentioned above. Beside this, the study has shown that the displacement index can indicate the state of stability of slope. A slope becomes unstable if the displacement index is less than 48.04, 73.31, 54.25 and 53.22 for rotational slide, planar slide, slide flow and fluid flow respectively. It

also appears that flowage index within slide process group (RS and PS) indicate the degree of surficiality and speed of failure action, i.e. higher the flowage value from its mean, more the surficial and faster will be the movement. However, further field observation is needed to confirm its validity.

4.4 MULTIVARIATE DISCRIMINATION CRITERIA FOR SLOPE MOVEMENTS

The usefulness of the various morphometric indices towards prediction of various slope movement processes has been demonstrated in the three test areas. However, it is evident that one single index is not good enough to identify such processes. There is, therefore, a need to develop a simple multivariate statistical criteria to differentiate between two similar slope movement processes employing all the five slope morphometric indices simultaneously. The technique of discriminant function analysis has been applied to achieve this goal. The basic philosophy of this technique is briefly mentioned here.

4.4.1 Philosophy of Discriminant Function Analysis

If there are two data groups of known origin, and each group contains number of variables. The problem therefore, would be to find out a linear combination of these variables producing the maximum difference between two previously defined groups. If one can find a function which produces a significant difference, then it can be used to allocate new samples of unknown origin into one of the original groups.

A linear discriminant function transforms an original set of

mesurements on a sample into a single discriminant score. This score or transform variable represents the sample's position along a line defined by the linear discriminant function. Therefore, discriminant function is a way of collapsing a multivariate problem down in to a problem which involves only one variable. A good mathematical account of this method is given by Kendall (1946), Rao (1952) and Davis (1973).

This method gives a linear combination $R = \sum_{i=1}^{n} a_i x_i$ in which X_i (i= 1,2,3 .....,n) are the `n' discriminant variables. Then the discriminant constant as are chosen in such a way so that the mathematical distance between the clusters of points of two groups is maximized and at the same time the spread within each cluster is minimised.

Knowing `a_i', the discriminant scores R_i (i=1,2,3,....,n) can be computed for the samples of both the groups. A discriminant index R_o which is a point along the discriminant function line, and is exactly halfway betwen the center of group one and center of group two, is worked out and is used as criteria to differentiate between two groups. The domain of one group is characterised by discriminant scores more than R_o while in the other group, values are less than R_o. A `distance' measure which is called `Mahalnobs' or generalized distance D^2, between the means of the discriminant scores R_1 and R_2 of the two groups is worked out as the difference between R_1 and R_2. The significance of separation between the two groups' means is tested through well known F-statistic.

4.4.2 Application of Discriminant Function Analysis

This technique has been used in the present study to workout the discriminant functions and criteria to allocate an unknown sample (slope section) to one of the groups of all possible slope movement processes, based on simultaneous use of five morphometric indices determined for 60 slope section samples.

The discriminant constants determined for various pairs of movement processes are summarised in Table 4.13. The discriminant score means and distance measure, D^2 found in this investigation are presented in Table 4.14.

Table 4.13 : Discriminant Constants for Discrimination Between **Various Slope Movement Process Group**

Morphometric index	Discriminant Constant for different pair of process group					
	FF VS SF	FF VS PS	FF VS RS	SF VS PS	SF VS RS	PS VS RS
Classification index (c)	5.5931	1.0535	3.0603	1.1906	1.4086	-0.5306
Dilation index (d)	-4.2424	-7.6783	-11.3112	2.1812	-9.9840	-13.5728
Flowage index (f)	0.0100	0.0346	0.0579	-0.0592	-0.0084	-0.0171
Displacement index (s)	0.0342	0.0432	-0.1196	0.0412	-0.0086	-0.0033
Tenuity index (f)	-0.0669	-4.8809	-5.2498	-9.8985	-2.3680	22.346

FF = Fluid-Flow, SF = Slide Flow,
PS = Planar Slide, RS = Rotational Slide

c,d,f,s,t are the variables indicating classification, dilation, flowage, displacement and tenuity indices.

4.4.3 Discriminant Function and Discriminant Criteria

Based on discriminant constants (Table 4.13) and mean discriminant scores of pairs of groups (Table 4.14), the discriminant function and the criteria to differentiate one process against the other have been worked out as hereunder:

Table 4.14 : Discriminant Score Means and Distance Measure D^2

Discriminant Score Parameter	Pairs of Slope Movement Process Group					
	Group 1 2 SF FF	Group 1 2 PS FF	Group 1 2 RS FF	Group 1 2 PS SF	Group 1 2 RS SF	Group 1 2 RS PS
R_1	23.9809 (SF)	6.3437 (PS)	9.7212 (RS)	3.7887 (PS)	2.4181 (RS)	16.9234 (RS)
R_2	6.9939 (FF)	-12.6042 (FF)	-19.4752 (FF)	-11.4752 (SF)	-5.7251 (SF)	4.2027 (PS)
R_o	15.4874	-3.1302	-5.0055	-3.8432	-1.6535	10.5630
D^2	16.99	18.95	29.45	15.26	8.14	12.72
F Statistic	19.02	29.25	32.99	20.30	7.99	16.92

R_1 and R_o = Means of Discriminant score of Group 1 & 2 respectively

$R_o = (R_1+R_2)/2$

D^2 = Mahalnobis Distance between two groups

F-statistic - Significant at 1% level

(a) Discrimination Between Fluid Flow (FF) and Slide Flow (SF)

Discriminant Function, R=5.5931c-4.2442d+0.0100f+0.0342s-0.0669t

Mean Discriminant score for SF, R_1 = 23.9809

Mean Discriminant score for FF, R_2 = 6.9939

Mean of R_1 & R_2, R_o = 15.4874 , $R_o = (R_1+R_2)/2$

D^2 = 16.99

F = 19.02

D^2 is significant at 1% level with 5 and 25 degree of freedom, indicating the distance between the two groups is significant.

Discriminant criterion - Let P be the discriminant score of a new slope section

if P < 15.4874, the samples belong to FF

if P > 15.4874, the sample belong to SF

Figure 4.7 depicts the discriminant function as linear plot of scores. Unknown test samples have been correctly plotted and classified to the slope movement group to which these actually belong.

(b) Discrimination Between Fluid Flow (FF) and Planar Slide (PS)

Discriminant Function, R=1.0537c-7.6783d+0.0346f+0.0432s-4.8809t

Mean Discriminant score for PS, R_1 = 6.3437

Mean Discriminant score for FF, R_2 = -12.6042

Mean of R_1 & R_2, R_o = -3.1302, $R_o = (R_1+R_2)/2$

D^2 = 18.95

F = 29.25

D^2 is significant at 1% level with 5 and 30 degree of freedom, indicating the distance between the two groups is significant.

Discriminant criterion - Let P be the discriminant score of a new slope section

if P < -3.1302, the samples belongs to FF

if P > -3.1302, the sample belongs to PS

Figure 4.8 depicts the discriminant function as linear plot of scores. Unknown test samples have been correctly plotted and

classified to the slope movement group to which these actually belong.

(c) Discrimination Between Fluid Flow (FF) and Rotational Slide (RS)

Discriminant Function, R=3.0603c-11.3112d+0.0579f+0.1196s-5.2498t

Mean Discriminant score for RS, R_1 = 9.7212

Mean Discriminant score for FF, R_2 = -19.7323

Mean of R_1 & R_2, R_o = -5.0055, $R_o = (R_1+R_2)/2$

D^2 = 29.45

F = 32.99

D^2 is significant at 1% level with 5 and 21 degree of freedom, indicating the distance between the two groups is significant.

Discriminant criterion - Let P be the discriminant score of a new slope section

if P < -5.0055, the samples belong to FF

if P > -5.0055, the sample belong to RS

Figure 4.9 depicts the discriminant function as linear plot of scores. Unknown test samples have been correctly plotted and classified to the slope movement group to which these actually belong.

(d) Discrimination Between Slide Flow (SF) and Planar Slide (PS)

Discriminant Function, R=1.1906c-2.1812d-0.0592f+0.0412s-9.8985t

Mean Discriminant score for PS, R_1 = 3.7887

Mean Discriminant score for SF, R_2 = -11.4752

Mean of R_1 & R_2, R_o = -3.8432, $R_o = (R_1+R_2)/2$

D^2 = 15.26

F = 20.30

D^2 is significant at 1% level with 5 and 27 degree of freedom, indicating the distance between the two groups is significant.

Discriminant criterion - Let P be the discriminant score of a new slope section

if P < -3.8432, the sample belong to SF

if P > -3.8432, the sample belong to PS

Figure 4.10 depicts the discriminant function as linear plot of scores. Unknown test samples have been correctly plotted and classified to the slope movement group to which these actually belong.

(e) Discrimination Between Slide Flow (SF) and Rotational Slide (RS)

Discriminant Function, R=1.4086c-9.9840d-0.0084f+0.0086s-2.3680t

Mean Discriminant score for RS, R_1 = 2.4181

Mean Discriminant score for SF, R_2 = -5.7251

Mean of R_1 & R_2, R_o = -1.6535 , $R_o = (R_1+R_2)/2$

D^2 = 8.14

F = 7.99

D^2 is significant at 1% level with 5 and 18 degree of freedom, indicating the distance between the two groups is significant.

Discriminant criterion - Let P be the discriminant score of a new slope section

if P < -1.6535, the sample belong to SF

if P > -1.6535, the sample belong to RS

Figure 4.11 depicts the discriminant function as linear plot of scores. Unknown test samples have been correctly plotted and

classified to the slope movement group to which these actually belong.

(f) Discrimination Between Planar Slide (PS) and Rotational Slide (RS

Discriminant Function, R=-0.5306c-13.5728d-0.0171f+0.0033s-22.346t

Mean Discriminant score for PS, R_1 = 16.9234

Mean Discriminant score for SF, R_2 = 4.2027

Mean of R_1 & R_2, R_o = 10.5630 , $R_o = (R_1+R_2)/2$

D^2 = 12.72

F = 16.92

D^2 is significant at 1% level with 5 and 27 degree of freedom, indicating the distance between the two groups is significant.

Discriminant criterion - Let P be the discriminant score of a new slope section

if P < 10.5630, the sample belong to SF

if P > 10.5630, the sample belong to RS

Figure 4.12 depicts the discriminant function as linear plot of scores. Unknown test samples have been correctly plotted and classified to the slope movement group to which these actually belong.

The multivariate discriminant analysis of slope morphometric indices suggest that these indices are fairly effective in distiguishing various process groups.

4.4.4 Discriminant Function as Search Technique

All the discriminant variables included in discriminant

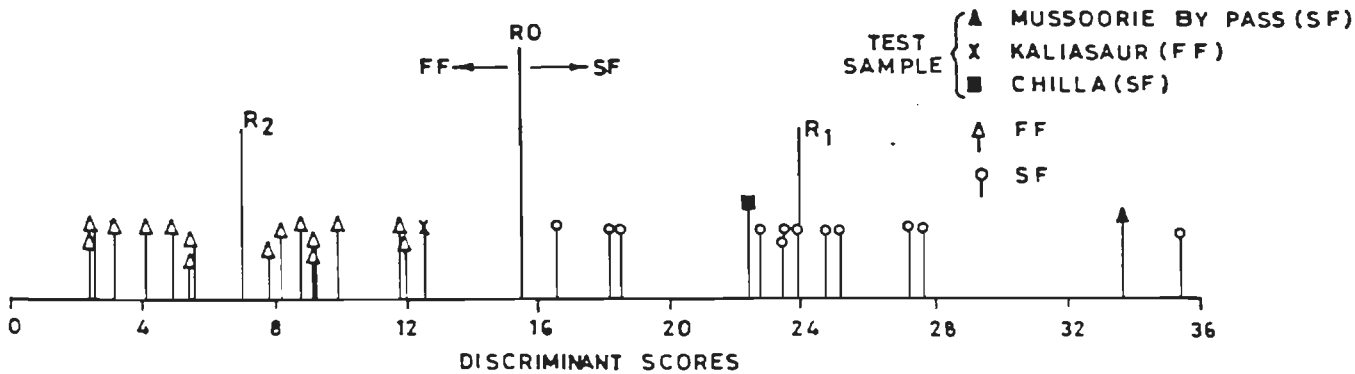

Fig. 4.7: LOCATION OF SAMPLES ON DISCRIMINANT FUNCTION LINE FOR DIFFERENTATION BETWEEN SLIDE FLOW (SF) AND FLUID-FLOW (FF)

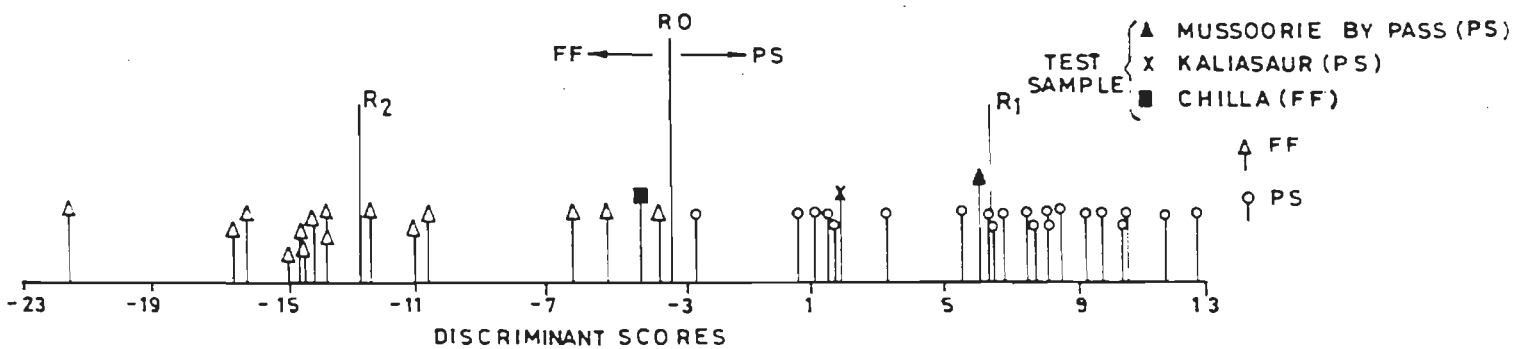

Fig. 4.8: LOCATION OF SAMPLES ON DISCRIMINANT FUNCTION LINE FOR DIFFERENTATION BETWEEN PLANAR SLIDE (PS) AND FLUID-FLOW (FF)

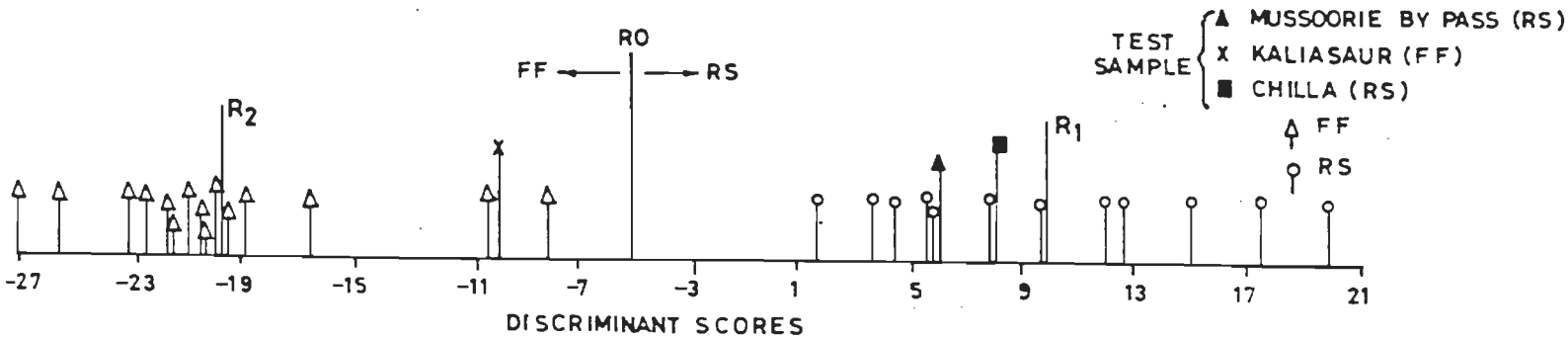

Fig. 4.9: LOCATION OF SAMPLES ON DISCRIMINANT FUNCTION LINE FOR DIFFERENTIATION BETWEEN ROTATIONAL SLIDE (RS) AND FLUID-FLOW (FF)

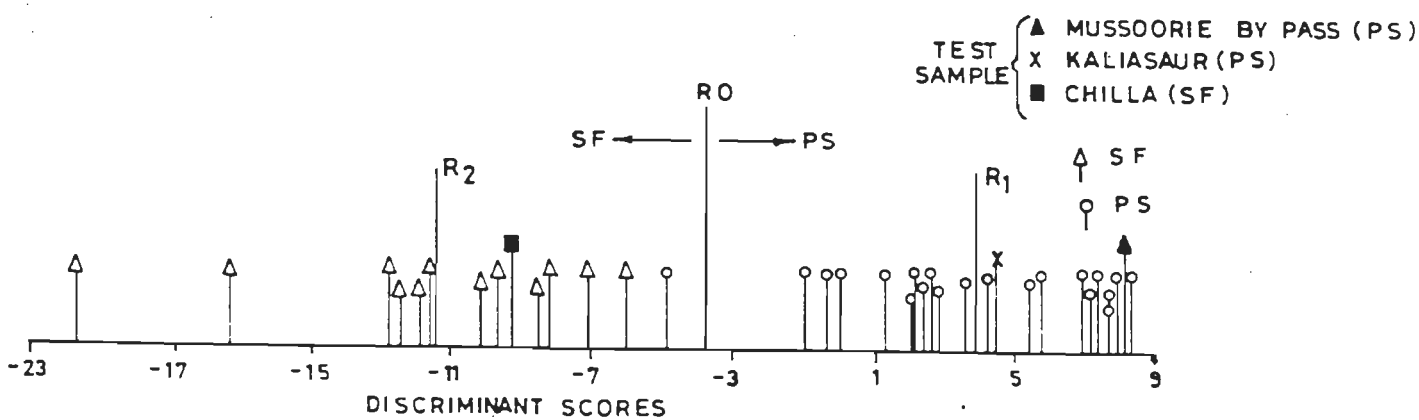

Fig. 4.10: LOCATION OF SAMPLES ON DISCRIMINANT FUNCTION LINE FOR DIFFERENTIATION BETWEEN PLANAR SLIDE(PS) AND SLIDE-FLOW(SF)

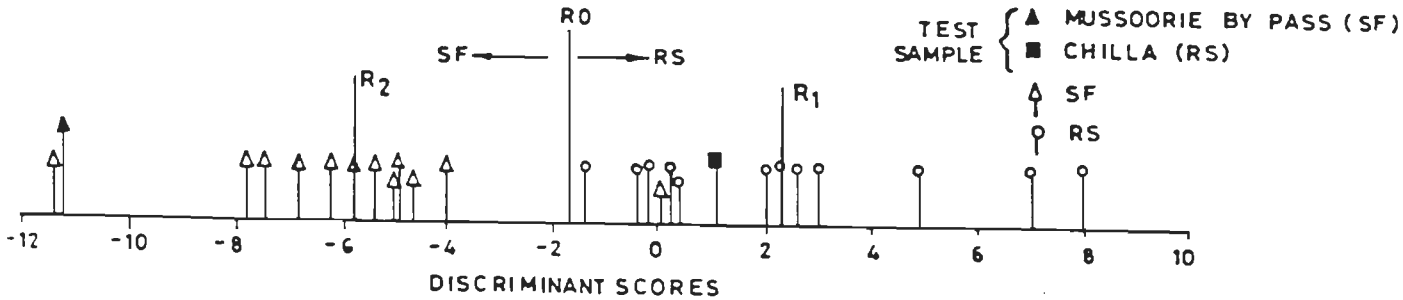

Fig. 4.11: LOCATION OF SAMPLES ON DISRIMINANT LINE FOR DIFFERENTIATION BETWEEN ROTATIONAL SLIDE (RS) AND SLIDE—FLOW (SF)

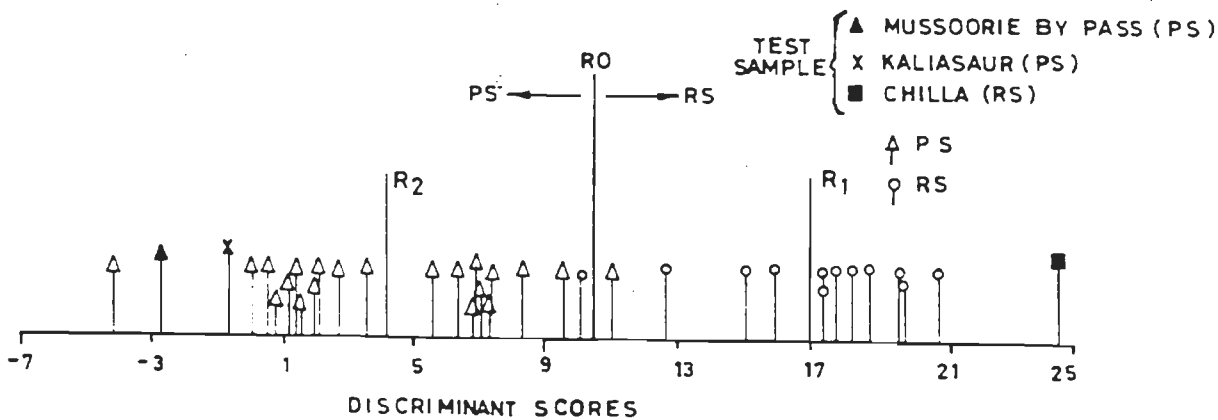

Fig. 4.12: LOCATION OF SAMPLES ON DISCRIMINANT FUNCTION LINE FOR DIFFERENTIATION BETWEEN ROTATIONAL SLIDE (RS) AND PLANAR SLIDE (PS)

function may not be equally useful in distinguishing one group from the other. Therefore, those variables that are not especially helpful may be eliminated to help in easing the computational process. Discriminant analysis can help in identifying meaningful variables from a large set. Following Davis (1973), the relative contribution of variable `j' to the distance between two group means may be measured by a quantity E_j,

$$E_j = \frac{\lambda_j D_j}{D^2}$$

where λ_j is the jth coefficient, and D_j is the difference between jth means of the two groups. This is a measure of only the direct contribution of the variable. It does not consider interaction between variables. If two or more of the variables in the discriminant function are not independent, their interaction may contribute to D^2 to a greater extent than the value E_j suggest. In the present study the percent contribution of each indices in discriminating two slope movement process is presented in Table 4.15.

These contributions help in searching the extent to which variables (in morphometric indices) participate in differentiating two groups on multivariate basis. Hence, as indicated in Table 4.15, the most important indices to discriminate between FF and SF are CI and DI; between FF and PS, are DI, TI and CI; between FF and RS are DI and CI; between SF

and PS are TI and CI; between SF and RS are CI and DI and between PS and RS is TI.

Table 4.15: Relative Contribution of Each Indices to Discriminate **Between Various Slope Movement Process**

Movphometric Index	Pairs of Various Slope Movement Processes					
	FF and SF	**FF and PS**	**FF and RS**	**SF and PS**	**SF and RS**	**PS and RS**
Classification index (CI)	82.6221	29.4801	53.0184	21.7768	44.8594	0.8283
Dilation index (DI)	27.2088	57.7435	55.1029	-4.8009	42.3015	1.0543
Flowage index (FI)	-9.7878	-36.3133	-3.2241	12.7577	-0.2037	-4.6843
Displacement index (DPI)	-0.3381	3.9491	3.2338	5.1536	0.6566	0.6539
Tenuity index (TI)	0.2949	45.1407	20.8689	65.1127	12.2836	102.1479

FF=Fluid FLow, SF=Slide Flow, PS=Planar Slide, RS=Rotation Slide

4.4.5 Bivariate and Univariate Plots As Tools for Discrimination

In discriminating between various process group, classification index followed by Dilation and Tenuity indices are the most important variables. A brief description of the most suitable indices for discrimination between each process group is given below :

a) The most important indices to discriminate between Fluid Flow (FF) and Slide Flow (SF) are classification and Dilation indices (Table 4.15). The bivariate plot (Fig. 4.13) between

these two indices clearly brings out two distinct fields for these slope movement processes. It can be used towards the allocation of any unknown sample to its movemnt class. Test samples when plotted in this plot, were correctly classified in slope movement group to which these actually belonged as observed in the Figure 4.13.

b) The indices which appear to contribute most in the discrimination between fluid flow and planar slide are (Figures 4.14, 4.15 and 4.16) classification, dilation and tenuity indices (Table 4.15). Each of the three, possible bivariate plots between these indices clearly bring out distinct fields for these slope movement processes, which can be used to classify any unknown sample to its movement class. Test samples when plotted in these plots, were correctly allocated to the slope movement group to which these actually belonged, as observed in Figures 4.14, 4.15 and 4.16.

c) The most important indices to discriminate between fluid flow and rotational slide (RS) are classification and dilation indices (Table 4.15). The bivariate plot between these indices (Fig. 4.17) clearly bring out distinct fields for these slope movement processes, which can be used towards the allocation of any unknown sample to its movement class. Test samples when plotted in this plot, were correctly classified into slope movement group to which these actually belonged, as observed in Figure 4.17.

d) The indices which weigh most to discriminate between slide flow (SF) and planar slide (PS) are classification and tenuity

indices (Table 4.15). The bivariate plot between these indices (Fig.4.18) clearly bring out distinct fields for these slope movement processes, which can be used towards the classification of any unknown sample to its movement class. Test samples when plotted in this plot, were correctly classified into slope movement group to which these actually belonged, as observed in Figure 4.18.

e) The most suitable indices to discriminate between slide flow (SF) and rotational slide (RS) are classification and dilation indices (Table 4.15). The bivariate plot between these indices (Fig. 4.19), clearly bring out distinct fields for these slope movement processes, which can be used towards the classification of any unknown sample to its movement class. Test samples when plotted in this plot, were correctly classified into slope movement group to which these actually belonged, as observed in figure 4.19.

f) The most suitable index to discriminate between planar slide (PS) and rotational slide (RS) is tenuity index (Table 4.15). The unvariate plot between these indices (Fig. 4.20) clearly bringout two distinct fields for these slope movement processes, which can be used towards the allocation of any unknown sample to its movement class. Test samples when plotted in this plot were correctly classified into slope movement group to which these actually belonged, as observed in Figure 4.20.

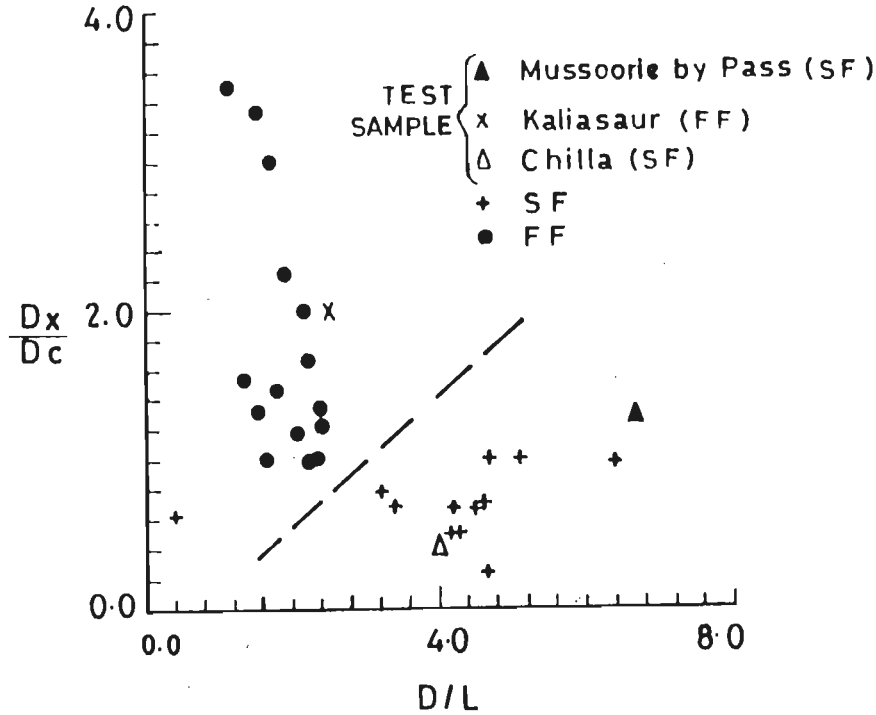

Fig. 4.13: LOCATION OF TEST SAMPLES ON THE BIVARIATE PLOT BETWEEN CLASSIFICATION (D/L) AND DILATION ($\frac{Dx}{Dc}$) INDICES SHOWING DISTINCT FIELDS FOR SLIDE FLOW (SF) AND FLUID-FLOW (FF)

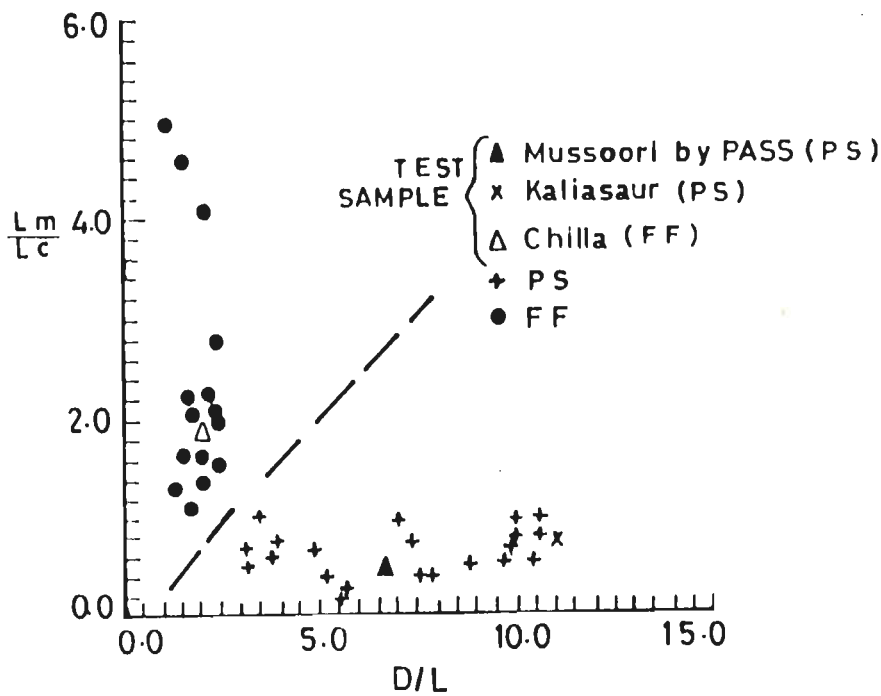

Fig. 4.14: LOCATION OF TEST SAMPLES ON THE BIVARIATE PLOT BETWEEN CLASSFICATION (D/L) AND TENUITY (Lm/Lc) SHOWING DISTINCT FIELDS FOR PLANAR SLIDE (PS) AND FLUID-FLOW (FF)

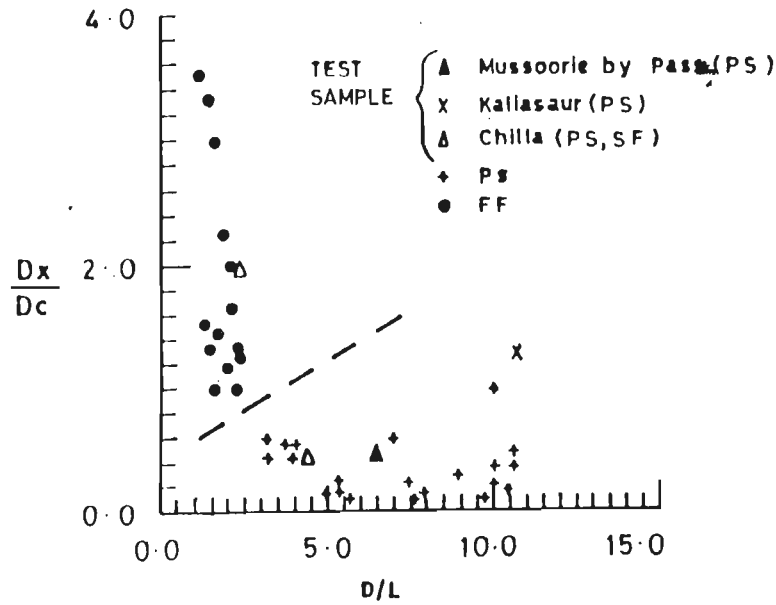

FIG.4.15: LOCATION OF TEST SAMPLES ON THE BIVARIATE PLOT BETWEEN CLASSIFICATION (D/L) AND DILATION $(\frac{Dx}{Dc})$ INDICES SHOWING DISTINCT FIELDS FOR PLANAR SLIDE (Ps) AND FLUID-FLOW (FF)

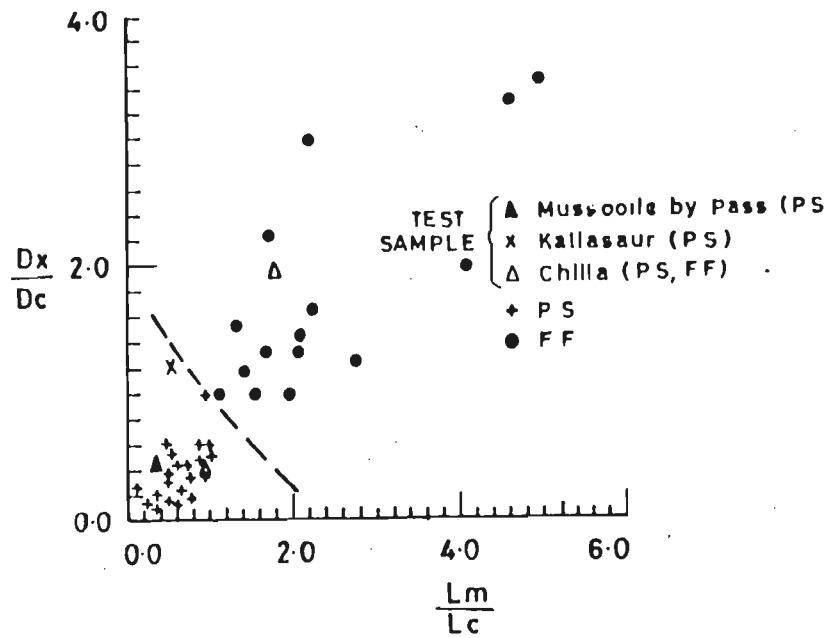

FIG.4.16: LOCATION OF TEST SAMPLES ON THE BIVARIATE PLOT BETWEEN TENUITY $(\frac{Lm}{Lc})$ AND DILATION $(\frac{Dx}{Lc})$ INDICES SHOWING DISTINCT FIELDS FOR PLANAR SLIDE (PS) AND FLUID-FLOW (FF)

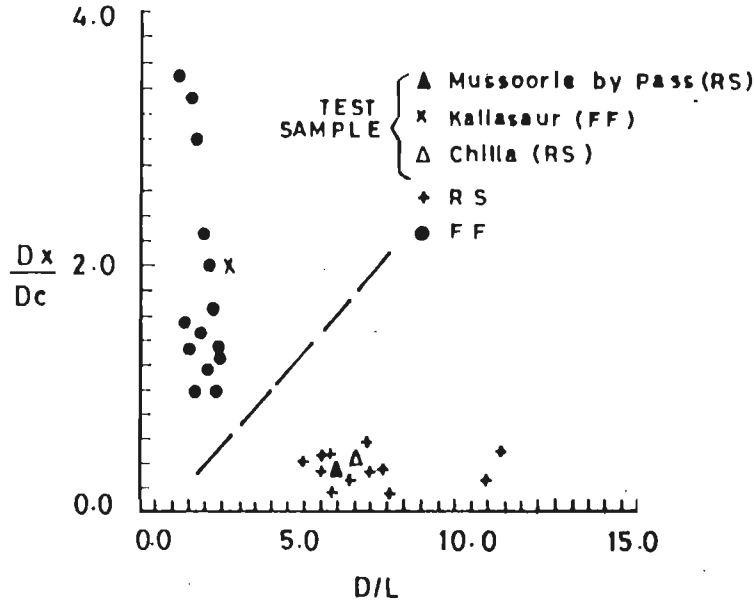

FIG. 4.17: LOCATION OF TEST SAMPLES ON THE BIVARI-ATE PLOT BETWEEN CLASSIFICATION (D/L) AND DILATION $(\frac{Dx}{Dc})$ INDICES SHOWING DISTINCT FIELDS FOR ROTATIONAL SLIDE (Rs) AND FLUID FLOW (FF)

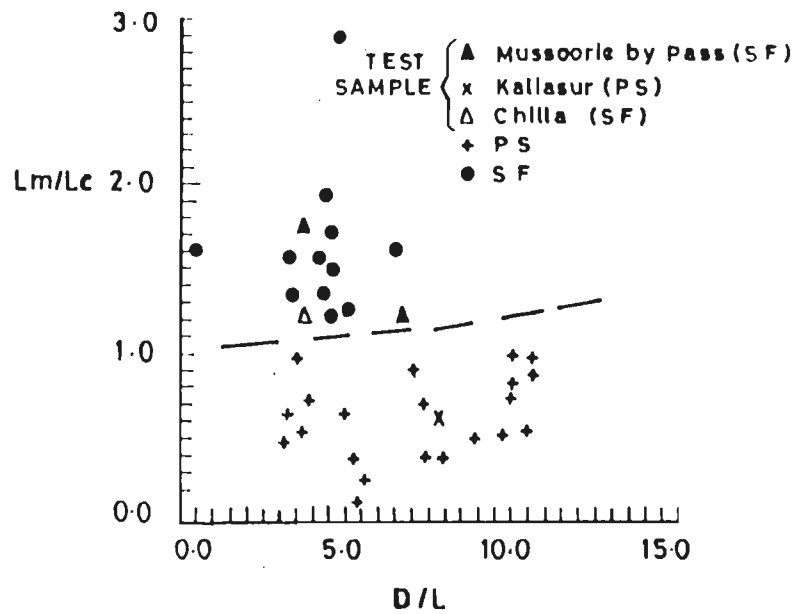

FIG. 4.18: LOCATION OF TEST SAMPLES ON THE BIVAR-IATE PLOT BETWEEN CLASSIFICATION (D/L) AND TENUITY INDICES SHOWING DISTINCT FIELDS FOR PLANAR SLIDE (Ps) AND SLIDE FLOW (SF)

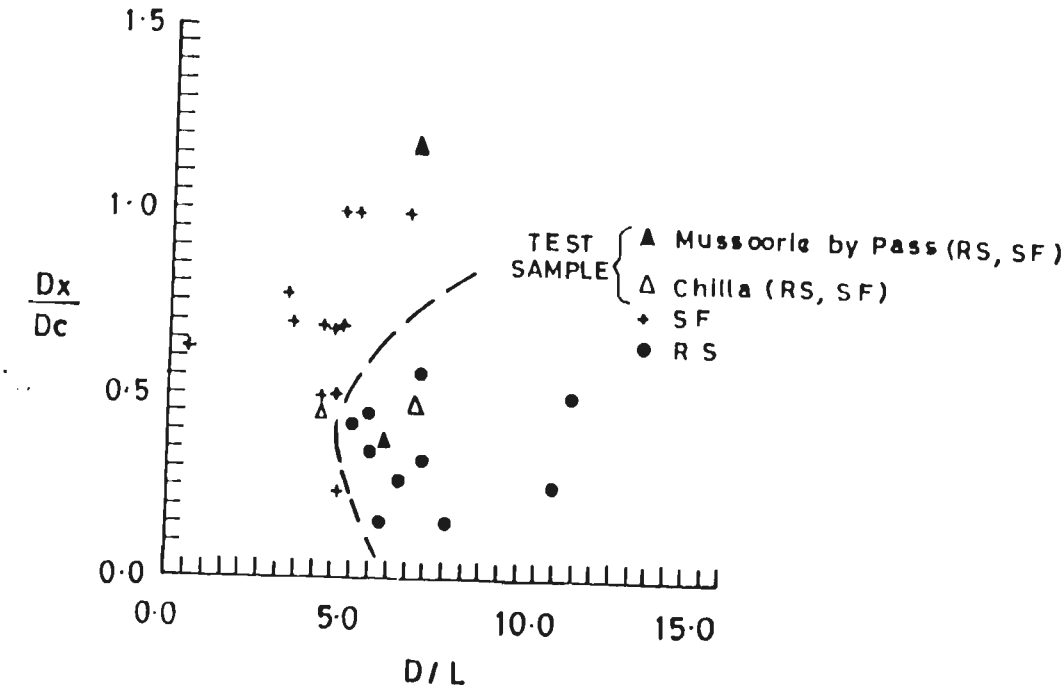

FIG. 4.19: LOCATION OF TEST SAMPLES ON THE BIVARI-ATE PLOT BETWEEN CLASSIFICATION (D/L) AND DILATION INDICES SHOWING DISTINCT FIELDS FOR ROTATIONAL SLIDE (Rs) AND SLIDE FLOW (SF)

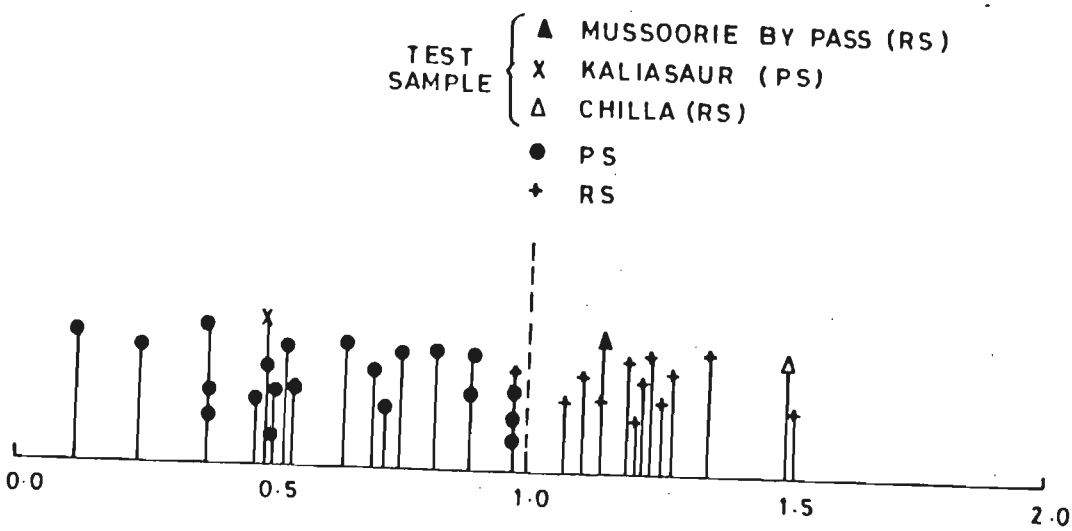

Fig. 4.20: LOCATION OF TEST SAMPLES ON THE UNIVARIAT PLOT OF TENUITY (Lm/Lc) SHOWING DISTINCT FIELDS FOR ROTATIONAL SLIDE (RS) AND PLANAR SLIDE (PS)

4.4.6 Usefulness of Bivariate and Univariate Plots

The morphometric indices for three test areas namely Mussoorie Bypass, Kaliasaur and Chilla were computed using slope sections indicating different movement procsses. When these indices were subjected to the above mentioned bivariate and univariate approach as shown in Figures 4.13-4.20, they clearly demonstrated the usefulness of such a technique developed through search process of discriminate function analysis. In view of this, the approach both graphical and quantitative can be used towards the classification of slope movement. The advantage of the presently developed technique is that, besides being easy to use, the data can be extracted from topographic contour maps of such a terrain as against other researchers whose data base were field observations. The technique may also be used to prepare hazard zonation map on the basis of these indices, particularly displacement index.

4.5 SUMMARY

Landslip form can be interpreted to give an indication of processes that are periodically or continually sculpturing the face of earth. Hence, reconstruction of its related genetic events can be made by morphological analysis of the resultant form. In doing so, Crozier (1973) derived significant morphometric indices on the basis of sixty six landslips and found them useful in identifying the nature of slope movement and process involved in it. His studies were based on three dimensional slope face measurement in a terrain characterised

largely by broad concavo-convex slopes with very few bedrock outcrops and free faces in Newzealand. In the present investigation of an altogether different nature of terrain exhibiting typical rugged topography, high relief, steep sided valleys and poor soil and regolith mantle cover, the critical values of various indices given by Crozier (1973) could not be applied as such. However, a similar approach was made to obtain limit of these indices on the basis of two dimensional, sixty slope profiles drawn from contour map of this terrain.

Displacement Index (DPI) appears to help in suggesting the potential of failure of a section. A slope section is likely to become unstable if displacement index is less than 48.04, 73.31, 54.25 and 53.22 for rotational slide, planar slide, slide flow and fluid flow respectively.

With a view to work out a simple quantitative statistically significant criteria to differentiate between the various slope movement processes based on simultaneous use of all the five morphometric indices, multivariate discriminant function analysis was used. The multivariate criteria have been developed and tested successfully to discriminate between slide flow from fluid flow, from planar slide, fluid flow from rotational slide, planar slide from slide flow, rotational slide from slide flow and planar slide from rotational slide.

Discriminant analysis when used as search technique, helped in highlighting the morphometric indices which contribute

signifiantly in discriminating various slope movement processes. Based on these indices bivariate and univariate plots have been prepared. These plots can also be used as tools to examine and find out the slope movement process at a given site.

CHAPTER - 5

LANDSLIDES IN RELATION TO DEVELOPMENTAL ACTIVITIES IN THE AREA

5.1 INTRODUCTION

In the mountain realm like Himalaya, the problem of hillslope instability and slope movement are particularly severe. The recent developmental activities particularly the road construction activities in these hilly regions have greatly contributed to the instability of hillslopes and increased the incidents of landslides manifold. In the present chapter an attempt has been made to investigate the hillslope instability along the only major motorable road extending from Byasi to Devaprayag. The results of these investigations are presented herewith.

5.2 CLASSIFICATION OF ROADSIDE SLOPE INSTABILITY IN THE AREA - GENERAL

The sliding phenomena which involves a variety of processes and factors give rise to numerous possibilities of classification. Here several classification schemes have been forwarded by various geoscientists, on the basis of the following parameters: i) Character of the material i.e. bed rock, debris, soil etc.; ii) Amount of water content; iii) Type of movement, i.e. fall, topple, slide and flow; iv) Rapidity of movement; v) Cause of triggering movement viz, earthquake, excess water, mass;

vi) Nature of slip surface i.e. planar or rotational; vii) Slide location viz., sub-aerial or subaqueous; viii) Geometry and morphology of resulting topography; ix) Environmental setting; x) Regional and physiographic aspects; vi) Size of the slide; xii) degree of activity, viz., active or dormant; viii) Size of the material involved; xiv) Mechanics involved; and xv) Climate. Of the many classification schemes such as those given by Terzaghi (1929), Sharp (1938), Savage (1951), Varnes (1958, 1978), Zaruba and Mencl (1969) and Coastes (1977), the one give by Varnes (1978) is simple, systematic and easy to use. Varnes classification scheme envisages the following six types of slope movements (Table 5.1).

1) **Falls-** In falls a mass of any size is detached from steep slope or cliff, along a surface on which little or no shear displacement takes place. The mass in motion travels most of the distance through air by free fall, movement by leaps and bounds and rolling of fragments of bed rock or soil.

2) **Topple** - Movement due to forces that cause an overturning movement about a pivot point below the centre of gravity of a unit, under the action of gravity and forces exerted by adjacent units or by fluids in cracks.

3) **Slide** - Movement involves shear displacement along one or several surfaces or within a relatively narrow zone, which are visible or may reasonably be inferred. Slides have been further divided into rotational and translational. In rotational slide,

TABLE 5.1 : CLASSIFICATION OF SLOPE MOVEMENTS (After Varnes, 1978)

TYPE OF MOVEMENT		TYPE OF MATERIAL		
		BED ROCK	ENGINEERING SOILS Predominantly coarse	ENGINEERING SOILS Predominantly fine
FALLS		Rock fall	Debris fall	Earth fall
TOPPLES		Rock topple	Debris topple	Earth topple
ROTATIONAL SLIDES	FEW UNITS	Rock slump	Debris slump	Earth slump
TRANSLATIONAL	FEW UNITS	Rock block slide	Debris block slide	Earth block slide
	MANY UNITS	Rock slide	Debris slide	Earth slide
LATERAL SPREADS		Rock spread	Debris spread	Earth spread
FLOWS		Rock flow(deep creep)	Debris flow	Earth flow (Soil creep)
COMPLEX		Combination of two or more principal types of movements.		

surface of rupture is curved concave upward along which the movement has taken place. The movement is rotational about an axis that are parallel to the slope. The top portion of the slide mass moves downward with the surface tilting backward. Slump are generally considered as rotational. Translational movement predominantly takes place along more or less planar or less gently undulatory surfaces. Movement frequently is structurally controlled by surfaces of weakness, such as faults, joints, bedding planes, and variation in shear strength between layers of bedded deposits.

4) **Lateral Spreads** - In spreads the dominant mode of movement is lateral extension accomodated by shear or tensile fractures. Two types may be distinguished: i) Distributed movement result in overall extension but without a recognised or well-defined controlling basal shear surface or zone of plastic flow. These appear to occur predominantly in bedrock, especially on the crest of ridges, ii) Movement may involve fracturing and extension of coherent material, either bedrock or soil, owing to liquefaction or plastic flow of subjacent material. The coherent upper units may subside, translate, rotate or disintegrate or they may liquify and flow.

5) **Flows** - They are generally confined in unconsolidated material, either fast or slow. Depending on particle size and velocity of movement two types may be recognized, i) Bedrock flow movement which is extremely slow, include deformations that are distributed among many large or small fractures, or even

microfractures, without concentration of displacement along a thorough-going fracture. The movement may result in folding, bending, bulging or other manifestations of plastic behaviour, ii) Debris and earth flow movement which is usually rapid, the relative displacement within the mass are commonly larger and more closely distributed and the general appearance is more obviously that of a body that has behaved like a fluid. Moreover, the fluidizing effect of water due to very high velocity (>2m/sec) is, as a rule, a part of the process. Slip surfaces within the moving mass are usually not visible or are short lived, and the boundary between moving mass and material in place may be a sharp surface of differential movement or a zone of disturbed shear.

6) **Complex** - Movement is by a combination of one or more of the five principal types of movement described above. Many landslides are complex although one type of movement is generally dominant over the others at certain areas within a slide or at a particular time.

5.3 TYPES OF HILLSLOPE INSTABILITY ALONG THE ROAD

Field investigations were carried out with a view to assess the nature, type and mode of failures of problematic slopes along the road between Byasi and Devaprayag and also in the accessible parts of hillslopes both uphill and downhill adjoining the road. Varnes (1978) classification was followed for categorising various types of existing landfailures in the area. In this

section of the road a total of 21 landslides were identified as shown in Fig. 5.1. The salient features of each slide area as observed are listed in Table 5.2. The photographs of these slide areas depicting variations in the mode of failures are shown in Figs. 5.2 to 5.15.

A perusal of Table 5.2 indicates the following types of instabilities.

i) **Rock slide** - It is the most problematic and common type of slope movement. It consists predominantly of rock fragments of varying sizes as well as blocks with associated soils. The movement is generally translational along planar surfaces cutting the slope (Figs. 5.2, 5.7, 5.8, 5.12). The exposed surfaces are found either moderate to steeply dipping bedding plane or joint planes. The next common type of slope failure in this area is wedge failure (Figs. 5.4, 5.6, 5.10 and 5.11). In this the movement is also translational along the intersection of two planar surfaces or axis of two joint planes cutting the slope. Field observations have indicated that the dimension of wedges are not big possibly due to close spacing of joints.

ii) **Debris slide** - Debris slides are also common in the area. These occur in slopes composed of weathered and loose materials. Some planar discontinuity surfaces also occur as remanence of the parent bed rock and translational slide generally occur along such weak planes producing debris slides. This type of slide is observed at km 60 from Rishikesh in quartzite (Fig. 5.13) and

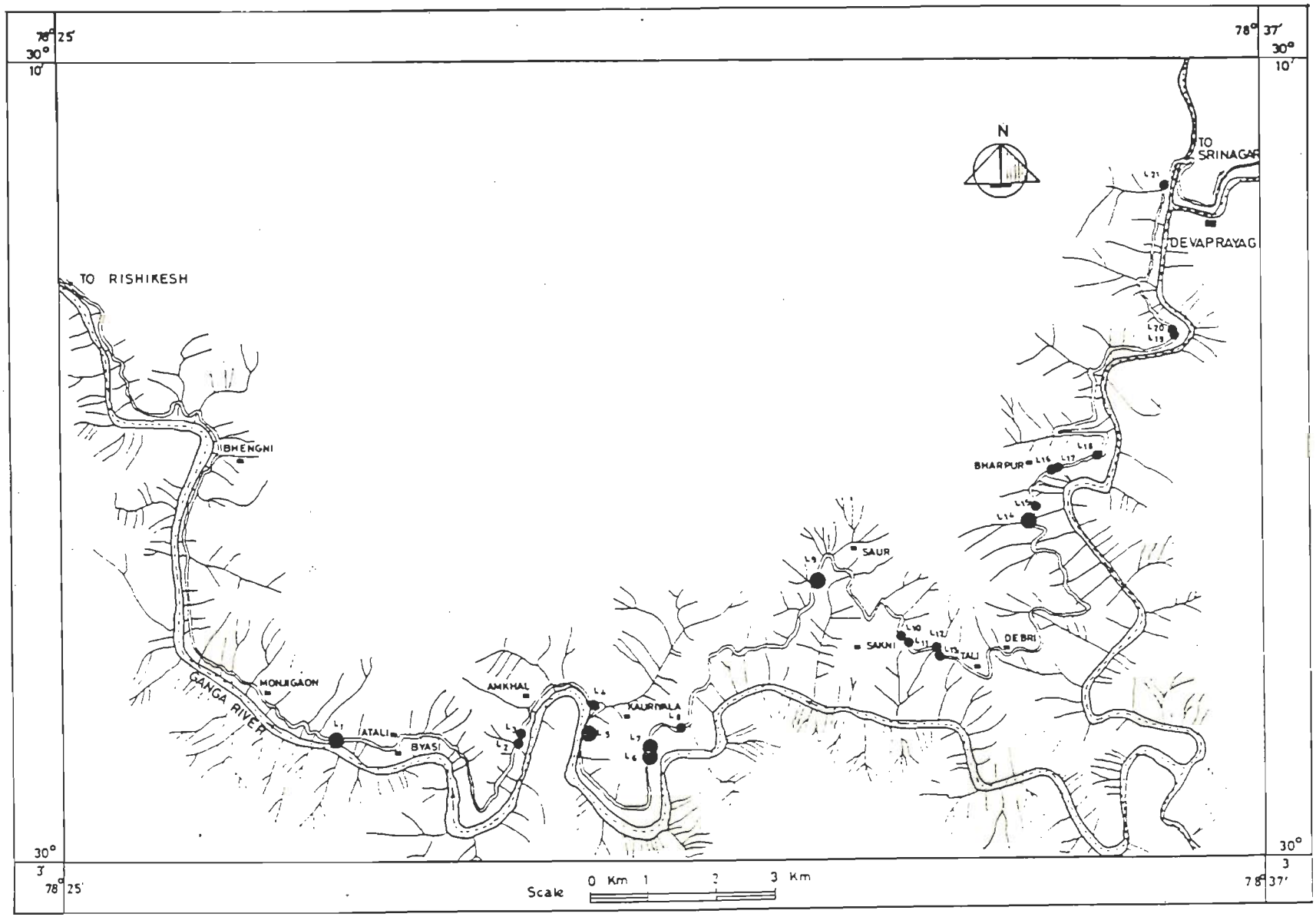

Fig. 5.1. INVENTORY OF LANDSLIDE AREAS INVESTIGATED ALONG THE ROAD

Table 5.2 : Details of Reconnaissance Survey of the Area Along the Road Between Byasi to Devaprayag

Slide designation (1)	Location (km) (2)	Mode of failure (3)	Dimension (sq.m) (4)	Type of material (5)	Landuse (6)	Causitive factor (7)	Slope and dominent discontinuities (dip direction/dip) (8)	Soil/rock (9)
L_1	32	Mainly planar otherwise wedge failure associated with debris flow	4829	Blocks and fragments of quartzite associated with slope wash.	Low to medium vegetation in slide zone, dense around it. Rectangular growth of vegetation observed, small agriculture farm 500 m behind crown.	Heavy precipitation, saturation and pore water pressure causing reduction in cohesion and friction angle, unfavourable joint orientation. Road construction activity.	Slope N209/49 Joints N190/36 N27/30 N111/62 N290/88	Rock exposures at middle of slope and crown, debris accumulation at toe region.
L_2	35	Rock avalanches	2312	Blocks of quartzite common.	Low to medium vegetation in slide area.	Heavy precipitation, reduction in cohesion and sliding friction of blocks. Steep slope.	Slope N140/45-67 Joints N215/62 N25/54 N302/42 N97/29	Mostly rock exposure in slide zone with occasional soil cover.
L_3	35.3	Occasional wedge failure and rock fall.	1800	Blocky quartzite associated with slope wash.	No vegetation near crown, medium in form of bushes at middle slope of the slide zone.	Heavy precipitation, pore water pressure causes reduction in shearing strength of blocks. Steep slope.	Slope N120/60-75 Joints N215/62 N25/54 N302/42 N97/29	Mostly rock exposure in slide zone with occasional soil cover.
L_4	38	planar failure common associated with debris slide	2158	Flakes of slate	No vegetation in slide zone, low around it, 400m behind crown there is agriculture farm and school.	Failure under saturation, unfavourable joint orientation, Road construction activity.	Slope N215/47 Joints N210/50 N24/48 N309/38 N88/31	Rock exposure in slide zone associated with thick soil cover behind crown.

Contd.. Table 5.2

(1)	(2)	(3)	(4)	(5)	(6)	(7)	(8)	(9)
L_5	38.5	Mainly planar associated with occasional wedge and debris slide	2552	Blocks of quartzite associated with slope wash.	Very low to low vegetation in and around slide zone, with few trees tilted towards the free face.	Heavy precispitation, failure under saturation, unfavourable joint orientation.	Slope N25/50 N270/36 N322/74 Joints N36/32 N74/35 N315/44 N210/41	Rock exposures, highly fractured at middle of slope. Occasionally thin soil cover present.
L_6	42	Wedge failure common, planar failure otherwise associated with debris slide.	2340	Blocks and small frangments of quartzite and shale common.	Low to medium vegetation in and around slide zone, with tilted trees at the periphery towards direction of slide.	Failure due to over saturation. Unfavourable joint orientation Regolithic nature of rock at crown.	Slope N40/60 Joints N13/50 N201/31 N289/80 N98/56	Rock exposures common near crown region, middle and toe regions covered with debris.
L_7	42	Occasional plane failure.	1320	Blocky silt stone with small fragments of slate.	Low vegetation in and around slide zone.	Heavy precipitation, pore water pressure, steep slope.	Slope N90/75 N20/55 Joints N18/41 N316/48 N208/42 N105/68	Rock exposure in slide zone. Thin cover of soil around it.
L_8	43	Rock avalanches	2870	Blocks and small fragments of limestone common.	Low and medium vegetation in and around slide zone, with trees tilted towards direction of slide.	Heavy precipitation, steep slope, medium to highly weathered rock mass.	Slope N150/45-70 Joints N210/56 N92/58	Nearly 30 cm soil cover at toe. Rock exposure at the middle and crown of sliding zone.

Contd.. Table 5.2

(1)	(2)	(3)	(4)	(5)	(6)	(7)	(8)	(9)
L_9	46	Occasional planar failure.	420	Small blocks of quartzite common.	No vegetation in slide area. Dense around it.	Unfavourable joint orientation, Regolithic nature of rock mass. Road construction activity.	Slope N107/56 Joints N108/42 N302/20 N221/85 N46/82	Rock exposures in sliding zone. Rocks are more weathered and fractured at crown compare with toe region. Thick soil cover behind crown.
L_{10}	51.1	Rock, debris avalanches	1800	Quartzite fragments associated with sandy soil.	Very low to medium vegetation in and around slide zone with trees tilted towards direction of slope. 100 m away from this zone at the height of 80 to 100 m from road level agriculture farm is present.	Heavy precipitation causes reduction in shearing strength and cohesion. Steep slope.	Slope N275/48 Joints N202/72 N38/63	Thick soil cover in and around the slide zone, few weathered rock exposure present.
L_{11}	51.4	Rock-debris slide	1210	Quartzite fragments common.	Low to medium vegetation in slide zone. Dense around it.	Regolithic nature of rock mass. Folding.	Slope N260/37 Joints N80/35 N42/68 N221/72 N302/31	Rock exposure associated with few thin soil cover zones in failed area. Thick soil cover behind crown.
L_{12}	52	Mainly rock fall associated with planar failure.	360	Blocks and fragments of quartzite.	Low vegetation in slide zone, dense around it.	Heavy precipitation, highly weathered and fractured rock mass. Folding. Road construction activity.	Slope N175/78 Joints N290/80 N105/63 N31/57	Rocks are thinly bedded and fractured. No soil cover present.

Contd.. Table 5.2

(1)	(2)	(3)	(4)	(5)	(6)	(7)	(8)	(9)
L_{13}	52	Rock cumb debris slide.	380	Fragments of shale and quartzite common.	No vegetation in slide zone, medium around it.	Heavy precipitation, highly weathered nature of rock mass. Steep slope. Fan folding. Road construction activity.	Slope N185/70 Joints N25/52 N99/65	Weathered rock exposure associated with thin soil cover at few places in slide zone.
L_{14}	58.5	Wedge failure common otherwise planar failure.	800	Blocks and small fragments of quartzite.	No vegetation in slide zone. Low to medium around it.	Heavy precipitation, Pore water pressure, unfavourable joint orientation, road construction activity.	Slope N92/39 N74/60 N56/70 Joints N97/33 N50/72 N228/88 N317/36	Rock exposures in and around slide zone. No soil cover present.
L_{15}	58.8	Occasional wedge failure	480	Blocks and fragments of quartzite associated with small fragments of shale.	Vegetation very low in slide zone and low to medium around it, with trees tilted in direction of slope. Near it, there is a zone of debris slide which has been provided toe support and step wise protection wall.	Heavy precipitation causing reduction in sliding friction and cohesion of blocks having unsupported toe.	Slope N145/49 Joints N35/25 N84/43 N325/28 N205/50	Rock exposure in slide zone. They are regolithic in nature at crown and tabular at toe region. No soil cover present.
L_{16}	60	Planar failure with occasional rock fall.	985	Fragments of quartzite common.	Vegetation low in slide zone and dense around it, with trees tilted towards slide direction.	Heavy precipitation, unfavourable joint orientation. Regolithic nature of rock mass. Steep slope. Road construction activity.	Slope N92/71 Joints N295/63 N92/43 N38/67	Rocks are highly fractured and weathered with no soil cover in sliding zone.

Contd.. Table 5.2

(1)	(2)	(3)	(4)	(5)	(6)	(7)	(8)	(9)
L_{17}	60	Debris slide	355	Small fragments of quartzite, shale and sandy material.	Vegetation low in slide zone and medium around it.	Heavy precipitation, reduction of friction angle and cohesion due to saturation, steep slope. Unfavourable drainage orientation.	Slope N55/55 Joints N95/53 N104/47 N44/58 N298/52	Rocks are highly fractured thinly bedded, associated with thick debris cover in slide zone.
L_{18}	61	Planar failure common.	2325	Blocks and fragments of quartzite.	Vegetation low in the middle and toe of slide zone. Dense around it, with trees tilted in direction of failure. Some shopes and Schools are situated behind crown.	Heavy precipitation, unfavourable joint orientation, steep slope.	Slope N175/70-47 Joints N300/35 N180/41 N92/36 N30/60	Rocks are highly fractured and weathered near crown associated with thin soil cover in slide zone and thick around it.
L_{19}	65	Debris slide	2334	Blocks and small fragments of quartzite,phyllite and sandy materials.	Vegetation low in slide zone, dense around it, with some trees tilted in direction of failure. Step wise protection wall has been provided.	Heavy precipitation, failure due to over saturation, highly weathered and fractured nature of rock mass. Steep slope.	Slope N125/46 Joints N45/25 N110/42 N283/60	Rocks are highly weathered and fractured associated with thick soil and debris cover in and around slide zone.
L_{20}	65	Debris slide	1670	Fragments of phyllite and sandy material.	Vegetation low in slide zone dense around it. Retaining wall has been provided at toe which partly has been broken.	Heavy precipitation, reduction of cohesion and friction due to saturation. Steep slope Road construction activity.	Slope N140/60 Joints N45/30 N105/45 N283/60	Rock exposure at crown are highly weathered and fractured with thick debris cover at middle and toe of slide zone.

Contd.. Table 5.2

(1)	(2)	(3)	(4)	(5)	(6)	(7)	(8)	(9)
L_{21}	70	Rotational slide	1822	Small fragments of phyllite and sandy material.	No vegetation in slide zone, low to medium around it. Retaining wall has been provided at toe which is partly broken.	Failure under saturation due to reduction of friction angle and cohesion. Steep slope. Road construction activity.	Slope N107/40 Joints N289/49 N97/60 N30/35	Thick debris and soil cover in and around slide zone. Few rock exposures which are highly weathered present.

Fig. 5.2 : Planar Slide in Well Jointed and Fractured Quartzite (32 km from Rishikesh)

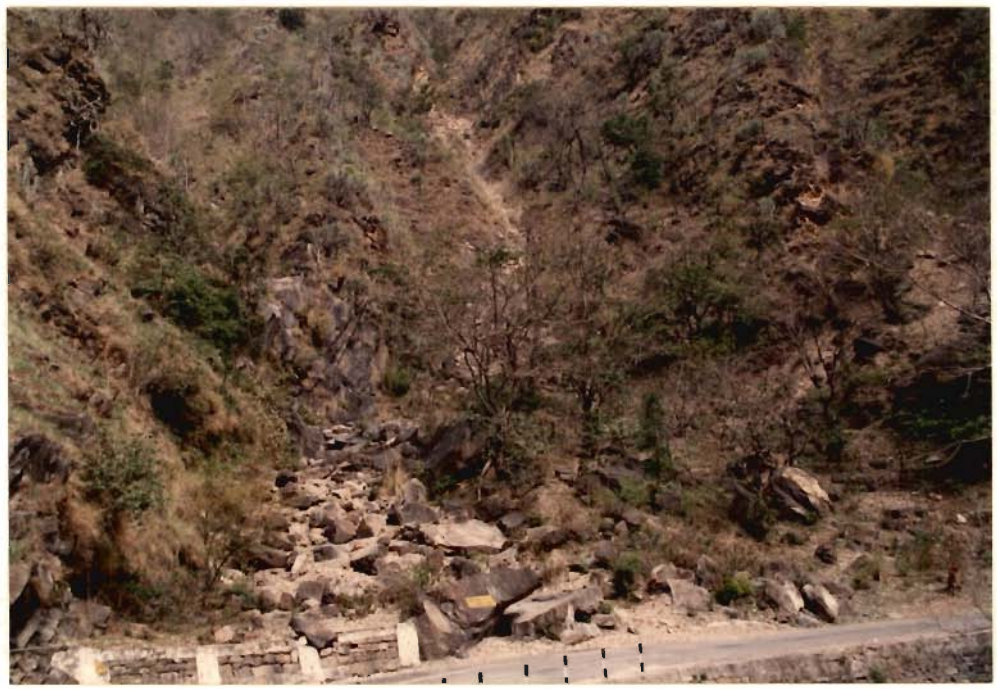

Fig. 5.3 : Rock Avalanches in Jointed Quartzite (35 km from Rishikesh)

Fig. 5.4 : Occasional Wedge Failure and Rock Fall in Jointed Quartzite (35.3 km from Rishikesh)

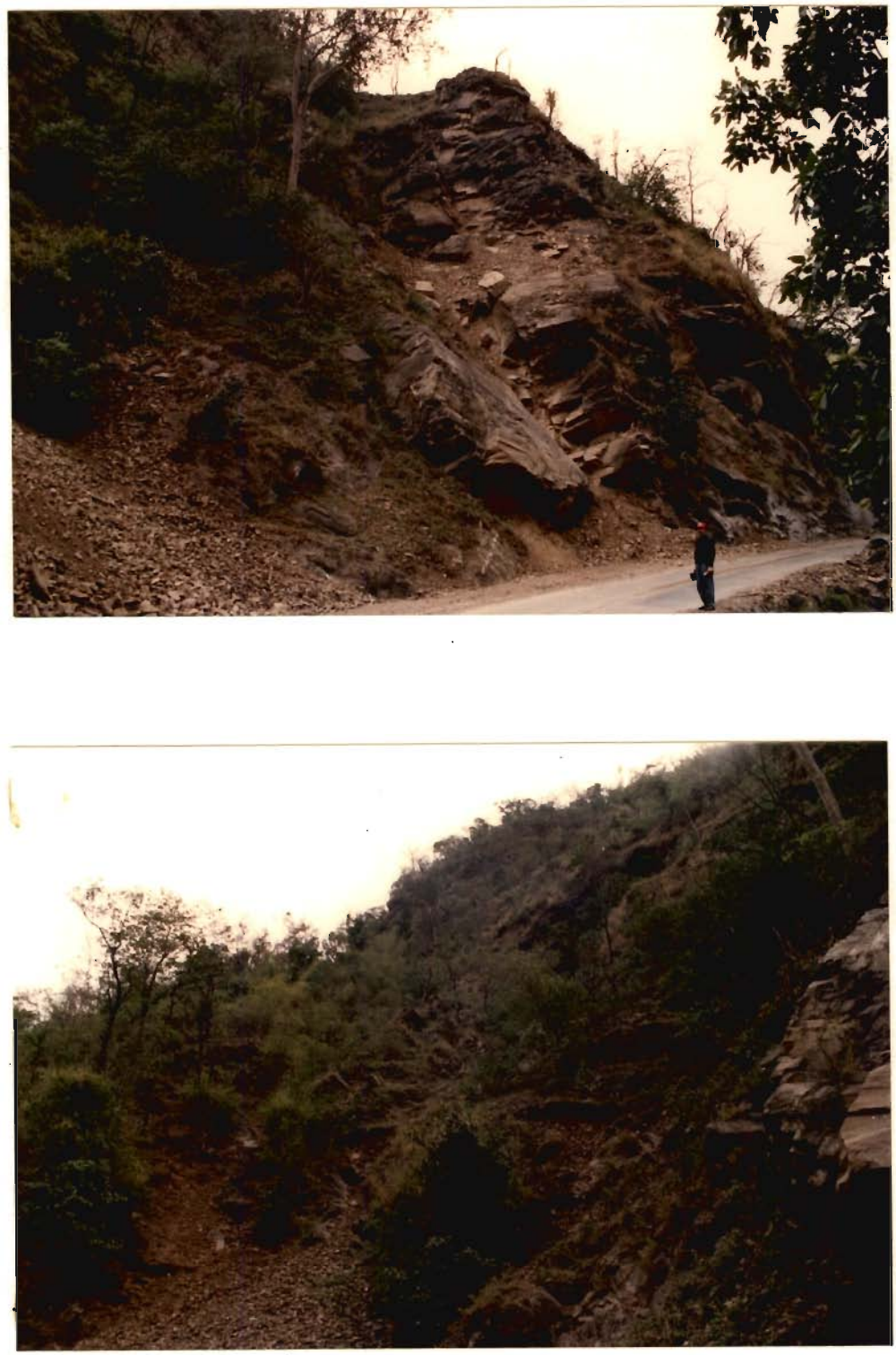

Fig. 5.5 : Large Planar Failure in Well Jointed Quartizte (38.5 km from Rishikesh)

Fig. 5.6 : Wedge Failure in Highly Jointed and Fractured Quartzite (42 km from Rishikesh)

Fig. 5.7 : Occassional Planar Failure in Well Jointed Silt-stone (42 km from Rishikesh)

Fig. 5.8 : Planar Slide in Highly Jointed and Fractured Quartzite (46 km from Rishikesh)

Fig. 5.9 : Rock Avalanches in Jointed and Weathered Limestone (43 km from Rishikesh)

Fig. 5.10 : Wedge Failure in Well Jointed Quartzite (52.8 km from Rishikesh)

Fig. 5.11 : Wedge Cum Planar Failure in Well Jointed Quartzite (52.5 km from Rishikesh)

Fig. 5.12 : Planar Slide Cum Debris Avalanches in Well Jointed Quartzite (61 km from Rishikesh)

Fig. 5.13 : Debris slide in Weathered Phyllite (65 km from Rishikesh)

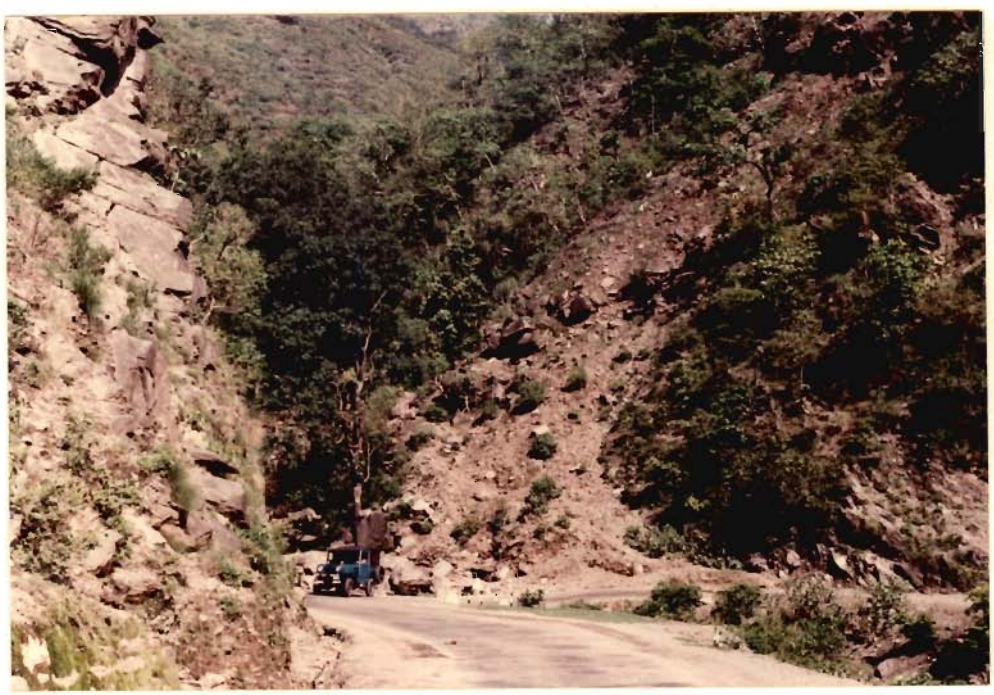

Fig. 5.14 : Debris Slide in Weathered Phyllite and Quartzite (65 km from Rishikesh)

Fig. 5.15 : Rotational Slide in Highly Weathered Phyllite (70 km from Rishikesh)

most frequently in phyllites which are more vulnerable to weathering processes. A typical example of debris slide in phyllite is seen at km 65 from Rishikesh (Fig. 5.14).

iii) **Debris slump** - This type of slope failure is not common. It is marked by rotational movement and usually occurs in homogeneous debris material derived from deep weathering of phyllite. The movement is rotational about an axis, parallel to the slope as is indicated by the back-ward tilting of head portion of slided mass and characterised by presence of steep scarps and crown crown cracks. A typical example of the debris slump is seen near Devaprayag at km 70 on the deeply weathered phyllite. The failure is initiated due to slope excavations for road construction and saturation during monsoon.

iv) **Rock fall** - This type of the failure occurs by free fall of the rock material from naturally occurring steep or steep road cut face which are well jointed and fractured. Figures 3.12 and 5.4 are examples of rock fall in the highly disturbed quartzite at km 35.3 and 52 from Rishikesh.

v) **Flows** - Flow in the area along the road section, generally are rare and rapid. The relative displacement within the mass are commonly larger and the body behaves like a fluid. This type of movement have been observed at km 35 in quartzite (Fig. 5.3) and at km 43 in limestone (Fig. 5.9) from rishikesh.

vi) **Complex** - This type of slope failure is very common in the area. These are characterised by combination of different types

of movements. As such most of the slides are complex, but they are classified according to their most dominant mode of movement. Figures 5.5, 5.6, 5.11, 5.12 are examples of complex type of slope movement.

5.4 DETERMINATION OF PARAMETERS FOR STABILITY ANALYSIS

On the basis of slide dimensions, accessibility, extent of instability, and rock/soil ratio, six sites were selected. Detailed investigations aiming at stability analysis, using Slope Mass Rating (SMR) and limit equilibrium method of simulating field observations with the help of computer, for the sites under study (L_1, L_5, L_6, L_7, L_9 and L_{14}; Figs. 5.2, 5.5, 5.6, 5.7, 5.8 and 5.11) were carried out.

5.4.1 Stability Parameters

Romana (1985) has made an important contribution by modifying Rock Mass Rating (RMR) given by Bieniawiski (1979) for the assessment of stability of rock slopes. He developed a factorial approach for rating the discontinuity orientation parameter in RMR system, based on field data. Recognizing that rock slope stability is governed by the behaviour of the discontinuities, his modification of RMR system involved subtracting the newly proposed adjustment factors for the discontinuity orientation and adding new adjustment factors for assessment of stability.

There are six parameters used in Slope Mass Rating (SMR) for assessment of rock stability. These are described and determined

for the sites under study:

a) Uniaxial compressive strength of intact rock material

b) Rock Quality Designation

c) Spacing of Discontinuities

d) Condition of Discontinuities

e) Ground water condition (in joint)

f) Orientation of Discontinuities

A) Uniaxial Compressive Strength of Joint Wall and Intact Rock

The stability of rock mass is influenced by its strength. However the presence of network of defective planes or surfaces of discontinuities such as joint surfaces, bedding planes and fractures in rock mass influence its mechanical and physical properties. The strength of rock mass decreases whenever these defective surfaces are found and is affected by their attitude, geometry, spatial distribution and the number of such discontinuity surfaces. Therefore the shearing strength of rock mass, in a way is found to be largely governed by the presence of discontinuities and rock mass is anisotropic in its strength and deformational properties. It is, therefore, not surprising to observe that the surfaces of failure in hard rock follow the preexisting surfaces of weakness in the rock mass. Such failures do not take place generally through the intact rock material to a great extent unless the rock itself is quite soft and therefore has low strength.

According to Barton et al. (1977), strength along the discontinuity surfaces is governed by the strength of asperities.

Thus JCS (Joint Wall Compressive Strength) need to be determined in the field under natural conditions. Various workers like Barton et al. (1977), Jesch et al. (1979) have recommended the use of L-type Schmidt Hammer for measurement of joint wall compressive strength.

A-1 Determination of JCS using L-type Schmidt Rebound Hammer

Schmidt Rebound Hammer designated specially to test the strength of concrete is also widely in use for rock material classification. This is a simple device for recording the rebound of a spring loaded plunger after its impact on a surface. The L-type rebound hammer, used in the present study has impact energy of 0.075 m kg.

Miller (1965) found a correlation between rebound number (ranging 10 to 60) and the uniaxial compressive strength (q_c) of the rock.

$$\log_{10} q_c = 0.00088\ \gamma R + 1.01 \qquad (5.1)$$

where

q_c = uniaxial compressive strength , UCS(Mn/m^2)

γ = Dry Density of Rock (kN/m^3)

R = Rebound Number

Aufmuth (1974), Irfan and Dearman (1978), Jesch et al (1979) and Karnataka Engineering Research Station (1985) have found

different relationship as given below:

$$\log UCS = 1.831 \log R + 1.533 \quad \text{(Aufmuth ,1974)} \qquad (5.2)$$

$$UCS = 7.752\ R - 213.349 \quad \text{(Irfan and Dearmam,1978)} \qquad (5.3)$$

$$UCS = 3.540\ R - 37.268 \quad \text{(Jesch et al.,1979)} \qquad (5.4)$$

$$UCS = 0.005\ R + 44.1 \quad \text{Karnatak Engineering Research Station (1985)} \qquad (5.5)$$

where UCS = Uniaxial compressive strength

R = Schmidt Hammer value.

The published relationship between Schmidt Hammer values and uniaxial compressive strength, however differed widely and significantly. Keeping in view the problem of estimating compressive strength using Schmidt Rebound Hammer and also considering the fact that their tests had been conducted on very smooth surfaces of cores and cubes, which are rarely encountered in nature, oriented samples from the field were collected for six selected sites, which consists mainly of quartzite and silt stone. The samples were large enough with average dimensions of 30 cm x 20 cm x 15 cm to help to take hammer readings at different parts on the same joint surface.

A-2 Experimental Setup and Test Procedure

In order to determine JCS with the help of rebound hammer, a small pit was constructed (80 cm length, 50 cm width and 40 cm depth) in the laboratory and filled with very fine and slightly moist sand up to 30 cm and compacted. The samples were placed firmly in the fine sand. A spirit level was also used to ensure

horizontal position of samples in space. The joint faces of the samples were thoroughly checked and made free from sand particles. Surfaces of nearly 160 joint faces were tested in natural dry condition, taking 30 readings on each joint face with L-type hammer vertically downward (Fig. 5.16). Then, samples were kept for a period of two weeks in a pool (3m length, 2 m with and 1.25 m depth) filled with water. The same procedure was adopted as mentioned before to measure the rebound number in natural wet condition (Table 5.3). Thirty specimens were randomly selected. They were cut into 25 mm cubes. Two cubes were prepared from each joint surface. All the cubes and their faces were properly marked before the testing. Care was taken to have final smooth finishing towards the ends of specimen to 0.05 mm by using different meshes (Fig. 5.17). Samples were then kept in water under low pressure vacuum condition for a period of two weeks.

All the specimen were tested following IS : 9413-1979, under ten tonne capacity universal testing machine. The loading plate was brought down slowly so as to be in contact with the top of specimen (Fig. 5.18). Load on the specimen was applied continuously at a constant stress rate till the failure occurred. The maximum load on specimen was recorded. The unconfined compressive strength of the specimen were determined. The results are presented in Table 5.3.

A-3 Analysis and Discussion

The density (γ) and average of 10 highest rebound number for each discontinuity surface were calculated both in dry and wet

Fig. 5.16 : Measurement of Uniaxial Compression Strength (JCS) by L-type Rebound Hammer

Fig. 5.17 : Rock Cubes Preparation for Measurement of Uniaxial Compressive Strength (JCS)

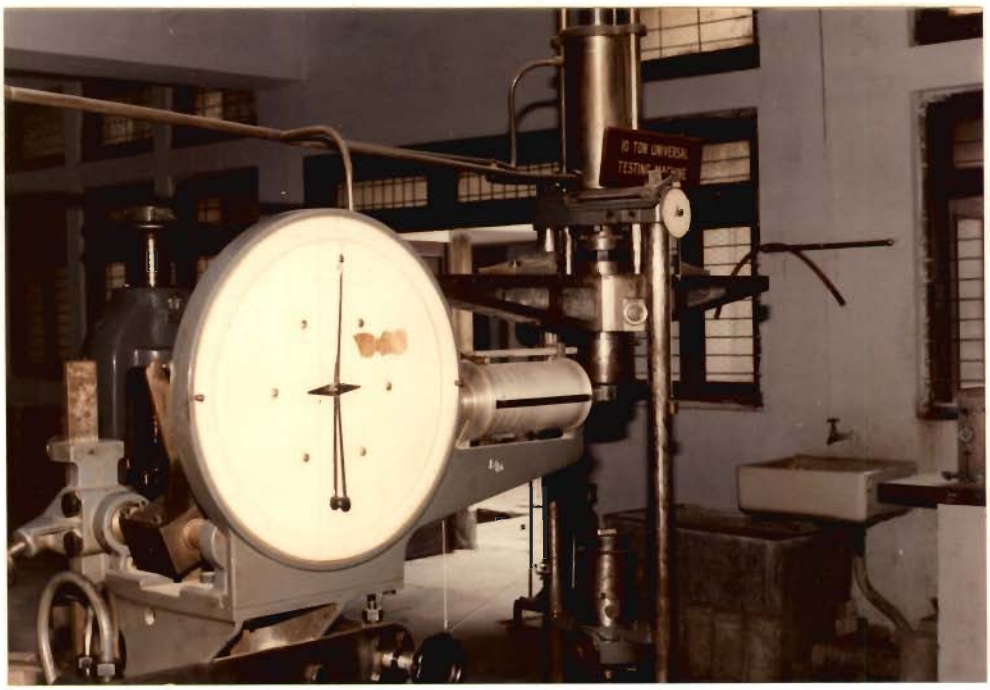

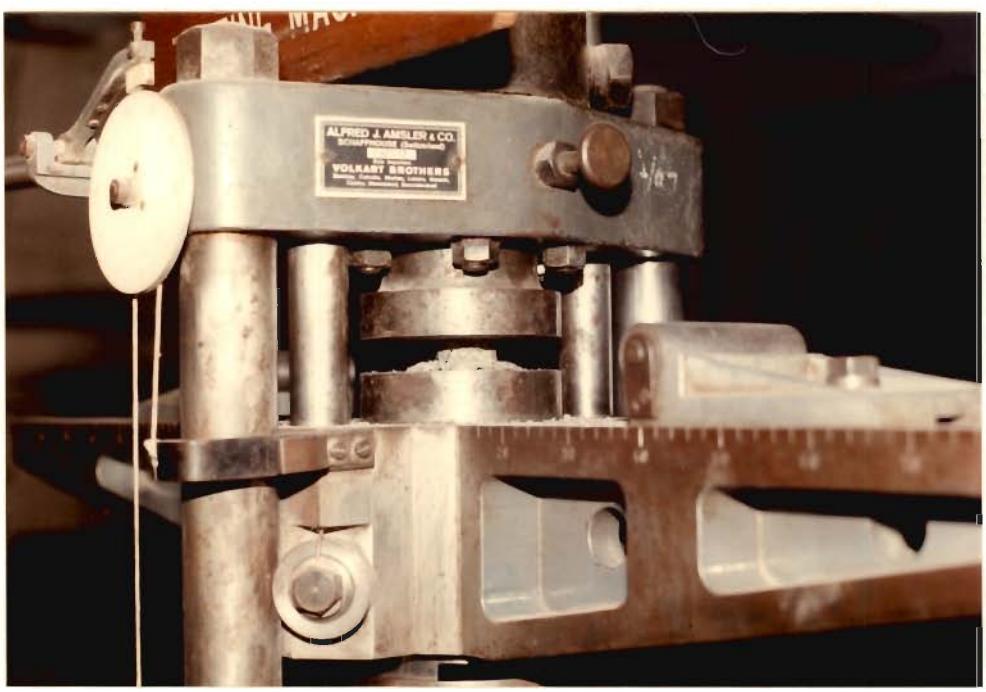

Fig. 5.18 : Determination of JCS by 10 Tons Universal Testing Machine

conditions (Table 5.3). Then, average uniaxial compressive strength of two specimens (cubes) for each joint surface as observed in the laboratory under wet condition, was plotted against the estimated uniaxial compressive strength obtained from L-type rebound hammer, following Miller's equation 5.1 (of relationship between rebound number and uniaxial compressive strength). The plot indicated that no correlation exists between observed and estimated uniaxial compressive strength (Figs. 5.19, 5.20). However, on examining the surface roughness of discontinuity surfaces under study, it was noted , that it may estimate the observed uniaxial compressive strength, if it is applied on smooth natural surfaces of joint walls.

Hence, the use of hammer should be restricted on smooth natural surfaces. While Miller's equation is used, it appears the hammer is expected to give more reliable result, when applied in dry condition (Fig. 5.19). Attempt to obtain a linear relationship between observed and estimated uniaxial compressive strength using rebound value (γ_R) did not yield any result (Fig. 4.21). Therefore, in the present study the uniaxial compressive strength of joint walls and intact determined in the laboratory were used and are presented in Tables 5.5 to 5.10.

B) Rock Quality Designation (RQD)

Deere et al. (1967) suggested a modified core recovery procedure to provide a Rock Quality Designation (RQD) for a given core interval. The RQD value is the percentage obtained by dividing the sum of lengths of all core pieces equal to or

Table 5.3 : Showing the Density of Rock and Rebound Number (L-type hammer) Under Dry and Wet conditions

Joint Orientation		density (dry)	density (wet)	Rebound number (average of 30 reading (dry)	Rebound number (average of 30 (wet)	Rebound number (average of ten hight reading) (dry)	Rebound Number (average of ten highest reading) (wet)	UCS
dip	dip direction	kN/m³	kN/m³					
81	N110	25.87	25.91	33.8	31.4	37.0	36.3	153.09
57	N216	25.60	25.74	39.2	29.4	42.4	34.2	166.07
57	N75	24.56	24.69	40.8	35.6	44.6	39.6	100.64
53	N205	24.49	24.53	39.0	34.0	43.2	38.2	116.69
49	N13	25.61	25.71	45.6	41.9	47.8	45.3	161.20
75	N315	26.25	26.43	46.2	41.0	48.9	43.6	142.50
23	N243	26.60	26.70	34.4	30.3	36.9	34.6	152.41
35	N210	26.06	26.15	31.0	23.0	33.6	25.6	122.15
50	N200	26.49	26.57	42.8	37.7	45.1	41.9	148.80
86	N83	26.27	26.35	45.6	40.9	48.9	44.7	148.40
52	N200	26.03	26.10	39.0	38.0	45.2	41.6	155.18
83	N105	24.24	24.93	42.0	32.0	47.8	38.0	157.41
52	N20	26.14	26.24	40.0	37.4	41.4	41.3	110.76
43	N192	26.38	26.43	38.6	33.7	42.1	38.8	131.36
52	N202	26.37	26.42	41.3	35.8	45.2	39.8	155.36
82	N95	26.43	26.48	43.7	40.6	46.3	43.4	114.56
77	N319	25.84	26.11	45.6	42.6	50.5	45.9	110.62
63	N70	26.78	26.93	41.7	35.7	46.4	41.5	133.38
53	N205	26.89	27.01	41.8	35.5	45.5	39.9	116.66
47	N192	25.89	25.97	31.6	29.2	35.0	32.7	86.34
52	N209	26.32	26.42	44.8	39.6	47.7	43.3	92.02
75	N91	25.91	25.98	43.6	39.2	46.8	46.0	149.87
49	N14	26.02	26.18	45.5	43.8	49.2	46.3	109.61

Contd.. Table 5.3

Joint Orientation		density (dry)	density (wet)	Rebound number (average of 30 reading (dry)	Rebound number (average of 30 (wet)	Rebound number (average of ten hight reading) (dry)	Rebound Number (average of ten highest reading) (wet)	*UCS
dip	dip direction	kN/m³	kN/m³					
46	N18	25.67	25.77	45.0	43.7	49.5	46.6	109.91
43	N92	26.24	26.30	42.4	36.0	47.2	40.1	104.57
59	N318	25.20	25.48	35.7	34.6	39.3	38.2	141.62
36	N92	26.76	26.85	35.0	29.0	39.2	32.9	126.95
38	N90	26.25	26.35	27.0	25.0	36.0	35.5	127.42
50	N200	26.10	26.19	44.1	38.1	47.3	42.4	113.31
61	N17	25.66	25.79	44.1	41.5	47.4	44.4	113.30

*UCS = Uniaxial Compressive Strength in wet condition measured in the lab.(MN/m²)

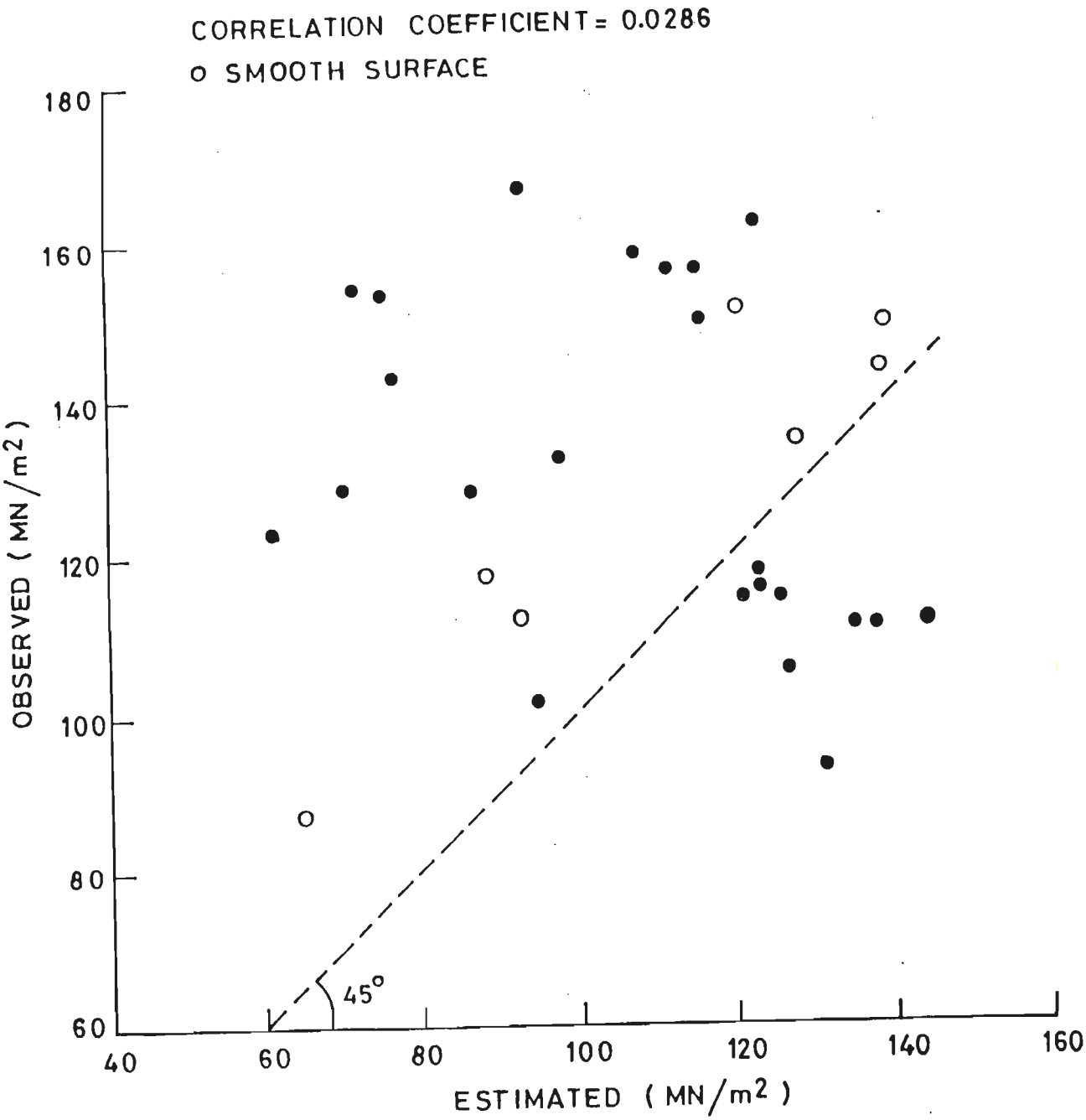

Fig. 5.19: OBSERVED Vs COMPUTED JOINT WALL COMPRESSIVE STRENGTH (MILLER, 1963) IN DRY CONDITION

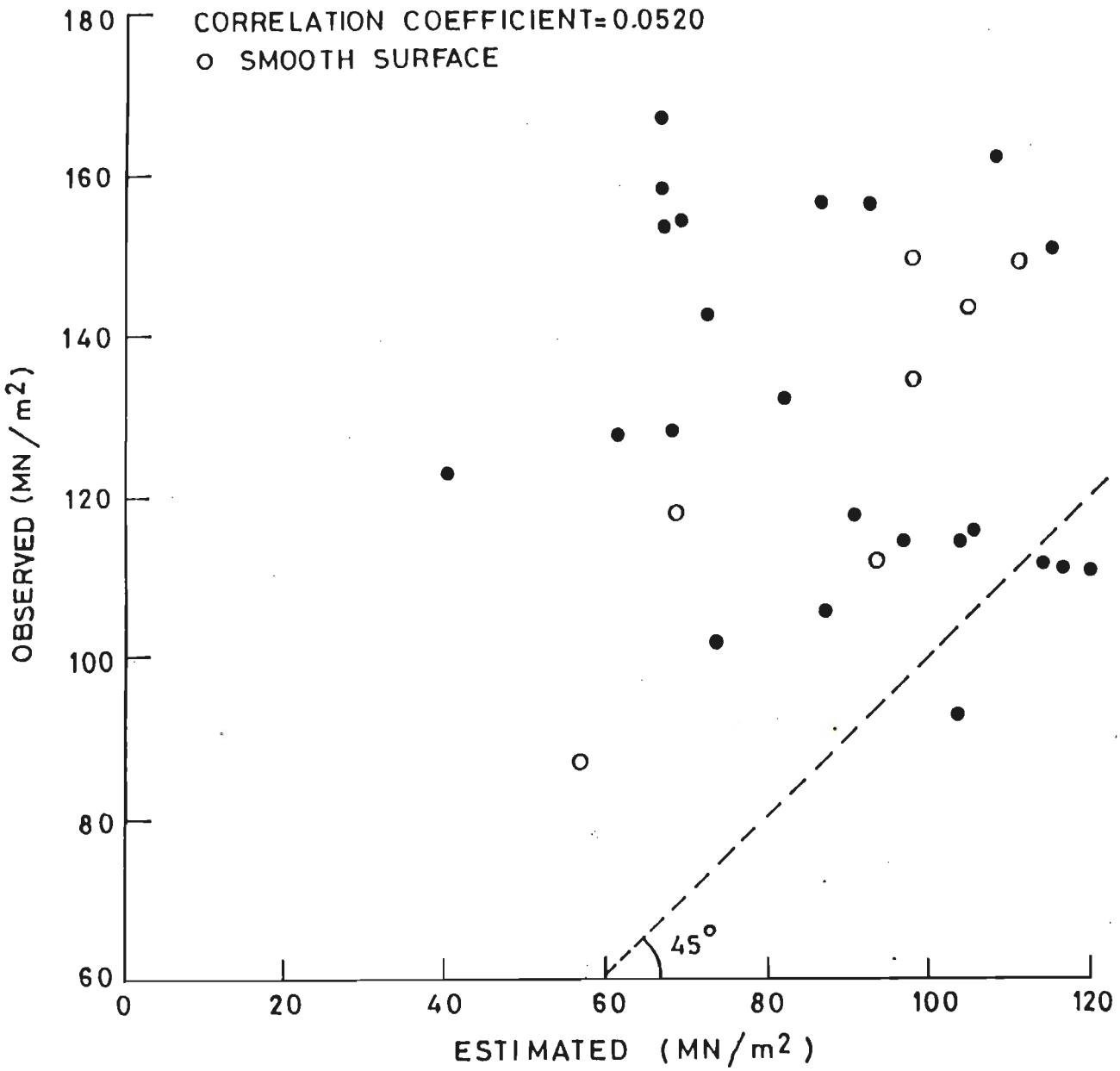

Fig. 5.20: OBSERVED Vs COMPUTED JOINT WALL COMPRESSIVE STRENGTH (MILLER,1963) IN WET CONDITION

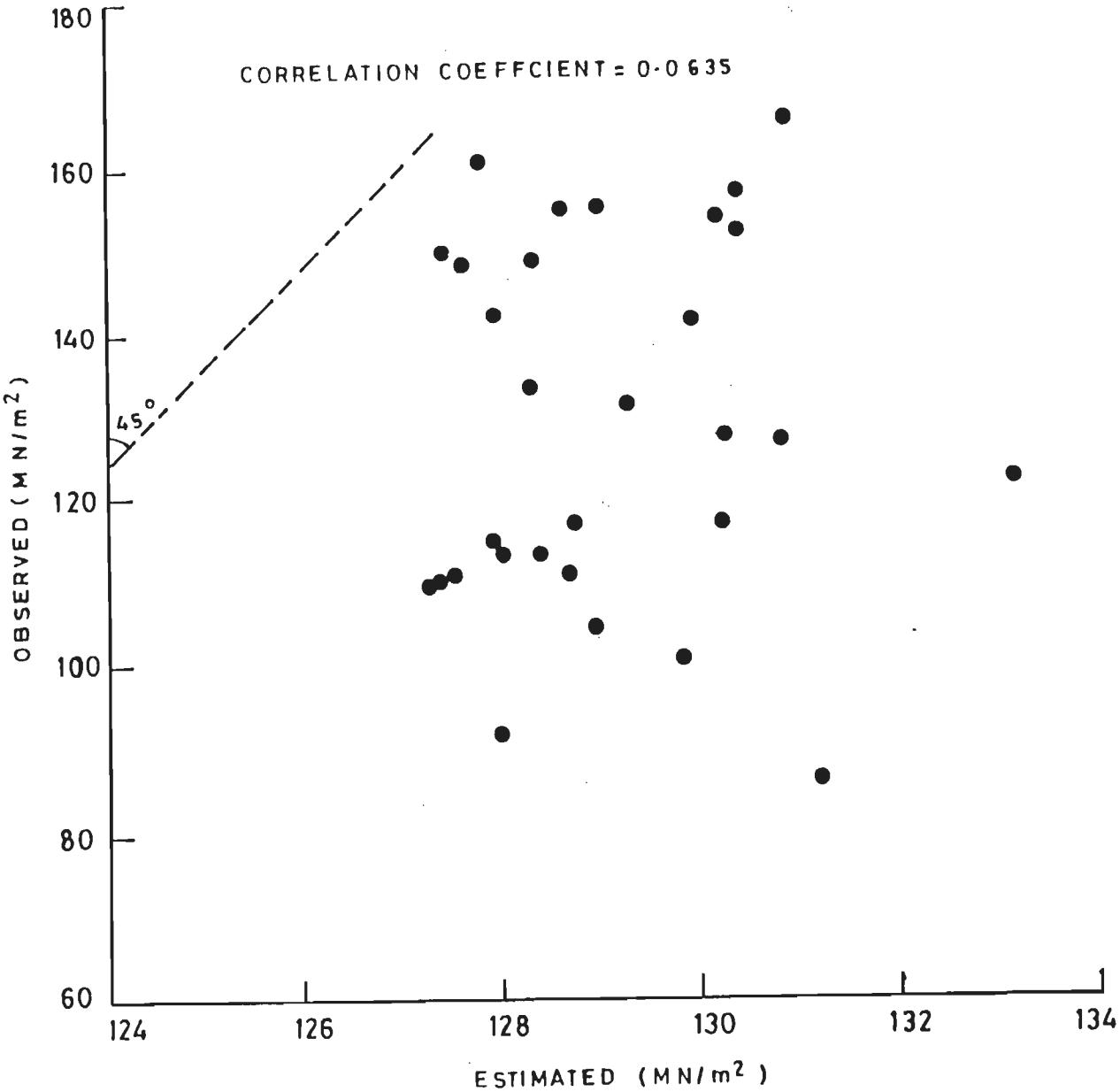

Fig. 5.21: OBSERVED VS COMPUTED JOINT COMPRESIVE STRENGTH IN WET CONDITION.

greater than 10 cm long, to the total drill run. Smaller core pieces may be assumed to be the result of closely spaced discontinuities, shearing, faulting or weathering, causing decrease in rock mass quality. An RQD of 100 percent indicates hundred percent core recovery with all pieces equal to or greater than 10 cm in length. Thus it does not imply an unjointed rock mass.

For the present study RQD has been obtained from the following Barton's correlation (Barton et al. , 1974).

$$RQD = 115 - 3.3Jv \qquad (5.6)$$

where, Jv = sum number of joints per meter for each joint set present. Volumatric Joint Count (Jv) was done in the field as per IS: 11315-1987. A measuring tape of 5 m was placed perpendicular to the relevant joint and number of joints were counted along it. The calculated Jv and their corresponding RQD are listed in Table 5.4.

Table 5.4: Calculated Jv and RQD Values for Six Selected Sites

SITE	**I**	**II**	**III**	**IV**	**V**	**VI**
Jv	19.36	11.65	10.84	8.63	12.26	9.32
RQD %	51.00	76.00	79.00	86.00	74.00	84.00

The table shows that the RQD value is minimum for site I, moderate for sites II, III and V and high for sites IV and VI. These variations in RQD could be due to presence or absence of

shear zone, close spacing of discontinuities and variations in the extent of weathering.

C) Spacing of Discontinuities

The spacing of discontinuities affects overall rock mass strength or quality. Even strongest intact rock is reduced to show poor strength when closely spaced joints are encountered. Conversely, where the spacing is large, the behaviour of rock mass will be strongly influenced by the intact properties. However, exception also exists in case of widely spaced daylighting joints that create a kinematically unstable state. The closely spaced joint surfaces encountered in the slope tend to cause numerous rockfalls or raveling of the surface, whereas widely spaced joints may tend to cause massive catastrophic block failures.

In the present study, measurements of spacing of joints were carried out as per IS: 11315-1987. For this purpose a measuring tape of 5 m length was used. The tape was held along the exposure such that the surface of the discontinuity set being measured was approximately perpendicular to the tape and all the distances between adjacent discontinuities were recorded. Spacing variation or frequency of joints was not constant throughout the rock mass for a joint set. Therefore, several measurements were recorded for each joint set and the most common (modal) spacing was recorded and presented in Tables 5.5 to 5.10 (Art. 5.7). It is evident from these Tables that the joints have

close to moderately close spacing in the sites under study.

D) Condition of Joints

This parameter includes continuity, roughness of joint surfaces, weathering, opening or separation and the infilling material of the joint wall rock. The term continuity implies the aerial extent or size of a discontinuity within a plane. It can be roughly quantified by observing the discontinuity trace lengths on the surface of exposures. It is one of the most important rock mass parameters, but one of the most difficult to quantify except in crude forms (Duncan 1965; Jennings, 1971). In the present work, continuity is estimated along dip and strike direction. Several observations for each joint set were taken and modal trace length for each set were recorded following IS: 11315-1987 procedure. These observations are shown in Tables 5.5 to 5.10 (Art. 5.7) for each site. The observations clearly revealed that continuity on an average for planes involved in failure show low to medium persistence, especially for site-III, where due to low persistence of discontinuities stepwise mode of failure has taken place.

In general terms, the roughness of discontinuity wall can be characterised by a waviness and unevenness. In practice, dip affects the direction of shear displacement of the discontinuity plane, and waviness affects the shear strength. In present study unevenness was measured by visual estimation using roughness profile of IS: 11315-1987 and waviness was quantified using Brunton compass. Wherever the potential sliding direction was

found clear, the Brunton compass was placed along the same direction and amount of inclination were recorded on a straight line at constant interval (2-5 cm). Otherwise the measurements were taken along true dip following the same procedure. For each surface approximately 20 to 25 readings for waviness were taken and standard deviation was calculated. The measurements are shown in Tables 5.5 to 5.10. It is clear from the data shown in these Tables that site VI has the maximum and site I the minimum roughness.

Weathering state of rock has a significant influence on the engineering properties of a rock mass. Rock masses are frequently weathered near the surface. The weathering generally affects the walls of discontinuities more than the interior blocks. This results in a wall strength which is some fraction of what would be measured on the comparatively fresher rock found in the interior of rock blocks. Hence, description of the state of weathering is, therefore, an essential part, while describing the wall strength. Tables 6.5 to 6.1, exhibits the state of joint wall rock weathering for each discontinuity set present at different sites according to IS: 11315-1987. As indicated in Tables the weathering of joint wall on an average has been found to be restricted maximum to discoloration or rusting of joint walls.

Filling is a term used for the gouge material generally clay, silt, etc. between the adjacent rock walls of discontinuities. The perpendicular distance between the adjacent

rock walls is considered as the width of the filled discontinuity. Jaeger (1967) noted that, if infilling is sufficiently thick, the wall of the discontinuities will not touch and the strength properties will be those of infilling materials. The sites investigated have shown that joint planes are generally unfilled and wherever fillings were present the maximum and minimum widths were measured which are presented in Tables 5.5 to 5.10.

Separation or aperture is the perpendicular distance separating the adjacent rock walls of an open discontinuity, in which the intervening space is air or water. Air or water filled large aperture or openness can result from shear displacement of discontinuities showing appreciable unevenness and waviness. Aperture is recorded from point of view of both their loosening and conducting capacity. For the six selected sites aperture or separation of joint planes were measured across each discontinuity. Since the separation was found to vary from point to point, the average separation for each discontinuity was calculated and the measurements are presented in Tables 5.5 to 5.10. As evident from these Tables, site VI has shown maximum separation of joint planes followed by site V, whereas at site I, separation has been found to be minimum.

E) Ground Water Condition (in joint)

Since most of the failure has taken place during monsoon, the presence of water in joints play an important role in

triggering most of the rock failure than any other causes. During heavy rains, the rate of recharge of the ground water through pores, surfaces of discontinuities such as joints, cracks, bedding plane etc., is more than the rate of discharge of ground water. This results in saturation of rock mass which ultimately increases the pore water pressure and in turn reduces the shear strength of the joint wall rock. The rating of ground water condition was determined according to field observations and other joint wall properties. The rating for sites under study are presented in Table 5.11.

F) Orientation of Discontinuities

The orientation of discontinuities relative to slope face largely controls the possibility of unstable conditions. The importance of orientation increases when other conditions for deformation are also present, such as low shear strength, sufficient number of joints and unfavourable attitudes of discontinuities set for slip to occur.

Brunton campass was used for measurement of dip and dip direction of various joint sets. Approximately 200 readings were taken at each site. Poles of measured discontinuities were plotted using polar equal net. Schmidt contouring method was used to determine pole densities, and central value of highest concentration poles were taken as representing the mean orientation of the joint sets. Schmidt net was used to plot great circles with respect to pole densities. Figures 5.22 to 5.25

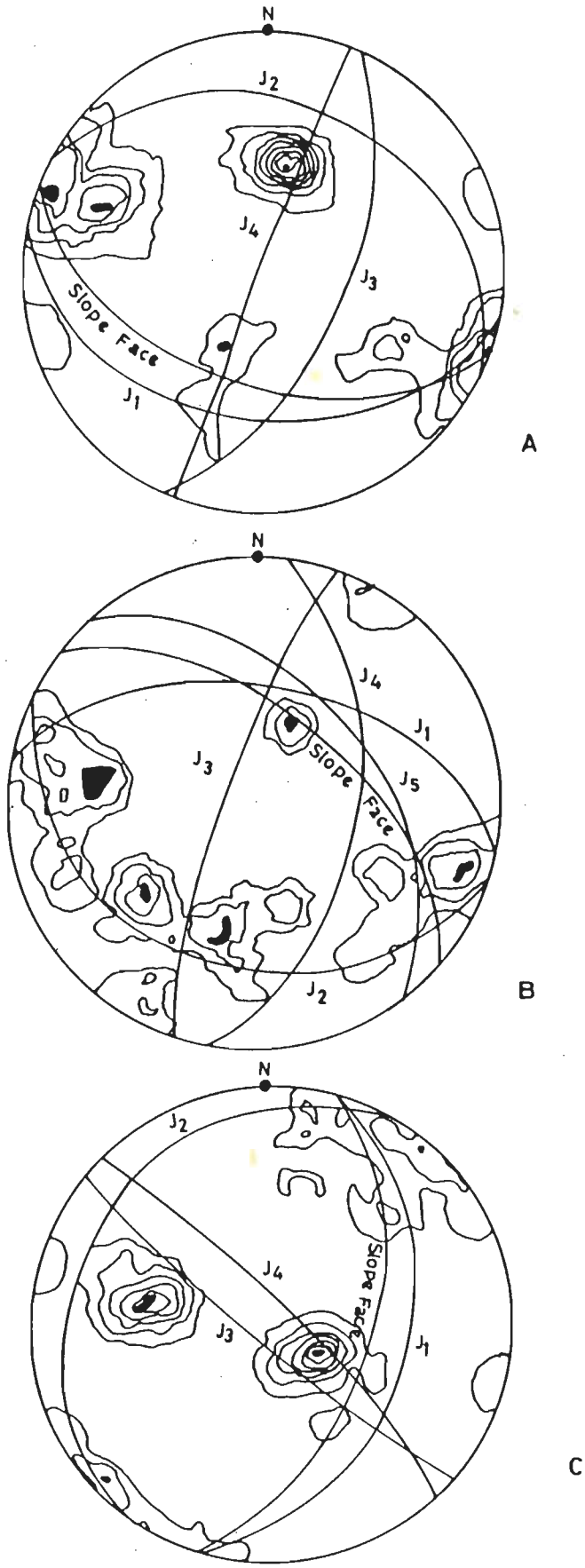

Fig. 5.22: STEREOGRAPHIC PLOTS OF JOINTS AND SLOPE AT SITES L_1 (A), L_6 (B) AND L_9 (C)

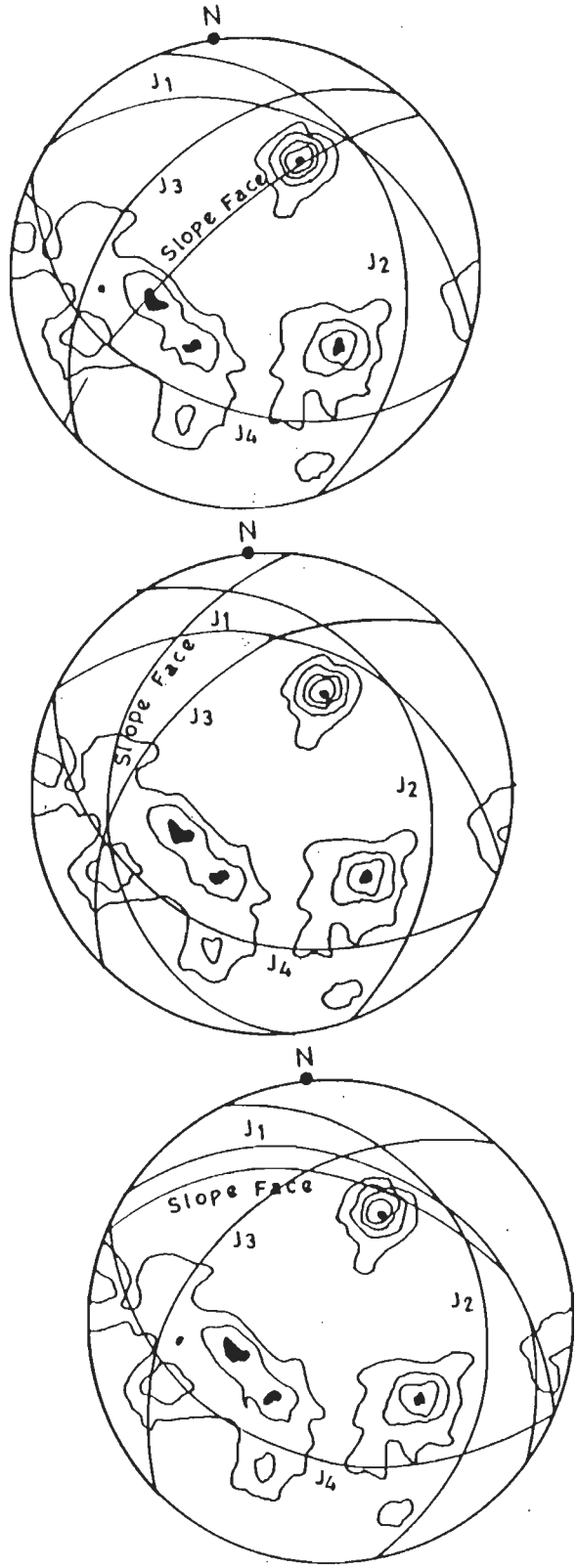

Fig. 5.23 : STEREOGRAPHIC PLOTS OF JOINTS AND SLOPE AT SITE L_5

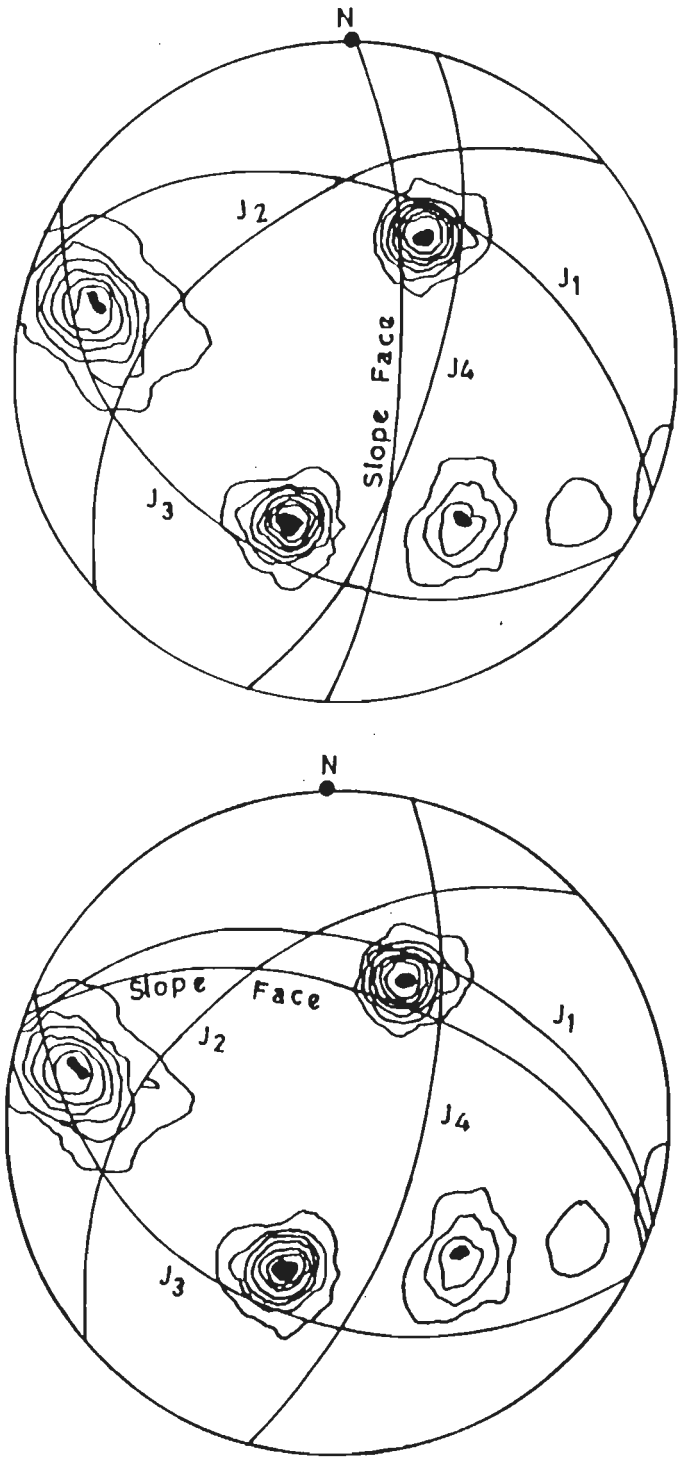

Fig. 5.24: STEREOGAPHIC PLOTS OF JOINTS AND SLOPE AT SITE L7

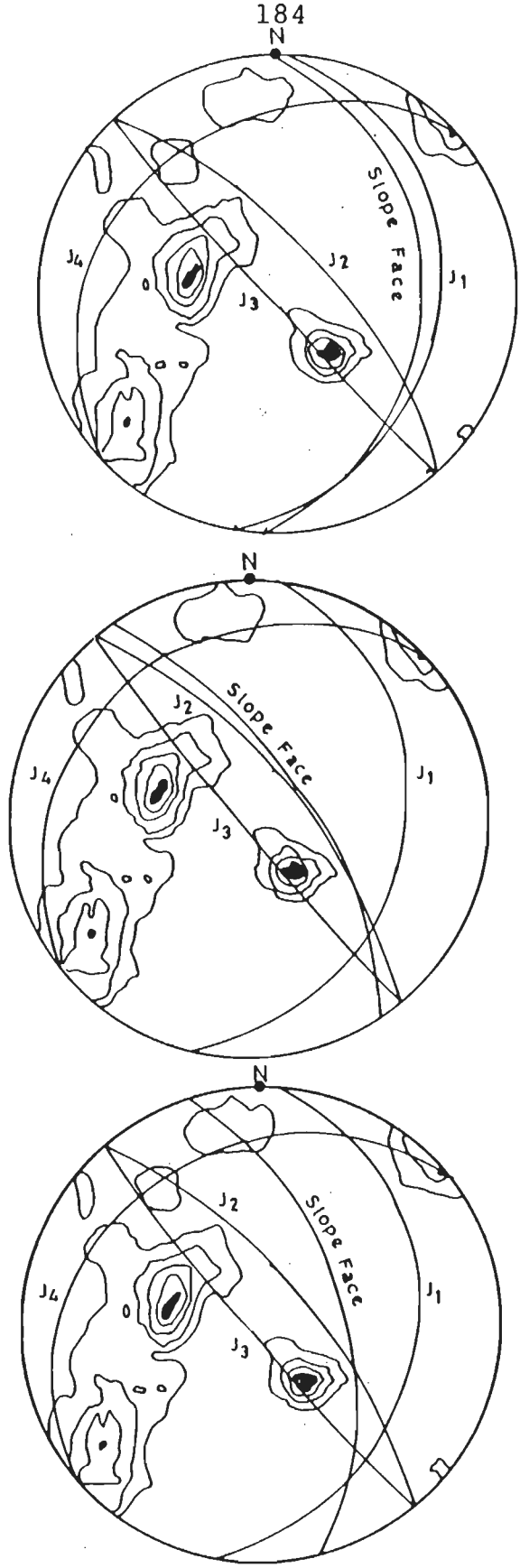

Fig. 525: STEREOGRAPHIC PLOTS OF JOINTS AND SLOPE AT SITE L_{14}.

illustrate different probable mode of failure with respect to slope orientation at different sites.

5.5 STABILITY ANALYSIS

Slope Mass Rating is a system of classification developed by Romana (1985) as an extension of Beiniawiski's (1979) Rock Mass Rating (Appendix-I). In order to assess slope instability, rock parameters like attitude of discontinuities, slope orientation, mode of failure and excavation method must be known. Rock mass quality is determined for sites under study by adding the ratings given to each stability parameter following Bieniawiski's (1979) RMR classification. Based on the value of RMR, slopes are categorised into different stability condition as very poor, poor, fair, good and very good.

SMR `Slope Mass Rating' is obtained from RMR by adding a factorial adjustment factor, the final calculation is of the form:

$$SMR = RMR_{basic} + (F_1 x F_2 x F_3) + F_4 \qquad (5.7)$$

where

SMR = Slope Mass Rating

RMR_{basic} = Rock Mass Rating (Sum of all rating as per table A I.1, App. I)

F_1 - reflects parallelism between the slope and the discontinuity strike. It varies between 1.00 (when both are parallel) to 0.15 (where the angle between the slope strike and strike of discontinuity surface is more than 30^{o}).

F_2 - refers to the dip of discontinuity plane in plane mode of failure. It ranges between 1.00 (for dips > 45^o) to 0.65 (for dip < 20, Appendix -I).

F_3 - refers to angular difference between discontinuity dip angle and the slope angle (i.e. dip angle - slope angle, (Appendix-I). It ranges from zero (for angular difference > 10^o) to -60 (for angular difference < -10^o).

F_4 - Adjustment factor for the method of excavation. It ranges from +15 (for natural slopes) to -8 (for defficient blasting, Appendix-I).

The original classification has provision for planar sliding failure only. In the classification adopted for the study, the wedge failure have also been included. For that purpose the plunge of the line of intersection has been taken for stability analysis in place of dip of the plane (Anbalagan et al. 1992).

5.5.1 Slope Mass Rating of Sites Under Study

Sites I, II, III, IV and VI are close to the road, but no scares of blasting or irregular fracture is observed, except site I, where irregular fractures are not confined to the site and are present every where. Thus, it can be attributed to its proximity to the shear zone. Moreover slopes at these sites are not cut slopes, but explosives have been used for construction of the road about 30 years back. Therefore F_4 is taken as 10. F_4 at site V is taken as zero, since, irregular fractures are

intensified at this site. Besides, it is a cutslope and excavaton is done mostly through mechanical method.

The basic RMR values are listed in Table 5.11. The sites under study have been analysed for their stability using SMR technique and following observations were drawn:

i) **SMR of site I** - This site (Figs. 3.11 , 5.2) has slope angle of 49^{o} towards SSW and trends ESE to WNW. There are four planes of weakness (Fig. 5.21A) dipping 36°, 30°, 62° and 88° due N190 N27, N11 and N290 respectively. The most unfavourable joint orientation is in N190/36° direction (for detail see Table 5.12). Joint walls are moderately rusted. The continuity of joints varies between 1 to 2 m along dip and 4 m to more than 30 m along strike with minimum and maximum roughness, average spacing and separation of 1.5 to 2°, 9-14 cm to 25-43 cm and 0.5 to 2.5 mm respectively. The uniaxial compressive strength of joint wall (quartzite) is found to be above 100 MN/sq.m for each jolint set (Table 5.5). The RMR and SMR values are estimated to be 55 and 22 respectively (Tables 5.11, 5.12). The mode of failure is large planar with no wedge failure.

(ii) **SMR of Site II** - The site (Fig. 5.5) has been studied with respect to surface slope angles of 74°, 36°, 50° towards WNW, W and NNE, trending ESE to WNW, E-W and WNE-SSW. There are four planes of weakness (Fig. 5.23) diping 32°, 35°, 44° and 41° due N36, N74, N315 and N210. The most unfavourable joint orientations are in N36/32° and N315/44° directions. The

weathering of joint walls varies between fresh to moderately discoloured. Roughness, average spacing and average separation are found to vary between 1.6 to 3.6°, 30-61 cm to 21-110 cm and 0.5-2 m to 0.5 - 4.5 mm respectively. The continuity of joints ranges between 2.7m to more than 15 m along strike and 1.2 to 3.4 m along dip. The uniaxial compressive strength of joint wall (quartzite) is above 100 MN/sq.m for all joint sets (Table 5.6). The estimated RMR is 62 (Table 5.11) and SMR are 28, 58 and 43 with respect to different slope orientation (for detail see Table 5.13). Considering the most unfavourable discontinuity and slope orientation, it can be placed in SMR class IV (Planar or large wedge). The observed mode of failure at this site is planar to large planar with no wedge failure.

iii) **SMR of Site III** - The site (Fig. 5.6) has slope angle of 60° towards NNE and trends ESE-WNW. There are five planes of weakness dipping 50°, 31°, 80°, 56° and 50° due N13, N201, N289, N98 and N50 respectively (Fig. 5.22B). The most unfavourable joint orientations are in N13/50°, N50/50° and N98/56° directions (for detail see Table 5.14). Weathering of joint wall vary from slightly to moderately discoloured and rusting. The uniaxial compressive strength (quartzite) for all except joint set having orientation of N13/50° is above 100 MN/sq.m. The continuity of joints varies between 1.5 to 6 m along strike and 0.7 to 2 m along dip. Minimum and maximum roughness, average spacing and average separation at this site varies between 0.5-2.4° to 5.4°, 60 cm to more than 100 cm, 0.5-3 to 9 mm respectively (Table

5.7). The RMR was calculated to be 59 (Table 5.11). Field observations indicate that the site is dominantly characterised by wedge mode of failure. Hence, plunge of line of intersection of two planes involved were considered for the most unfavourable condition and SMR estimated to be 18 (Table 5.14), which places it in SMR class V (large planar or soil like). Besides wedge mode of failure, small planar failure also occur in N98156° direction at this site and SMR with respect to this discontinuity plane is calculated to be 26 and falls within SMR class IV (planar or large wedges). thus minimum SMR is 18 for this site.

iv) **SMR of Site IV** - The site (Fig. 5.7) has been studied with respect to surface slope angles of 75° and 55° towards E and NNE, trending E-W and NNE-SSW. There are four planes of weakness dipping 41°, 48°, 42°, 68° due N18, N315, N208 and N105 respectively (Fig. 5.24). The most unfavourable joint orientation is in N18/41° (For details, see Table 5.15). Weathering of joint wall (silt-stone) varies from slightly to moderately discoloured. Minimum and maximum average roughness, spacing and separation ranges between 1.4 to 2.6°, 26.40 to more than 100 cm and 1 to 12 mm respectively. The continuity varies between 0.4 to more than 20m along strike and 1.2 to 2 m along dip. The uniaxial compressive strength of all joint walls are above 100 MN/sq.m (Table 5.8). RMR is calculated to be 65 (Table 5.11). The SMR are 64 and 24 for different slope orientations (Table 5.15). Considering the most unfavaourable condition (joint of N18/41° orientation with respect to N20/55° slope direction) the minimum

SMR is estimated to be 24. Field observations did not confirm planar movement with respect to this slope direction and SMR equal to 24 does not represent the actual failure and field condition as far as stability is concerned.

v) **SMR of site V** - The site (Figs. 3.13, 5.8) has slope angle of 56° towards ESE and trends NNE-SSW. There are four planes of weakness dipping 42°, 20°, 85° and 82° due N302, N221 and N46 respectively. The most unfavourable joint orientation is in N108/42° direction. Weathering of joint (quartzite) wall vary from fresh to slightly discoloured in all joint sets except joint having dip amount of 42° due N108, which is highly discoloured, with rusting on the surface. The continuity vary between 0.8 to more than 60 m along strike and 0.3 to 1.5 along dip. Minimum and maximum roughness, average spacing and separation ranges between 1.6° to 5.6-7.5°, 27-31 cm to 40-70 cm, 0.65-3 to 15 mm respectively. The uniaxial compressive strength of all joint walls is above 100 MN/s.qm (Table 5.9). The RMR is estimated to be 57 (Table 5.11). The SMR for this site is calculated to be 6 (Table 5.16). Field observations indicate this site is characterized by planar mode of failure of much lower magnitude as compared to site I and II. This rating places it in SMR class V (large planar or soil like) which does not represent true/observed stability condition at this site.

vi) **SMR of site VI** - The site (Fig. 5.11) has been studied with respect to surface slope angles of about 40°, 70° and 60° towards E, NE, ENE, trending in E-W, NE-SW and ENE-WSW directions. There

are four planes of weakness dipping 33°, 72°, 88° and 26° due N97, N50, N228 and N317 respectively. The most unfavourable joint orientations are in N97/33°, N50/72° and N228/88° (Fig. 5.25). Weathering of joint wall vary between slightly to moderately discoloured. Continuity ranges between 3 m to more than 60 m along strike and 2 to 6 m along dip. Minimum and maximum roughness, average spacing and average separation varies between 3.4 to 4.0°, 31-42 to 80-90 cm and 3 to 9 mm respectively. The uniaxial compressive strength (quartzite) of all joint walls except joint orientation of N97/33° is above 100 MN/sq.m (Table 5.10). RMR is estimated to be 62 (Table 5.11). The SMR for slope orientations of N92/39°, N57/70° and N74/60° are calculated to be 42, 66, 55 respectively (Table 5.17). Thus minimum SMR is 42. The failure at this site involves thin wedges and planar failure confined to the face of slope only.

5.5.2 Efficacy of SMR Approach of Stability Analysis

Although sites I, II, IV and III and V, may be placed in class IV and V of SMR classification respectively, but extent of failure as observed in the field is comparatively high at site I followed by site II and least at site IV. The extent of failure at site III is also much higher than site V. The results obtained show that descriptive mode of failure are not matching with SMR classes. Further, it seems, when SMR value approaches the upper class (class I), it can represent the true stability condition. Conversely, towards the lower class (class V), at certain situation it appears to be misleading. Based on the

results obtained and through study of field observations (Table 5.5 - 5.10), it appears where continuity of discontinuity surfaces along dip is less than 5% of the height of affected slope, the slope mass rating does not give a true picture of the stability conditions and its usefulness appears to be limited.

5.6 THREE DIMENSIONAL STABILITY ANALYSIS

The Slope Mass Rating (SMR) method of analysis as mentioned above did not work in certain situations. Hence another approach based on Hoek and Bray's (1981) short solution was applied to carry out stability analysis of these six sites.

The stability analysis of discontinuity controlled slopes generally involves two interrelated stages, i) most unfavourable discontinuities out of all surfaces of defects must be identified ii) Each joint defined block must be analysed to determine the factor of safety (F) which is defined as the ratio of the total force available to resist sliding to the total force tending to induce sliding. Under different conditions, the factor of safety has been worked out by Hoek and Bray's (1981) short solution. The details of these common equations are given in Appendix II.

Computer analysis of slope for estimating factor of safety (F) is the approach in the present slope stability study. In this technique, by iterative changes in `c' and `ϕ' values for a given slope parameter, the value of `F' is estimated continually till the actual field conditions get simulated ($F \leq 1.0$) . At this stage the values of `c' and `ϕ' are finally chosen to conduct

stability analysis in the similar geological situation of hill slope in the nearby area.

A computer program `SASW' developed by Sharma (1990) based on Hoek and Bray's (1981) short solution has been used to workout factor of safety in dynamic dry and wet conditions. It is pertinent to add that the execuation file of this program was allowed to be used. This program allows that either of the planes of discontinuity may be labelled 1 or 2. Further, a check on whether the two planes do form a wedge is included. Depending upon the geometry of the wedge and the magnitude of water pressure acting on each plane, contact may be lost on either plane and this contingency is provided in this program. The program has also provision of assigning values of cohesion and friction angle for each joint . This program in addition to above defined parameters also calculates the dynamic displacement and critical acceleration by earthquakes.

Bieniawiski (1979) proposed a simple and reliable geomechanical classification of rocks based on extensive field data, to workout a narrow range of cohesion (c) and internal friction angle (ϕ). The summation of the rating given to each of the parameter, as discussed in section 5.4.1, gives a single numerical value called Rock Mass Rating (RMR), which in turn is used to find C & ϕ (Appendix-III). Since C & ϕ found from RMR technique forms the basis for back slope analysis, it is important to note that affect of joint orientation and water condition be considered only in one of these two approaches

namely RMR and Back analysis to avoid double accounting of parametres. Since the program used for Back slope analysis already incorporates these parameters (water pressure and joint orientation), the RMR was accordingly worked out taking this philosophy into account to get `c' & `ϕ' values for Back analysis of slope.

The value of `c' & `ϕ' obtained from such a modified RMR for these sites are (Appendix-III) estimated to range between 2-4 kg/cm^2 and 25 - 45^o respectively. The `c' and `ϕ' affect the value of factor of safety under a given hillslope condition. However, the factor of safety is more sensitive to `c' than `ϕ'. Hence, considering the basic geological parameters of each joint set, a conservative value of `$\phi$' was assigned. The `c' values were simulated till field condition was created. The values of `c' and `ϕ' thus work out for each site are presented in Table 5.12-17.

5.7 RESULTS AND DISCUSSION

Inquiries from the local people and DGBR (Director General of Border Road) officials responsible for the maintenance of the road, revealed that these slide areas always get activated during monsoon. Therefore `c' and `ϕ' values calculated from RMR in dry condition were changed in such a manner that field condition or mode of failure, were simulated in wet condition. The area of study falls within zone IV of seismic map of India (IS: 1893-1970). Hence, in the present study, horizontal seismic

coefficient is taken as 0.05 under dry condition. Results obtained are presented in Tables 5.12 - 17 and discussed below.

i) **Site I** - This site is characterised by formation of one plane and two wedges with respect to surface slope angle of 49° due N200. The `c' and `ϕ' values vary between 2.5 to 5 t/sq.m and 32 to 33° respectively. The estimated factor of safety in wet and dry dynamic condition are presented in Table 5.12. The water pressure is of the order of 4.2 t/sq.m, which is positive on both discontinuity planes J_3 and J_4, having their plunge of line of intersection in N200/5° direction. Thus, increasing factor of safety from 39.65 in dry dynamic to 88.56 in wet condition. Conversely the effect is negative on planes J_1 and J_4 having their plunge of line of intersection in N200/36° direction, inducing a decrease on factor of safety from 1.61 in dry dynamic to 1.02 in wet condition. In case of N190/36° joint plane, the water pressure reduces factor of safety from 1.51 to 0.85, causing a planar failure (Table 5.12). So the minimum factor of safty of slope is less than 1 as expected.

ii) **Site II** - This site has been analysed with respect to surface slope angles of 74°, 36° and 50° due N322, N270 and N25. The estimated `c' and `ϕ' values ranges between 3 to 6 t/sq.m and 33 to 35° respectively. The calculated factor of safety are presented in Table 5.13. In case of N322/74° slope orientation, intersection of J_1 and J_3 form a wedge in dry dynamic condition, having plunge of their line of intersection in N8/36° direction. In wet condition the contact is lost on discontinuity Plane J_1

due to pore water pressure of the order of 6.7 t/sq.m, reducing factor of safety from 1.67 to 0.85. Joint Plane of N315/44° orientation has factor of safety of 1.23 under dry dynamic condition and decreases to 0.84 in wet condition. Back slope analysis with respect to 270/36° slope orientation indicated formation of a wedge by intersection of two discontinuity planes J_3 and J_4 with factor of safety of 2.99 in dry dynamic condition. The contact is maintained on joint plane J_4 under wet condition with factor of safety of 18.97, implying thereby a positive water pressure acting on this plane. Analysis of this site with respect to surface slope angle of 50° due N25, indicated a planar failure as observed in the field with factor of safety of 0.95 and formation of two wedges with factor of safety above 1 in wet condition. Hence, it is inferred that this site remains stable under dry dynamic condition as indicated by a factor of safety of 1.44 and 1.23 involving unfavourable joint orientations J_1 and J_3. In monsoon the minimum factor of safty is less than 1 as expected.

iii) **Site III** - The site has been analysed with slope orientation of N60/40°. The cohesion, internal friction angle ranges between 4.5 to 12 t/sq.m and 32 to 35° respectively (Table 5.14). Calculated water pressure is of the order of 13.3 t/sq.m. The dominant mode of slope movement is wedge failure. The wedge formed by intersection of J_1 and J_4 discontinuities has factor of safety of 0.99 in wet condition and increases to 1.35 under dry dynamic condition. The J_1 and J_5 joint planes also form a wedge

having its plunge of line of intersection in N30/48° direction. The factor of safety of this wedge is 0.69 in wet condition and increases to 1.35 under dry dynamic condition. The wedge formed by intersection of J_4 and J_5 joint planes under dry, dynamic condition loses its contact on J_4 and factor of safety decreases from 1.59 to 0.35 inducing a planar mode of slope movement in wet condition, as expected.

iv) **Site IV** - This site is analysed with respect to surface slope angles of 75° and 55° due N90 and N20. The cohesion and internal friction angle varies between 10 to 19 t/sq.m and 32 to 35° respectively. The calcualted water pressure is found to be 8.3 t/sq.m. The planar failure in N18/41° direction, observed in the field with respect to N90/75° slope orientation, is anticipated to be due to water pressure acting on this plane, thus reducing factor of safety to 0.87 (Table 5.15), whereas, in dry dynamic condition the same plane forms a wedge with the discontinuity plane in N105/68° direction, thus increasing factor of safety from 0.87 to 1.93. The factor of safety at this site with slope orientation of N20/55° changes from 2.41 to 3.74 under wet condition. As indicated in Fig. 5.24 and SMR value of this site (Table 5.15), a planar failure with respect to this slope orientation (N20/55°) is expected. But field observations did not conform such a movement (in N18/41 direction). This is probably due to effect of cohesion, which is estimated to be 19 t/sq.m along this discontinuity surface.

v) **Site V** - This site is characterised with slope orientation of N107/56°. The values of cohesion and internal friction angle is

worked out to vary between 3-10 t/sq.m and 31 to 34° respectively (Table 5.16). The water pressure is estimated to be of the order of 3.8 t/sq.m. Factor of safety at this site under dry dynamic condition varies between 1.40 to 25.61 and changes from 0.85 to 479.79 under wet condition. Planar failure observed at this site appears to be due to water pressure acting on J_1 (N108/42°) discontinuity plane. Conversely, the factor of safety of N302/20°. Joint plane increases to 479.79, implying thereby a positive water pressure acting on this plane.

vi) **Site VI** - This site shows a wide range of change in its slope direction. Hence, the site has been analysed with respect to surface slope angles of 39°, 60° and 70° due N92, N74 and N50. The cohesion and internal friction angle is found to vary between 2.5 to 3 t/sq.m and 30 to 33° respectively (Table 5.17). The water pressure acting on each discontinuity plane is estimated to be 4.2 t/sq.m. Factor of safety with respect to slope orientation of N92/39° has been calculated to vary between 1.14 to 31.26 in dry dynamic condition. Conversely, movement of a thin wedge confined to the face of slope reduces factor of safety to 0.00 under wet condition as the result of floating of the wedge due to water pressure acting on J_1 and J_3 discontinuity planes, confirming field observation. Back analysis of slope with surface angle of 60° due N70, revealed that observed (field) planar failure involving J_1 discontinuity plane is due to water pressure acting on this discontinuity surface. The factor of safety of the same joint plane has been calculated to be 1.23

Table 5.5 : Basic Geological Parameters and Measurements for Site I (L_1)

Joint orientation (Degree)		Roughness angle (Degree)	Weathering of joint wall	Continuity (m)	Average spacing (cm)	Filling (mm)	Average separation (mm)	JCS by rebound hammer (MN/sq.m)		JCS by uniaxial compression test in wet condition (MN/sq.m)
Dip	Dip direction							Dry	Wet	
36	190	1.5	Moderate rusting	>30 along strike 2 along dip	9-14	5mm thick clay seen at few places	2.5	75	50	153.0
30	27	2.0	-do-	>15 along strike 1.5-1.8 along dip	21-40	-	1.4	52	38	141.0
62	111	1.7	-do-	>10 along strike 1 along dip	25-43	-	1.8	72	70	155.0
88	290	1.5	-do-	4 along strike 2 along dip	8-25	-	0.5	62	42	132.0

Table 5.6 : Basic Geological Parameters and Measurements for Site- II (L_5)

Joint orientation (Degree)		Roughness angle (Degree)	Weathering of joint wall	Continuity (m)	Average spacing (cm)	Filling (mm)	Average separation (mm)	JCS by rebound hammer (MN/sq.m)		JCS by uniaxial compression test in wet condition (MN/sq.m)
Dip	Dip direction							Dry	Wet	
32	36	1.6	Fresh to slightly discolored	3 along strike 1.5-2 along dip	60-80	-	0.5-2	92	91	110
35	74	2.0	-do-	2.7 along strike 1.2 along dip	modal 30-50	-	0.5-4.5	94	73	100
44	315	1.7-4.0	moderately discolored	4 along strike 3.4 along dip	21-110 modal 35	-	2.3	92	85	142
41	210	3.6	fresh to slightly discolored	>15 along strike 3 along dip	30-61 modal 45	-	1.7	90	60	166

Table 5.7 : Basic Geological Parameters and Measurements for Site- III (L_a)

Joint orientation (Degree)		Roughness angle (Degree)	Weathering of joint wall	Continuity (m)	Average spacing (cm)	Filling (mm)	Average separation (mm)	JCS by rebound hammer (MN/sq.m)		JCS by uniaxial compression test in wet condition (MN/sq.m)
Dip	Dip direction							Dry	Wet	
50	13	1.2	Moderately discolored	4 along strike 3 along dip modal 1.5	50-120 modal 60	-	0.5-3	70	52	90
31	201	1.9	-do-	>2 along strike 1.8 along dip	55-100 modal 65	-	2	87	68	116
80	289	5.4	Moderate rusting	2-6 along strike 2 along dip	55-60	-	1-6	143	113	110
56	98	0.5-2.4	-do-	2-6 along strike 2-2.5 along dip	50-65	-	9	75	55	101
50	50	2.2	Slightly discolored	0.8-1.7 along strike 0.7 along dip	100-115	-	3	80	75	134

Table 5.8 : Basic Geological Parameters and Measurements for Site- IV (L_7)

Joint orientation (Degree)		Roughness angle (Degree)	Weathering of joint wall	Continuity (m)	Average spacing (cm)	Filling (mm)	Average separation (mm)	JCS by rebound hammer (MN/sq.m)		JCS by uniaxial compression test in wet condition (MN/sq.m)
Dip	Dip direction							Dry	Wet	
41	18	2.6	Slightly discolored	2- 5 along strike 1.5-1.9 along dip	70	-	0.5-4	80	68	110
48	316	NA.	-do-	6 along strike 2 along dip	100-110	-	1	78	70	155
42	208	1.8	-do-	>20 along strike 1.7 along dip	26-40	-	2	90	82	155
68	105	1.4	moderately discolored	4 along strike 2 along dip	54	-	12	88	72	114

Table 5.9 : Basic Geological Parameters and Measurements for Site- V (L_9)

Joint orientation (Degree)		Roughness angle (degree)	Weathering of joint wall	Continuity (m)	Average spacing (cm)	Filling (mm)	Average separation (mm)	JCS by rebound hammer (MN/sq.m)		JCS by uniaxial compression test in wet condition (MN/sq.m)
Dip	Dip direction							Dry	Wet	
42	108	5.6-7.5	Highly discolored with rusting on the surface	3 along strike 0.7-1.5 along dip	27 - 31	Quartz coating 1- 5 thick	0.65-3	100	92	110
20	302	1.6	Fresh to slightly discolored	>60 along strike 1.5 along dip	40 - 70	Dark green clay 2-18 thick	1 - 2	135	102	118
85	221	5.6	Fresh	1 along strike 0.25-0.40 along dip	30 - 50	Quartz coating 2-4 thick	2 - 4	125	100	120
82	46	4.0	Fresh	0.8 along strike 0.30 - 0.50 along dip	29 - 40	-	2 - 6	70	56	134

Table 5.10 : Basic Geological Parameters and Measurements of Site- VI (L_{14})

Joint orientation (Degree)		Roughness angle (Degree)	Weathering of joint wall	Continuity (m)	Average spacing (cm)	Filling (mm)	Average separation (mm)	JCS by rebound hammer (MN/sqm)		JCS by uniaxial compression test in wet condition (MN/sq.m)
Dip	Dip direction							Dry	Wet	
33	97	3.75	Moderately discolored	<3 along strike 2.5 along dip	40 - 50	-	9	45	40	97
72	50	4.9	Slightly discolored	4 along strike 5 along dip	31 - 42	-	3.6	110	108	141
88	228	4.8	-do-	4 along strike 4 along dip	40 - 55	-	3.4	102	90	105
26	317	3.4	-do-	>60 along strike 3 along dip	80 - 90	-	3	95	84	124

Table 5.11 : Basic Rock Mass Rating for Selected Sites.

Site	Uniaxial compressive strength	RQD	Joint spacing	Joint condition	Ground water	RMR
I	12	13	9	12	9	55
II	12	17	10	13	10	62
III	12	17	11	10	9	59
IV	12	17	12	14	10	65
V	12	13	11	12	9	57
VI	12	17	11	13	9	62

Table 5.12 : SMR and Factor of Safty of Site - I (L_1)

Joint orientation (Degree)		Slope orientation (Degree)		SMR	Height (m) H	Density (t/cu.m)	Cohesion (t/sq.m) C	Angle of Internal friction (deg.) ϕ	Movement Orientation (Degree)		Type of movement	Factor of safety	
Dip	Dip direction	Dip	Dip direction						Dip	Dip direction		Dry dyn.	Wet
36	190	49	200	22	25	2.567	2.5	32	36	190	Plane	1.51	0.85
30	27						5	33	36	200	Wedge	1.61	1.02
62	111						4	33	5	200	Wedge	39.65	88.56
88	290						5	32					

Table 5.13 : SMR and Factor of Safty of Site - II (L_8)

Joint orientation (Degree)		Slope orientation (Degree)		SMR	Hei-ght (m) H	Density (t/cu.m)	Cohesion (t/sq m) C	Angle of Internal friction (deg.) ϕ	Movement Orientation (Degree)		Type of movement	Factor of safety	
Dip	Dip direction	Dip	Dip direction						Dip	Dip direction		Dry dyn.	Wet
32	36						3	33					
									30	8	Wedge/		
		74	322	28					32	36	plane	1.67	0.85
									23	20	wedge	2.44	2.17
									44	315	plane	1.23	0.84
35	74						6	34					
		36	270	58	40	2.610			44	315	wedge/	2.99	18.97
									30	261	plane		
44	315						6	35					
									32	36	Plane	1.44	0.95
		50	25	43					30	8	wedge	1.57	1.14
									23	20	wedge	2.53	2.20
41	210						4	35					

Table 5.14 : SMR and Factor of Safty of Site - III (L_6)

Joint orientation (Degree)		Slope orientation (Degree)		SMR	Height (m) H	Density (t/cu.m)	Cohesion (t/sq m) C	Angle of Internal friction ø	Movement Orientation (Degree)		Type of movement	Factor of safety	
Dip	Dip direction	Dip	Dip direction						Dip	Dip direction		Dry dyn.	Wet
50	13	60	40	18	80	2.612	12	33	80	289	Plane	2.50	14.93
									44	48	Wedge	1.53	0.99
31	201						7	33					
									48	30	Wedge	1.35	0.69
80	289						4.5	35					
									13	16	Wedge	7.23	7.21
56	98						10	32					
									42	9	Wedge	1.75	1.09
50	50						9	33					
									50 56	60 98	wedge/ plane	1.59	0.35

Table 5.15 : SMR and Factor of Safty of Site - IV (L_7)

Joint orientation (Degree)		Slope orientation (Degree)		SMR	Height (m) H	Density (t/cu.m)	Cohesion (t/sq m) C	Angle of Internal friction (deg.) ϕ	Movement Orientation (Degree)		Type of movement	Factor of safety	
Dip	Dip direction	Dip	Dip direction						Dip	Dip direction		Dry dyn.	Wet
41	18						19	35					
									41	35	wedge/		
									41	18	plane	1.91	0.87
		75	90	64	65				23	25	Wedge	3.73	3.31
48	316						13	35					
						2.680							
42	208						12	33					
									41	18	plane	2.89	2.41
		55	20	24	50				41	35	Wedge	2.91	2.45
									23	25	Wedge	4.03	3.74
68	105						10	32					

Table 5.16 : SMR and Factor of Safty of Site - V (L_5)

Joint orientation (Degree)		Slope orientation (Degree)		SMR	Height (m) H	Density (t/cu.m)	Cohesion (t/sq m) C	Angle of Internal friction (deg.) ø	Movement Orientation (Degree)		Type of movement	Factor of safety	
Dip	Dip direction	Dip	Dip direction						Dip	Dip direction		Dry dyn.	Wet
42	108						3	34					
									20	302	Plane	9.91	479.79
20	302						2.5	33					
		56	107	6	23	2.624			42	108	Plane	1.40	0.85
85	221						9	31					
									22	143	Wedge	25.61	25.31
82	46						10	31					

Table 5.17 : SMR and Factor of Safty of Site - VI (L_{14})

Joint orientation (Degree)		Slope orientation (Degree)		SMR	Height (m) H	Density (t/cu.m)	Cohesion (t/sq m) C	Angle of Internal friction (deg.) ø	Movement Orientation (Degree)		Type of movement	Factor of safety	
Dip	Dip direction	Dip	Dip direction						Dip	Dip direction		Dry dyn.	Wet
33	97	39	92	42	25	2.648	2.5	30	72	50	plane	2.31	30.36
									33	97	plane/ wedge	2.61	0.00
									26	140			
									14	19	wedge/ plane	4.30	147.12
									26	317			
									1	141	wedge	31.26	38.93
72	50	70	56	66			3	33	33	97	plane/ wedge	1.14	0.00
									30	129			
									11	24	Wedge	3.47	3.64
									1	141	Wedge	31.39	38.95
88	228	60	74	55			3	33	33	97	Plane	1.23	0.63
									11	24	Wedge	3.54	3.65
									1	141	Wedge	30.85	38.87
26	317						2.5	33					

under dry dynamic condition.

From the analysis made above and the results presented in the Table 5.12-17, it is observed that the factor of safety for all the these six sites gets reduced and becomes less than one under wet condition. This indicates prevalence of sliding forces over resisting forces acting on these sites. This is the reason why during monsoon periods, these sites become unstable. In dry dynamic condition, the factor of safety is more than one, i.e., resistive forces are more than the sliding forces and therefore, no failure takes place during dry season at these critical sites. The stability of hillslopes under dry dynamic condition is further proved by the fact that an earthquake of 6.8 magnitude on 19th October, 1992, which devastated the areas in and around Uttarkashi (situated about 35 km to the north of study area), had no effect in destabilisation of these sites. Thus, instability of these sites during rainy season can be reduced by providing appropriate horizontal drains in form of drill holes with folded geofabric.

Another limitation of SMR should also be mentioned that radius of curvature of the slope in plan affects the stability of slopes (Hoek and Bray,1981). Concave slopes are more stable than convex slopes. This factor should be considered in the SMR.

5.8 SUMMARY

The developmental activity has affected the hillslope adjoining the road section at a number of places by various type of slope movement, particularly planar and wedge failure. The

landslides perpetually have been a cause of great concern and difficulties mainly towards transportation or road communication. Field observations at locations L_1, L_4, L_7, L_9, L_{12}, L_{14}, L_{15}, L_{16} and L_{18} indicate that the road construction has day lighted the weakest surface of discontinuities, which has made these areas vulnerable to slope movement during monsoon.

While doing stability analysis of six selected sites, namely L_1, L_5, L_6, L_7, L_9 and L_{14} using SMR technique, it was observed that L-type rebound hammer applied on natural surfaces of rock masses to estimate uniaxial compressive strength did not yield any correlation with observed uniaxial strength as determined in the laboratory.

SMR was used to categorise the stability condition of these sites. On the basis of this stability study approach, these site have been categorised as unstable (L_1) with planar or large wedge failures, unstable (L_5) with planar or large wedge failures, very unstable (L_6) with large planar or soil like failure, unstable (L_7) with planar or large wedge failures, very unstable (L_9) with large planar or soil-like failure and partially stable (L_{14}) with some joints or many wedge failure. Whereas the conclusion drawn tally with actual observation for sites I, II and VI, the SMR appear to have not worked for the sites namely III, IV and V. A critical examination of these sites indicates that when the of continuity of joints along dip is less than 5 percent of the affected slope height, it appears SMR gives an inadequate picture of stability condition because of major role of $C / \gamma H$.

Back analysis of slope based on Hoek and Bray's (1981) short solution suggests that all these slopes are unstable in wet conditions and are stable under dry dynamic condition. This conclusion is supported by the fact that year after year, these slopes fail during monsoon season, due to dual action of pore water in form of pressures acting to destabilise the slope and decrease the strength of wet rock mass. It is also important to note that these sites located on zone IV of seismic map of India, remained unaffected by an earthquake of 6.5 magnitude which devastated the area in and around Uttarkashi (situated 35 km to the north of study area). In view of instability of the slopes during monsoon, where SMR recommends reexcavation at sites L_6 and L_9, extensive correction at sites L_1, L_5, L_7 and systematic support for site L_{14}, the back slope analysis recommends provision of adequate subsurface drainage to stabilise them.

CHAPTER - 6

SYNTHESIS, SUMMARY AND CONCLUSION

Himalaya is the youngest and the loftiest mountain range in the world. It stands out as a very prominent physiographic unit on the northern part of Indian subcontinent. Its origin is attributed to collision of the Indian plate with the Eurasian plate. Himalaya is still rising due to continual subduction of Indian plate. This geodynamically active terrain witnesses intense landslide during monsoon and frequent earthquakes. Landslide phenomenon is not omnipresent in this terrain. Slope instability is found to occur and recur in the areas characterised by unique combination of topographic, structural, lithologic, hydrologic, climatic and vegetative features. Also, these factors act and interact to change the sculpture of a watershed. If this is so, then the geomorphic parameters may have some relationship with the instability of the terrain. Hence, with this hypothesis, the present study was taken up as an endeavour mainly towards the identification, evaluation and forecasting of hazardous zones of instability due to landslide through the geomorphometric signatures imprinted on the instability prone Garhwal region of Lesser Himalaya, in the district Tehri Garhwal.

The area of study lies in Kumaun tectonic zone of the Lesser Himalaya in the Garhwal region, which is separated in the north

from the Garhwal tectonic zone by the North Almora Thrust and from the Siwalik in the South by the Main Boundary Thrust. The terrain under study covers an area of about 102 sq.km and is characterised by a typical ridge and valley topography. It is bounded in the east, south and west by the river Ganga and in the north by a ridge.

The rocks exposed in the area form part of two major lithostratigraphic successions - the Lansdowne Formation of Precambrian. Kumaun Super group dominantly consists of Quartzite of Bijni Member associated with Phyllite of the Amri Member, and the younger succession comprising of the Blaini Formation which consists mainly of boulder bed, variegated purple green shale and siltstone, the Krol Formation which largely consists of limestone and dolomite with calcareous shale, the Tal Formation which is made up of quartzite, slate, shale and shell limestone and the Subathu Formation consisting mainly of greenish splintery shale. The Bijni Member of Lansdowne Formation has angular unconformable contact with overlying younger stratigraphic units. Between Phulchatti Quartzite and Manikat Shell Limestone of Upper Tal an unconformity exists, and the contact of the Subathu Formation with underlying rocks is marked by a disconformity. In the south western part of the area, Bijni Quartzite overlies the Subathu Formation (Eocene) and this abnormal position is due to a major reverse fault known as Singtali Fault (Kumar et al., 1979) or the Garhwal Thrust (Auden, 1937), which trends in general, WNW-ESE with steep southerly dips varying between 70° to 80°.

These rocks, in general, have four sets of joints dipping in NE, SSW, ESE and NW directions.

With a view to investigate role of physiographic elevation, slope, structure, vegetation cover and lithology on land instability specially the landslides, various types of maps characterising the terrain and landslide were prepared, using toposheets, aerial photographs and field observations.

A close study of elevation distribution in this rugged area indicates that about 88% of the terrain has elevation between 400 to 1500 m. Nearly 38% of the area has elevation less than 900 m and approximately 50% of the area has elevation between 900 to 1500 m of which about 30% falls within 1000 to 1300 m. Approximately 1% of the terrain has elevation above 1900 m. Field observations indicated that valley have small flood plains and relatively steep sloping faces.

Slope classification map of the area clearly indicates that slopes are steep near the upper parts of ridges and in general, highly variable. The hillface having slope angle more than 25° constitute 86% of the area. Approximately 76% of the hillface is occupied with slope angle varying between 25 to 40°. The area covered by ridge top is about 3% of the total area. The terrain has high gradient and appears to be in youth stage. In other words natural processes like weathering and erosion are very active.

Landuse (vegetation cover) map indicates that nearly 7% of the area is characterised by very dense forest. The vegetation cover for categories of dense and moderately dense is 26% and 30% respectively, implying thereby, that the total forest cover in the area is nearly 63%. Approximately 37% of area is characterised by sparse, agricultural and barren lands, of which 22% of hillface is occupied by sparse vegetation. The agricultural land constitute about 11% of the area and only about 3% of the area is barren. Further observations indicate that vegetation cover at higher altitudes relatively decreases, specially along the ridges where it ranges from moderately dense and in general sparse. On the other hand, low altitude areas are characterised by very dense to dense vegetation. Field observations also revealed that with increase of elevation the growth of secondary vegetation also decreases.

The geological map on the basis of field studies was modified after Kumar (1979). The oldest stratigraphic unit i.e. Lansdowne Formation consisting mainly of quartzite with some phyllite constitute 71% of the area. The Blaini Formation, the Krol Formation, the Lower Tal Member and Upper Tal Member (Quartzitic) and the Subathu Formation constitute about 5%, 10%, 3%, 9% and less than 1% of the total area respectively. Therefore, quartzite forms about 80% of the total area of study.

Landslide map prepared on the basis of aerial photographs and topographic map coupled with field investigation, revealed that total of 13.42 sq.km of the terrain forming about 13% of

the total area has been affected by landslide activity. It is observed that, in general, landslide density is high close to slopes in the upper parts of ridges. A synoptic view of landslide map revealed that landslide areas in general, are elongated. This may be due to the fact that the area has high gradient thus, they are directional in their movement. Field observations indicated that slope provides a natural surface for landslides. The slopes on the steep rock face is influenced by frequent action of weathering processes. The weathering of free face causes debris avalanches and slide. These type of failures were common around Bargan village and frequently observed along the road.

Superimposition of landslide map on contour map indicates that landslide activity is found to occur at any elevation but it is not uniformly distributed. In general, with increase in elevation, the landslide affected area increases. Nevertheless, the landslide area distribution shows four modes (peaks). The primary mode indicates that maximum percent landslide area is found at elevations above 1800 m. Such regions are of very small aerial extent (only about 1.5% of the total area of the terrain). They are found on hillslopes close to the ridges. These landslide prone areas are poor or devoid of vegetation. The second, third and fourth modes related to landslide areas found at elevation ranges of 100-1300 m, 1500-1600 m and 500 - 600 m, have aerial extents of about 17%, 4% and 7% of the total terrain.

The landuse (vegetation cover) map reveals that vegetation cover at upper parts of ridges with hillslope of 1100-1300 and 1500-1600 m elevations are moderately dense and in general sparse. Field observations indicated that with increase of elevation, scanty growth of secondary vegetation decreases. Slope map of the area reveals that in general, slopes are steeper at upper part of ridges as compared to low level areas. The sharp edge of ridges indicates that slopes in general are retreating towards ridges, thus erosion near ridges is intensified. The fourth mode of slope failure is at elevation between 500 - 600 m which is generally found along hillslopes near the road runing parallel to river Ganga.

Superimposition of landslide map on slope map indicates that landslide activity is not uniformly distributed with respect to different slope facet. It shows a bimodal pattern. The primary mode reveals that the maximum slope failure is found in the facet V with slope angle of 30 to 35°. This appears to be due to proximity of this facet in general to ridges which are characterised by moderate to sparse vegetation cover. The landslide activities are also intensified in facet with slope angle between 40-45°. This facet with vegetation cover ranging from dense to moderately dense, are often close to the ridges and lies entirely in the western part of the area where amount of precipitation is relatively more. The facet with slope angle between 20 - 25° has a large aerial extent and characterised by moderately dense to barren and dominantly sparse vegetation

cover. The aerial extent of facet with slope angle between 25, 30° is largest in the area with dominantly dense to sparse vegetation cover.

Vegetation cover map coupled with landslide map indicates that landslide area distribution has some relation with vegetation cover. As the density of natural vegetation decreases, landslide area increases. It is observed that maximum landslide areas occur in natural lands. Although the barren areas have relatively low aerial extent of about 3.66 sq.km, they are affected maximum by landslide activity. It is observed that barren lands are usually associated with steep slopes of upper part of ridges.

Landslide activity has affected each and every stratigraphic unit. The Lower Krol of 2.22 sq.km aerial extent which consists mainly of limestone, dolomite and calcareous shale has been affected the most followed by Bijni Member of Lansdowne Formation. The Lower Krol member is exposed in the western part of the area where rainfall is comparatively high. The instability of slopes of this member is thus not only due to physical processes but also due to chemical processes. The Bijni Quartzite of Lansdowne Formation has an aerial extent of 72.16 sq.km. Thus, most of land failures are found associated with it.

The major fault (Singtali Fault) in the southwestern part of the area although has caused tremendous fracturing of Bijni and Phulchatti quartzites in its proximity, but landslide activity is

not a common phenomenon except along the road where in most places it runs parallel to the strike of the rocks. The relatively higher stability is probably due to fracturing of rocks which has affected their weathering characteristics and thus produced soil favourable for luxuriant vegetation on relatively gently sloping surfaces in the vicinity of shear zone. Field observations indicate that the slope movement is also governed by occurrence, orientation and trend of local structures, such as bedding plane and joints, whenever they are day lighted on a slope.

Distribution of landslide area in relation to various attributes like slope structures, vegetation cover, climate, lithology and topographic elevation indicates certain pattern in its occurrence when these factors are considered on univariate basis. The morphometric parameters which result as the sum effect of these factors may have correlation with landslide areas. With this premise, 19 morphometric parameters were measured from 26 third order drainage basins in quartzite terrain which constitute about 81% (72% Bijni Member and 9% Upper Tal Formation) of the total area of investigation.

The analysis based on `Pearson's Correlation Matrix' indicates that Fraction landslide area (Ls) has significant correlation of 0.86, 0.82, 0.63 and -0.55 with Drainage texture (DT), Stream Frequency (SF), Drainage Density (DD) and Basin circularity (BC) respectively.

Drainage Texture (DT) shows very high positive correlation coefficients of 0.95 and 0.95 with Drainage Density (DD) and Stream Frequency (SF) respectively. Such a correlation is natural to occur as the drainage texture is defined as the product of drainage density and stream frequency. It also shows negative correlation of -0.48 and -0.49 with BR and BC respectively, suggesting that elongated basins with low relief has maximum drainage texture but it is not uniform in the area as indicated by low rate of change in correlation coefficient.

Drainage Density (DD) is also correlated positively with Stream Frequency (SF, 0.85) and Ruggedness Number (RN, 0.66), besides Drainage Texture (DT, 0.95). This indicates that as overall number of drainaes in the area increases their overall length also increases and energy entered into system in form of precipitation is dissipiated both through lengthening and expansion of drainage network. Its correlation with RN indicates that with increase in elevation the energy (rainfall) is dissipiated more through overall lengthening of drainage network than its branching. However, it is not uniform throughout the area as indicated by low rate of change in correlation coefficient.

Stream Frequency (SF) shows significant positive correlation of 0.54 with LR_1 besides drainage density (DD) and drainage texture (DT) and negative correlation of -0.49, -0.57 and -0.47 with BL, BR and L_2 respectively. This probably indicates that as dissection of the area increases length of first order stream

increases. The negative correlation with BL and BR suggests that as dissection increases the length and relief of basin decreases. But these are not uniform throughout the area as indicated by low rate of change.

Basin circularity (BC) shows positive significant correlation of 0.56 with basin elongation (BE), beside drainage texture (DT). The correlation between BC and BE at the low rate of change probably indicates that there are some structural controls which help in development of basin circularity in the area (Chorley, 1969). Basin shape does not show correlation with F_1,$F_2$$L_1$,$L_2$,$L_3$,BA and BL. It may prove that basin shape does not have a direct pronounced control over drainage network development. Basin area shows high positive correlation of 0.88, 0.95, 0.93, 0.96, 0.91, 0.96, 0.58, 0.96 with BF_2, F_1, F_2, L_1, L_2, L_3, BR and BL respectively. Thus, the ratio of hillslope area occupied by basin to the basin length does not increase as drainage network expands in size. Basin relief has significant positive correlation of 0.48, 0.46, 0.67, 0.49, 0.58 and 0.71 with F_1, L_1, L_2, L_3, BA and BL respectively, implying thereby that as relief increases the frequency of first order streams, length of first, second and third order streams with different rate of change increases. The rate of change in correlation coefficient indicates that relief has maximum effect on length of second order streams and minimizes on other parameters. Its correlation with BL suggests that tendency is to erode and the area is characterised by retreating slopes which are usually

dominated by rill and channel erosion. Hence, it appears the present topography is the result of accelerated erosion of slopes towards ridges.

Drainage Texture (DT) is directly related to Drainage Density (DD), Stream Frequency (SF), Ruggedness number (RN), Basin Circularity (BC) and Basin Relief (BR). Stream Frequency (SF) is directly related to Basin Length (BL), length of second order stream (L_2), Basin Relief (BR) and length ratio of first to second order stream (LR_1). Moreover, SF is largely dependent on rock type (Horton, 1945). Drainage Density is a sensitive parameter to other basin characters like vegetation cover, slope, structure, mean annual rainfall (Carlston, 1963; Williams and Fowler, 1969), rainfall intensity (Chorely and Morgan, 1962). Drainage texture is product of drainage density and stream frequency.

Fraction of landslide area (Ls) in a basin has hightest statistically significant correlation coefficient of about 0.86 with drainage texture (DT). Hence, it is only single morphometric parameter in a basin that has in it the influence of many morphometric parameters which in turn, are reflections of sum effect of elevation, slope, lithology, structural features, vegetation cover, climate and hydrological conditions. Based on regression analysis the following relationship between fraction landslide area (Ls) and drainage texture (DT) has been worked out

$$Ls = 0.0279 + 0.0052\ DT \qquad (6.1)$$

This relationship when tested to estimate fraction landslide area in four randomly selected drainage basins in the area was found to be useful within the error limit of 25 percent.

Despite the usefulness of drainage texture as an indicator of instability of a terrain, this parameter can not be used to study instability condition at local level of a particular hillslope section. Also, it does not indicate the nature or type of failure and processes of instability involved on hillslope. Nevertheless, it indicates that morphological features can be very useful in investigation of stability of hillslopes. Crozier (1973) derived six significant morphometric indices namely the Classification, Dilation, Flowage, Displacement, Tenuity and Viscous flow based on three dimensional concavo-convex slope measurements for five slope movement processes namely Rotation slide (RS), Planar slide (PS), Slide flow (SF) Viscous flow (VS) and Fluid flow (FF). A similar approach was made to obtain these indices on the basis of two dimensional, sixty slope profiles drawn from contour map of the area.

The mean values of five morphometric indices namely Classification (CI), Dilation (DI), Flowage (FI), Displacement (DPI) and Tenuity (TI) were found to be 7.68, 0.35, 75.92, 48.04 and 1.20 for Rotational slide (RS) respectively. Likewise the mean values of five above mentioned indices for planar slide (PS) were calculated to be 7.32, 0.36, 44.00, 73.31 and 0.62 respectively. Similarly for Slide flow (SF) the mean values for Classification, Dilation, Flowage, Displacement and Tenuity

indices were found to be 4.39, 0.70, 73.14, 54.25 and 1.62 respectively. The computed mean for Fluid Flow (FF) was calculated to be 1.88, 1.78, 215.15, 53.22 and 2.37 for Classification, Dilation, Flowage, Displacement and Tenuity indices respectively. The efficacy of the modified parameters as predictive critical limits for the slope movement processes involved in landslip was established when this approach was applied successfully to three different areas of similar topography located at 122 km NNW (Mussoorie Bypass), 80 km NNE (Kaliasaur) and 57 km SSW (Chilla) of the area of study.

The difference in the values of some indices for each slope movement process group as compared to values obtained by Crozier, may possibly be due to marked difference in field conditions. It is important to mention that the critical limits for the morphometric indices given by Crozier (1973), are based on sixty six landslips in a terrain made up largely of concavo-convex slope with very few bed rock outcrops, free faces and thick soil mantle in Newzealand. However, the present study is based on sixty slope profiles drawn from enlarged contour map of this part of Himalayan terrain exhibiting rugged topography, high relief, steeply sloping valley faces, many bed rock outcrops, poor soil and regolith mantle cover. In view of these differences in the nature of the terrain, it is concluded that for the terrain of the type found in the area of study, the morphometric indices as worked out herein and whose efficacy has been proved in three different hilly areas, may be used in similar terrains to

indicate the instability of slopes and probable processes of slope movement.

Displacement index (DPI) has been found to be useful in indicating the instability potential of a slope section in this terrain. A section may fail by rotational slide if DPI is less than 48; by planar slide, if DPI is less than 73; by slide flow, if DPI is less than 54 and by fluid flow, if DPI is less than 53.22 .

Multivariate discriminant function criteria based on simultaneous use of these five slope morphometric indices have been worked out statistically to differentiate between various classes of slope movements. To differentiate between slide flow (SF) and fluid flow (FF), if the discriminate score computed through the discriminate function is less than 15.48, then the slope movement can be classified as likely to take place by Fluid Flow. If it is more than 15.48, the slope movement may take place by Slide Flow. Like wise to differentiate between the planar slide (PS) and fluid flow (FF), rotational slide (RS) and fluid flow (FF), planar slide and slide flow, rotational slide and slide flow, rotational slide and planar slide the discriminant indices have been worked out as -3.13, -5.01, -3.84, -1.65 and 10.56 respectively.

The efficacy of the discriminant criteria was established when test samples of slope section from three apriori unknown areas were correctly classified to the class of movement to which

they actually belong.

Discriminant analysis has also been used as search technique to identify the indices which contribute significantly in differentiating two similar slope movement processes. It is found that the most important indices to discriminate between FF and SF are CI and DI; between FF and PS are DI, TI and CI; between FF and RS are DI and CI; between SF and PS are TI and CI; between SF and RS are CI and DI and between PS and RS is TI with decreasing order of their contribution On the basis of these, simple bivariate and unvariate plots were prepared for use as tools in identifying likely slope movement processes affecting the slope morphology. The important morphometric indices of each process group for three test areas namely Mussoorie Bypass, Kaliasaur and Chilla, when plotted on these plots, clearly demonstrated the usefulness of such a technique developed through search process of discriminant function analysis.

The developmental activity has affected the hillslope stability of the area. Along the road section, at a number of places various types of slope movement are observed. The landslides perpetually have been a cause of great concern and difficulties mainly towards transportation or road communication. Field investigations were carried out with a view to assess the nature, type and mode of failure of problematic slopes along the road between Byasi to Devaprayag and also in the accessible parts of hillslope both uphill and downhill adjoining the road. In this section of the road a total of 21 slope failures were

identified. Field observations at a number of locations indicated that the road construction has day lighted the weakest surface of discontinuities, which has made these areas vulnerable to slope movement during monsoon. On the basis of slide dimensions, accessibility, extent of failure and rock/soil ratio, six sites were selected for stability analysis.

While doing stability analysis of six selected sites, namely L_1, L_5, L_6, L_7, L_9 and L_{14} using SMR (Slope Mass Rating) technique, it was observed that L-type rebound hammer, applied on natural surfaces of rock masses failed in certain conditions to estimate uniaxial compressive strength determined in the laboratory. However, on examining the surface roughness of discontinuity surfaces under study, it is observed that it can estimate the uniaxial compressive strength of rock masses if it is applied on smooth and dry natural surfaces of joint walls and not on rough surfaces. Hence, it appears that the hammer may be useful when applied to such natural surfaces of rock mass. Also it gives relatively more reliable reading when applied in dry condition, using Miller's equation.

Slope Mass Rating (SMR) is used to categorise the stability condition of these sites. The SMR values of site L_1, L_5, L_6, L_7, L_9 and L_{14} are calculated to be 22, 28, 18, 24, 6, 42. On the basis of this stability study approach, these sites have been categorised as unstable (L_1,L_5) with planar or large wedge failures (class IV), as against the field observation of unstable with large planar and no wedge failure; very unstable (L_6) with

safety are 0.85 , 0.84 , 0.35 , 0.87, 0.85 and 0.00 for the sites L_1, L_5, L_6, L_7, L_9 and L_{14} respectively. The corresponding factor of safety under dry dynamic condition are 1.51 , 1.23 , 1.35 , 1.91 , 1.40 and 1.14 . Hence, it is concluded that all these slopes are unstable in wet condition and remain stable under dry dynamic condition. This conclusion is supported by the fact that year after year, these slopes fail during monsoon season due to dual action of pore water pressure. Its adverse action decreases the strength of the rock mass along the discontinuity surfaces. Thus, increase in the pore water pressure destabilise the slopes. It is also important to note that these sites located on zone IV of seismic map of India, remained unaffected by an earthquake of 6.5 magnitude which devastated the area in and around Uttarkashi (situated 35 km to the north of study area). In view of instability of the slopes, during monsoon, where SMR recommends reexcavation at sites L_6 and L_9, extensive correction at sites L_1, L_5 and L_7 and systematic support for site L_{14}, the computer slope analysis recommends provision of subsurface drainage to stabilise them.

6.1 CONCLUSIONS

Thus, on the basis of this study the following salient conclusions have been drawn:

1) Morphometric parameters in a drainage basin can help to estimate the Fraction Landslide area (LS) in a basin. Of all the morphometric paramrters Drainage Texture (DT) shows statistically very high positive correlation with the

large planar or soil-like failures (class IV), as against field observation of unstable with small planar and many wedges; unstable (L_7) with planar or large wedge failure (class IV), as against field observation of partially stable with occasional planar failures; very unstable (L_9) with large planar or soil like failure (class V), as against unstable with many small plane failures and partially stable (L_{14}) with some joints or many wedge failures (class III) which has also been observed in the field. Hence, it is concluded that descriptive mode of failure is not matching in the present field condition. Although sites L_1, L_5, L_7 and L_6 and L_9, may be placed in class IV and V of SMR classification respectively, the extent of failure as observed in the field is comparatively high at site L_1 followed by L_5 and least at site L_7. The extent of failure at site L_6 is also much higher than site L_9, thus failures of different magnitude are placed within the same class and the extent of failure cannot be inferred from SMR classification. Considering the wide range of each SMR class, the interpreted stability conditions for sites L_6, L_7 and L_9 do not match with actual field observations. On critical examination of these sites, it appears where continuity of discontinuity surfaces (Joint surface) along dip is less than 5% of the height of affected slope, Slope Mass Rating does not give a true picture of the stability conditions in this situation and its usefulness appears to be limited.

Slope stability analysis based on short solution of Hoek and Bray (1981) suggests that in wet condition, factors of

fraction landslide area. This parameter and Eq. 3.3 can be used in similar terrains to estimate it with an error of the order of 25 percent.

2) Slope profile morphometry (Modified after Crozier) can give an indication of instability and type of slope movement process. New critical limits have been found as predictive limits of slope instability conditions in a terrain of rugged topography with high relief, steep slopes and low soil and regolith mantle cover. The method has been verified by 3 large complex landslides.

3) The road constructions in the area have affected the stability of hillslopes.

4) The Slope Mass Rating (SMR) technique of predicting of slope stability does not hold good in toto in the present field conditions. It appears to hold good when the continuity discontinuity surface along the dip is more than 5% of the height of affected slope because of high value of $C / \gamma H$.

5) L-type rebound hammer frequently used to estimate uniaxial compressive strength, holds good only on smooth and dry natural discontinuity surfaces of rock mass and not on natural rough surfaces. The Miller's correlation (Eq. 5.1) was based on hammer tests on polished surfaces and not natural joints.

REFERENCES

Acharya, S.K. and Rao, K.K., 1981, Geotectonic evoluation of the Himalaya- A model. Geol. Surv. India Misc. Publ., Vol. 41(4): 1155-142.

Anbalagan, R., Awasthi, A.K., Singh, B., 1990, Geo-environmental hazards of Ninital area-An urgent needs for regeneration and hazard management. Int. Conf. on environmental Planning and Management, Roorkee: 8-15.

Anbalagan, R., 1992a, Terrain evaluation and landslide hazard zonation for environmental regeneration and landuse planning in mountainious terrain. Int. Symp. on Landslide Christchurch, Newzealand.

Anbalagan, R., 1992b, Landslide evaluation and zonation mapping in mountanious terrain. J. Engg. Geol. Elseviers, Amesterdam (In Press).

Anbalagan, R., Sharma, S., Raghuvanshi, T.K., 1992, Rock mass stability evalution using modified SMR aprroch. Proc. sixth national symposium on rock mechanics , Banglore :258-268.

Auden, J.B., 1934, The Geology of the Krol Belt. Rec. Geol. Surv. India, vol. 67: 357-454.

Auden, J.B. 1937, The structure of the Himalaya in Garhwal. Rec. Geol. Surv. India, vol. 71: 407-433.

Auden, J.B. 1949, In Director General's report for 1939. Rec. Geol. Surv. India., vol. 78: 74-78.

Aufmuth, R.E., 1974, Site engineering indexing of rock. Am. Soc. Test. mater. Spec. Tech. Publ. 554: 81-99.

Azmi, R.J. , Joshi, M.N. and Juyal, K.P. , 1981, Discovery of the Cambro-Ordovician Conodont from Mussorie Tal Phosphorite: its significance in correlation of Lesser Himalaya. In : Contemporary Geoscientific Researches in Himalaya, Voi. 1. (ed.) Sinha, A.K. , Bishen Singh Mahendra Pal Singh, Dehra Dun : 245-250.

Azmi, R.J., and Joshi, M.N., 1983, Conodont and other Biostratigraphic on the age and evolution of the Krol belt. Himalayan Geol. Voi. 11 :198-223.

Barton, N., Lien, R., and Lunde, J., 1974, Engineering classification of rock masses for the design of tunnel support. Rock Mech., Vol. 6(4) : 189-236.

Barton, N., and Choubey, V., 1977, The shear strength of rock joints in theory and practice. Rock mech., Vol. 10(1-2) : 1-54.

Bassi, U.K., 1968, Geology of the area between river Ganga and river Huinl (East of Rishikesh) Distt. Pauri Garhwal, U.P., Unpublished M.Sc. Tech., Thesis, University of Roorkee, Roorkee, India.

Beaty, C.B., 1962, Asymmetry of stream patterns and topography in Bitter-root Range, Montanna. J. Geol., 70 (3): 347-354.

Belcher, D.J., 1960, Photo-interpretation in engineering, Manual of Photographic interpretaton. (Ed.) Colwell, R.N., Am. Soc. Photogrammetry: 403-456.

Bharktia, D.K. and Gupta, R.P., 1982, Lineament-tectonic interpretations from Landsat images in Garhwal-Kumaun Himalaya. Him. Geol. Vol.12: 1-13.

Bieniawski, Z.T. 1979, The Geomechanics classification in rock engineering applications. Proc. 4th Int. Cong. on rock Mech., ISRM Montreux, Balkema, Rotterdum, Vol. 2: 51-58.

Bose, S.C., 1966, Fluvio-glacial geomorphology and occupance in the Alaknanda valley. (Abs.) Pr. Ind. Sci. Cong. Ass., 53rd Session, pt. 3: 196 p.

Burdon, D.J., 1966, The largest karst spring. J. Hyd.,vol. 4:p. 104.

Carlston, C.W., 1963, Drainage density and stream-flow U.S. Geol. Survey Prof. Paper 422C.

Chansarkar, R.A., 1970, Tentative terrain types in Kumaun hills, (Abs.). Pr. Ind. Sci. Cong. Ass., 57th session, Pt. 3:229 P.

Chorley, R.J.,Malm ,D.E.G., and Pogorzelski, H.A.,1957, A new standard for estimating Basin shape. Amer. J. Sci. Vol. 255 : 138-41 .

Chorley, R.J., 1957, Illustrating laws of morphometry. Geol. Mag., Vol. 94: 140-150.

Chorley, R.J. and Morgan, M.A., 1962, Comparison of morphometric features, Unaka mountains Tennesse and North Carolina, and Dartmoor, England. Geol. Soc. Am. Bull., Vol. 73 : 17-34.

Chorley, R.J., 1969, The drainage basin as the fundamental geomorphic unit. In: Water, Earth and Man, (ed.)Chorly, R.J., London: 77-100.

Choubey, V.D. and Litoria, P.K., 1990 , Landslide hazard zonation in Garhwal Himalaya - A terrain evaluation approch. Proc. six international congress , International Association of

Engineering Geology, Vol. 1, (ed.) Price, D.G., Amesterdam : 65-72.

Coates, D.R., 1977, Landslide Prespective, In: Reviews in Engineering Geology: Landslides, (Ed.) Coates, D.R., Geol. Soc. Am. 3: 3-28.

Cooke, R.U., Doornkamp, J.C., 1974, Geomorphology in Environmental Management. Clarendam, Oxford : 432 p.

Crozier, M.J., 1968, Earth-flows and Related Environmental factors of Eastern Otago. J. Hydrol. (N.Z.), Vol. 7(1): 4-12.

Crozier, M.J., 1969a, Earth flow occurance during high intensity rainfall in eastern Otago, New Zealand. Eng. Geol. Vol. 3: 325-334.

Crozier, M.J., 1969b, Landslip Morphology, Process and slope. 41st Anzaas Congress, Adelaide.

Crozier, M.J., 1973, Techniques for morphometric analysis. Zeitsehr. fur Geomorph., Vol 17(1): 78-101.

Crozier, M.J., 1984, field assessment of slope instability. In: Slope instability (Eds.) Brunsden, D. and Prior, D. , John Wiley and sons , New York : 103-142.

Crozier, M.J., 1986, Landslides: Causes, Consequences and Environment. Croom Helm Australia Pty. Ltd. Surry Hills, 252p.

Dalrymple, J.B., Blong, R.J. and Conacher, A.J., 1968, An hypothetical nine-unit land-surface model, Zeitschr. fur Geomorph., Vol. 12: 60-76.

Davis, J.C., 1973, Statistics and data analysis in geology, John Wiley and Sons, Inc., New York: 550 p.

Deere, D.U., Hendron, A.S., Patton, F.D., and Cording, E.J., 1967, Design of surface and near surface construction in rock. Proc. 8th Symp. Rock Mech., Am. Inst. Min. Metall. and Pet. Eng., Minneapolis, Minn. : 237-302.

Dhaundiyal, J.N. and Kumar, G., 1976, On the Geology of the Garhwal synform, Tehri Garhwal and Garhwal districts, U.P.. Seminar, 125th Ann. Celebrations, Geol. Surv. India, Northern Region, Lucknow, Nov. 1976, (preprint).

Dixon, W.J. and Mass, F.J., 1951, Introduction to statistical analysis. McGraw-Hill, Inc.: 623 p.

Duncan, N., 1965, Geology and Rock Mechanics in Civil Engineering Practice. Water Power: 23-32.

East, T.J., 1978, Mass movement landforms in Baroon pocket, South-east Queensland, a study of form and process. Queensland Geographical Journal (3rd series) 4:37-67.

Fuches, G. and Sinha, A.K., 1978, The tectonic of Garhwal-Kumaun Lesser Himalaya, Jahrb. Geol. B-A., Vol. 121(2): 219-241.

Gairola, V.K., 1975, On the petrology and structure of the Central Crystallines of the Garhwal Himalaya, Uttar Pradesh. Him. Geol., Vol. 5: 455-467.

Ganeshan, T.M. and Thussu, J.L., 1978, Geology of parts of Tons velley, Garhwal Himalaya, with special reference to old fold trends. J. Geol. Soc. India, Vol. 19: 285-291.

Gansser, A., 1964, Geology of the Himalayas. Inter. Science Publishers, London: 289 p.

Gaur, G.C.S. and Dave, V.K.S., 1978, Geology and structure of a part of Garhwal syncline, Rishikesh , Garhwal Himalaya. Him. Geol. , Vol. 8(1) : 524-529.
University of Roorkee, Roorkee, India.

Gillbert, L.B. and Auden, J.B., 1932, Note on a glacier in the Arwa valley, British Garhwal. Rec. Geol. Surv. India, Vol. : 388-404.

Goswami, K.C., 1977, Stratigraphy and structure of the Simla and krol belts in parts of Alaknanda and Nayar valleys, Distt. Pauri Garhwal, U.P.. Unpublished M.Sc. Tech., Thesis, University of Roorkee, Roorkee, India.

Gregory, K.J. and Walling, D.E., 1973, Drainage basin form and processes: a geomorphological approach. Edward Arnold, London: 458 p.

Hazara, P.C. and Raina, B.N., 1972, Geomorphology of the Himalayas. Geol. Surv., India, Misc. Publ., Vol. 15: 47-52.

Heim, A. and Gansser, A., 1939, Central Himalaya, Geological observation of the swiss expedition in 1936. Mem. Soc. Helv. Sci. Nat., Vol. 73: 1-245.

Herbert, J.D., 1848, Geological map of the mountain provinces between the river Satluj and Kali. J. Asiatic Soc., Vol. 21 (Appendix).

Hoek, E. and Bray, J., 1981, Rock slope engineering. 3rd ed. Inst. Min. Metall. Engg., London: 358 p.

Horton, R.E., 1932, Drainage basin characteristics. Trans. Amer. Geophy., Vol. 13: 350-361.

Horton, R.E., 1945, Erosional developments of streams and their drainage basins, hydrophysical approach to quantitative morphology. Bull. Geol. Soc. Am., Vol. 56: 275-370.

Irfan, T.Y. and Dearman, W.R. 1978, Engineering classification and index properties of a weathered granit Bull. Int. Assoc. Eng. Geol., Vol. 17: 79-90.

IS: 1893-1970, Criteria for earthquake resistant design of structures.

IS: 9143-1979, On method for Determination of unconfined compressive strength of Rock Materials.

IS: 11315 (part I-X) - 1987, Methods for Quantitative Description of Discontinuities in Rock Masses.

Ives, J.D. and Messerli, B., 1981, Mountain hazard mapping in Nepal:Introduction to an applied mountain research project. Mountain Research and Development, Vol. 1(3-4): 223-230.

Jain, A.K., 1971, Stratigraphy and tectonics of Lesser Himalayan region of Uttarkashi, Garhwal Himalaya. Him. Geol., Vol. 1: 25-28.

Jain, A.K., 1981, Stratigraphy , petrography and paleogeography of the Late Palaeozoic diamictites of the Lesser Himalaya. Sedi. Geol. ,Vol. 30 : 43-78.

Jain, A.K., 1987, Kinematics of the Transverse Lineaments, regional tectonics and Holocene stress field in the Garhwal Himalaya. J. Geol. Soc. India, Vol. 30(3): 169-186.

Jennings, J.E., 1971, A mathematical theory for calculation of the stability of slopes in open cast mines. In: planning open pit mines, Johannes burg (Ed.) Van Rensbury, P.W.J., Proc. Open

pit Mining Symp. Johnsburg, South Africa Inst. of Min. and Metall., Balkema, Amesterdam: 87-102.

Jesch, R.L., Johnson, R.B., Belscher, D. B., Yaghjian, A.D., Steppe, M.C., and Fleming, R.W., 1979, High resolution sensing techniques for slope stability studies. Rep. No. FHWA-RD-79-32, U.S. Dept. of Commerce Natl. Bur., Standards, Boulder Colo.: 138p.

Johnson, R.B. and DeGraff, V.J. , 1988, Principales of engineering geology. John Wiley and sons , Singapore : 497p.

Joshi, B.C., 1987, Geo-environmental studies in parts of Ramganga catchment, Kumaun Himalayas, Ph.D. Thesis, Roorkee University, Roorkee, India.

Judson, S. and Andrews, G.W., 1955, Pattern and form of some valleys in the driftless areas, Wisconsin. J. Geol., 63: 328-336.

Kalvoda, I., 1972, Geomorphological studies in the Himalaya with special reference to the landslides and allied phenomenon. Him. Geol. Vol. 2: 301-316.

Karnataka Engineering Research Station, 1985, Rock classification by hardness. Central Borad of Irrigation and Power Research Scheme applied to river valley project, New Delhi: 77-101.

Kaushik, S.D., 1972, Geomorphology of rejuvenation in the Garhwal Himalaya. Geol. Surv. India, Misc. Publ., Vol. 15: 61-64.

Kaushik, S.D. and Sharma, V.D., 1972a, Geomorphology of the Bugyal ridges in the Garhwal Himalaya. Geol. Surv. India Misc. Publ., Vol. 15: 45-46.

Kaushik, S.D. and Sharma, V.D., 1972b, Geomorphology of the transverse gorge of the Alaknanda. Geol. Surv. India Misc. Publ., Vol. 15: 65-68.

Kendall, M.G., 1946, The advance theory of statistics. Vol. II, Charles. Griffin and Co. Ltd., London: 521 p.

Khan, A.A., Dubey, U.S., Sehgal, M.N. and Awasthi, S.C. 1982, Terraces in the Himalayan Tributaries of the Ganges in U.P.. J. Geol. Soc. India, Vol. 23: 392-401.

Khattri, K.N., Chandra, R., Gaur, V.K., Sarkar, I. and Kumar, S., 1989, New seismological results on the tectonic of Garhwal Himalaya, Proc. Indian Acad. Sci. (Earth Planet. Sci.), Vol. 98(1): 91-109.

Kumar, G., 1970, Alaknanda Tragedy: A geotechnic evaluation. Proc. Sem. River Valley projects, Roorkee University, Roorkee.

Kumar, G., Prakash, G. and Singh, K.N., 1974, Geology of the Devaprayag - Dwarahat area, Garhwal Himalaya, U.P.. Him. Geol., Vol. 4: 323-347.

Kumar, G. and Agarwal, N.C., 1975, Geology of the Srinagar-Nandprayag area (Alaknanda Valley), Chamoli Garhwal and Tehri Garhwal distt., Kumaun Himalaya, U.P.. Him. Geol., Vol. 5: 29-59.

Kumar, G., and Dhaundiyal, J.N., 1979, Stratigraphy and structure of `Garhwal synform', Garhwal and Tehri Garhwal districts, U.P., A reappraisal. Him. Geol., Vol. 9(1) : 18-41.

Kumar, G., 1981, Stratigraphy and Tectonics of Lesser Himalaya of Kumaun, Uttar Pradesh.In: Contemporary Geoscientific Research

in Himalaya, Vol.1. (ed.) Sinha, A.K., Bishen Singh Mahendra Pal Singh, Dehra Dun: 61-70.

Langstaff, T.C., 1928, The Nanda Devi group and source of Nandakani. Geogr. J., Vol. 71: 417-430.

Lavania, B.V.K. ,Srivastava, L.S., 1987, A simplified approach to evaluation of earthquake induced displacements. Seminar on Earth and rock fill Dams, Lucknow.

McLean, R.F., Davidson, C.F., 1968, The role of mass movement in shoare platform development along the Gisborn Coastline, Newzealand. Earth Sci. J., Vol. 2: 15-25.

Medlicott, H.B., 1864, On the geological structure and relationship of the southern portion of the Himalayan range between the rivers Ganges and Ravee. Mem. Geol. Surv. India, Vol. 3(2): 1-212.

Mehrotra, G.S. and Bhandari, R.K., 1988, A Geological Appraisal of slope instability and proposed remedial measures at Kaliasaur slide on National highway, Garhwal Himalaya. Second Int. Conf. on case histories in Geotech. Engg., Missouri (USA).

Middlemiss, C.S., 1885, A fossiliferous series in the Lower Himalaya, Garhwal. Rec. Geol. Surv. India, Vol. 18:73-77.

Middlemiss, C.S. 1887a, Physical geology of west British Garhwal. Rec. Geol. Surv. India, Vol. 20: 26-40.

Middlemiss, C.S., 1887b, Crystalline and metamorphic rocks of the Lower Himalayas, Garhwal and Kumaun Section (1). Rec Geol. Surv. India, Vol. 20: 134-143.

Middlemiss, C.S., 1890, Physical geology of the sub-Himalaya of Garhwal and Kumaun. Mem. Geol. Surv. India,Vol. 24(2): 59-200.

Miller, R.P.,1965, Engineering Classification and index properties for intact rock. ph.D. Thesis, Univ. Ill.:1-322p.

Mithal, R.S., Chansarkar, R.A. and Gaur, G.C.S., 1972, Geomorphic studies of the Birahi Ganga, Garhwal Himalaya. Him. Geol., Vol. 2: 415-430.

Morgan, R.P.C., 1970, Climatic Geomorphology: its scope and future. Geographical, Vol. 6: 26-35.

Morisawa, M.E., 1962, Quantitative geomorphology of some watersheds in Appalachian Plateau. Bull. Geol. Soc. Am., Vol. 73: 1025-1046.

Morisawa, M.E., 1963, Distribution of stream flow direction in drainage patterns. J. Geol., Vol. 71(4): 528-529.

Morisawa, M.E., 1968, Streams, their dynamics and morphology, McGraw-Hill, New York: 175 p.

Morisawa, M.E., 1985, Rivers, Longman Inc., New York: 222p.

Negi, S.S., Pandey, B.K. and Sinha, A.K., 1982, Slope in Rudraprayag - Tilwara- Mayali area of Garhwal Himalaya with special reference to slope stability. Him. Geol., Vol. 12: 330-344.

Nityanand and Prasad, C., 1972, Alaknanda Tragedy: A Geomorphological appraisal. Nat. Geog. J., Varanasi, Vol. 18(34): 206-212.

Nunnaly, N.R., and Witmer, R.E., 1970, Remote sensing for landuse studies. photogrammetric Engg., Vol. 36: 449-453.

Oldham, R.D., 1883, Note on the Geology of jaunsar and Lower Himalaya. Rec. Geol. Surv. India, Vol. 16: 193-198.

Ollier, C.D., 1977, Terrain Classification: Methods, Application and Principles.In: applied Geomorphology, (Ed.) Hails, J.R., Elsevier - New York: 277-316.

Pachauri, A.K., 1970, Terrain; A classification. Bhuvigyan, Vol. 2(2): p 101.

Pachauri, A.K. and Krishna, A.P., 1984, Terrain classification of a part of Himalayas using multistage sampling Technique. 5th Asian Conf. Remote Sensing (Kathmandu).

Pachauri, A.K. and Manoj, P., 1992, Landslide hazard mapping based on geological attributes. J. Engg. Geol., Vol. 32: 81-100.

Pande, I.C., 1974, Tectonic interpretation of the geology of Nainital area. Him. Geol., Vol. 4: 532-546.

Pandy, L.M., 1986, Litho-control and prime morphometric parameters: Study of a Lesser Himalayan basin. Nat. Geogr. J. India, Varanasi, Vol. 32(3): 192-200.

Pant, C., 1975, Observations of the fossil valleys and epigenetic gorges of the Bhagirathi and Alaknanda rivers. Him. Geol., Vol. 5: 193-206.

Pilgrim, G.E. and West, W.D., 1928, The structure and correlation of the Simla rocks. Mem. Geol. Surv., India, Vol. 53: 1-140.

Powar, K.B., 1980, Stratigraphy of the Lesser Himalaya sediments of Nainital-Almora area, Kumaun Himalaya.In: stratigraphy and correlations of the Lesser Himalayan Formations (eds.) Valdiya, K.S. and Bhatia, S.B., Hindustan Publ. Corp., Delhi :49-58.

Prasad, B. , Maithy, P.K., Kumar , G. and Raina, B.K. , 1990, Precambrian - Cambrian Acritarchs from the Blaini - Krol -

Tal Sequence of Mussoorie Syncline, Garhwal Lesser Himalaya, India. Mem. Geol. Soc. of India , Vol. 16 :19- 32.

Prasad, C. and Verma, V.k., 1980, Slope failure - A case study in the catchment areas of Alaknanda and Bhagirathi rivers, Garhwal Himalaya, India. Proc. Int. Symp. on landslides, New Delhi, Vol. 1: 41-44.

Prasad, C. and Rawat, S.S., 1985, Study of planar surfaces and lineament zones in area between Devaprayag and Rishikesh, Garhwal Himalaya. Publ. Cent. Adv. Stud. Geol. Punjab Univ., Chandigarh, (N.S.), Vol. 1: 227-284.

Raina, B.N., 1972, Photogeology and Himalayan Geology. Him. Geol., Vol. 2: 527-536.

Raina, B.N., 1978, A review of the Stratigraphy and Structure of the Lesser Himalaya of Uttar Pradesh and Himachal Pradesh. Tectonic Geology of the Himalaya, Today and Tomorrow's Printers and Publishers, New Delhi, India: 79-112.

Rao, C.R., 1952, Advanced statistical Methods in Biometric Research. John Willey and Sons., New York: 390p.

Rau, M.A., 1974, Vegetation and physiography of Himalaya, in Ecology and Biogeography in India, (Ed.) Mani, M.S., Dr. W. Junk, b.v. Publishers, The Haque.

Rib, H.T. and Liang, T., 1978, Recognition and identification. In: landslides; analysis and control, Spl. Rept., 176, (Eds.) Schuster, R.L. and Krizek, R.J., Transportation Research Board, Nat. Acad. Sci., Washington, D.C.: 34-80.

Romana, M., 1985, New adjustment ratings for application of Bieniawski classifiction to slopes. Int. Symp. on the role of

rock mechanics, Zacatecas : 49-53.

Roy, A.B. and Valdiya, K.S., 1988, Tectonometamorphic evolution of the Great Himalayan Thrust Sheets in Garhwal Region, Kumaun Himalaya, J. Geol. Soc. India, Vol. 32(2): 106-124.

Rupke, J. 1968, Note on the Blaini Boulder Beds of Tehri Garhwal, Kumaun Himalaya. J. Geol. Soc. India, 9: 171-177.

Rupke, J., 1974, Stratigraphic and structure evolution of the Kumaun Lesser Himalaya. Sed. Geol., Vol. 11(2,4): 83-265.

Ryabchikov, A., 1975, The changing face of the Earth. progress publications, Moscow: 205p.

Saklani, P.S. 1970, Metamorphism in rocks of Garhwal Nappe of Garhwal Himalaya. Centr. Adv. Stud. Geol., Punjab Univ. Chandigarh, Vol. 7: 115-118.

Saklani, P.S. 1971, Structure and Tectonics of the Pratapnagar area, Garhwal Himalaya. Him. Geol., Vol. 1:75-91.

Saklani, P.S., 1972a, Lithostratigraphy and structure of the area between the Bhagirathi and Bhilangana rivers, Garhwal Himlaya. Him. Geol. Vol. 2: 342-355.

Saklani, P.S., 1972b, Metamorphism in rocks of Parautochthonous zones of Mukhem area, Garhwal Himalaya. Indian Mineralogist, Vol. 13: 69-73.

Savage, C.N. , 1951, Masswasting, classification and damage in Ohio. Ohio J. Sci., 51 (2) : 299-308.

Saxena, P.B., 1980, A study of landslide and its land depletion in Alaknanda Valley (Garhwal Himalaya). Him. Geol., Vol. 9 :32-41.

Schumm, S. A., 1956, Evolution of drainage systems and slopes in bad lands of Perth Amboy, New Jersey. Bull. Geol. Soc. AM., Vol. 67 : 597-646.

Schwan, W., 1981, Key struture of Minor Tectonics, Major Tectonics forms and shortening Kinematics in Himalaya. In: Contemporary Geoscientific Researches in HImalaya, Vol.1 (ed.) Sinha, A.K., Bishen Singh Mahendra Pal singh, Dehra-Dun: 13-20.

Selby, M.J., 1967, Aspects of the Geomorphology of the Grywacke Ranges Bordering the Lower and Middle Waikato Basins. Earth Sci. Jour., Vol. 1: 37-58.

Selby, M.J., 1976, Slope erosion due to extreme rainfall. A case study from Newzealand. Geografiska Annuler, Vol.3(A):131-8.

Selby, M.J., 1982, Controls on stability and inclinations of hillslopes formed on hard rock. Earth surface processes and landforms, Vol. 7 : 489-497.

Shandilya, A.K. and Prasad, C., 1982, Geomorphic studies of lineament zones in Garhwal Himalaya. Him. Geol., Vol. 12: 31-39.

Sharma, A.K., 1990, Softwae for 3-D wedge analysis of rock slopes with graphic. Unpublished M.E. Thesis, Deptt. of Civil Engg., University of Roorkee, Roorkee, India.

Sharma, R.P. and Virdi, N.s., 1976, Tectonic evolution of Simla and Kumaun Himalaya, based on Landsat-I Multispectral Imagery and aerial photo-interpretation, Proc. Int. Him. Geol. Sem., New Delhi, Vol. 2(A) : 115-132.

Sharma, R.P., 1977, The role of multispectral imagery in the elucidation of tectonic frame-work and economic potentials of Kumaun and Simla Himalaya. Him. Geol., Vol. 7: 77-99.

Sharpe, C.F.S., 1938, Landslides and Related Phenomena. Cooper Square Publ., Inc., New York: 137 p.

Skempton, A.W., 1953, Soil mechanics in relation to geology. proc. of yorkshire Geological society 29 Pt. 1(3): 33-62.

Srivastava, R.N. and Ahmad, A., 1979, Geology and structure of Alaknanda Valley, Garhwal Himalaya. Him. Geol., Vol. 9: 225-254.

Stimpson, B.S., 1976, Physical properties of rock. University of California, Berkeley :70p.

Strachey, R., 1851, On the geology of part of the Himalaya Mountains and Tibet. Quart. J. Geol. Soc., London, Vol. 7: 292-310.

Strahler, A.N., 1952, Hypsometric (area, altitude) analysis of erosional topography. Bull. Geol. Soc. Am., Vol. 63: 1117-1142.

Strahler, A.N., 1956, Quantitative Slope analysis. Bull. Geol. Soc. Am., Vol. 67: 571-596.

Strahler, A.N., 1957, Quantitative analysis of watershed geomorphology. Trans. Am. Geophys. Union, Vol. 38: 919 p.

Strahler, A.N., 1958, Dimensional analysis applied to fluvially eroded landforms. Bull. Geol. Soc. Am., Vol. 69: 1-279.

Strahler, A.N., 1964, Quantitative geomorphology of drainage basins and channel networks. In: Hand book of applied Hydrology, (ed.)Chow, V.T., McGraw-Hill, New york: 4-39.

Strahler, A.N., 1971, Physical Geography. John Wiley & Sons, New York: 733p.

Talukdar, S.N. and Sudhakar, R., 1963, Structure of southern edge of Himalaya of North India. Geol. Surv. India Misc. Publ. , Vol. 1 : 185-195.

Terzaghi, K., 1929, Effect of minor geologic details on the safty of dams. Am. Inst. Min. Metall., Tech. Publ., 215: 31-44.

Thakur, V.C., 1980, Tectonics of the Central Crystallines of Western Himalaya. Tectonophysics, Vol. 62: 41-154.

Valdiya, K.S., 1964, The unfossiliferous formations of the Lesser Himalaya and their correlation. XXII, Int. Geol. Cong., Vol. 11 : 15-35.

Valdiya, K.S., 1975, Lithology and age of the Tal Formation in Garhwal, and implications on stratigraphic scheme of krol belt in Kumaun Himalaya. J. Geol. Soc. India, Vol. 16(2) : 119-134.

Valdiya, K.S., 1976, Himalayan transverse faults and folds and their parallelism with subsurface structures of the Northen Indian Plains. Tectonophysics, Vol. 32 : 353-386.

Valdiya, K.S., 1978, Extension and analogues of the Chali Nappe in Kumaun Himalaya. Ind. J. Earth Sci., Vol. 55: 1-19.

Valdiya, K.S., 1980a, Stratigraphic scheme of the sedimentary units of the Kumaun Lesser Himalaya. In: Stratigraphy and correlation of the Lesser Himalayan Formation, (eds.) Valdiya K.S.,and Bhatia, S.B., Hindustan Publ. Corp., Delhi:7-48.

Valdiya, K.S., 1980b, Geology of Kumaun Lesser Himalaya. W.I.H.G., Dehra Dun: 291p.

Varnes, D.J., 1958, Landslide types and process, In: Landslides and Engineering practice. (Ed.) Eckel, E.B., Highway Research Board special report 29, NAS-NRC Publication 544 : 20-47.

Varnes, D.J., 1978, Slope movement types and processes, In: landslides: analysis and control. Sp. report. 176, (eds.) schuster, R.L. and Krizek, r.J., Transportation Research Board, Nat. Acd. Sci. Washington, D.C. : 11-33.

Virdi, N.S., 1986, Lithostratigraphy and structure of central crystallines in the Alaknanda and Dhauliganga valleys of Garhwal, U.P.. Cur. Trends Geol., Vol. 9: 156-166.

William, R.E. and Flower, P.M., 1969. A preliminary report on an empirical analysis of drainage network adjustment to precipitation input. J. Hyd. Vol. 8 : 227-238.

Woldenberg, M.J., 1969, Spatial order in fluvial systems :Horton's law derived from mixed hexagonal hierarchies of drainage basin areas . Geol. Soc. Amer. Bull. 80 :97-112.

Yatsu, E. 1965, Rock control in geomorphology. Tokyo: 135p.

Young, A., 1961, Characteristic and limiting slope angles. Zeit. fur Geomorphologie , Vol. 5 : 126-131.

Zaruba, G. and Mencl, V., 1969, Landslides and their control. American Elsevier Publ. Co., New York: 214 p.

Zimmermann, M., Bischsel, M. and Kienholz, H. , 1986 , Mountain hazard mapping in Khumbu Himal, Nepal, with prototype map, scale 1:50,000. Mount. Res. and Dev., Vol. 6(1) : 29-40.

APPENDIX - I

CALCULATION OF SLOPE MASS RATING (ROMANA, 1985)

TABLE AI.1 BIENIAWSKI (1779) RATINGS FOR RMR

PARAMETER		RANGES OF VALUES						
1 Strength of Intact rock material	Point load strength index (MPa)	>10	4-10	2-4	1-2	For this load range, unixial compressive test is preferred		
	Unixial Compressive (MPa)	>250	100-250	50-100	25-50	5-25	1-	<1
	Rating	15	12	7	4	2	1	0
2 Drill core quality RQD(%)		90 -100	75 -90	50 -75	25 -50		<25	
	Rating	20	17	13	8		3	
3 Spacing of discontinuities		>2m	0.6-2m	200-600mm	60-200mm		<60 mm	
	Rating	20	15	10	8		5	
4 Condition of discontinuities		Very rough surfaces. Not continous. No separation. Unweathered wall rock	Slightly rough surfaces. Separation <1mm; Slightly weathered walls.	Slightly rough surfaces. Separation <1mm; Highly weathered walls.	Slickensided surfaces.or Gauge <5mm thick, or Separation 1-5 mm Continuous		Soft gauge> 5 mm or Separation> 5 mm Continous	
	Rating	30	25	20	10		0	
5 Ground water in joint		Completely dry	Damp	Wet	Dripping		Flowing	
	Rating	15	10	7	4		0	

TABLE AI.2 ADJUSTMENT RATING FOR JOINTS

Cont.

CASE		Very Favoruable	Favourable	Fair	Unfavourable	Very unfavourable
P T	$\lvert\alpha_j - \alpha_s\rvert$	$>30^\circ$	30°-20°	20°-10°	10°-5°	$<5^\circ$
P/T	$\lvert\alpha_j - \alpha_s - 180^\circ\rvert$					
	F_1	0.15	0.40	0.70	0.85	1.00
P	$\lvert\beta_j\rvert$	$<20^\circ$	20°-30°	30°-35°	35°-45°	$>45^\circ$
P	F_2	0.15	0.40	0.70	0.85	1.00
T	F_2	1	1	1	1	1
P	$\beta_j - \beta_s$	$>10^\circ$	10°-0°	0°	0°-(-10°)	$<-10^\circ$
T	$\beta_j + \beta_s$	$<110^\circ$	110°-120°	$>120^\circ$	--	--
P/T	F_3	0	-6	-25	-50	-60

P Plane fallure
T Toppling fallure

α_s slope dip direction α_j Joint dip direction

β_j slope dip β_j Joint dip

TABLE AI.3 ADJUSTMENT RATING FOR METHODS OF EXCAVATION OF SLOPES

Method	Natural	Prespliting	Smooth blasting	Blasting or Mechanical	Defficient
F_4	+15	+10	+8	0	-8

$$SMR = RMR_{basic} + (F_1 x F_2 x F_3) + F_4$$

TABLE A I.4 TENTATIVE DESCRIPTION OF SMR CLASSES

Contd.

Class No.	V	IV	III	II	I
SMR	0-20	21-40	41-60	61-00	81-100
Description	Very poor	poor	FAir	Good	Very good
Stability	very Unstable	Unstable	Partially stable	Stable	Fully stable
Failures	Large planar or soil-like	Planar or Large wedges	Some joints or Many wedges	Some blocks	None
Support	Reexcavation	Extensive Correction	Systematic	Occasional	None

APPENDIX - II

SHORT METHOD OF ANALYSIS OF TETRAHEDRAL WEDGE (HOEK AND BRAY, 1981)

Here, in the analysis of a wedge, a horizontal slope crest and no tension crack is considered (Fig. AII.1). Each plane may have different friction angle and cohesive strength. The influence of water pressure of each plane is also included in the analysis. The analysis does not include the effect of externally applied load.

The discontinuities are denoted by 1 and 2, the upper ground surface by 3 and the slope face by 4. The data required for the analysis are:

Γ = the unit weight of the rock

H = The height of the crest of the slope (wedge) above the intersection 'O'.

ψ = Dip of each plane

α = Dip direction of each plane

C = Cohesion for planes 1 and 2

ϕ = Friction angle for planes 1 and 2

u = Average water pressure of each of the planes 1 and 2.

If the slope face overhangs over the toe of the slope, the index 'n' is assigned the value of '-1'.

If the slope face does not overhang over the toe of the slope the index 'n' is assigned the value '+1'.

F = Factor of safety against wedge sliding calculated as the ratio of the resisting of the actuating shear forces.

A = Area of a face of the wedge

W = Weight of the wedge

N = Effective normal reaction on a plane

S = Actuating shear force on a plane

X,Y,Z= Co-ordinate axes with origin at 'O'. The Z-axis is directed vertically upwards, the Y-axis is in the dip direction of plane '2'.

$\bar{a}$ = Unit vector in the direction of the normal to plane '1' with components (ax,ay,az)

$\bar{b}$ = Unit vector in the direction of the normal to plane '2' with components (bx, by, bz)

$\bar{f}$ = Unit vector in the direction of the normal to plane '4' with components (fx,fy,fz)

$\bar{g}$ = Vector in the direction of the line of intersection of planes '1' and '4' with components (gx,gy,gz)

$\bar{i}$ = Vector in the direction of the line of intersection of planes '1' and '2' with components (ix, iy, iz)

If the discontinuities are completely filled with water and that the water pressure varies from zero at the free face to a maximum, at some point on the line of intersection then

$$u1 = u2 = \Gamma w . Hw / 6 \qquad \text{(AII.1)}$$

where,

Γw = Unit weight of water and

Hw = Over all height of the wedge.

$i = -iz$ (AII.2)

q = Component of g in the direction of b

r = Component of a in the direction of b

$k = |i|^2 = ix^2 + iy^2 + iz^2$ (AII.3)

$1 = W/A2$ (AII.4)

$p = A1/A2$ (AII.5)

$(ax,ay,az) = (\text{Sin}\psi 1.\text{Sin}(\alpha 1-\alpha 2),$

$\text{Sin}\psi 1.\text{Cos}(\alpha 1-\alpha 2), \text{Cos}\psi 1)$ (AII.6)

$(fx,fy,fz) = (\text{Sin}\psi 4.\text{Sin}(\alpha 4-\alpha 2),$

$\text{Sin}\psi 4.\text{Cos}(\alpha 4-\alpha 2), \text{Cos}\psi 4)$ (AII.6)

$(bx,by,bz) = (0, \text{Sin}\psi 2, \text{Cos}\psi 2)$ (AII.8)

$\psi 3$ & $\alpha 3 = 0$

AII.2 Condition for no Wedge formation

If following two conditions are satisfied, then no wedge is formed

i) $nq/i > 0$ (AII.9)

or if, $n(fz-q/i)\ \tan\psi 3 > \sqrt{(1-fz)^2}$ (AII.10)

ii) $\sigma 3 = \alpha 4 \pm (1-\eta)\ \pi/2$ (AII.11)

where

$i = ax.by$ (AII.12)

$gz = fx.ay - fx.ax$ (AII.13)

$q = by\ (fz.ax - fx.az) + bz.gz$ (AII.14)

AII.3 Equations of discontinuities, slope face and slope crest planes

Discontinuity Plane 1

$$ax.x + ay.y + az.z = 0 \qquad \text{(AII.15)}$$

Discontinuity Plane 2

$$bx.x + by.y + bz.z = 0 \qquad \text{(AII.16)}$$

Crest Plane 3

$$Z = H \qquad \text{(AII.17)}$$

Slope face Plane 4

$$fx.x + fy.y + fz.z = 0 \qquad \text{(AII.18)}$$

AII.4 Co-ordinates of Wedge formed

For calculating the point of intersections of different planes (Fig. AII.1). Point 'a' is the intersecting point of plane 1,3 & 4. Point 'b' is the intersecting point of plane 2,3 & 4. Point 'c' is the intersecting point of planes 1,2 & 3. The point 'd' is assumed as the origin of the coordinate axes system.

From equations AII.15, AII.16 & AII.18 the coordinate of point 'a' is

$$Xa = \frac{H(ay.fz-az.fy)}{ax.fy-ay.fx} \qquad \text{(AII.19)}$$

$$Ya = \frac{H(fx.az-fz.ax)}{ax.fy-ay.fx} \qquad \text{(AII.20)}$$

$$Za = H \qquad \text{(AII.21)}$$

From equations AII.16, AII.17 & AII.18 the coordinate of point 'b' is

$$Xb = \frac{H(fy.bz-fz.by)}{fx.by-bx.fy} \qquad (AII.22)$$

$$Yb = \frac{-H.bz}{by} \qquad (AII.23)$$

$$Zb = H \qquad (AII.24)$$

From equation AII.15, AII.16 & AII.17 the coordinate of point 'c' is

$$Xc = \frac{H(ay.bz-by.az)}{ax.by-by.ay} \qquad (AII.25)$$

$$Yc = \frac{-H.bz}{by} \qquad (AII.26)$$

$$Zb = H \qquad (AII.27)$$

and Coordinate of point 'd' is (0,0,0)

AII.5 Volume of Wedge

$$Volume = H/6\ [\{Xa(Yb-Yc) + Xb\ (Yc-Ya) + Yc(Ya-Yb)\}] \qquad (AII.28)$$

AII.6 Dip of Intersection line

$$= ASIN\ [z(3)/\sqrt{\{x(3)\}^2 + \{Y(3)\}^2 + \{Z(3)\}^2}] \qquad (AII.29)$$

AII.7 Effect of Sub-mergence

$$u1\&u2 = Yw.Hw/6.\ (1-RWL^2)/H^2 \qquad \text{(AII.30)}$$

$$Hw = (H - RWL).\ PORE \qquad \text{(AII.31)}$$

AII.8 Effective Unit Weight

$$\Gamma s = \Gamma - \Gamma w.\ RWL^3/H^3 \qquad \text{(AII.32)}$$

AII.9 Contact on Both the Planes (Plane '1' & '2')

$$n1 = [\{1/k\ (az-r.bz)\}-p.u1]\ p/|p| = N1/A2 \qquad \text{(AII.33)}$$

$$n2 = [\{1/k\ (bz-r.az)\}-u2] = N2/A2 \qquad \text{(AII.34)}$$

where

$$p = -by.fx/gz \qquad \text{(AII.35)}$$

$$r = ay.by + az.bz \qquad \text{(AII.36)}$$

$$k = 1 - r^2 \qquad \text{(AII.37)}$$

$$1 = \frac{\Gamma.H.q}{3q_z} \qquad \text{(AII.38)}$$

If n1>0 and N2>0, then the wedge is in contact with both the planes and so, sliding will take place along line of intersection.

Hence, (Factor of Safety)

Fstatic = Resisting Force (Q)/Actuating Shear Force (S)

$$Fstatic = \frac{n1.\tan\phi1 + n2\tan\phi2 + |p|.C1 + C2}{1i\ \sqrt{k}} \qquad (AII.39)$$

$$S = 1i \times A2 / \sqrt{k} \qquad (AII.40)$$

$$Fdynamic = \frac{S.Q - E[Q^2+B(S^2-E^2)]^{1/2}}{S^2 - E^2} \qquad (AII.41)$$

Where E = Earthquake force

$$= W \times \alpha h$$

$$= |1.\alpha h)| \qquad (AII.42)$$

$$B = \frac{\tan^2\phi1 + \tan^2\phi2 - 2r.\tan\phi1.\tan\phi2}{k} \qquad (AII.43)$$

$$r = ay.by + az.bz \qquad (AII.44)$$

$$k = 1 - r^2 \qquad (AII.45)$$

S = Shear force on plane 1 & 2 = $A2.1i/\sqrt{k}$ (AII.46)

Q = Resisting force on plane 1 & 2

$$= n1.\tan\phi1 + n2.\tan\phi2 + |p|.C1 + C2 \qquad (AII.47)$$

AII.10 Contact of plane '1' only

$$m1 = 1.az - r.u2 - p.u1).p/|p| = N1/A2 \qquad \text{(AII.48)}$$

If n2 < 0 and m1 > 0, then the wedge has contact on plane '1' only and it will slide only along plan '1'

$$Fstatic = \frac{m1.\tan\phi1 + |p|.C1}{\{1^2(1-az^2) + k.u_2^2 + 2(r.az-bz)1.u2\}^{1/2}} \qquad \text{(AII.49)}$$

where $1 = W/A2$ (AII.50)

$$P = -by.fx/qz \qquad \text{(AII.51)}$$

$$u2 = \Gamma w.Hw/6.\ (1-RWL^2)/H^2 \qquad \text{(AII.52)}$$

$$k = |i|^2 \qquad \text{(AII.53)}$$

$$m1^2 = N1/A2 \qquad \text{(AII.54)}$$

$$Fdynamic = \frac{S.Q - E\ [Q^2+\tan^2\phi1)(S^2-E^2)]^{1/2}}{S^2 - E^2} \qquad \text{(AII.55)}$$

where

$$E = w.\alpha h = |1.\alpha h| \qquad \text{(AII.56)}$$

S = Shear force on plane 1

$$= \{1^2(1-az^2) + k.u2^2 + 2\ (r.az-bz)1.u^2\}^{1/2} \qquad \text{(AII.57)}$$

Q = Resisting force on plane '1'

$$= m1.\tan\ \phi1 + |p|.C1 \qquad \text{(AII.58)}$$

AII.11 Contact on Plane '2' only

$$m2 = (1.bz - r.p.u1-u2) = N2/A2 \qquad \text{(AII.59)}$$

If n1 < 0 and m2 > 0, then the wedge has contact on plane '2' only and the wedge will slide only along plane '2'. In this case

$$Fstatic = \frac{m2.\tan\phi2 + C2}{\{l^2.by^2+k.p^2.ul^2+2(r.bz-az)p.l.ul\}^{1/2}} \qquad (AII.60)$$

$$Fdynamic = \frac{S.Q. - E[Q^2+\tan^2\phi2\ (S^2-E^2)^{1/2}}{S^2 - E^2} \qquad (AII.61)$$

where Q = Resisting force on plane '2'

$$= m2.\tan\phi2 + C2 \qquad (AII.62)$$

S = Shear force on plane '2'

$$= [l^2.by^2+k.p^2.ul^2+2(r.bz-az)p.l.ul]^{1/2} \qquad (AII.63)$$

AII.12 Floating Wedge

If m1 < 0 and m2 < 0, in such case the contact of wedge is lost on both the planes due to very high seepage forces on both the planes and wedge floats over plane '1' and '2', sometimes it may overturn or topple down also.

In this condition, factor of safety of wedge becomes ZERO.

AII.13 Dynamic Displacement (Lavania et al.,1987)

Displacement of wedge (DIS) = $308.5)\alpha h\ (1-p)^{1.19}\ e^{-7.174p}$

where

αh = Horizontal component of earthquake acceleration

$P = \alpha cr/\alpha h$

αcr= Critical acceleration

= αh when factor of safety of wedge equal to unity.

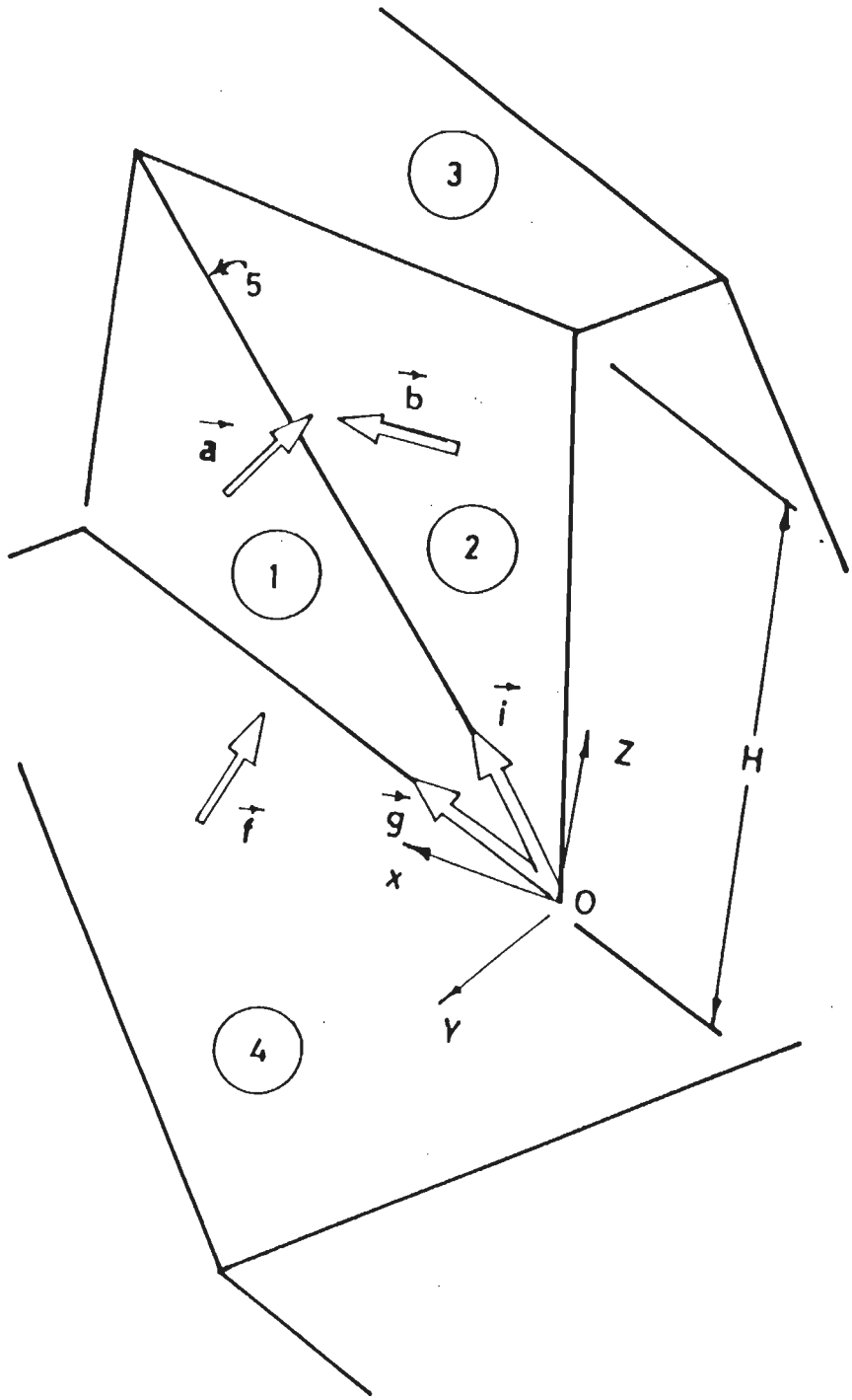

Fig.All 1: PICTORIAL VIEW OF TETRAHEDRAL WEDGE SLIDING SHOWING UNIT VECTORS AND OTHER DETAILS

APPENDIX - III

Tables for Estimation of `c' and `ϕ' from Basic RMR

Class No.	I	II	III	IV	V
Description	Very good rock	Good rock	Fair rock	Poor rock	Very poor rock
RMR	100-81	80-61	60-41	40-21	<20

TABLE AII2 MEANING OF ROCK CLASSES

Class No.	I	II	III	IV	V
Average Stand-up time	10 years for 15m span	6 months for 8m span	1 week for 5m span	10 hours for 2.5m span	30 minute for 1m span
Cohesion of the rock mass	4kg/cm^2	3-4 kg/cm^2	2-3.0 kg/cm^2	1-2.0 kg/cm^2	0-1 kg cm
Friction angle of the rockmass	>45°	35°-45°	25°-35°	15°-25°	15°

APPENDIX - IV

Slope Morphomertic Indices for Sixty Slope Profiles in Area of Study

Process Group (1)	Classification Index (2)	Dilation Index (3)	Flowage Index (4)	Displacement Index (5)	Tenuity Index (6)
RS	10.5	0.26	67.88	73.39	1.26
	6.43	0.27	93.07	47.50	1.27
	6.86	0.56	49.17	50.00	1.11
	10.97	0.50	53.57	43.75	1.07
	5.83	0.16	82.60	64.80	0.98
	7.57	0.16	100.80	48.00	1.20
	5.07	0.42	66.19	34.74	1.14
	5.55	0.45	74.25	45.00	1.35
	6.98	0.32	93.50	28.12	1.37
	5.60	0.35	80.10	45.77	1.23
	7.00	0.33	81.68	34.24	1.21
	5.44	0.45	68.24	61.11	1.24
PS					
	7.93	0.15	32.78	90.70	0.38
	10.08	0.37	51.88	58.80	0.82
	9.00	0.30	32.66	76.50	0.49
	10.00	0.21	59.00	56.52	0.75
	3.25	0.46	34.60	74.28	0.64
	10.67	0.37	61.38	58.97	0.97
	5.62	0.12	32.90	82.78	0.25
	7.06	0.61	34.66	81.48	0.89
	7.50	0.25	52.99	46.67	0.70
	5.37	0.27	41.07	75.00	0.12

Contd.. App. - IV

(1)	(2)	(3)	(4)	(5)	(6)
	10.67	0.50	44.74	80.54	0.89
	10.47	0.17	62.92	75.80	0.53
	10.06	0.98	98.07	91.50	0.98
	7.61	0.11	33.09	89.92	0.38
	9.75	0.12	44.62	74.90	0.51
	5.00	0.16	54.42	76.05	0.64
	6.29	0.22	30.10	78.94	0.38
	3.20	0.61	18.80	84.00	0.48
	3.77	0.55	24.37	77.77	0.54
	3.52	0.60	39.33	40.83	0.98
	4.00	0.46	39.00	67.59	0.72
SF					
	3.21	0.78	34.22	51.85	1.56
	4.23	0.69	41.62	54.17	1.35
	4.16	0.50	78.26	55.65	1.56
	4.52	0.68	48.00	62.50	1.50
	3.38	0.70	20.68	69.00	1.34
	4.70	0.99	74.28	74.20	2.86
	5.09	0.98	121.42	71.42	1.25
	6.44	1.00	161.53	69.23	1.61
	4.50	0.68	54.85	38.09	1.71
	4.25	0.50	96.43	33.33	1.93
	4.70	0.24	93.34	38.04	1.23
	3.50	0.61	62.70	33.33	1.60

Contd.. App. - IV

(1)	(2)	(3)	(4)	(5)	(6)
FF					
	1.63	1.00	109.30	90.70	1.09
	2.06	1.17	23.92	48.80	1.41
	1.51	3.33	580.0	60.00	4.57
	1.90	2.25	213.06	56.80	1.70
	2.38	1.25	68.80	42.22	2.75
	1.09	3.50	608.60	95.16	4.93
	2.12	2.00	407.31	53.66	4.07
	1.60	1.33	57.31	51.02	1.68
	2.30	1.00	154.83	56.46	1.55
	1.66	3.00	436.00	54.45	2.18
	2.19	1.66	147.58	38.80	2.23
	2.35	1.10	197.05	41.17	1.97
	1.32	1.53	70.09	79.56	1.32
	1.76	1.46	95.94	32.80	2.08
	2.34	1.33	68.53	38.46	2.07

ERRATA

Page	Line	Printed	Corrected
ii	12	carrier	career
38	5	th	the
46	10	hte	the
46	18	damarcation	demarcation
86	17	fracture landslide	fraction landslide
97	22	Skewpton	skempton
169	19	Fig. 4.21	Fig. 5.21
170	5	hight	highest
205	3	RMR	RMR_{basic}
223	13	drainaes	drainages
233	17	high value	low value
249		Skemton	skempton

C/ϕH = denoted as value of cohesion